OUKA
The University of Osaka
Institutional Knowledge Archive

Title	Chemical and Biotechnological Strategies to Enhance the Catalytic Efficiency and Utility of Hemoprotein-Based Biocatalysis for Aldoxime Dehydration
Author(s)	阿部, 美笛
Citation	大阪大学, 2026, 博士論文
Version Type	VoR
URL	https://doi.org/10.18910/105420
rights	
Note	

The University of Osaka Institutional Knowledge Archive : OUKA

https://ir.library.osaka-u.ac.jp/

The University of Osaka

Doctoral Dissertation

Chemical and Biotechnological Strategies to Enhance the Catalytic Efficiency and Utility of Hemoprotein-Based Biocatalysis for Aldoxime Dehydration

(アルドキシム脱水反応におけるヘムタンパク質を基盤としたバイオ触媒の

高活性化とその応用拡張をめざした化学的・生物工学的戦略)

January 2026

Miteki Abe

Graduate School of Engineering,
The University of Osaka

Contents

General Introduction 1

Chapter 1

Reconstituted Myoglobin with Iron Porphycene Catalyzes Aldoxime Dehydration with a Broad Substrate Scope

1-1. Introduction 14

1-2. Results and discussion 16

1-3. Summary 29

1-4. Experimental section 30

References 36

Chapter 2

Enhancement of Heme Biosynthesis via 5-Aminolevulinate Pathway Engineering in E. coli to Improve Hemoprotein-Based Biocatalysis

2-1. Introduction 40

2-2. Results and discussion 41

2-3. Summary 52

2-4. Experimental section 52

References 74

Chapter 3

Whole-Cell Aldoxime Dehydration in Organic Media Using Organic Solvent-Tolerant Bacterial Hosts

3-1. Introduction 78

3-2. Results and discussion 79

3-3. Summary 84

3-4. Experimental section 84

References 89

Conclusion 91

Acknowledgements 93

General introduction

Biocatalyst formats

Both purified enzymes and whole-cell catalysts have become established formats for biocatalytic processes, each offering distinct advantages for synthetic applications[1]. Purified enzymes act as well-defined catalysts that can be added directly to the reaction mixture, allowing for optimization of conditions to achieve high activity, selectivity, and substrate scope. However, processes relying on isolated enzymes must still address challenges such as stability and production cost[2]. In contrast, whole-cell systems employ enzymes within their native intracellular environment. The conservation of cellular machinery enables access to metabolic pathways, cofactor-regeneration systems, and multi-step enzymatic cascades without additional engineering[3]. However, this format has limitations: substrates and products must cross the cell membrane, which can limit mass transfer, and endogenous metabolic activities can lead to side reactions, cofactor depletion, or degradation of substrates and products[3,4]. These factors lead to lower yields and more complex reaction control, making whole-cell systems less predictable than purified enzymes. However, whole-cell catalysis remains attractive when cofactor recycling or cellular robustness provide advantages that outweigh the challenges associated with transport limitations or metabolic interference. As such, it continues to serve as a practical and cost-effective option for numerous biotransformations[5]. Taken together, the choice between purified enzymes and whole-cell catalysts depends on the balance between catalytic performance, operational simplicity, and cost. In either case, the practical implementation of biocatalysis requires reliable production of the target enzyme, making the selection of an appropriate expression host a critical factor. Among the available systems, *E. coli* remains the most widely used platform for recombinant enzyme production.

E. coli expression system for enzyme production

Escherichia coli (*E. coli*) has long been recognized as one of the most effective hosts for recombinant protein production. Its role as a robust protein expression host is well-established, and it remains the most widely used expression platform in both academic and industrial fields. The popularity of *E. coli* stems from the availability of diverse expression tools. These include a wide range of expression plasmids, numerous engineered strains, and well-optimized culture strategies enabling high-level production of heterologous proteins[6–10]. In principle, the workflow for obtaining a recombinant enzyme is straightforward: the gene of a target protein is cloned into a suitable vector, introduced into host cells, cultured to induce expression, then purified and characterized[11] (Fig. 1). In practice, however, this process often faces challenges such as the formation of insoluble inclusion bodies, loss of enzyme activity due to misfolding, or even complete failure to produce the target protein. To address these limitations, numerous strategies have been explored in previous studies. For example, the addition of a fusion tag during protein expression can improve the stability and solubility of the target protein[12]. Furthermore, induction at low temperatures helps prevent misfolding[13]. In addition, host engineering and selection of codons optimized for the expression host can significantly improve protein expression efficiency[14]. Therefore, despite inherent challenges, *E. coli* remains a robust and versatile platform for recombinant protein production. In addition to optimizing recombinant protein expression, the intracellular metabolic environment of the host cell plays a crucial role in determining whether the

expressed enzyme attains its functional, cofactor-bound form. In particular, many hemoproteins require sufficient heme supply for proper folding and catalytic activity. Therefore, understanding the heme biosynthesis pathway in *E. coli* is essential for rationally improving the production and functionality of heme-dependent enzymes.

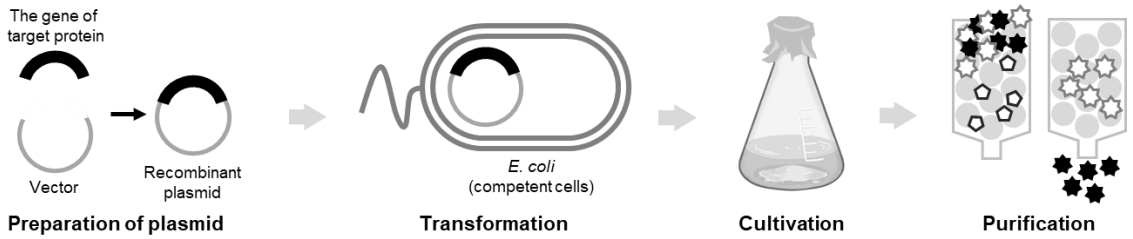


Figure 1. Workflow for obtaining recombinant enzymes.

Heme biosynthesis pathway

Heme biosynthesis constitutes a fundamental metabolic process conserved across bacteria, archaea, and eukaryotes and is tightly integrated with central carbon and amino acid metabolism. Despite this conservation, distinct biosynthetic routes and regulatory strategies have evolved to accommodate differences in cellular organization, metabolic demand, and environmental conditions.

The final product of glycolysis, pyruvate, is oxidatively decarboxylated to acetyl-CoA by the pyruvate dehydrogenase complex under aerobic conditions and subsequently enters the tricarboxylic acid (TCA) cycle. Within the TCA cycle, isocitrate is converted to α-ketoglutarate by isocitrate dehydrogenase, generating a key metabolic intermediate that links central carbon metabolism with amino acid biosynthesis[15]. Thus, central carbon metabolism provides essential precursors for multiple biosynthetic pathways, including heme biosynthesis.

Heme biosynthesis starts from 5-aminolevulinic acid (ALA), which is produced via two distinct pathways depending on the organism: the C4 and C5 pathways (Fig. 2) [16]. In the C4 pathway found in animals, fungi, and α-proteobacteria, ALA synthase (ALAS) catalyzes the condensation of glycine (which is usually supplied via the serine pathway from 3-phosphoglycerate, an intermediate of glycolysis[17]) and succinyl-CoA to produce ALA. In contrast, the C5 pathway found in plants, archaea, and many bacteria, synthesizes ALA from L-glutamate through the sequential actions of glutamyl-tRNA synthetase (GluRS), glutamyl-tRNA reductase (GluTR), and glutamate-1-semialdehyde aminomutase (GSAM).

ALA is subsequently converted into porphobilinogen (PBG) by porphobilinogen synthase (PBGS, also known as ALA dehydratase). Four PBG molecules are then polymerized by porphobilinogen deaminase (PBGD) to generate the unstable linear tetrapyrrole 1-hydroxymethylbilane (HMB), which is cyclized by uroporphyrinogen III synthase (UROS) to form uroporphyrinogen III (Uro III). From Uro III, heme is synthesized through two alternative downstream pathways. In the classical protoporphyrin-dependent (PPD) pathway, which operates in eukaryotes and α-proteobacteria, Uro III is sequentially converted into coproporphyrinogen III, protoporphyrinogen IX, and protoporphyrin IX by uroporphyrinogen decarboxylase (UROD), coproporphyrinogen oxidase (CPO), and protoporphyrinogen oxidase (PPO), respectively, followed by iron insertion catalyzed by ferrochelatase (FECH). In contrast, Actinobacteria and Firmicutes utilize the noncanonical coproporphyrin-dependent (CPD) pathway. In this

route, Uro III is first converted to coproporphyrinogen III as in the classical pathway, after which coproporphyrinogen III is oxidized to coproporphyrin III. Coproporphyrin III is then converted to coproheme by coproporphyrin ferrochelatase (CPFC), and finally to heme through a hydrogen peroxide-dependent reaction catalyzed by heme synthase (HS)[18,19].

In organisms utilizing the C5 pathway, heme exerts feedback control over its own biosynthesis by regulating the activity and stability of GluTR, the first committed enzyme of the C5 pathway. Accumulation of heme promotes GluTR destabilization and proteolytic degradation, thereby limiting ALA formation and maintaining intracellular heme homeostasis[20,21]. In contrast, in the C4 pathway, heme biosynthesis is tightly regulated through multilayered control of ALAS. When intracellular heme concentration increases, heme binds to regulatory motifs on ALAS, inhibiting its transport to the mitochondria and/or promoting enzyme destabilization. This feedback regulation reduces ALAS activity, maintaining the balance of heme production and protecting the cell from heme-induced toxicity[22]. Together, these pathways and regulatory mechanisms underscore that heme biosynthesis is tightly coupled to central metabolism and subject to strict control to maintain cellular homeostasis. Since the structure and reactivity of heme-dependent enzymes are intimately linked to the properties of their porphyrin cofactors, the cellular mechanisms governing heme biosynthesis and homeostasis are directly relevant to the functional assembly of hemoproteins. This connection provides the conceptual bridge to reconstitution approaches, where apoprotein scaffolds can be combined with native heme or structurally modified metalloporphyrinoids to dissect or redesign catalytic behavior.

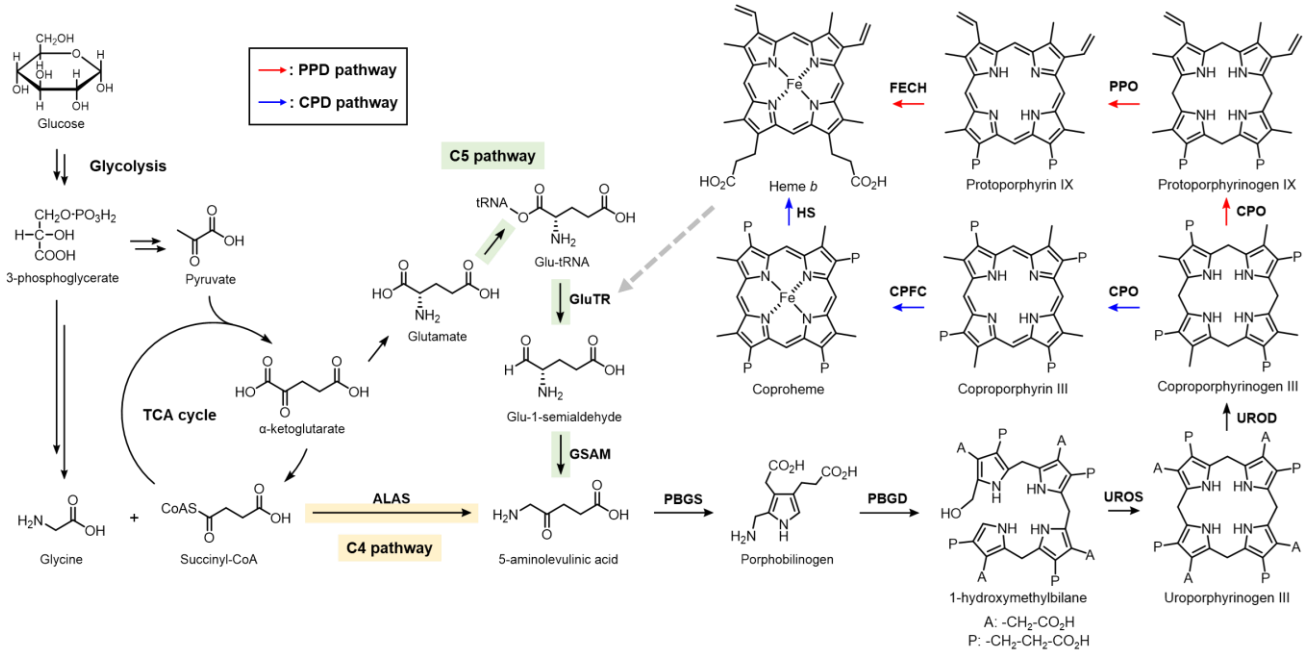


Figure 2. The biosynthetic pathway of heme and its derivatives.

Reconstitution of heme proteins

Heme proteins, which have iron porphyrin (heme) as a cofactor, constitute a highly versatile group of metalloproteins in biological systems. They mediate a wide range of essential functions, including the storage and

transport of oxygen and nitric oxide, catalysis, and electron transfer. The remarkable functional diversity of these proteins arises from the unique interactions between the heme cofactor and the surrounding protein matrix within the heme pocket. Under acidic conditions, the native heme can be selectively removed to generate the corresponding apoprotein. Crucially, the resulting apoprotein scaffold can be reconstituted not only with the native heme but also with modified heme derivatives or artificial metalloporphyrinoids (Fig. 3). Such reconstitution modulates the interactions within the heme pocket and enables the fine-tuning or even redirection of protein function. This approach thus provides a powerful strategy for elucidating structure–function relationships and for engineering novel biocatalysts with enhanced or tailored reactivity[23–25].

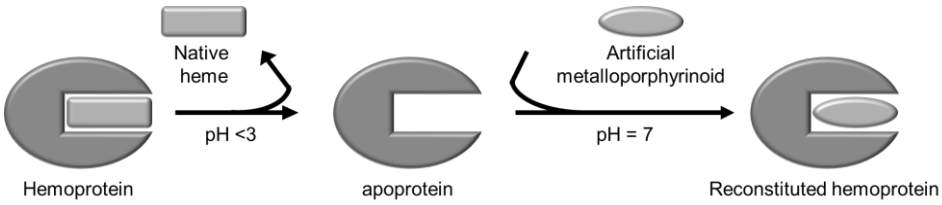


Figure 3. Representative scheme of hemoprotein reconstitution.

Building on this concept, several emblematic artificial metalloenzymes have been developed to demonstrate the potential of this strategy, by reconstituting hemoproteins with artificial metal cofactors. A representative example is myoglobin (Mb) reconstituted with iron porphycene (FePc), a constitutional isomer of porphyrin. In this case, the modification of the macrocyclic framework markedly alters the electronic structure of the metal center (Fig. 4a). Replacement of native heme with FePc enhances the oxidative reactivity of Mb, resulting in an approximately 11-fold increase in the H_2O_2-dependent oxidation of guaiacol at pH 7.0 compared with native Mb[26]. In addition to this enhanced peroxidase activity, FePc-reconstituted Mb (rMb(FePc)) enables abiological transformations such as olefin cyclopropanation via a spectroscopically observable iron–carbene intermediate, demonstrating that subtle modifications of the porphyrinoid framework can induce new catalytic functions within an otherwise unchanged protein scaffold[27].

The potential for reconstituted hemoproteins has been further expanded by metal substitution within artificial porphyrinoid cofactors. A notable case is Mb reconstituted with manganese porphycene (MnPc), which catalyzes H_2O_2-driven hydroxylation of inert C(sp^3)–H bonds[28,29] (Fig. 4b). In contrast to native Mb and FePc-containing Mb (rMb(FePc)), MnPc-containing Mb (rMb(MnPc)) promotes alkane hydroxylation through a Compound I–like Mn–oxo species. Importantly, the corresponding MnPc complex shows no catalytic activity in the absence of the protein matrix, indicating that the heme pocket plays an essential role in the generation and stabilization of the reactive intermediate.

As an alternative strategy, Hartwig and co-workers utilized the native transporters of *E. coli* Nissle 1917 strain to introduce iridium mesoporphyrin IX into the cells, enabling its incorporation into expressed cytochrome P450 variants (Fig. 4c). The resulting artificial metalloenzymes were assembled in vivo and used as a whole-cell catalyst to promote carbene insertion reactions[30].

These representative examples demonstrate that reconstitution of hemoproteins with artificial metal cofactors provides a modular and versatile platform for engineering artificial metalloenzymes. By decoupling catalytic function from native heme while preserving the structural features of the protein scaffold, this strategy

provides access to new reactivity patterns and offers powerful opportunities for the rational design of biohybrid catalysts. Nevertheless, numerous synthetically valuable functional groups are still produced primarily through chemical methods. Among these, nitriles represent an important class of compounds with broad industrial relevance. The following section outlines major strategies for nitrile synthesis and the limitations that motivate the search for milder catalytic approaches.

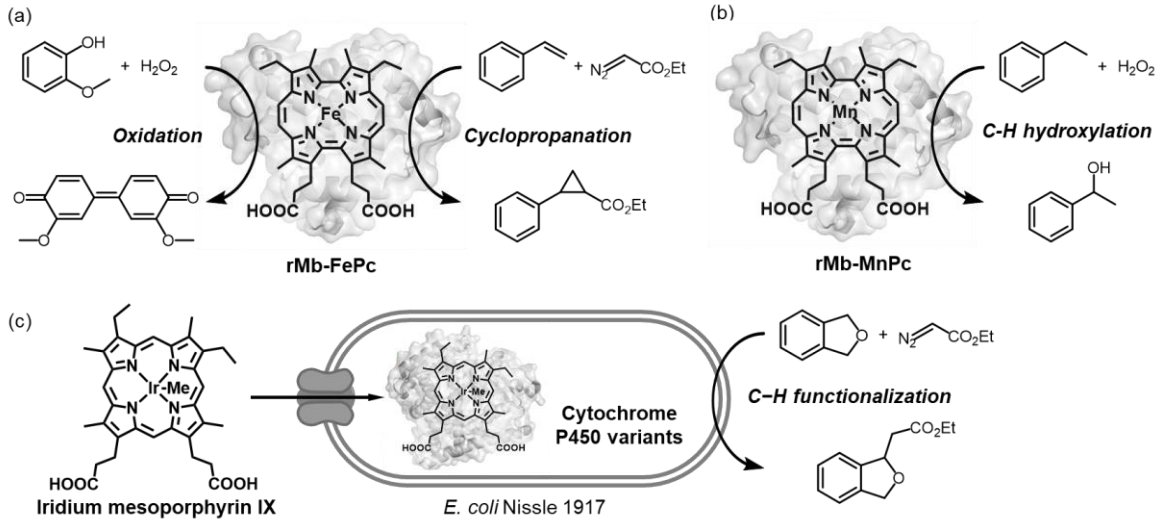


Figure 4. (a) H_2O_2-dependent oxidation of guaiacol and cyclopropanation catalyzed by rMb-FePc. (b) C–H hydroxylation catalyzed by rMb-MnPc. (c) C–H functionalization catalyzed by whole-cell catalysts comprising cytochrome P450 variants reconstituted with iridium mesoporphyrin IX.

Nitrile synthesis

Nitriles are widely used as intermediates and starting materials in the chemical industry because of the versatile reactivity of the polar unsaturated −C≡N group. Their susceptibility to nucleophilic addition, hydrolysis, and reduction enables efficient conversion of nitriles into a broad range of fundamental synthetic building blocks, including imines, ketones, amides, carboxylic acids, amines, and aldehydes[31–36]. Beyond these classical transformations, nitriles also serve as valuable partners in transition metal-catalyzed reactions such as alkyne insertion, annulation, cycloaddition, and C–H functionalization, as well as in nucleophilic or radical cascade processes. This enables efficient access to diverse carbocycles, heterocycles, and functionalized aromatic frameworks[37].

The representative industrial methods for nitrile synthesis are hydrocyanation and ammoxidation. Hydrocyanation was first reported in 1950s as a straightforward protocol for obtaining the corresponding nitriles from readily available raw materials through the hydrocyanation of alkenes[38]. A major drawback of this methodology is that it requires the use of hydrogen cyanide (HCN), which is highly toxic and hazardous to handle in industrial settings. Over the past few decades, concerns about the use of these harmful chemicals have led to the development of alternative strategies aimed at replacing them with safer reagents. Several approaches have now been developed that allow for the hydrocyanation of alkenes without directly handling HCN[39]. For example, transition-metal-catalyzed protocols using Ni or Pd complexes have enabled hydrocyanation with in situ generated cyanide species[40–44]. On the other hand, ammoxidation emerged in 1960s as an industrial process for the synthesis of

acrylonitrile, most notably through the Sohio process[45]. This method made it possible to convert simple alkenes such as propene into valuable nitriles on a large scale with relatively high efficiency, and the ammoxidation became the basis for commercial nitrile production. However, despite its industrial success, the process has several inherent limitations. Generally, this reaction is limited to simple substrates with few substituents, and undesirable side reactions often occur with more complex molecules[46]. The need for harsh reaction conditions and carefully optimized catalysts, combined with these factors, limits the broad applicability of ammoxidation for introducing nitrile groups into structurally complex compounds. To overcome this limitation, researchers have explored the ammoxidation of aldehydes, amines, and alcohols as alternative pathways to nitriles[47–49]. Among these, alcohols have attracted particular attention because they are readily available, chemically stable, and can be obtained from biomass resources. In recent years, various heterogeneous catalysts have been developed for the synthesis of nitriles via the ammoxidation of alcohols, however, challenges remain, including the need for high temperature or high oxygen pressure, insufficient catalytic activity and stability, and a lack of clarity regarding the structure–activity relationships. Addressing these challenges will require the design of more efficient and sustainable catalysts[50].

Moreover, numerous other approaches to nitrile synthesis have been developed so far[51]. For example, the dehydration of aldoximes represents a straightforward synthetic route that can convert aldehydes into the corresponding nitriles, usually with high yields. Recent advances have expanded this transformation beyond conventional reagent-based dehydrations; however, many established non-enzymatic protocols still rely on relatively harsh conditions. For example, organoselenium-mediated oxidative dehydrations typically require stoichiometric oxidants such as hydrogen peroxide and proceed via high-valent selenium intermediates[52,53]. Conversely, the oxalyl chloride/DMSO-activated process employs highly electrophilic chlorinating reagent[54]. Although these approaches are synthetically useful, their operational safety and environmental compatibility remain limited, highlighting the need for milder alternatives such as enzyme-catalyzed aldoxime dehydrations. In this context, enzyme-catalyzed aldoxime dehydration has emerged as a particularly attractive strategy, with aldoxime dehydratase (Oxd) representing a key biocatalyst for environmentally benign nitrile synthesis.

Aldoxime dehydratase

Aldoxime dehydratase (Oxd) was first reported in 1998 by Asano and Kato from *Bacillus sp*. OxB-1[55], and the three-dimensional structure of Oxd derived from *Rhodococcus erythropolis* PR4 was subsequently elucidated by Aono and co-workers in 2009 through X-ray crystallographic analysis[56] (Fig. 5a). Oxd is a heme-dependent enzyme that contains heme *b* as a prosthetic group and catalyzes the highly efficient dehydration of aldoximes to the corresponding nitriles. This enzyme family exhibits broad substrate specificity, and most Oxd enzymes show high catalytic activity toward both aliphatic and aromatic aldoximes[57,58]. The catalytic mechanism of Oxd has been proposed based on structural and mutational analyses[59] (Fig. 5b). Initially, the substrate is bound within the heme pocket through interactions with the side chain of Ser219. Subsequently, the protonated His320 donates a proton to the hydroxyl group of the aldoxime substrate, facilitating its elimination as a water molecule. In this process, the substrate bound to the ferrous heme cofactor is polarized through the interaction, increasing the basicity of the substrate's hydroxyl group, and further promoting its elimination as a water molecule through hydrogen bonding

with Ser219. The substrate's α-carbon is oriented toward His320, forming a hydrogen bond between the substrate's α-proton and the hydroxyl group of Ser219, thereby stabilizing the reaction intermediate. At this stage, the substrate adopts a linear Fe=N–C configuration, with His320 positioned optimally to abstract the α-proton and thereby facilitate nitrile formation. Finally, the protonated imidazole ring of His320 donates a proton to Arg178, the enzyme returns to its initial state. Two reaction intermediates, called OS-I (a heme-bound aldoxime complex) and OS-II (a dehydrated heme–substrate complex), were experimentally detected by spectroscopic analyses[60]. Notably, Arg178, Ser219, and His320 are strictly conserved among Oxd enzymes from different organisms, strongly suggesting that these residues play similar crucial roles throughout this enzyme family. Due to its high efficiency, broad substrate scope, and mild reaction conditions, Oxd has attracted considerable attention as a biocatalyst for environmentally friendly nitrile synthesis.

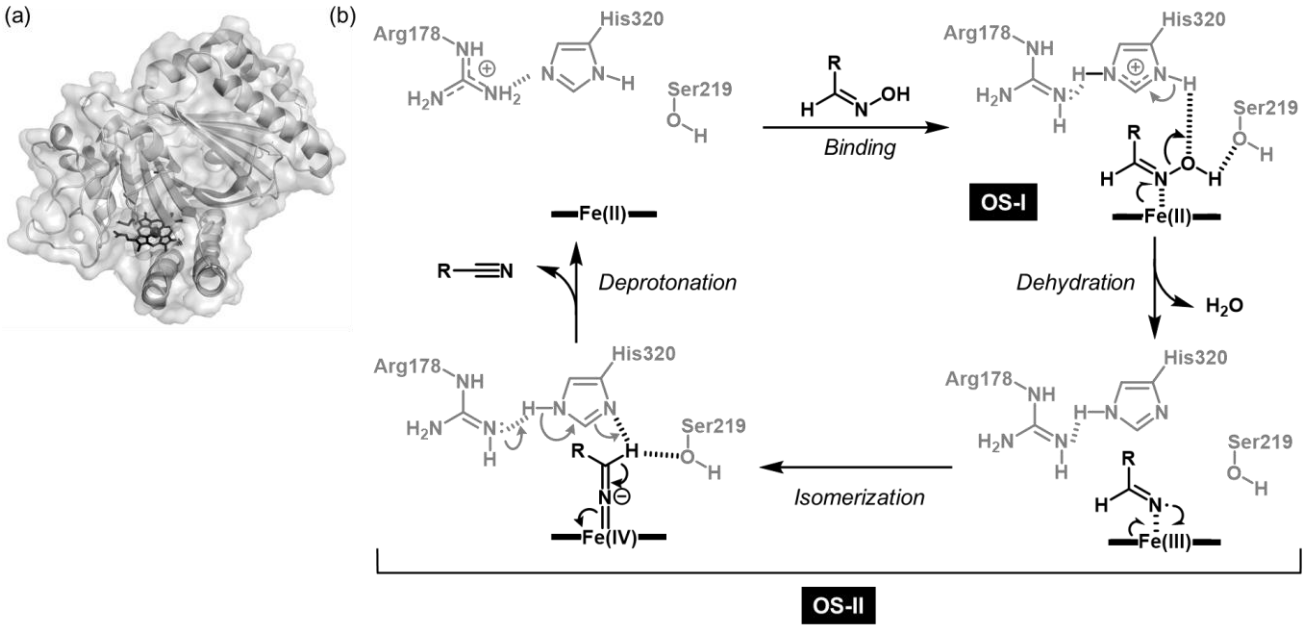


Figure 5. (a) X-ray crystal structure of Oxd (PDB: 3A15). (b) A plausible reaction mechanism for the nitrile synthesis by Oxd.

Outline of this thesis

In recent years, the development of environmentally friendly chemical processes has become increasingly important for realizing a sustainable society. In this context, enzymes have attracted significant attention from both academia and industry as biocatalysts because of their high chemoselectivity and stereoselectivity under mild reaction conditions. Among various enzymes, hemoproteins are particularly noteworthy as versatile platforms due to the reactivity of their metal center and the tunability of their structure. However, several challenges remain as barriers to the practical application of hemoproteins as biocatalysts. Their substrate scope is often limited to native or closely related substrates, and catalytic activity frequently decreases or disappears for non-native substrates. In addition, during heterologous overexpression in *E. coli*, intracellular supply of the heme cofactor is frequently insufficient, leading to the formation of inactive apoproteins. Furthermore, since most heme-dependent biocatalytic reactions occur in aqueous media, application to poorly water-soluble substrates is difficult. To address these limitations, this study aims to expand the utility of heme-based biocatalysts using chemical and bioengineering approaches. Chapter 1 describes the development of an artificial metalloenzyme for the aldoxime dehydration that accommodates a broader range of substrates than native enzymes. Chapter 2 describes increasing intracellular heme supply by introducing a heterologous heme biosynthetic pathway. Chapter 3 describes the construction of a whole-cell biocatalytic system that functions in organic solvents, enabling efficient biotransformations under non-aqueous conditions.

Chapter 1: Reconstituted Myoglobin with Iron Porphycene Catalyzes Aldoxime Dehydration with a Broad Substrate Scope

The enzymatic aldoxime dehydration represents a valuable strategy for the synthesis of diverse nitrile compounds under mild conditions. However, Oxds have the disadvantage of having a narrow substrate scope and frequently exhibiting reduced activity toward non-natural substrates. To overcome these limitations, Mb with a promiscuous reaction environment and FePc as an artificial cofactor having distinctive electronic properties were used. Then, an artificial metalloenzyme responsible for nitrile synthesis was created by reconstituting Mb with FePc. The obtained rMb-FePc was found to catalyze the transformation of various substrates into nitriles under neutral and ambient conditions, achieving a turnover number (TON) of 9300 for aliphatic aldoximes. Furthermore, by introducing site-directed mutations to mimic the reaction site of the Oxd, the initial reaction rate was enhanced more than 24-fold.

Chapter 2: Enhancement of Heme Biosynthesis via 5-Aminolevulinate Pathway Engineering in *E. coli* to Improve Hemoprotein-Based Biocatalysis

Recombinant production of hemoproteins in *E. coli* is often limited by regulatory mechanisms, and intracellular heme concentration levels are further constrained by inherent limitations of the heme biosynthetic pathway. Overexpression often leads to the accumulation of inactive apo forms, so adding ALA to the culture medium is necessary to increase the yield of hemoproteins. However, 5-ALA is expensive, accounting for approximately 60%

of the culture costs. To overcome this limitation, a self-sufficient ALA production system was constructed in *E. coli* by introducing the C4 pathway, which is absent in the native host. Specifically, the C4 pathway was established by expressing ALA synthase derived from *Paracoccus denitrificans* (PdALAS). Pyridine hemochromagen assay demonstrated that this system effectively promoted the production of heme cofactors in 15 different hemoproteins. Furthermore, the utility of PdALAS-based C4 pathway engineering was validated through biocatalytic reactions employing diverse hemoproteins. In seven representative transformations, catalytic activities were markedly improved.

Chapter 3: Whole-Cell Aldoxime Dehydration in Organic Media Using Organic Solvent-Tolerant Bacterial Hosts

Enzymatic reactions are generally performed in aqueous systems, which imposes significant limitations on the solubility of hydrophobic substrates and consequently restricts both reaction efficiency and scale. Moreover, *E. coli*, a widely used host for whole-cell biocatalysts, exhibits poor tolerance to organic solvents and is therefore unsuitable for applications in non-aqueous environments. To address these challenges, this study focused on *Rhodococcus* species, which are known for their excellent resistance to organic solvents, and aimed to establish a whole-cell biocatalytic system capable of efficient nitrile synthesis under organic solvent conditions. The whole-cell biocatalyst based on *Rhodococcus erythropolis* L88 demonstrated high catalytic activity in hexane, quantitatively producing the desired nitrile in a short reaction time. Subsequently, the catalytic performance of the *Rhodococcus*-based system was compared to that of a conventional *E. coli*-based system under hexane conditions. Whereas the *E. coli* system almost completely lost its activity, the *Rhodococcus*-based catalyst promoted the hydration of aldoximes quantitatively within 30 minutes of the reaction initiation. Furthermore, the substrate scope of this catalytic system was evaluated. As a result, it was confirmed that various aldoximes could be efficiently dehydrated, even on a preparative scale.

References

[1] R. A. Sheldon, J. M. Woodley, "Role of Biocatalysis in Sustainable Chemistry" *Chem. Rev.* **2018**, *118*, 801–838.

[2] S. Wu, R. Snajdrova, J. C. Moore, K. Baldenius, U. T. Bornscheuer, "Biocatalysis: Enzymatic Synthesis for Industrial Applications" *Angew. Chem. Int. Ed.* **2021**, *60*, 88–119.

[3] N. Ladkau, A. Schmid, B. Bühler, "The microbial cell — functional unit for energy dependent multistep biocatalysis" *Curr. Opin. Biotech.* **2014**, *30*, 178–189.

[4] B. Lin, Y. Tao, "Whole-cell biocatalysts by design" *Microb. Cell. Fact.* **2017**, *16*, 106.

[5] J. Wachtmeister, D. Rother, "Recent advances in whole cell biocatalysis techniques bridging from investigative to industrial scale" *Curr. Opin. Biotech.* **2016**, *42*, 169–177.

[6] F. Baneyx, "Recombinant protein expression in *Escherichia coli*" *Curr. Opin. Biotech.* **1999**, *10*, 411–421.

[7] S. C. Makrides, "Strategies for achieving high-level expression of genes in Escherichia coli" *Microbiol. Rev.* **1996**, *60*, 512–538.

[8] R. C. Stevens, "Design of high-throughput methods of protein production for structural biology" *Structure* **2000**, *8*, R177–R185.

[9] S. Jana, J. K. Deb, "Retraction Note: Strategies for efficient production of heterologous proteins in Escherichia coli" *Appl. Microbiol. Biotechnol.* **2014**, *98*, 5787–5787.

[10] H. P. Sørensen, K. K. Mortensen, "Advanced genetic strategies for recombinant protein expression in *Escherichia coli*" *J. Biotech.* **2005**, *115*, 113–128.

[11] G. L. Rosano, E. A. Ceccarelli, "Recombinant protein expression in Escherichia coli: advances and challenges" *Front. Microbiol.* **2014**, *5*, 172.

[12] K. Terpe, "Overview of tag protein fusions: from molecular and biochemical fundamentals to commercial systems" *Appl. Microbiol. Biotechnol.* **2003**, *60*, 523–533.

[13] H. P. Sørensen, K. K. Mortensen, "Soluble expression of recombinant proteins in the cytoplasm of Escherichia coli" *Microb. Cell. Fact.* **2005**, *4*, 1.

[14] C. Gustafsson, S. Govindarajan, J. Minshull, "Codon bias and heterologous protein expression" *Trends Biotechnol.* **2004**, *22*, 346–353.

[15] L. F. Huergo, R. Dixon, "The Emergence of 2-Oxoglutarate as a Master Regulator Metabolite" *Microbiol. Mol. Biol. Rev.* **2015**, *79*, 419–435.

[16] F. Yu, Z. Wang, Z. Zhang, J. Zhou, J. Li, J. Chen, G. Du, X. Zhao, "Biosynthesis, acquisition, regulation, and upcycling of heme: recent advances" *Crit. Rev. Biotechnol.* **2024**, *44*, 1422–1438.

[17] H. E. Umbarger, "Amino Acid Biosynthesis and its Regulation" *Ann. Rev. Biochem.* **1978**, *47*, 533–606.

[18] S. A. Swenson, C. M. Moore, J. R. Marcero, A. E. Medlock, A. R. Reddi, O. Khalimonchuk, S. A. Swenson, C. M. Moore, J. R. Marcero, A. E. Medlock, A. R. Reddi, O. Khalimonchuk, "From Synthesis to Utilization: The Ins and Outs of Mitochondrial Heme" *Cells* **2020**, *9*, DOI 10.3390/cells9030579.

[19] Q. Yang, J. Zhao, Y. Zheng, T. Chen, Z. Wang, Q. Yang, J. Zhao, Y. Zheng, T. Chen, Z. Wang, "Microbial Synthesis of Heme b: Biosynthetic Pathways, Current Strategies, Detection, and Future Prospects" *Molecules* **2023**, *28*, DOI 10.3390/molecules28083633.

[20] U. C. Vothknecht, C. G. Kannangara, D. von Wettstein, "Barley glutamyl tRNAGlu reductase: Mutations

affecting haem inhibition and enzyme activity" *Phytochem.* **1998**, *47*, 513–519.

[21] B. Pontoppidan, C. G. Kannangara, "Purification and partial characterisation of barley glutamyl-tRNAGlu reductase, the enzyme that directs glutamate to chlorophyll biosynthesis" *European J. Biochem.* **1994**, *225*, 529–537.

[22] A. C. W. Franken, B. C. Lokman, A. F. J. Ram, P. J. Punt, C. A. M. J. J. van den Hondel, S. de Weert, "Heme biosynthesis and its regulation: towards understanding and improvement of heme biosynthesis in filamentous fungi" *Appl Microbiol. Biotechnol.* **2011**, *91*, 447–460.

[23] Y.-W. Lin, "Rational design of metalloenzymes: From single to multiple active sites" *Coord. Chem. Rev.* **2017**, *336*, 1–27.

[24] F. Schwizer, Y. Okamoto, T. Heinisch, Y. Gu, M. M. Pellizzoni, V. Lebrun, R. Reuter, V. Köhler, J. C. Lewis, T. R. Ward, "Artificial Metalloenzymes: Reaction Scope and Optimization Strategies" *Chem. Rev.* **2018**, *118*, 142–231.

[25] K. Oohora, A. Onoda, T. Hayashi, "Hemoproteins Reconstituted with Artificial Metal Complexes as Biohybrid Catalysts" *Acc. Chem. Res.* **2019**, *52*, 945–954.

[26] T. Hayashi, D. Murata, M. Makino, H. Sugimoto, T. Matsuo, H. Sato, Y. Shiro, Y. Hisaeda, "Crystal Structure and Peroxidase Activity of Myoglobin Reconstituted with Iron Porphycene" *Inorg. Chem.* **2006**, *45*, 10530–10536.

[27] K. Oohora, H. Meichin, L. Zhao, M. W. Wolf, A. Nakayama, J. Hasegawa, N. Lehnert, T. Hayashi, "Catalytic Cyclopropanation by Myoglobin Reconstituted with Iron Porphycene: Acceleration of Catalysis due to Rapid Formation of the Carbene Species" *J. Am. Chem. Soc.* **2017**, *139*, 17265–17268.

[28] K. Oohora, Y. Kihira, E. Mizohata, T. Inoue, T. Hayashi, "C(sp^3)–H Bond Hydroxylation Catalyzed by Myoglobin Reconstituted with Manganese Porphycene" *J. Am. Chem. Soc.* **2013**, *135*, 17282–17285.

[29] K. Oohora, H. Meichin, Y. Kihira, H. Sugimoto, Y. Shiro, T. Hayashi, "Manganese(V) Porphycene Complex Responsible for Inert C–H Bond Hydroxylation in a Myoglobin Matrix" *J. Am. Chem. Soc.* **2017**, *139*, 18460–18463.

[30] Z. Liu, J. Huang, Y. Gu, D. S. Clark, A. Mukhopadhyay, J. D. Keasling, J. F. Hartwig, "Assembly and Evolution of Artificial Metalloenzymes within *E. coli* Nissle 1917 for Enantioselective and Site-Selective Functionalization of C─H and C═C Bonds" *J. Am. Chem. Soc.* **2022**, *144*, 883–890.

[31] S. Lange, S. Elangovan, C. Cordes, A. Spannenberg, H. Jiao, H. Junge, S. Bachmann, M. Scalone, C. Topf, K. Junge, M. Beller, "Selective catalytic hydrogenation of nitriles to primary amines using iron pincer complexes" *Catal. Sci. Technol.* **2016**, *6*, 4768–4772.

[32] D. Kim, B. Kang, S. H. Hong, "Ruthenium-catalyzed selective imine synthesis from nitriles and secondary alcohols under hydrogen acceptor- and base-free conditions" *Org. Chem. Front.* **2016**, *3*, 475–479.

[33] F.-E. Essebbar, H. Ben El Ayouchia, H. Anane, S.-E. Stiriba, "Recent Advances in Metal-Based Catalysts for Nitrile Hydration to Amides: Mechanistic Aspects" *The Chemical Record* **2025**, *0*, e202500155.

[34] R. Mouselmani, A. Hachem, A. Alaaeddine, E. Métay, M. Lemaire, "Reduction of aromatic nitriles into aldehydes using calcium hypophosphite and a nickel precursor" *Org. Biomol. Chem.* **2018**, *16*, 6600–6605.

[35] M. Hatano, K. Kuwano, R. Asukai, A. Nagayoshi, H. Hoshihara, T. Hirata, M. Umezawa, S. Tsubaki, T.

Yoshikawa, K. Sakata, “Zinc chloride-catalyzed Grignard addition reaction of aromatic nitriles” *Chem. Sci.* **2024**, *15*, 8569–8577.

[36] C. M. Starks, *Hydrolysis of Nitriles to Carboxylic Acids*, **1970**, US3542822A.

[37] A. Rakshit, H. N. Dhara, A. K. Sahoo, B. K. Patel, “The Renaissance of Organo Nitriles in Organic Synthesis” *Chem. Asian J.* **2022**, *17*, e202200792.

[38] P. Jr. Arthur, D. C. England, B. C. Pratt, G. M. Whitman, “Addition of Hydrogen Cyanide to Unsaturated Compounds” *J. Am. Chem. Soc.* **1954**, *76*, 5364–5367.

[39] R. Chinchilla, A. Baeza, “Hydrocyanation of Non-Activated Alkenes Without Handling HCN” *Eur. J. Org. Chem.* **2024**, *27*, e202400527.

[40] B. N. Bhawal, J. C. Reisenbauer, C. Ehinger, B. Morandi, “Overcoming Selectivity Issues in Reversible Catalysis: A Transfer Hydrocyanation Exhibiting High Kinetic Control” *J. Am. Chem. Soc.* **2020**, *142*, 10914–10920.

[41] X. Fang, P. Yu, B. Morandi, “Catalytic reversible alkene-nitrile interconversion through controllable transfer hydrocyanation” *Science* **2016**, *351*, 832–836.

[42] J. C. Reisenbauer, B. N. Bhawal, N. Jelmini, B. Morandi, “Development of an Operationally Simple, Scalable, and HCN-Free Transfer Hydrocyanation Protocol Using an Air-Stable Nickel Precatalyst” *Org. Process Res. Dev.* **2022**, *26*, 1165–1173.

[43] A. Bhunia, K. Bergander, A. Studer, “Cooperative Palladium/Lewis Acid-Catalyzed Transfer Hydrocyanation of Alkenes and Alkynes Using 1-Methylcyclohexa-2,5-diene-1-carbonitrile” *J. Am. Chem. Soc.* **2018**, *140*, 16353–16359.

[44] N. L. Frye, A. Bhunia, A. Studer, “Nickel-Catalyzed Markovnikov Transfer Hydrocyanation in the Absence of Lewis Acid” *Org. Lett.* **2020**, *22*, 4456–4460.

[45] J. J. D. Idol, *Process for the Manufacture of Acrylonitrile*, **1959**, US2904580A.

[46] A. Martin, V. N. Kalevaru, “Heterogeneously Catalyzed Ammoxidation: A Valuable Tool for One-Step Synthesis of Nitriles” *ChemCatChem* **2010**, *2*, 1504–1522.

[47] H. Zhao, X. Sun, D. Xu, Q. Zhu, Y. Zhu, Z. Dong, “Fe-based *N*-doped dendritic catalysts for catalytic ammoxidation of aromatic aldehydes to aromatic nitriles” *J. Colloid Interf. Sci.* **2020**, *565*, 177–185.

[48] J. Vilím, T. Knaus, F. G. Mutti, “Catalytic Promiscuity of Galactose Oxidase: A Mild Synthesis of Nitriles from Alcohols, Air, and Ammonia” *Angew. Chem. Int. Ed.* **2018**, *57*, 14240–14244.

[49] R. V. Jagadeesh, H. Junge, M. Beller, “‘Nanorust’-catalyzed Benign Oxidation of Amines for Selective Synthesis of Nitriles” *ChemSusChem* **2015**, *8*, 92–96.

[50] Z. Qi, C. Hu, Y. Zhong, C. Cai, G.-P. Lu, “The ammoxidation of alcohols over heterogeneous catalysts for the green synthesis of nitriles” *Org. Chem. Front.* **2021**, *8*, 3137–3149.

[51] D. T. Mowry, “The Preparation of Nitriles.” *Chem. Rev.* **1948**, *42*, 189–283.

[52] L. Yu, H. Li, X. Zhang, J. Ye, J. Liu, Q. Xu, M. Lautens, “Organoselenium-Catalyzed Mild Dehydration of Aldoximes: An Unexpected Practical Method for Organonitrile Synthesis” *Org. Lett.* **2014**, *16*, 1346–1349.

[53] X. Zhang, J. Sun, Y. Ding, L. Yu, “Dehydration of Aldoximes Using PhSe(O)OH as the Pre-Catalyst in Air” *Org. Lett.* **2015**, *17*, 5840–5842.

[54] R. Ding, Y. Liu, M. Han, W. Jiao, J. Li, H. Tian, B. Sun, "Synthesis of Nitriles from Primary Amides or Aldoximes under Conditions of a Catalytic Swern Oxidation" *J. Org. Chem.* **2018**, *83*, 12939–12944.

[55] Y. Asano, Y. Kato, "Z-phenylacetaldoxime degradation by a novel aldoxime dehydratase from Bacillus sp. strain OxB-1" *FEMS Microbiol. Lett.* **1998**, *158*, 185–190.

[56] H. Sawai, H. Sugimoto, Y. Kato, Y. Asano, Y. Shiro, S. Aono, "X-ray Crystal Structure of Michaelis Complex of Aldoxime Dehydratase" *J. Biol. Chem.* **2009**, *284*, 32089–32096.

[57] T. Betke, J. Higuchi, P. Rommelmann, K. Oike, T. Nomura, Y. Kato, Y. Asano, H. Gröger, "Biocatalytic Synthesis of Nitriles through Dehydration of Aldoximes: The Substrate Scope of Aldoxime Dehydratases" *ChemBioChem* **2018**, *19*, 768–779.

[58] A. Hinzmann, T. Betke, Y. Asano, H. Gröger, "Synthetic Processes toward Nitriles without the Use of Cyanide: A Biocatalytic Concept Based on Dehydration of Aldoximes in Water" *Chem. Eur. J.* **2021**, *27*, 5313–5321.

[59] J. Nomura, H. Hashimoto, T. Ohta, Y. Hashimoto, K. Wada, Y. Naruta, K.-I. Oinuma, M. Kobayashi, "Crystal structure of aldoxime dehydratase and its catalytic mechanism involved in carbon-nitrogen triple-bond synthesis" *Proc. Nat. Acad. Sci. USA* **2013**, *110*, 2810–2815.

[60] K. Konishi, T. Ohta, K.-I. Oinuma, Y. Hashimoto, T. Kitagawa, M. Kobayashi, "Discovery of a reaction intermediate of aliphatic aldoxime dehydratase involving heme as an active center" *Proc. Nat. Acad. Sci. USA* **2006**, *103*, 564–568.

Chapter 1
Reconstituted Myoglobin with Iron Porphycene Catalyzes Aldoxime Dehydration with a Broad Substrate Scope

Reproduced in part with permission from [*ACS Catal.,* **2024**, *14,* 13081-13087.]
DOI: 10.1021/acscatal.4c03220

1-1. Introduction

Biocatalytic dehydration of aldoximes is a practical synthetic method for obtaining a variety of nitrile-containing compounds[1-4], offering a valuable alternative to conventional nitrile synthesis methods such as ammoxidation and hydrocyanation, which often require harsh conditions, toxic cyanide sources, or precious metal catalysts[5]. The biocatalytic reaction proceeds under mild conditions and avoids the use of hazardous reagents, making it attractive from both sustainability and safety perspectives[6-8]. However, aldoxime dehydratase[9], the natural enzyme responsible for this nitrile-forming reaction, sometimes loses its strong catalytic activity toward non-natural substrates with different chemical structures[3]. In particular, aldoxime substrates for the synthesis of pharmaceutically relevant product class of chiral α-amino nitriles, which serve as valuable intermediates for important drugs such as Vildagliptin[10-12] and Saxagliptin[13,14], gave negligible conversions when using natural aldoxime dehydratases[15]. Furthermore, less reactive *O*-alkyl aldoximes are not accepted as substrates at all[16]. To overcome this intrinsic limitation of natural enzymes and to expand the substrate scope of biocatalytic nitrile synthesis, the author sought to develop an artificial metalloenzyme capable of catalyzing aldoxime dehydration.

Artificial metalloenzymes using myoglobin as a protein scaffold are among the most well-studied classes of artificial metalloenzymes[17-23]. Since the myoglobin scaffold provides a promiscuous enzyme active site which can accommodate a wide range of substrates, myoglobin-based artificial metalloenzymes have been extensively utilized for various chemical transformations, such as NO reduction[24,25], CO_2 reduction[26], peroxidation[27-30], sulfoxidation[31-34], alkane hydroxylation[35-37], cyclopropanation[38-42], carbene insertion[43-45], and nitrene insertion[46,47]. These studies demonstrate that the reactivity of the metal center can be systematically tuned through cofactor engineering, enabling catalytic functions that are inaccessible to native heme enzymes. Through these studies, the author found that myoglobin reconstituted with an iron porphycene FePc (designated rMb(FePc)) has a great potential for use as an artificial metalloenzyme (Fig. 1-1b)[48]. Owing to the distinct electronic structure of the iron center imparted by the porphycene ligand, rMb(FePc) forms a stable Fe–O_2 complex [28,49,50] and efficiently promote the generation of Fe–carbene[39]/nitrene[47] intermediates.

Considering these unique catalytic properties of the FePc cofactor in combination with the versatile myoglobin scaffold, the author reasoned that rMb(FePc) could serve as an effective catalyst for aldoxime dehydration. Enzymatic aldoxime dehydration was proposed to proceed via a stepwise mechanism involving the steps of (i) inner

sphere electron transfer to promote the elimination of OH group and (ii) deprotonation to produce a nitrile[51]. Although native myoglobin with heme *b* does not have aldoxime dehydration activity, the author hypothesized that the distinct electronic structure of rMb(FePc) could promote this reaction. In particular, the lower Fe^{3+}/Fe^{2+} redox potential of rMb(FePc) (−193 mV vs NHE), compared to that of native myoglobin (+52 mV vs NHE)[49], is expected to enhance the inner-sphere electron-transfer step, thereby facilitating aldoxime dehydration (Fig. 1-1c). In addition to cofactor effects, the protein environment may also contribute to catalysis. rMb(FePc) has a histidine residue at distal position of the heme pocket(Fig. 1-1d,e). This distal histidine may function as a general acid-base catalyst, as it does in the mechanism of natural aldoxime dehydratases[51,52]. Based on these considerations, this study aims to establish a myoglobin-based artificial metalloenzyme for aldoxime dehydration by exploiting the electronic properties of a non-native cofactor within the myoglobin scaffold (Fig. 1-1f).

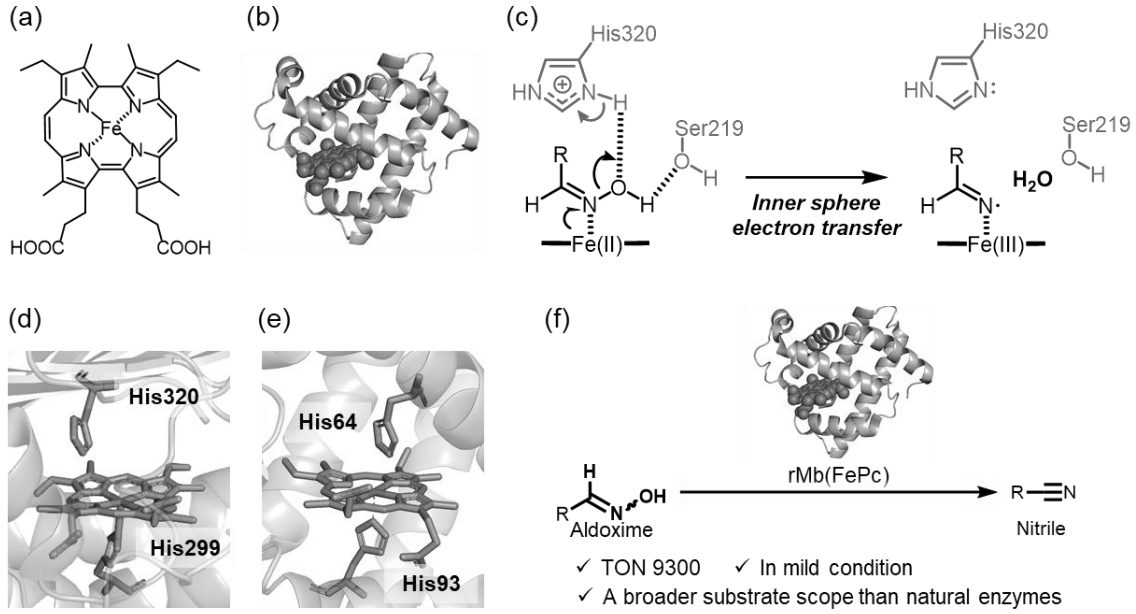


Figure 1-1. (a) Chemical structures of heme *b* and artificial cofactors. (b) Schematic representation of the reconstitution of myoglobin with an artificial cofactor. (c) The plausible reaction intermediate of Oxd. (d) Active site of Oxd (PDB: 3A15). (e) Active site of myoglobin. (f) Aldoxime dehydration using rMb(FePc) in this study.

1-2. Results and discussion

Aldoxime dehydration catalyzed by rMb(FePc)

Based on the hypothesis above, the author first tested the dehydration of butyraldehyde oxime (**1a**) as a model reaction for the rMb(FePc) catalyst. The reaction was performed in the reduced ferrous state with 0.02 mol% catalyst loading. Notably, rMb(FePc) exhibited excellent catalytic activity toward the dehydration of aldoxime **1a** under ambient temperature and neutral pH conditions (Fig. 1-2). Although a mixture of stereoisomers was used for the catalysis, both (*E*)- and (*Z*)-aldoximes were consumed rapidly. After 8 hours of reaction time, the target butyronitrile (**2a**) was obtained in 68% yield and the total turnover number (TON) of the catalyst reached 3400 (entry 1 in Table 1-1). Higher substrate loading has led to an increase in TON, although the product yields have decreased due to poor solubility of the substrate (Table 1-2). In contrast, the dehydration reaction does not proceed in the absence of rMb(FePc) (Table 1-1, entry 2). Little or no nitrile products are produced by native myoglobin with heme *b* or the FePc complex alone (entries 3 and 4 in Table 1-1). These results clearly indicate that both FePc and the secondary coordination sphere of myoglobin cooperatively contribute to the catalytic activity of rMb(FePc). Moreover, mutation of the distal His64 residue was found to significantly reduce the catalytic activity (entries 5 and 6 in Table 1-1). As the author envisioned, the distal histidine residue at the active site was suggested to be actively involved in the reaction mechanism as a general acid-base catalyst, similar to the mechanism of natural aldoxime dehydratases (Fig.1-1c)[51,52].

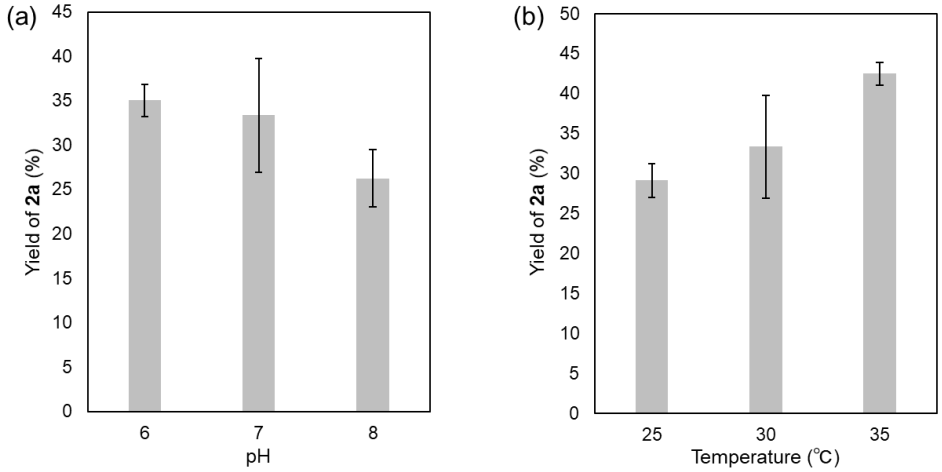
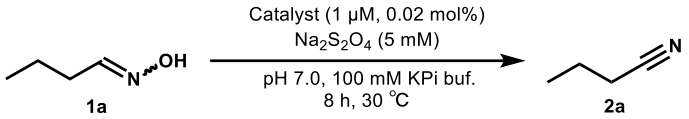


Figure 1-2. (a) pH dependency and (b) temperature dependency of the aldoxime dehydration (**1a**→**2a**) catalyzed by rMb(FePc). Reaction condition: rMb(FePc) (1.0 μM, 0.02 mol%), aldoxime **1a** (5.0 mM), $Na_2S_2O_4$ (5.0 mM) in KPi buffer (100 mM KPi, pH 6.0–8.0), 6h, 25–35 °C.

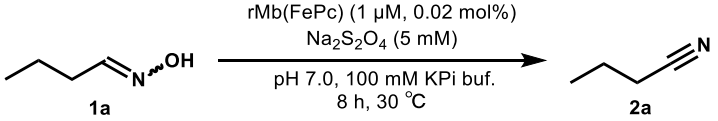
Table 1-1. Evaluation of aldoxime dehydration [a]



Entry	Catalyst	Yield (%)[b]	TON[b]
1	rMb(FePc)	68	3400
2	none	n.d.	–
3	native myoglobin	n.d.	–
4	FePc complex[c]	5	25
5	rMb^{H64A}(FePc)	3	150
6	rMb^{H64D}(FePc)	21	1100

[a] Conditions: [catalyst] = 1 μM or [FePc] = 10 μM, [**1a**] = 5 mM, [$Na_2S_2O_4$] = 5 mM in 100 mM potassium phosphate buffer (pH 7.0) at 30 °C for 8 h under a N_2 atmosphere. [b] Determined by GC-FID. [c] FePc complex (10 μM), dissolved in DMF, was added as catalyst.

Table 1-2. Dehydration of butyraldehyde oxime (**1a**) catalyzed by rMb(FePc) with increased substrate loading[a]



Entry	**1a** (mM)	Yield (%)[b]	TON[b]
1	5.0	68	3400
2	50	12	5800
3	100	5	5000

[a] Conditions: [rMb(FePc)] = 1 μM, [**1a**] = 5 mM, [$Na_2S_2O_4$] = 5 mM in 100 mM potassium phosphate buffer (pH 7.0) at 30 °C for 8 h under N_2 atmosphere. [b] Determined by GC-FID.

Investigation of substrate scope

With these promising results, the author next investigated the substrate scope of the aldoxime dehydration using rMb(FePc) as a catalyst (Fig. 1-3). The product yields were increased as the reaction time was extended to 24 hours. Butyronitrile (**2a**) and other alkyl nitriles **2b**–**2d** were obtained quantitatively in excellent yields from the corresponding aldoximes. Surprisingly, the total TON has reached 9300 in the case of isovaleronitrile (**2d**). rMb(FePc) also tolerates bulky substitutions at the α-position of aldoximes. Phenylacetaldoxime (**1e**), an original substrate of natural aldoxime dehydratases[9,53], was efficiently converted into phenylacetonitrile (**2e**) in 84% yield. Secondary and tertiary nitriles **2f**–**2h** were also formed by rMb(FePc) in high or moderate yields. In contrast,

rMb(FePc) showed decreased catalytic activities toward benzaldehyde oxime and its analogues **1i**–**1l**. This may be due to steric hindrance between the aromatic rings and the porphyrin ligand in the active site, which was also observed in the catalysis of natural aldoxime dehydratases[3]. Interestingly, the 2-isoxazoline derivative **1m** undergoes a ring opening reaction to form α-hydroxynitrile, and followed by formation of 4-chloro-3-hydroxybutyronitrile (**2m**) in 60% yield. Although **2m**, and also **2f**, having chiral centers were obtained as racemic mixture after 24 h, modest enantioenrichment of the products was observed at the early-stage of the reaction, implying the possibility of rMb(FePc) for the kinetic resolution (Fig. 1-4, 1-5). Furthermore, rMb(FePc) exhibits a high activity toward *N*-Boc-D-α-aminoaldoximes which are known to be inactive in the catalysis of natural aldoxime dehydratases[15]. The corresponding chiral α-aminonitriles **2n** and **2o**, which are pharmaceutically relevant compounds for drug synthesis, are obtained in 54% and 16% yields, respectively, retaining the stereocenters at the α-carbon of aminonitriles during the catalysis (Fig. 1-6).

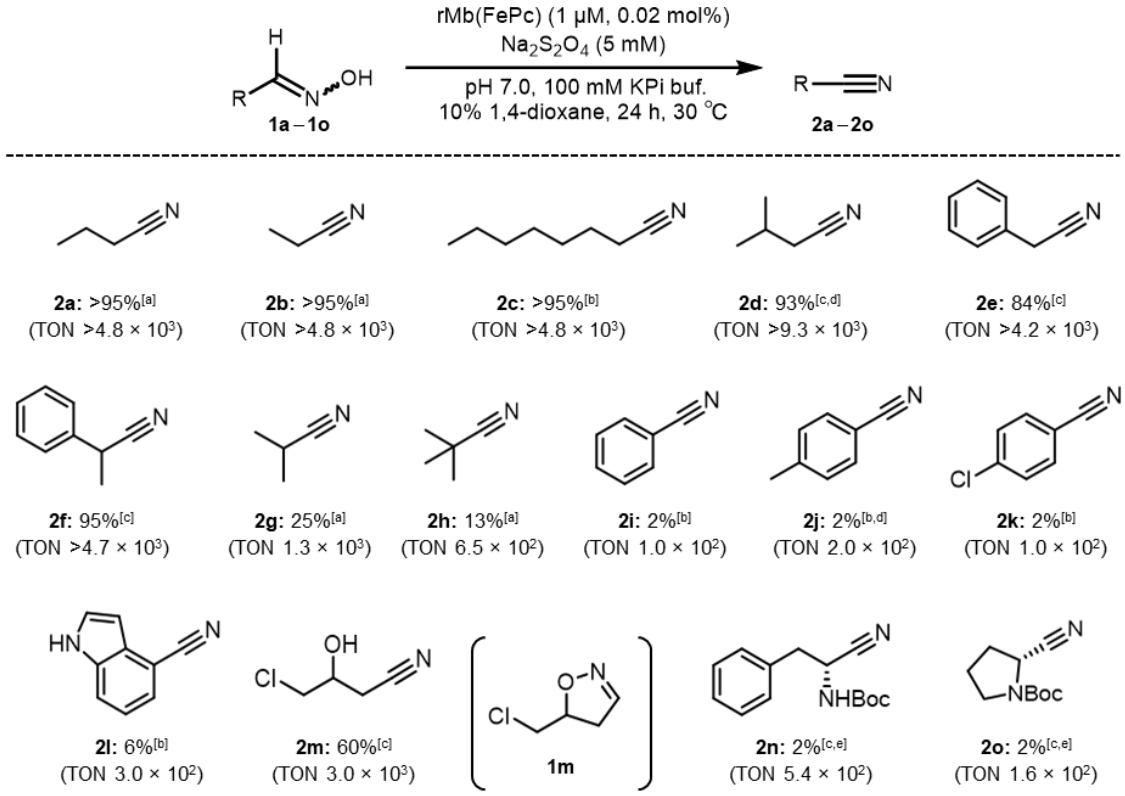


Figure 1-3. Substrate scope for aldoxime dehydration catalyzed by rMb(FePc). Conditions: [rMb(FePc)] = 1 μM, [aldoxime] = 5 mM, [$Na_2S_2O_4$] = 5 mM in 100 mM potassium phosphate buffer (pH 7.0) at 30 °C for 24 h under N_2 atmosphere. The product yields were determined by GC-FID.
[a] Determined by ^{1}H NMR. [b] DMF (10 v/v%) was added as cosolvent. [c]1,4-dioxane (10 v/v%) was added as cosolvent. [d] Aldoxime (10 mM). [e] rMb(FePc) (5.0 μM, 0.10 mol%).

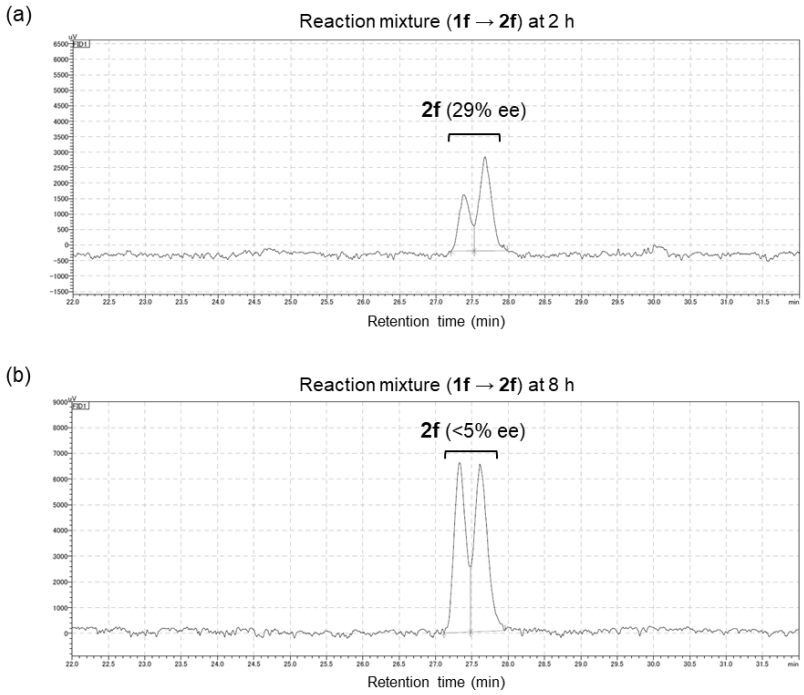


Figure 1-4. GC-FID chromatograms for the dehydration of **1f** promoted by rMb(FePc). Racemic aldoxime **1f** was used for the reaction. The reaction mixture was analyzed by GC-FID after incubation for (a) 2 hours and (b) 8 hours. Conditions: [rMb(FePc)] = 1 μM, [aldoxime] = 5 mM, [$Na_2S_2O_4$] = 5 mM in 100 mM potassium phosphate buffer (pH 7.0) containing 1,4-dioxane (10 v/v%) at 30 °C for 24 h under N_2 atmosphere.

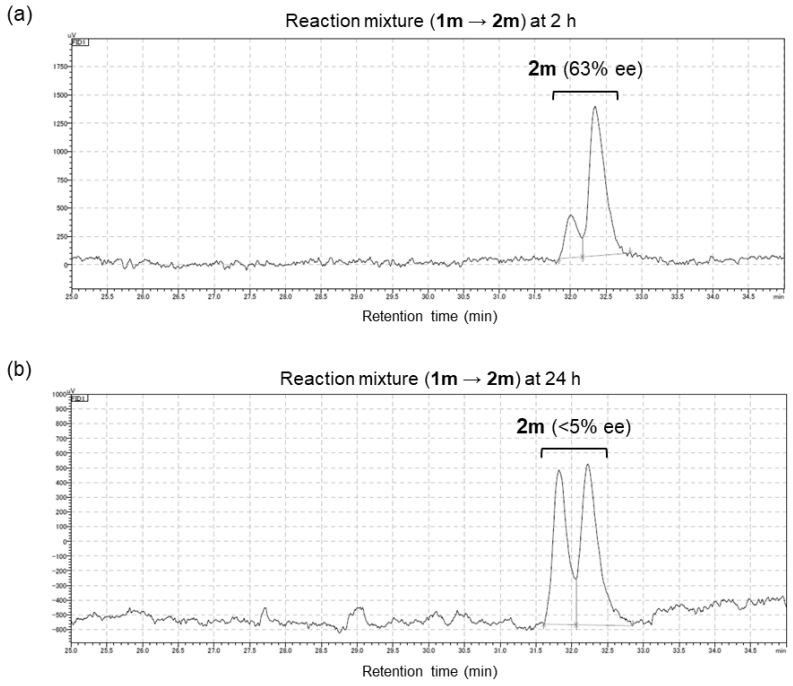


Figure 1-5. GC-FID chromatograms for the dehydration of **1m** promoted by rMb(FePc). Racemic aldoxime **1m** was used for the reaction. The reaction mixture was analyzed by GC-FID after incubation for (a) 2 hours and (b) 24 hours. Reaction conditions: rMb(FePc) (1.0 μM, 0.02 mol%), aldoxime **1m** (5.0 mM), $Na_2S_2O_4$ (5.0 mM) in KPi buffer (100 mM KPi, pH 7.0) containing 1,4-dioxane (10 v/v%), 30 °C.

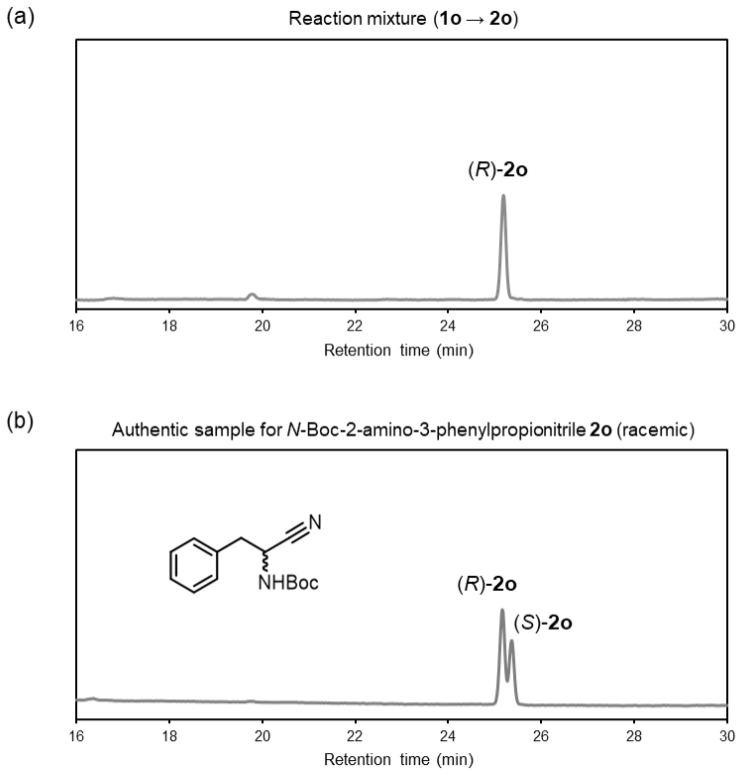


Figure 1-6. (a) GC-FID chromatogram for the reaction mixture of aldoxime dehydration (**1o→2o**) catalyzed by rMb(FePc). Enantiopure *N*-Boc-D-phenylalaninal oxime (**1o**) was used as a substrate for the dehydration reaction. Conditions: [rMb(FePc)] = 1 μM, [aldoxime] = 5 mM, [$Na_2S_2O_4$] = 5 mM in 100 mM potassium phosphate buffer (pH 7.0) containing 1,4-dioxane (10 v/v%) at 30 °C for 24 h under N_2 atmosphere. The reaction mixture was analyzed by GC-FID equipped with a SUPELCO Beta DEXTM 120 fused silica capillary column. (b) GC-FID chromatogram for the authentic samples of *N*-Boc-2-amino-3-phenylpropionitrile (**2o**).

Expanded substrate scope of rMb(FePc) compared with Oxd

To further evaluate the advantages of the artificial metalloenzyme systems presented here, the author next performed comparative experiments between rMb(FePc) and natural aldoxime dehydratase enzymes. Aldoxime dehydratase from *Rhodococcus erythropolis* PR4 (ReOxd), one of the most active and well-studied enzymes, was recombinantly prepared for the comparative experiments[53,54]. ReOxd exhibits extremely high catalytic activity toward dehydration of phenylacetaldoxime (**1e**) which is an original substrate of ReOxd in nature (Fig. 1-7)[53]. The Michelis-Menten kinetics revealed that k_{cat} value of the natural enzyme is 2800 times higher than that of rMb(FePc), while K_M values are comparable (Fig. 1-8). However, the catalytic performance of ReOxd clearly depends on the chemical structures of substrates. Particularly, as shown next, the artificial metalloenzyme showed higher catalytic activity than ReOxd for several aldoximes that differ from the natural substrate. For example, rMb(FePc) exhibits a two-fold faster initial ratio for the dehydration of *N*-Boc-α-aminoaldoximes **1n** and **1o** affording the pharmaceutically relevant chiral α-aminonitriles in higher yields (Fig. 1-9). These results clearly demonstrate the versatility of the catalytic systems using the artificial metalloenzyme.

Moreover, rMb(FePc) was found to show versatile catalytic activities toward *O*-alkyl aldoximes **3e**–**6e**

which are not accepted by the natural enzymes (Fig. 1-10)[16]. rMb(FePc) efficiently produces the corresponding nitriles through the elimination of methanol, ethanol, allyl alcohol, and benzyl alcohol, respectively. Accumulation of the eliminated alcohol was also confirmed by GC-MS analysis (Fig. 1-11). Moreover, it should be noted that total TONs of the rMb(FePc)-catalyzed dealcoholization of **3e**, **5e**, and **6e** exceed 450 within 24 hours (Fig. 1-10, black), while the natural enzyme ReOxd had little or no catalytic activity for these *O*-alkyl aldoximes (Fig. 1-10, gray). These sharply different results highlight the catalytic potential of the iron porphycene cofactor within the myoglobin scaffold.

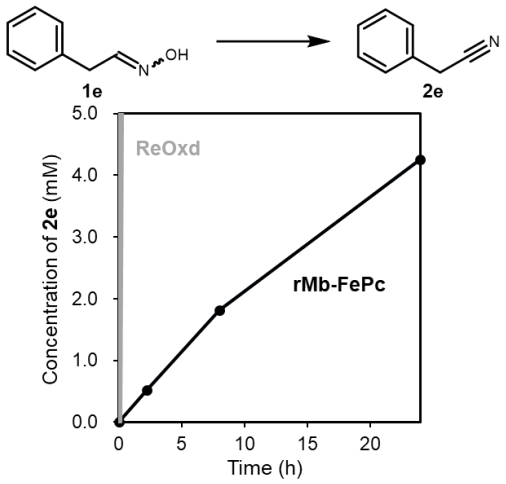


Figure 1-7. Time course for the formation of phenylacetonitrile (**2e**) catalyzed by rMb(FePc) (black) and ReOxd (gray). Catalytic reaction of ReOxd was completed within 10 minutes. Conditions: [rMb(FePc)] = 1 μM, [aldoxime] = 5 mM, [$Na_2S_2O_4$] = 5 mM in 100 mM potassium phosphate buffer (pH 7.0) containing 1,4-dioxane (10 v/v%) at 30 °C for 24 h under N_2 atmosphere. The product yields were determined by GC-FID.

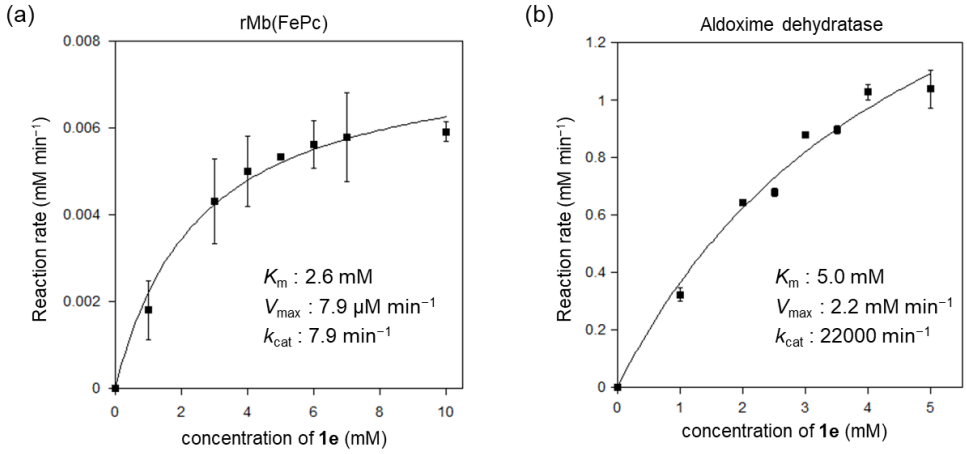


Figure 1-8. Michaelis-Menten plots for (a) rMb(FePc) and (b) aldoxime dehydratese with various concentration of aldoxime **1e**. Aldoxime dehydratase from *Pseudomonas chlororaphis* was used instead of ReOxd due to the low stability of ReOxd. Conditions: [rMb(FePc)] = 1 μM or [rMb(FePc)] = 0.1 μM, aldoxime **1e** (1–10 mM), $Na_2S_2O_4$ (5.0 mM) in KPi buffer (100 mM KPi, pH 7.0) containing 1,4-dioxane (10 v/v%) for rMb(FePc) or DMSO (5 v/v%) for aldoxime dehydratase at 30 °C under N_2 atmosphere..

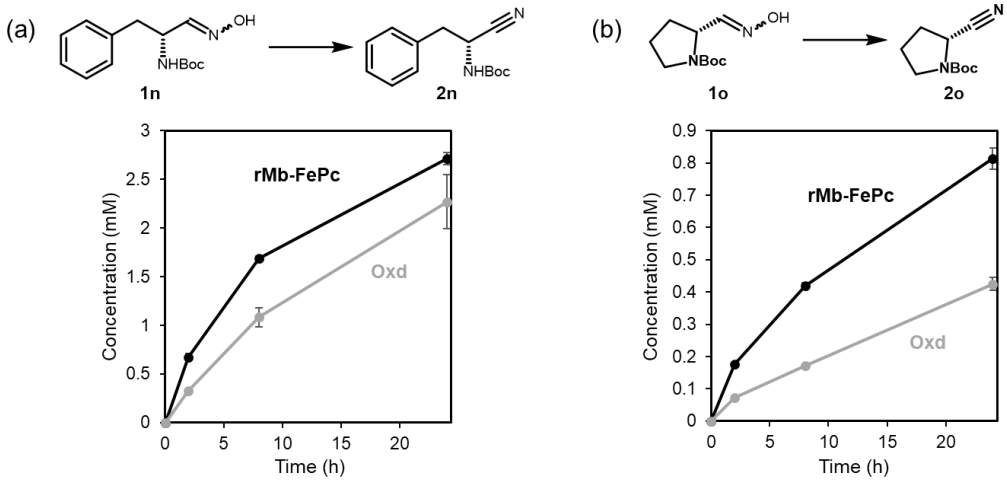


Figure 1-9. Time courses for the formation of (a) (*R*)-(*N*-Boc-2-amino)-3-phenylpropionitrile (**2n**) and (b) (*R*)-*N*-Boc-2-cyanopyrrolidine (**2o**) catalyzed by rMb(FePc) (black) and ReOxd (gray). Conditions: [rMb(FePc)] = 5 μM, [aldoxime] = 5 mM, [$Na_2S_2O_4$] = 5 mM in 100 mM potassium phosphate buffer (pH 7.0) containing 1,4-dioxane (10 v/v%) at 30 °C for 24 h under N_2 atmosphere. The product yields were determined by GC-FID.

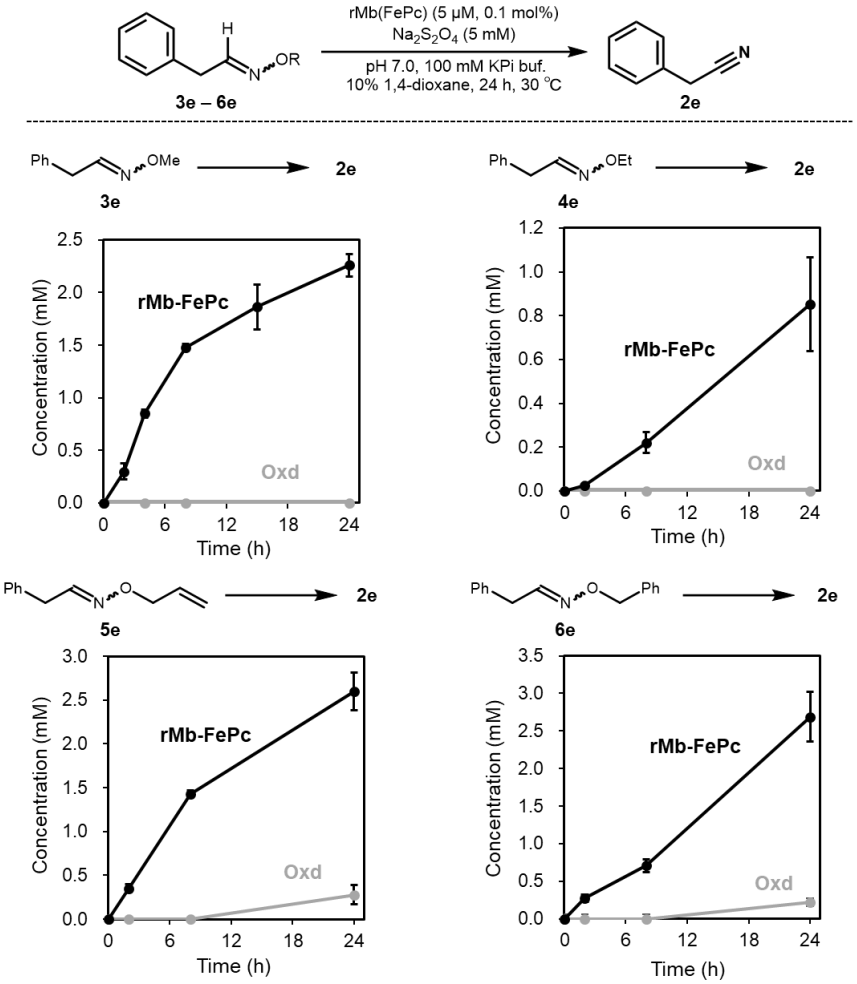


Figure 1-10. Dealcoholization of *O*-alkyl aldoximes **3e**–**6e** catalyzed by rMb(FePc) (black) and ReOxd (gray). Conditions: [catalyst] = 5 μM, [aldoxime] = 5 mM, [$Na_2S_2O_4$] = 5 mM in 100 mM potassium phosphate buffer (pH 7.0) containing 1,4-dioxane (10 v/v%) at 30 °C for 24 h under N_2 atmosphere. The product yields were determined by GC-FID.

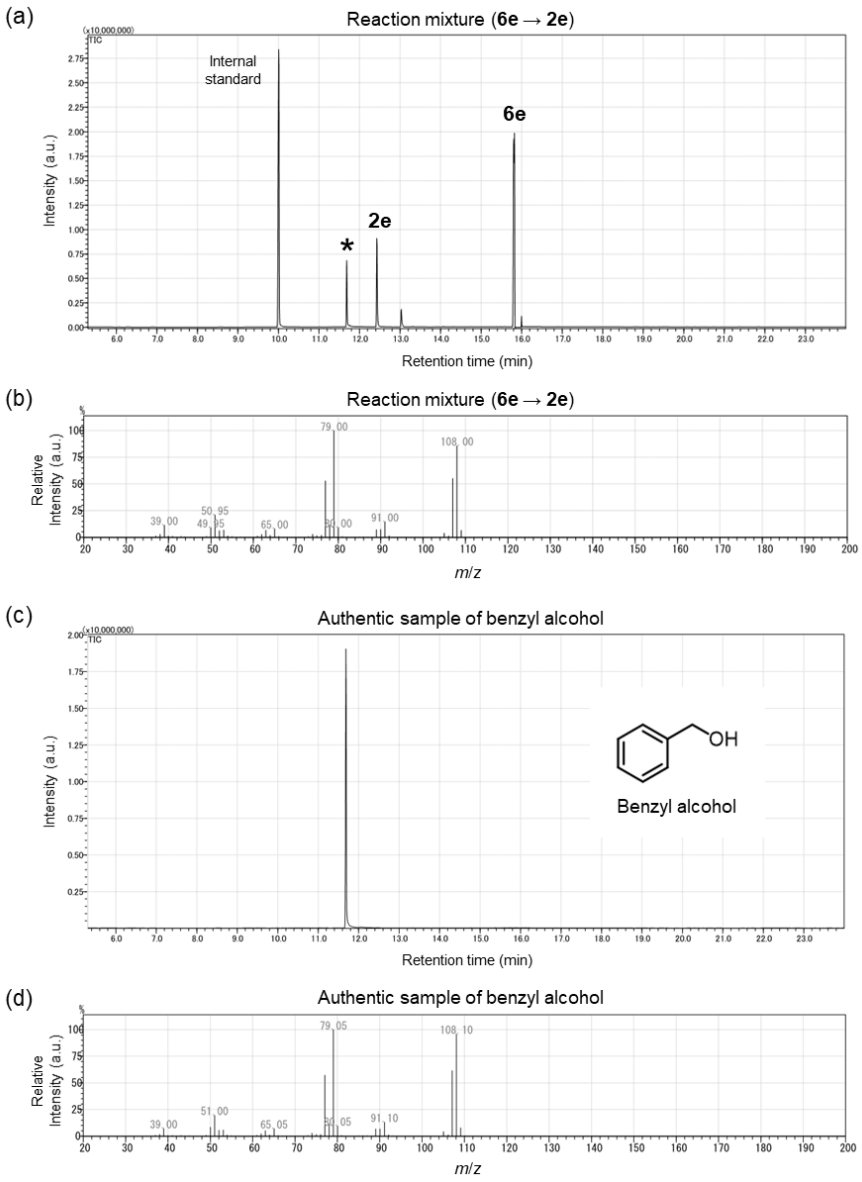


Figure 1-11. (a) GC-MS chromatogram for the reaction mixture of **6e** dealcoholization catalyzed by rMb(FePc) (total ion chromatogram). Cyclohexanol was added as an internal standard. The peak of benzyl alcohol was indicated with asterisk (retention time: 11.7 min). (b) Mass spectrum of the peak at 11.7 min for the analysis of the reaction mixture. (c) GC-MS chromatogram for the authentic sample of benzyl alcohol (total ion chromatogram). (d) Mass spectrum of the peak at 11.7 min for the analysis of the authentic sample.

Brønsted plot analysis

To further investigate the catalytic properties of rMb(FePc), Brønsted plot analysis was conducted using aldoxime **1e**, *O*-alkyl aldoximes **3e**–**6e**, and *O*-acetyl aldoxime **7e** as substrates. The plots for the rMb-FePc catalysis reveal a linear correlation between the reaction rates and pK_a values of the leaving groups (Fig.1-12a). This analysis clearly indicates that the rate-limiting HO/RO elimination step proceeds through the same reaction mechanism in the catalysis of rMb(FePc) even though the leaving groups are different. In contrast, the Brønsted plots for catalysis of ReOxd did not exhibit a clear correlation (Fig. 1-12b). In particular, the reaction rate for aldoxime **1e** dehydration

largely deviates from the plots for the other *O*-substituted substrates. This may be explained by the formation of a low-barrier hydrogen bond (LBHB) with the substrate, which is required for the catalysis of natural aldoxime dehydratases.[51] In fact, ReOxd possesses a conserved serine residue at the distal position of heme, and this serine residue is known to form an LBHB with the HO group of aldoximes to enhance the elimination rate of a water molecule (Fig. 1-13). In the case of *O*-substituted aldoximes **3e**–**8e**, the corresponding LBHB cannot be formed in the active site and therefore, the extremely high catalytic activity of ReOxd is considered to be specific for the *O*-unsubstituted aldoxime **1e**.

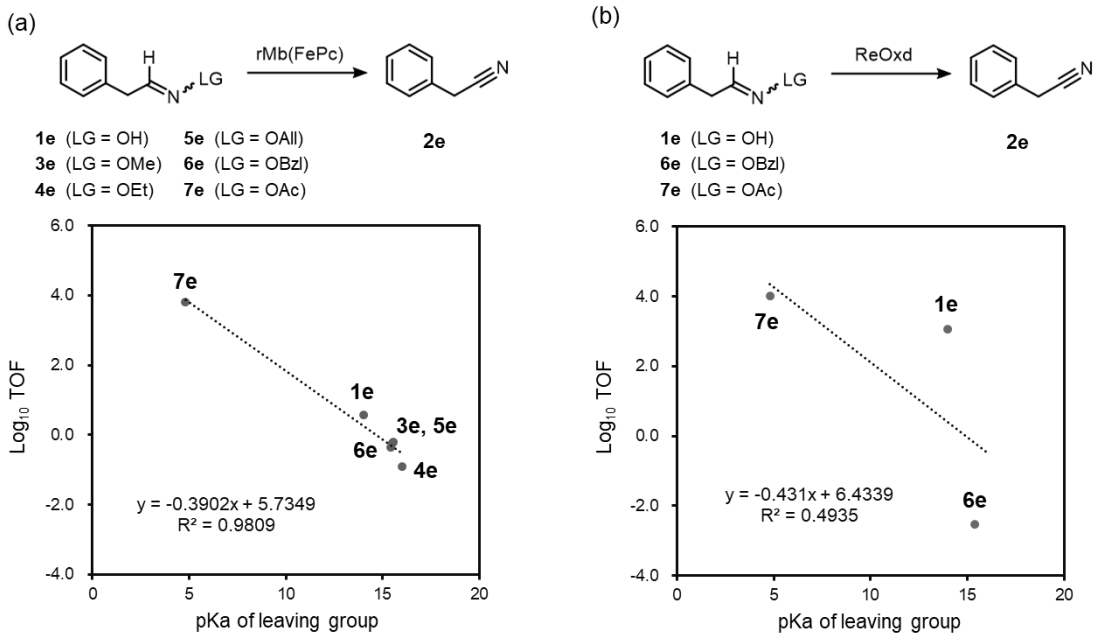


Figure 1-12. The Brønsted-type plots for the nitrile **2e** formation catalyzed by (a) rMb(FePc) and (b) ReOxd. The Log_{10} values of TOF (min^{-1}) for the reaction were plotted against pK_a values of the substrate leaving groups (LG). The pK_a values of water (= 14.0), MeOH (= 15.5), EtOH (= 16.0), allyl alcohol (= 15.5), benzyl alcohol (= 15.4), and AcOH (= 4.8) were used for the plots of **1e**, **3e**, **4e**, **5e**, **6e**, and **7e**, respectively.

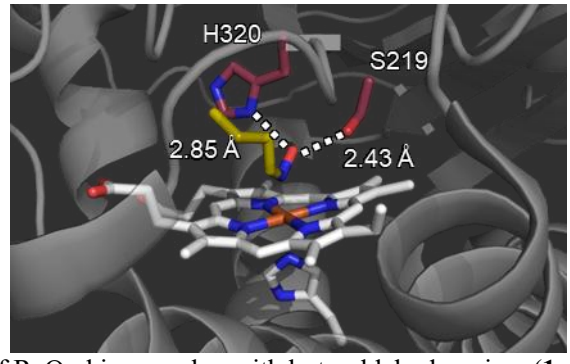


Figure 1-13. Crystal structure of ReOxd in complex with butyraldehyde oxime (**1a**) (PDB: 3A17).

Mechanistic insights: radical trapping and kinetic isotope effect studies

To gain insight into the underlying reaction mechanism, the author next examined whether the reaction proceeds via radical intermediates. Previous studies on native aldoxime dehydratases have proposed a mechanism involving Fe(III)–iminyl radical species (Fig. 1-1c)[51]. To test this hypothesis in my artificial metalloenzyme system, radical trapping experiments were performed using TEMPOL in the presence of 2-phenylcyclobutanone oxime (**1***) as a substrate. Under standard rMb(FePc) catalytic conditions, LC–MS analysis revealed the formation of the corresponding TEMPOL adduct (**2***) (Fig. 1-14). The detection of this adduct provides direct experimental evidence for the involvement of radical intermediates during the catalytic dehydration process.

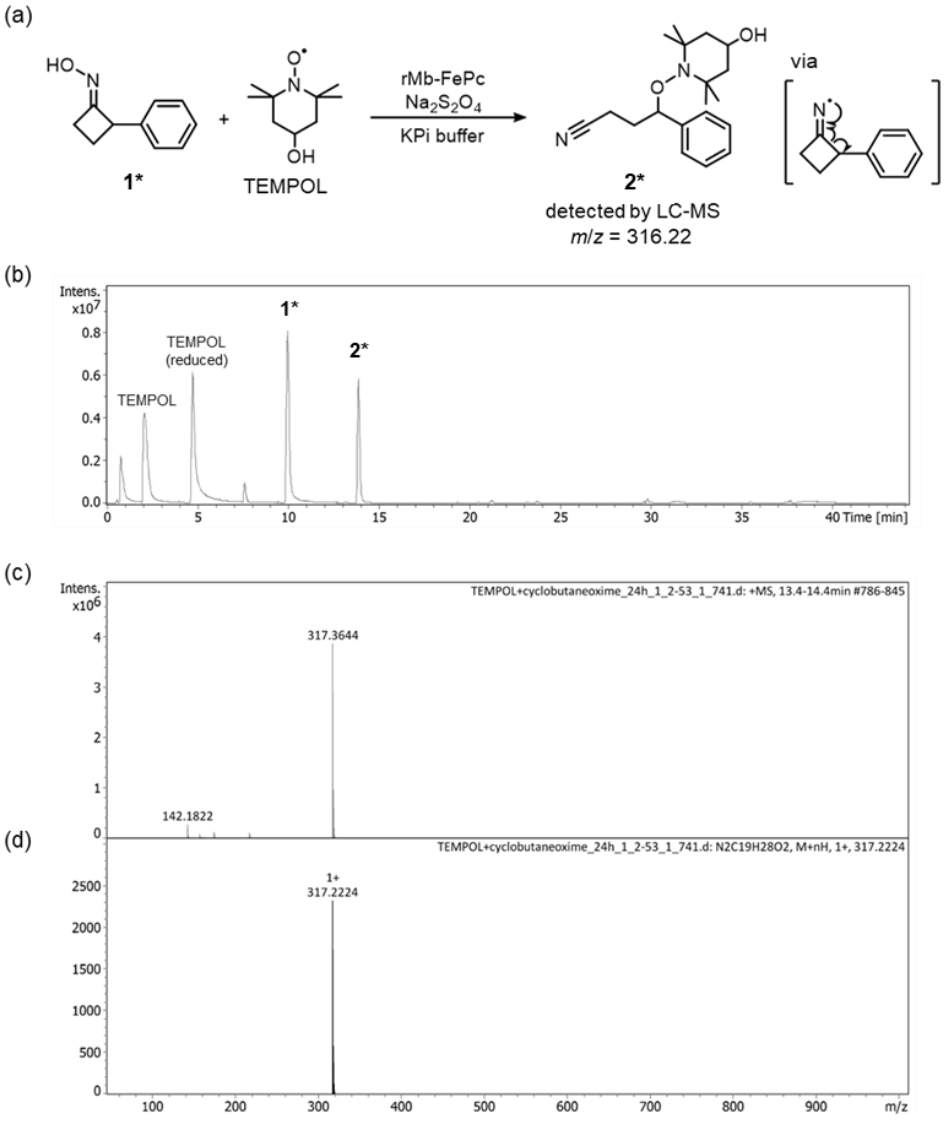


Figure 1-14. (a) Radical trapping experiment with TEMPOL using 2-phenyl cyclobutanone oxime (**1***) as a substrate. Conditions: [rMb(FePc)] = 5 μM, [**1***] = 5 mM, [TEMPOL] = 25 mM, [$Na_2S_2O_4$] = 5 mM in 100 mM potassium phosphate buffer (pH 7.0) containing 1,4-dioxane (10 v/v%) at 30 °C for 24 h under N_2 atmosphere. (b) LC-MS chromatogram for the radical trapping experiment (total ion chromatogram). The peak of TEMPOL adduct **2*** was indicated with asterisk (retention time: 13.8 min). (b) Mass spectrum of the peak at 13.4–14.4 min for the LC-MS analysis. (c) Simulated mass spectrum for the TEMPOL adduct. *m/z* calcd. for $N_2C_{19}H_{28}O_2$ $[M + H]^+$ 317.222, found 317.634.

To further elucidate the nature of the rate-determining step, kinetic isotope effect (KIE) experiments were performed for both rMb(FePc) and PcOxd. In these experiments, the time-course formation of the corresponding nitrile product was monitored using either the non-deuterated aldoxime (Fig. 1-15, gray) or the α-deuterated aldoxime (Fig. 1-15, black) as the substrate. As evident from the kinetic profiles, no discernible difference in the initial reaction rates was observed between the non-deuterated and α-deuterated substrates in either catalytic system. This lack of a detectable kinetic isotope effect indicates that α-C–H bond cleavage is not involved in the rate-determining step of the dehydration reaction in both the artificial metalloenzyme and the native enzyme.

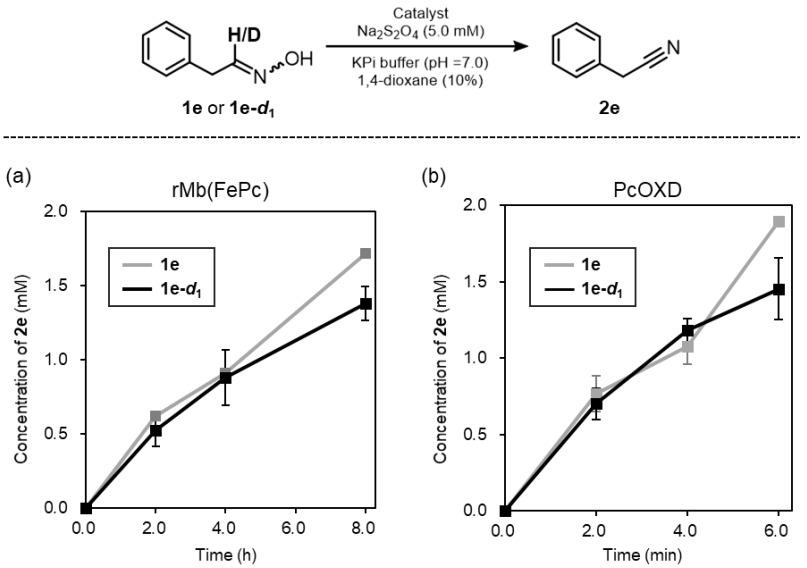
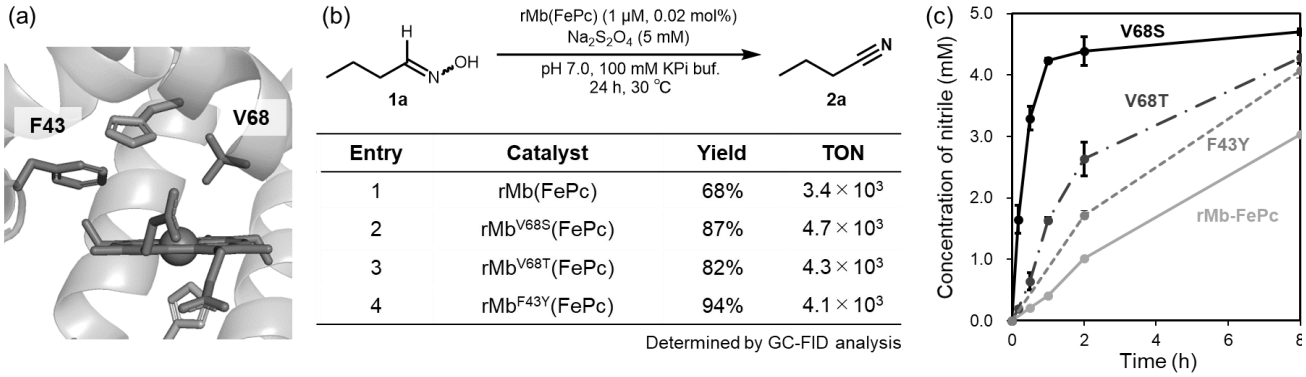


Figure 1-15. KIE studies using (a) rMb(FePc) and (b)PcOxd. Conditions: [rMb(FePc)] = 1 μM or [PcOxd] = 0.1 μM, [aldoxime] = 5 mM, [$Na_2S_2O_4$] = 5 mM at rMb(FePc) and 1 mM at PcOxd, in 100 mM potassium phosphate buffer (pH 7.0) containing 1,4-dioxane (10 v/v%) at 30 °C for 8 h under N_2 atmosphere.

Mechanism-inspired active site engineering of rMb(FePc) for aldoxime dehydration

Inspired by this catalytic mechanism of the natural aldoxime dehydratase, site-directed mutagenesis was next conducted to provide structures for the enzyme-like LBHB interactions in the active site of rMb(FePc) (Fig. 1-16). The author prepared rMb^{V68S}(FePc), rMb^{V68T}(FePc), and rMb^{F43Y}(FePc) variants in which a serine, threonine, or tyrosine residue was incorporated at the distal position adjacent to the His64 residue (Fig. 1-17, 1-18). Notably, these rMb(FePc) variants, especially the V68S variant, show enhanced catalytic activity toward the dehydration of aldoxime **1a** (entries 2 and 3 in Fig. 1-16b). The dehydration reaction is generally complete within 1 hour, and the turnover frequency (TOF) of rMb^{V68S}(FePc) reaches 165 min^{-1} which is 24-fold higher than that of rMb(FePc) without mutation (Fig. 1-16c). These results clearly support the contribution of the distal serine residue to catalytic activity of the artificial metalloenzymes. In contrast, rMb^{V68S}(FePc) exhibits lower catalytic activity for the dealcoholization reaction of *O*-methyl aldoxime **3a** compared to original rMb(FePc) (Fig. 1-19). Since *O*-methyl aldoxime **3a** does not have a protic hydroxyl group capable of forming an LBHB with the Ser68 residue, the V68S mutation does not enhance the dealcoholization activity of the variant, and this observation is consistent with the results for the natural aldoxime dehydratase enzyme.



Entry	Catalyst	Yield	TON
1	rMb(FePc)	68%	3.4×10^3
2	rMb^{V68S}(FePc)	87%	4.7×10^3
3	rMb^{V68T}(FePc)	82%	4.3×10^3
4	rMb^{F43Y}(FePc)	94%	4.1×10^3

Determined by GC-FID analysis

Figure 1-16. (a) Crystal structure of rMb(FePc) (PDB:2D6C). (b) Aldoxime dehydration catalyzed by rMb(FePc) variants. (c) Time course of **2a** formation catalyzed by rMb(FePc) (gray), rMb^{V68S}(FePc) (black), rMb^{V68T}(FePc) (dashed line), and rMb^{F43Y}(FePc) (dotted line). Conditions: [rMb(FePc) variants] = 1 μM, [aldoxime] = 5 mM, [$Na_2S_2O_4$] = 5 mM in 100 mM potassium phosphate buffer (pH 7.0) at 30 °C for 24 h under N_2 atmosphere. The product yields were determined by GC-FID.

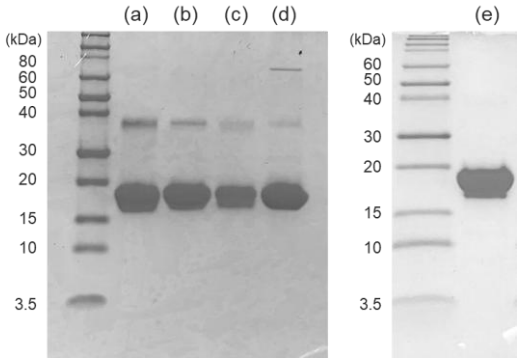


Figure 1-17. SDS-PAGE analysis of (a) Mb^{H64A} (19.3 kDa), (b) Mb^{H64D} (19.3 kDa), (c) Mb^{F43Y} (19.4 kDa), (d) Mb^{V68S} (19.3 kDa), and (e) Mb^{V68T} (19.3 kDa) purified by Strep-Tactin affinity chromatography.

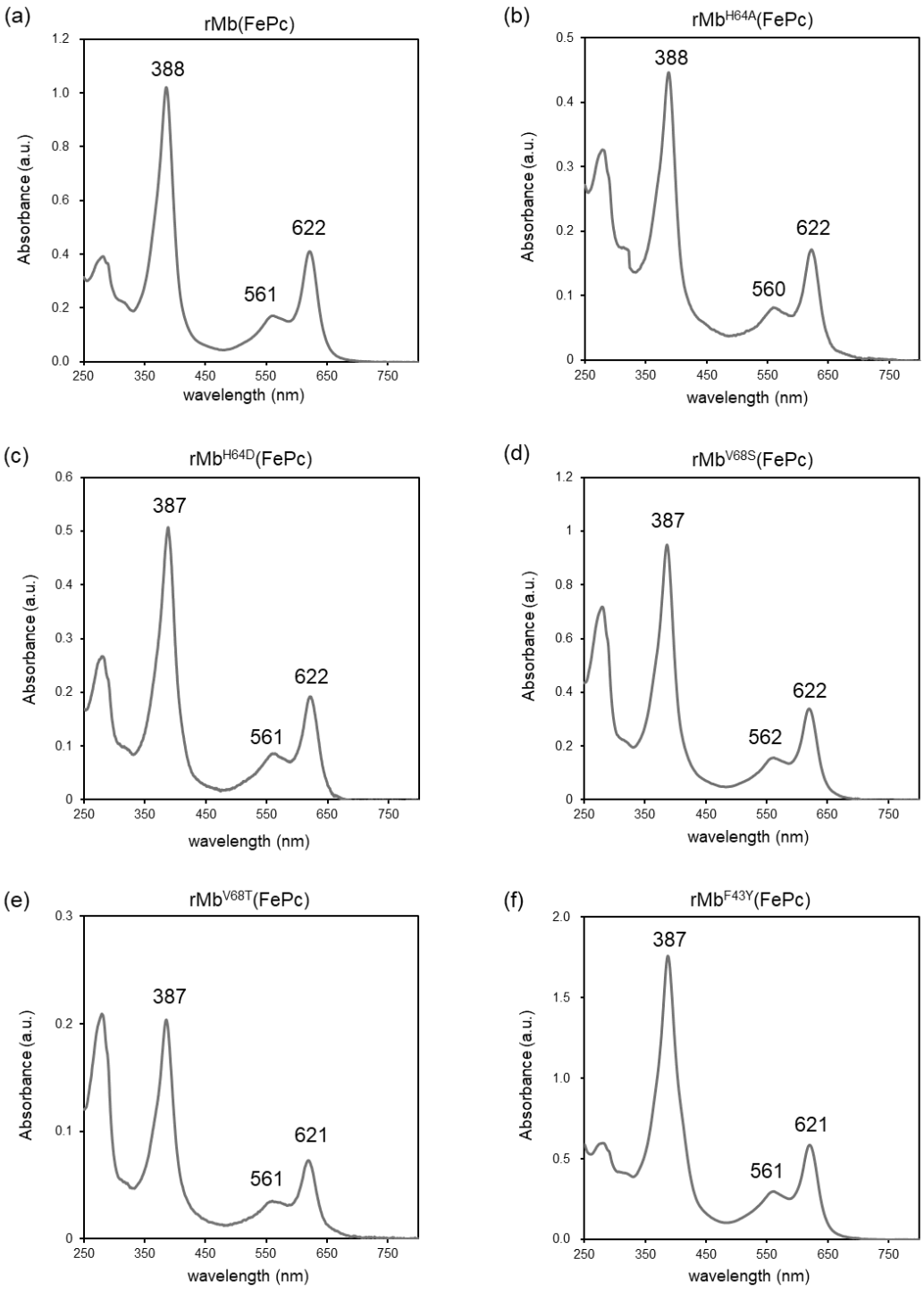


Figure 1-18. UV-vis spectra of (a) rMb(FePc), (b) rMb^{H64A}(FePc), (c) rMb^{H64D}(FePc), (d) rMb^{V68S}(FePc), (e) rMb^{V68T}(FePc), and (f) rMb^{F43Y}(FePc).

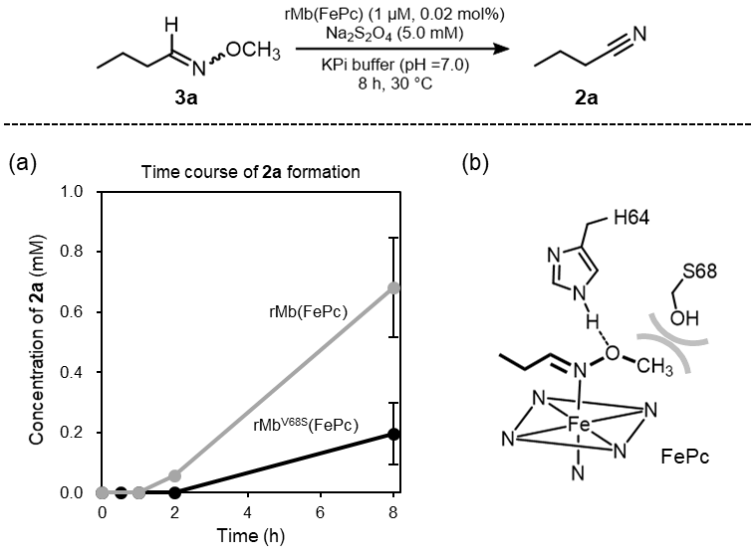


Figure 1-19. Dealcoholization of butyraldehyde *O*-methyloxime (**3a**) catalyzed by rMb(FePc) and rMb^{V68S}(FePc). (a) Time course for the formation of **2a**. (b) Plausible binding mode of the substrate in the active site of rMb^{V68S}(FePc).

1-3. Summary

In summary, aldoxime dehydration was performed by myoglobin reconstituted with the artificially created cofactor FePc. The rMb(FePc) catalyst exhibits high dehydration activity toward a wide range of aldoximes. In the dehydration of aliphatic aldoximes, the total TON reaches a maximum of 9300. Furthermore, less reactive *O*-alkyl aldoximes are also converted into corresponding nitriles by the artificial metalloenzyme, whereas natural aldoxime dehydratases lack activity for these substrates. A series of experiments including Brønsted plot analysis and site-directed mutagenesis of rMb(FePc) revealed the importance of the distal His and Ser residues in promoting the dehydration reactions, and these findings led to further enhancement of the rMb(FePc) activity in rational engineering of the myoglobin active site. The present results clearly reveal the versatile catalytic ability of my artificial metalloenzyme and provide new mechanistic insights into the design of biocatalysts for the nitrile synthesis.

1-4. Experimental section

Instruments

^{1}H NMR and ^{13}C NMR spectra were recorded on a Bruker NMR Advance III HD spectrometer (400 MHz). ^{1}H and ^{13}C NMR chemical shifts are reported relative to deuterated solvents. ESI-TOF MS analyses were performed on a Bruker micrOTOF focus II mass spectrometer. The GC experiments were performed on a Shimadzu GC-2010 Plus Gas Chromatograph equipped with DB-1 column (Agilent Technologies, Inc.) or SUPELCO Beta DEXTM 120 fused silica capillary column (Merck Ltd.). The GC-MS experiments were performed on a Shimadzu GCMS-QP2010 Ultra Gas Chromatograph Mass Spectrometer equipped with Rxi-5Sil MS column (GL Science). UV-vis spectra were measured with a Shimadzu UV-2700 spectrophotometer and Shimadzu UV-3600 Plus Spectrophotometer. PCR was performed using Bio-Rad T100^{TM} Thermal Cycler. Ultrapure water demineralized by a Merck Millipore Milli-Q Integral 3 Water Purification System was used.

Materials

All reagents of the highest guaranteed grade were purchased from TCI Co., Ltd., Merck Ltd., FUJIFILM Wako Pure Chemical Corporation and Nacalai Tesque, Inc., and used as received unless otherwise noted. Compounds **1a**–**1h**, **1j**–**1o**, **2n**, **2o**, **3a**, **3e**, **4e**, **5e**, **6e**, and **7e** were synthesized as described below. Aldoxime **1i** and authentic samples of nitriles **2a**–**2m** were purchased from TCI Co., Ltd., and used as received. The iron porphycene (FePc) was synthesized as described in the previous reports[39,49]. The native myoglobin (Mb) was purchased from Merck Ltd. and purified by column chromatography through a CM-cellulose column (FUJIFILM Wako Pure Chemical Corporation) before use. The Mb variants were recombinantly expressed and purified according to the previous reports with several modifications[56]. The gene of aldoxime dehydratases were amplified by PCR from genomic DNA of *Rhodococcus erythropolis* PR4 (NBRC 100887) which were purchased from Biological Resource Center, National Institute of Technology and Evaluation (NBRC). The amplified genes were cloned into pET-21b vector and expressed according to the standard protocol of pET-expression system. Oligonucleotides were obtained from Merck Ltd. Nucleotide sequences were determined by Eurofins Scientific SE, Inc.

Preparation of expression plasmids for Mb variants

Expression plasmids for Mb variants were prepared according to the standard protocol of the QuikChange II Site-Directed Mutagenesis Kit (Agilent Technologies Japan, Ltd.). A template plasmid containing Mb gene with strep-tag II sequence in pDEST14 vector was amplified by PCR using primers containing mutations at the target positions (Table 1-3). The PCR products were then treated with *Dpn*I restriction enzyme and transformed into chemically competent *E. coli* DH5α cells. The cells were inoculated on LB agar plates supplemented with 100 μg/mL ampicillin and incubated at 37 °C overnight. The single colonies were then transferred into 10 mL of an LB medium containing 100 μg/mL ampicillin and cultivated overnight at 37 °C. The cells were harvested by centrifugation at 4,000 *g* for 10 min, and the plasmids were purified according to the standard protocol of NucleoSpin Plasmid EasyPure (Takara Bio Inc.). The gene of Mb variants in each expression plasmid was analyzed by DNA sequencing (Eurofins Scientific SE, Inc.).

Table 1-3. Primers for preparation of Mb variants

Primer name	DNA sequence
H64A (forward)	CCTCCGAGGACTTGAAGAAAGCGGGCGTTACCGTGTTAACAGCAC
H64A (reverse)	GTGCTGTTAACACGGTAACGCCCGCTTTCTTCAAGTCCTCGGAGG
H64D (forward)	CCTCCGAGGACTTGAAGAAAGATGGCGTTACCGTGTTAACAGCAC
H64D (reverse)	GTGCTGTTAACACGGTAACGCCATCTTTCTTCAAGTCCTCGGAGG
F43Y (forward)	GCCATCCGGAAACGTTGGAGAAGTACGATCGCTTTAAACACCTGAAAACCG
F43Y (reverse)	CGGTTTTCAGGTGTTTAAAGCGATCGTACTTCTCCAACGTTTCCGGATGGC
V68T (forward)	GACTTGAAGAAACATGGCGTTACCACGTTAACAGCACTTGGTGCAATCCTC
V68T (reverse)	GAGGATTGCACCAAGTGCTGTTAACGTGGTAACGCCATGTTTCTTCAAGTC
V68S (forward)	GGACTTGAAGAAACATGGCGTTACCTCTTTAACAGCACTTGGTGCAATCC
V68S (reverse)	GGATTGCACCAAGTGCTGTTAAAGAGGTAACGCCATGTTTCTTCAAGTCC

(The nucleotide sequence containing mutation is highlighted by underline.)

Expression and purification of Mb variants

The expression plasmids encoding the gene of Mb variants with *Strep*-tag II was transformed into a chemically competent *E. coli* BL21-(DE3) strain. The transformant was then plated on an LB agar medium containing 100 μg/mL ampicillin and incubated at 37 °C overnight. A single colony was inoculated into 50 mL of an LB medium containing 100 μg/mL ampicillin and 180 μg/mL glucose and cultivated at 37 °C and 180 rpm. After OD_{600} reached approximately 0.8–1.0, 1.0 mL of the culture was transferred into 1.0 L of an SB medium (32 g/L tryptone, 20 g/L yeast extract, 5 g/L NaCl) containing 100 μg/mL ampicillin and 0.50 mM 5-aminolevulic acid and then cultivated at 37 °C and 150 rpm. After OD_{600} reached approximately 0.8–1.0, IPTG was added to a final concentration at 0.50 mM to induce the expression of Mb variants, and the cultivation was continued at 25 °C and 150 rpm for 16 h. The cells were harvested by centrifugation at 3,000 g for 10 min at 4 °C and stored at −80 °C. The frozen cell was thawed at room temperature and resuspended in Tris-HCl buffer (100 mM Tris-HCl, 150 mM NaCl, 1 mM EDTA, pH 8.0) supplemented with 1.0 mM PMSF. The cell was then lysed by sonication (Branson Sonifier 250) on an ice bath, and the supernatant was collected by centrifugation at 8,800 rpm for 10 min at 4 °C. After filtration with Millex-GV (0.22 μm), the supernatant was loaded on a Strep-Tactin column, and the purified Mb variants were eluted with Tris-HCl buffer (100 mM Tris-HCl, 150 mM NaCl, 1 mM EDTA, pH 8.0) containing 2.5 mM desthiobiotin. The eluate was further purified by ion exchange chromatography using DEAE Sepharose Fast Flow (GE healthcare) to remove desthiobiotin. The protein purity was checked by SDS-PAGE analysis, and the concentrations of the Mb variants were determined by UV-vis absorbance ($\varepsilon_{408} = 1.9 \times 10^5\ cm^{-1}M^{-1}$).

Preparation of rMb(FePc) variants

Removal of heme *b* from Mb and its variants was performed according to the literature with several

modifications[55]. An ice-cold solution of Mb (approximately 10 μM) was acidified to pH below 2.0 with 1.0 M HCl_{aq}. After the extraction of heme *b* with 2-butanone, the protein solution was sequentially dialyzed at 4 °C against (i) 10 mM KPi buffer (pH 6.0), (ii) 10 mM KPi buffer (pH 6.5), (iii) 10 mM KPi buffer (pH 7.0), and (iv) 100 mM KPi buffer (pH 7.0) to obtain a solution of apo-Mb. Next, the reconstitution of apo-Mb with FePc was performed according to the previous report[49]. To a solution of apo-Mb, 1.0 equivalent of FePc in pyridine/water (1/1) was added dropwise on ice. After incubation for 10 min, the mixture was dialyzed against 100 mM KPi buffer (pH 7.0) at 4 °C to remove pyridine. The resulting protein solution was then passed through CM sepharose Fast Flow (Cytiva) and HiTrap desalting columns (Cytiva) to separate free FePc cofactor. Purities and concentrations of rMb(FePc) and its variants were determined by UV-vis spectra ($\varepsilon_{388} = 9.1 \times 10^4$ $cm^{-1}M^{-1}$).

Preparation of the expression plasmid for ReOxd

The expression plasmid for ReOxd[53] was constructed according to the standard protocol of the NEBuilder HiFi DNA Assembly Cloning Kit (New England Biolabs Japan). The insert gene of ReOxd was amplified by PCR from the genomic DNA of *Rhodococcus erythropolis* PR4 (NBRC 100887) using PrimeSTAR® GXL DNA Polymerase (Takara Bio Inc.). The PCR product was then purified by agarose gel electrophoresis and assembled with a linearized pET-21b vector with the *Strep*-tag II sequence using NEBuilder HiFi DNA Assembly. The assembled product was then transformed into a chemically competent *E. coli* DH5α cell, and the resulting plasmid was purified using the NucleoSpin® Plasmid (Takara Bio Inc.).

Table 1-4. Primers used for the cloning of ReOxd

Primer name	DNA sequence
ReOxd (forward)	GTACTTTCAGGGGAAAATGGAATCTGCAATCAGTGAACATCTTCAATGCC
ReOxd (reverse)	AGCAGCCGGATCTTATTAGTGCGCGGCGGTGGTCACC
Vector (forward)	TAATAAGATCCGGCTGCTAACAAAGCC
Vector (reverse)	CATTTTCCCCTGAAAGTACAGGTTTTCTTTCTC

Expression and purification of ReOxd

The expression plasmid encoding the ReOxd gene with the *Strep*-tag II sequence vector was transformed into a chemically competent *E. coli* BL21-Gold(DE3) strain. Transformants were plated on an LB agar medium containing 100 μg/mL ampicillin and incubated overnight at 37 ºC. A single colony was then inoculated into 10 mL of an LB medium containing 100 μg/mL ampicillin and cultivated at 37 ºC and 180 rpm for 6 h. The culture (1.0 mL) was then transferred into 100 mL of an LB medium containing 100 μg/mL ampicillin and cultivated at 37 ºC at 150 rpm for additional 2.5 h. The cell culture (10 mL) was then transferred into 1.0 L of LB medium containing 100 μg/mL ampicillin and 0.50 mM 5-aminolevulic acid and cultivated at 37 ºC and 150 rpm. After the OD_{600} value reached approximately 0.6–0.7, IPTG was added to a final concentration at 0.20 mM to induce the expression of Oxd, and the cultivation was continued at 18 ºC and 150 rpm for 20 h. The cells were harvested by centrifugation at 8,800 rpm for 10 min at 4 ºC and stored at −80 ºC. Next, the frozen cells were thawed at room temperature and resuspended

in Tris-HCl buffer (100 mM Tris-HCl, 150 mM NaCl, 1 mM EDTA, pH 8.0). The cells were then lysed by sonication (Branson Sonifier 250) on an ice bath, followed by incubation with Benzonase (125 units/μL, 2.0 μL) (Merck Ltd.). The supernatant was collected by centrifugation at 8,800 rpm for 10 min at 4 ºC. After filtration through Millex-GV (0.22 μm), the supernatant was then loaded onto a Strep-Tactin column, and the purified Oxd was eluted with Tris-HCl buffer (100 mM Tris-HCl, 150 mM NaCl, 1 mM EDTA, pH 8.0) containing 2.5 mM desthiobiotin. The eluate was further purified by ion exchange chromatography using HiTrap DEAE Sepharose FF (Cytiva) to remove desthiobiotin. Purity of the protein was examined by SDS-PAGE analysis. The concentration of ReOxd was determined by UV-vis absorption at 407 nm according to the literature[57].

Procedure for aldoxime dehydration

To a 450 μL solution of rMb(FePc) (0.50 nmol or 2.5 nmol) or ReOxd (0.50 nmol or 2.5 nmol) in 100 mM KPi buffer (pH 7.0) containing $Na_2S_2O_4$ (2.5 μmol), aldoxime (2.5 μmol) in 1,4-dioxane (50 μL) was added at 30 °C under N_2 atmosphere. After incubation at 30 °C for the prescribed time period, the reaction was quenched by adding EtOAc or Et_2O (1.0 mL). To the mixture, benzyl alcohol (1.75 μmol) in acetonitrile (30 μL) was added as an internal standard. Finally, the organic layer was analyzed by GC-FID (Shimadzu GC-2010 Plus Gas Chromatograph) equipped with a DB-1 column (Agilent Technologies) to determine the yield of the product.

DNA Sequence

Mb:

ATGTGGTCGCATCCGCAGTTTGAGAAA*GAAAACCTGTACTTTCAGGGG*AAAGTGCTGTCTGAAGGCGAATGGCAACTGGT
CCTTCACGTTTGGGCTAAAGTCGAAGCCGATGTAGCGGGTCATGGTCAGGACATCCTGATTCGTCTGTTCAAAAGCCATC
CGGAAACGTTGGAGAAGTTCGATCGCTTTAAACACCTGAAAACCGAAGCTGAGATGAAAGCCTCCGAGGACTTGAAGA
AACATGGCGTTACCGTGTTAACAGCACTTGGTGCAATCCTCAAGAAGAAAGGTCATCACGAAGCTGAACTCAAACCACT
GGCACAGAGTCATGCGACTAAACACAAAATCCCGATCAAATATCTGGAGTTCATTAGCGAAGCCATTATTCACGTGTTACA
CTCACGTCATCCTGGCAATTTTGGCGCGGATGCGCAAGGAGCAATGAACAAAGCGCTGGAATTATTTCGCAAGGATATTG
CGGCCAAATACAAAGAACTGGGCTATCAGGGGTAA

(underline: Strep-tag II, *italic*: TEV protease cleavage site, black: Mb)

Mb^{H64A}:

ATGTGGTCGCATCCGCAGTTTGAGAAA*GAAAACCTGTACTTTCAGGGG*AAAGTGCTGTCTGAAGGCGAATGGCAACTGGT
CCTTCACGTTTGGGCTAAAGTCGAAGCCGATGTAGCGGGTCATGGTCAGGACATCCTGATTCGTCTGTTCAAAAGCCATC
CGGAAACGTTGGAGAAGTTCGATCGCTTTAAACACCTGAAAACCGAAGCTGAGATGAAAGCCTCCGAGGACTTGAAGA
AA**GCG**GGCGTTACCGTGTTAACAGCACTTGGTGCAATCCTCAAGAAGAAAGGTCATCACGAAGCTGAACTCAAACCACT
GGCACAGAGTCATGCGACTAAACACAAAATCCCGATCAAATATCTGGAGTTCATTAGCGAAGCCATTATTCACGTGTTACA
CTCACGTCATCCTGGCAATTTTGGCGCGGATGCGCAAGGAGCAATGAACAAAGCGCTGGAATTATTTCGCAAGGATATTG
CGGCCAAATACAAAGAACTGGGCTATCAGGGGTAA

(underline: Strep-tag II, *italic*: TEV protease cleavage site, black: Mb)

Mb^{H64D}:

ATGTGGTCGCATCCGCAGTTTGAGAAA*GAAAACCTGTACTTTCAGGGG*AAAGTGCTGTCTGAAGGCGAATGGCAACTGGT
CCTTCACGTTTGGGCTAAAGTCGAAGCCGATGTAGCGGGTCATGGTCAGGACATCCTGATTCGTCTGTTCAAAAGCCATC
CGGAAACGTTGGAGAAGTTCGATCGCTTTAAACACCTGAAAACCGAAGCTGAGATGAAAGCCTCCGAGGACTTGAAGA
AA**GAT**GGCGTTACCGTGTTAACAGCACTTGGTGCAATCCTCAAGAAGAAAGGTCATCACGAAGCTGAACTCAAACCACT
GGCACAGAGTCATGCGACTAAACACAAAATCCCGATCAAATATCTGGAGTTCATTAGCGAAGCCATTATTCACGTGTTACA
CTCACGTCATCCTGGCAATTTTGGCGCGGATGCGCAAGGAGCAATGAACAAAGCGCTGGAATTATTTCGCAAGGATATTG
CGGCCAAATACAAAGAACTGGGCTATCAGGGGTAA

(underline: Strep-tag II, *italic*: TEV protease cleavage site, black: Mb)

Mb^{F43Y}:

ATGTGGTCGCATCCGCAGTTTGAGAAA*GAAAACCTGTACTTTCAGGGG*AAAGTGCTGTCTGAAGGCGAATGGCAACTGGT
CCTTCACGTTTGGGCTAAAGTCGAAGCCGATGTAGCGGGTCATGGTCAGGACATCCTGATTCGTCTGTTCAAAAGCCATC
CGGAAACGTTGGAGAAG**TAC**GATCGCTTTAAACACCTGAAAACCGAAGCTGAGATGAAAGCCTCCGAGGACTTGAAGA
AACATGGCGTTACCGTGTTAACAGCACTTGGTGCAATCCTCAAGAAGAAAGGTCATCACGAAGCTGAACTCAAACCACT
GGCACAGAGTCATGCGACTAAACACAAAATCCCGATCAAATATCTGGAGTTCATTAGCGAAGCCATTATTCACGTGTTACA
CTCACGTCATCCTGGCAATTTTGGCGCGGATGCGCAAGGAGCAATGAACAAAGCGCTGGAATTATTTCGCAAGGATATTG
CGGCCAAATACAAAGAACTGGGCTATCAGGGGTAA

(underline: Strep-tag II, *italic*: TEV protease cleavage site, black: Mb)

Mb^{V68T}:

ATGTGGTCGCATCCGCAGTTTGAGAAA*GAAAACCTGTACTTTCAGGGG*AAAGTGCTGTCTGAAGGCGAATGGCAACTGGT
CCTTCACGTTTGGGCTAAAGTCGAAGCCGATGTAGCGGGTCATGGTCAGGACATCCTGATTCGTCTGTTCAAAAGCCATC
CGGAAACGTTGGAGAAGTTCGATCGCTTTAAACACCTGAAAACCGAAGCTGAGATGAAAGCCTCCGAGGACTTGAAGA
AACATGGCGTTACC**ACG**TTAACAGCACTTGGTGCAATCCTCAAGAAGAAAGGTCATCACGAAGCTGAACTCAAACCACT
GGCACAGAGTCATGCGACTAAACACAAAATCCCGATCAAATATCTGGAGTTCATTAGCGAAGCCATTATTCACGTGTTACA
CTCACGTCATCCTGGCAATTTTGGCGCGGATGCGCAAGGAGCAATGAACAAAGCGCTGGAATTATTTCGCAAGGATATTG
CGGCCAAATACAAAGAACTGGGCTATCAGGGGTAA

(underline: Strep-tag II, *italic*: TEV protease cleavage site, black: Mb)

Mb^{V68S}:

ATGTGGTCGCATCCGCAGTTTGAGAAA*GAAAACCTGTACTTTCAGGGG*AAAGTGCTGTCTGAAGGCGAATGGCAACTGGT
CCTTCACGTTTGGGCTAAAGTCGAAGCCGATGTAGCGGGTCATGGTCAGGACATCCTGATTCGTCTGTTCAAAAGCCATC
CGGAAACGTTGGAGAAGTTCGATCGCTTTAAACACCTGAAAACCGAAGCTGAGATGAAAGCCTCCGAGGACTTGAAGA
AACATGGCGTTACC**TCT**TTAACAGCACTTGGTGCAATCCTCAAGAAGAAAGGTCATCACGAAGCTGAACTCAAACCACT
GGCACAGAGTCATGCGACTAAACACAAAATCCCGATCAAATATCTGGAGTTCATTAGCGAAGCCATTATTCACGTGTTACA
CTCACGTCATCCTGGCAATTTTGGCGCGGATGCGCAAGGAGCAATGAACAAAGCGCTGGAATTATTTCGCAAGGATATTG
CGGCCAAATACAAAGAACTGGGCTATCAGGGGTAA

(underline: Strep-tag II, *italic*: TEV protease cleavage site, black: Mb)

ReOxd:

ATGTGGTCGCATCCGCAGTTTGAGAAA*GAAAACCTGTACTTTCAGGGG*AAAATGGAATCTGCAATCAGTGAACATCTTCAA
TGCCCGCGCACGCTGACCAGGCGCGTTCCGGATACCTATTCGCCACCATTTCCCATGTGGGTCGGGCGTGCGGACGACAC
ATTGCACCAGGTCGCGATGGGCTATCTCGGCGTGCAGTTCCGCGGCGAGGATCAGCGCTCGGCTGCACTGCAGTCCATGC
GGGATATTGTCGCCGGCTTCGACTTGCCGGACGGACCGGCACATCACGATCTCACTCACCATGTCGACAACCAGGGCTAC
GAGAATCTGATCGTGGTCGGGTACTGGAAAGATGTTTCTTCCCAACATCGTTGGAGCACATCAGCTCCGGTGGCCTCCTG
GTGGGAGTCCGAGGACCGCTTGTCCGACGGATTGGGGTTCTTCCGGGAGATCGTGGCACCGAGAGCCGAACAATTCGAA
ACGCTCTACGCGTTCCAGGACGATCTCCCCGGAGTGGGAGCCGTCATGGACGGTGTCAGCGGCGAGATCAACGAGCACG
GCTACTGGGGTTCGATGCGCGAGCGCTTTCCGATCTCCCAGACCGACTGGATGCAGGCCTCGGGCGAACTACGGGTCGTC
GCCGGTGACCCCCGCCGCAGGTGGACGCGTAGTAGTGCGGGGGCACGACAACATCGCACTGATCAGATCCGGGCAGGACT
GGGCCGACGCGGAAGCAGACGAGCGCAGCCTCTACCTCGACGAAATCCTGCCGACTCTTCAATCGGGCATGGACTTCCT
CCGCGACAACGGCCCGGCCGTCGGGTGCTACAGCAACCGTTTCGTACGCAATATCGACATCGACGGAAACTTCCTCGAC
CTGAGCTACAACATCGGTCACTGGGCCTCACTCGACCAACTCGAGCGGTGGTCGGAATCCCACCCGACCCATCTGCGGAT
CTTCACGACGTTCTTCCGGGTGGCCGAGGGCCTGTCGAAATTACGTCTCTACCATGAGGTCTCGGTATTCGATGCCGCCG
ATCAGCTGTACGAGTACATCAACTGCCATCCCGGGACCGGGATGCTGCGCGACGCGGTGACCACCGCCGCGCACTAA

(underline: Strep-tag II, *italic*: TEV protease cleavage site, black: ReOxd)

References

[1] K. Chen, Z. Wang, K. Ding, Y. Chen, Y. Asano, "Recent progress on discovery and research of aldoxime dehydratases" *Green Synth. Catal.* **2021**, *2*, 179–186.

[2] T. Betke, P. Rommelmann, K. Oike, Y. Asano, H. Gröger, "Cyanide-Free and Broadly Applicable Enantioselective Synthetic Platform for Chiral Nitriles through a Biocatalytic Approach" *Angew. Chem. Int. Ed.* **2017**, *56*, 12361–12366.

[3] T. Betke, J. Higuchi, P. Rommelmann, K. Oike, T. Nomura, Y. Kato, Y. Asano, H. Gröger, "Biocatalytic Synthesis of Nitriles through Dehydration of Aldoximes: The Substrate Scope of Aldoxime Dehydratases" *ChemBioChem* **2018**, *19*, 768–779.

[4] A. Hinzmann, T. Betke, Y. Asano, H. Gröger, "Synthetic Processes toward Nitriles without the Use of Cyanide: A Biocatalytic Concept Based on Dehydration of Aldoximes in Water" *Chem. Eur. J.* **2021**, *27*, 5313–5321.

[5] P. Pollak, G. Romeder, F. Hagedorn, H.-P. Gelbke, "Nitriles" in *Ullmann's Encyclopedia of Industrial Chemistry*, Wiley-VCH, **2000**.

[6] T. Betke, M. Maier, H. Gruber-Wölfler, H. Gröger, "Biocatalytic Production of Adiponitrile and Related Aliphatic Linear α,ω-Dinitriles" *Nat. Commun.* **2018**, *9*, 5112.

[7] A. Hinzmann, S. Glinski, M. Worm, H. Gröger, "Enzymatic Synthesis of Aliphatic Nitriles at a Substrate Loading of up to 1.4 kg/L: A Biocatalytic Record Achieved with a Heme Protein" *J. Org. Chem.* **2019**, *84*, 4867–4872.

[8] A. Hinzmann, M. Stricker, H. Gröger, "Chemoenzymatic Cascades toward Aliphatic Nitriles Starting from Biorenewable Feedstocks" *ACS Sustain. Chem. Eng.* **2020**, *8*, 17088–17096.

[9] Y. Asano, Y. Kato, "Z-phenylacetaldoxime degradation by a novel aldoxime dehydratase from *Bacillus* sp. strain OxB-1" *FEMS Microbiol. Lett.* **1998**, *158*, 185–190.

[10] E. B. Villhauer, "N-Substituted 2-cyanopyrrolidines" *WO2000034241A1*, **2000**.

[11] E. B. Villhauer, J. A. Brinkman, G. B. Naderi, B. F. Burkey, B. E. Dunning, K. Prasad, B. L. Mangold, M. E. Russell, T. E. Hughes, "1-[[(3-Hydroxy-1-adamantyl)amino]acetyl]-2-cyano-(S)-pyrrolidine: A Potent, Selective, and Orally Bioavailable Dipeptidyl Peptidase IV Inhibitor with Antihyperglycemic Properties" *J. Med. Chem.* **2003**, *46*, 2774–2789.

[12] L. Pellegatti, J. Sedelmeier, "Synthesis of Vildagliptin Utilizing Continuous Flow and Batch Technologies" *Org. Process Res. Dev.* **2015**, *19*, 551–554.

[13] T. C. Vu et al., "Methods and compounds producing dipeptidyl peptidase IV inhibitors and intermediates thereof" *WO200405285OA2*, **2004**.

[14] S. A. Savage, G. S. Jones, S. Kolotuchin, S. A. Ramrattan, T. Vu, R. E. Waltermire, "Preparation of Saxagliptin, a Novel DPP-IV Inhibitor" *Org. Process Res. Dev.* **2009**, *13*, 1169–1176.

[15] P. Rommelmann, *Synthese von Lactonen, Dioxinen und Nitrilen unter Verwendung von Bio- und Chemokatalysatoren*, Doctoral Thesis, Bielefeld University, **2018**.

[16] T. Betke, *Chemoenzymatic Synthesis of Nitriles and Lubricant Esters*, Doctoral Thesis, Bielefeld University, **2019**.

[17] Y. Lu, N. Yeung, N. Sieracki, N. M. Marshall, "Design of Functional Metalloproteins" *Nature* **2009**, *460*, 855–862.

[18] J. C. Lewis, "Artificial Metalloenzymes and Metallopeptide Catalysts for Organic Synthesis" *ACS Catal.* **2013**, *3*, 2954–2975.

[19] F. Schwizer et al., "Artificial Metalloenzymes: Reaction Scope and Optimization Strategies" *Chem. Rev.* **2018**, *118*, 142–231.

[20] O. F. Brandenberg, R. Fasan, F. H. Arnold, "Exploiting and Engineering Hemoproteins for Abiological Carbene and Nitrene Transfer Reactions" *Curr. Opin. Biotechnol.* **2017**, *47*, 102–111.

[21] R. B. Leveson-Gower, C. Mayer, G. Roelfes, "The Importance of Catalytic Promiscuity for Enzyme Design and Evolution" *Nat. Rev. Chem.* **2019**, *3*, 687–705.

[22] K. Oohora, A. Onoda, T. Hayashi, "Hemoproteins Reconstituted with Artificial Metal Complexes as Biohybrid Catalysts" *Acc. Chem. Res.* **2019**, *52*, 945–954.

[23] K. Oohora, T. Hayashi, "Myoglobins Engineered with Artificial Cofactors Serve as Artificial Metalloenzymes and Models of Natural Enzymes" *Dalton Trans.* **2021**, *50*, 1940–1949.

[24] X. Zhao, N. Yeung, B. S. Russell, D. K. Garner, Y. Lu, "Catalytic Reduction of NO to N_2O by a Designed Heme Copper Center in Myoglobin: Implications for the Role of Metal Ions" *J. Am. Chem. Soc.* **2006**, *128*, 6766–6767.

[25] N. Yeung, Y.-W. Lin, Y.-G. Gao, X. Zhao, B. S. Russell, L. Lei, K. D. Miner, H. Robinson, Y. Lu, "Rational Design of a Structural and Functional Nitric Oxide Reductase" *Nature* **2009**, *462*, 1079–1082.

[26] Y. Deng, S. Dwaraknath, W. O. Ouyang, C. J. Matsumoto, S. Ouchida, Y. Lu, "Engineering an Oxygen-Binding Protein for Photocatalytic CO_2 Reductions in Water" *Angew. Chem. Int. Ed.* **2023**, *62*, e202215719.

[27] H. Sato, T. Hayashi, T. Ando, Y. Hisaeda, T. Ueno, Y. Watanabe, "Hybridization of Modified-Heme Reconstitution and Distal Histidine Mutation to Functionalize Sperm Whale Myoglobin" *J. Am. Chem. Soc.* **2004**, *126*, 436–437.

[28] T. Hayashi, D. Murata, M. Makino, H. Sugimoto, T. Matsuo, H. Sato, Y. Shiro, Y. Hisaeda, "Crystal Structure and Peroxidase Activity of Myoglobin Reconstituted with Iron Porphycene" *Inorg. Chem.* **2006**, *45*, 10530–10536.

[29] T. Matsuo, A. Hayashi, M. Abe, T. Matsuda, Y. Hisaeda, T. Hayashi, "Meso-Unsubstituted Iron Corrole in Hemoproteins: Remarkable Differences in Effects on Peroxidase Activities between Myoglobin and Horseradish Peroxidase" *J. Am. Chem. Soc.* **2009**, *131*, 15124–15125.

[30] T. Matsuo, K. Fukumoto, T. Watanabe, T. Hayashi, "Precise Design of Artificial Cofactors for Enhancing Peroxidase Activity of Myoglobin: Myoglobin Mutant H64D Reconstituted with a 'Single-Winged Cofactor' Is Equivalent to Native Horseradish Peroxidase in Oxidation Activity" *Chem. Asian J.* **2011**, *6*, 2491–2499.

[31] M. Ohashi, T. Koshiyama, T. Ueno, M. Yanase, H. Fujii, Y. Watanabe, "Preparation of Artificial Metalloenzymes by Insertion of Chromium(III) Schiff Base Complexes into Apomyoglobin Mutants" *Angew. Chem. Int. Ed.* **2003**, *42*, 1005–1008.

[32] J. R. Carey, S. K. Ma, T. D. Pfister, D. K. Garner, H. K. Kim, J. A. Abramite, Z. Wang, Z. Guo, Y. Lu, "A Site-Selective Dual Anchoring Strategy for Artificial Metalloprotein Design" *J. Am. Chem. Soc.* **2004**, *126*, 10812–10813.

[33] T. Ueno, T. Koshiyama, M. Ohashi, K. Kondo, M. Kono, A. Suzuki, T. Yamane, Y. Watanabe, "Coordinated Design of Cofactor and Active Site Structures in Development of New Protein Catalysts" *J. Am. Chem. Soc.*

2005, *127*, 6556–6562.

[34] J.-L. Zhang, D. K. Garner, L. Liang, Q. Chen, Y. Lu, "Protein Scaffold of a Designed Metalloenzyme Enhances the Chemoselectivity in Sulfoxidation of Thioanisole" *Chem. Commun.* **2008**, *1665*, 1665–1667.

[35] K. Oohora, Y. Kihira, E. Mizohata, T. Inoue, T. Hayashi, "C(sp^3)–H Bond Hydroxylation Catalyzed by Myoglobin Reconstituted with Manganese Porphycene" *J. Am. Chem. Soc.* **2013**, *135*, 17282–17285.

[36] K. Oohora, H. Meichin, Y. Kihira, H. Sugimoto, Y. Shiro, T. Hayashi, "Manganese(V) Porphycene Complex Responsible for Inert C–H Bond Hydroxylation in a Myoglobin Matrix" *J. Am. Chem. Soc.* **2017**, *139*, 18460–18463.

[37] K. Oohora, Y. Kagawa, T. Nishiura, E. Mizohata, U. Schwaneberg, T. Hayashi, "Rational Design of an Artificial Ethylbenzene Hydroxylase Using a Molecular Dynamics Simulation to Enhance Enantioselectivity" *Chem. Lett.* **2023**, *53*, upad042.

[38] G. Sreenilayam, E. J. Moore, V. Steck, R. Fasan, "Stereoselective Olefin Cyclopropanation under Aerobic Conditions with an Artificial Enzyme Incorporating an Iron–Chlorin e6 Cofactor" *ACS Catal.* **2017**, *7*, 7629–7633.

[39] K. Oohora, H. Meichin, L. Zhao, M. W. Wolf, A. Nakayama, J. Y. Hasegawa, N. Lehnert, T. Hayashi, "Catalytic Cyclopropanation by Myoglobin Reconstituted with Iron Porphycene: Acceleration of Catalysis Due to Rapid Formation of the Carbene Species" *J. Am. Chem. Soc.* **2017**, *139*, 17265–17268.

[40] T. Hayashi, M. Tinzl, T. Mori, U. Krengel, J. Proppe, J. Soetbeer, D. Klose, G. Jeschke, M. Reiher, D. Hilvert, "Capture and Characterization of a Reactive Haem–Carbenoid Complex in an Artificial Metalloenzyme" *Nat. Catal.* **2018**, *1*, 578–584.

[41] D. M. Carminati, R. Fasan, "Stereoselective Cyclopropanation of Electron-Deficient Olefins with a Cofactor-Redesigned Carbene Transferase Featuring Radical Reactivity" *ACS Catal.* **2019**, *9*, 9683–9697.

[42] M. Pott, M. Tinzl, T. Hayashi, Y. Ota, D. Dunkelmann, P. R. E. Mittl, D. Hilvert, "Noncanonical Heme Ligands Steer Carbene Transfer Reactivity in an Artificial Metalloenzyme" *Angew. Chem. Int. Ed.* **2021**, *60*, 15063–15068.

[43] H. M. Key, P. Dydio, D. S. Clark, J. F. Hartwig, "Abiological Catalysis by Artificial Haem Proteins Containing Noble Metals in Place of Iron" *Nature* **2016**, *534*, 534–537.

[44] G. Sreenilayam, E. J. Moore, V. Steck, R. Fasan, "Metal Substitution Modulates the Reactivity and Extends the Reaction Scope of Myoglobin Carbene Transfer Catalysts" *Adv. Synth. Catal.* **2017**, *359*, 2076–2089.

[45] E. J. Moore, V. Steck, P. Bajaj, R. Fasan, "Chemoselective Cyclopropanation over Carbene Y–H Insertion Catalyzed by an Engineered Carbene Transferase" *J. Org. Chem.* **2018**, *83*, 7480–7490.

[46] M. Bordeaux, R. Singh, R. Fasan, "Intramolecular C(sp^3)–H Amination of Arylsulfonyl Azides with Engineered and Artificial Myoglobin-Based Catalysts" *Bioorg. Med. Chem.* **2014**, *22*, 5697–5704.

[47] Y. Kagawa, K. Oohora, T. Hayashi, "Intramolecular C–H Bond Amination Catalyzed by Myoglobin Reconstituted with Iron Porphycene" *J. Inorg. Biochem.* **2024**, *252*, 112459.

[48] T. Hayashi, "Metalloporphycene Is an Attractive Cofactor for Hemoproteins" *Bull. Chem. Soc. Jpn.* **2023**, *96*, 1331–1338.

[49] T. Hayashi, H. Dejima, T. Matsuo, H. Sato, D. Murata, Y. Hisaeda, "Blue Myoglobin Reconstituted with an Iron

Porphycene Shows Extremely High Oxygen Affinity" *J. Am. Chem. Soc.* **2002**, *124*, 11226–11227.

[50] T. Matsuo, H. Dejima, S. Hirota, D. Murata, H. Sato, T. Ikegami, H. Hori, Y. Hisaeda, T. Hayashi, "Ligand Binding Properties of Myoglobin Reconstituted with Iron Porphycene: Unusual O_2 Binding Selectivity against CO Binding" *J. Am. Chem. Soc.* **2004**, *126*, 16007–16017.

[51] J. Nomura, H. Hashimoto, T. Ohta, Y. Hashimoto, K. Wada, Y. Naruta, K. Oinuma, M. Kobayashi, "Crystal Structure of Aldoxime Dehydratase and Its Catalytic Mechanism Involved in Carbon–Nitrogen Triple-Bond Synthesis" *Proc. Natl. Acad. Sci. USA* **2013**, *110*, 2810–2815.

[52] K. Konishi, K. Ishida, K.-I. Oinuma, T. Ohta, Y. Hashimoto, H. Higashibata, T. Kitagawa, M. Kobayashi, "Identification of Crucial Histidines Involved in Carbon–Nitrogen Triple Bond Synthesis by Aldoxime Dehydratase" *J. Biol. Chem.* **2004**, *279*, 47619–47625.

[53] Y. Kato, S. Yoshida, S.-X. Xie, Y. Asano, "Aldoxime Dehydratase Co-existing with Nitrile Hydratase and Amidase in the Iron-Type Nitrile Hydratase-Producer *Rhodococcus* sp. N-771" *J. Biosci. Bioeng.* **2004**, *97*, 250–259.

[54] H. Sawai, H. Sugimoto, Y. Kato, Y. Asano, Y. Shiro, S. Aono, "X-ray Crystal Structure of Michaelis Complex of Aldoxime Dehydratase" *J. Biol. Chem.* **2009**, *284*, 32089–32096.

[55] F. W. J. Teale, "Cleavage of the Haem–Protein Link by Acid Methylethylketone" *Biochim. Biophys. Acta* **1959**, *35*, 543.

[56] K. Oohora, A. Onoda, H. Kitagishi, H. Yamaguchi, A. Harada, T. Hayashi, T. "A chemically-controlled supramolecular protein polymer formed by a myoglobin-based self-assembly system" *Chem. Sci.* **2011**, *2*, 1033–1038.

[57] Kobayashi, K.; Yoshioka, S.; Kato, Y.; Asano, Y.; Aono, S. Regulation of Aldoxime Dehydratase Activity by Redox-dependent Change in the Coordination Structure of the Aldoxime-Heme Complex. *J. Biol. Chem.* **2005**, *280*, 5486–5490.

Chapter 2
Enhancement of Heme Biosynthesis via 5-Aminolevulinate Pathway Engineering in *E. coli* to Improve Hemoprotein-Based Biocatalysis

Reproduced in part with permission from [*Angew. Chem. Int. Ed.,* **2025***, 64,* e202512156.]
DOI: 10.1002/ange.202512156

2-1. Introduction

With recent significant advances in biotechnology, biocatalysis has emerged as a powerful synthetic platform which provides straightforward access to a wide variety of chemical feedstocks[1]. In particular, chemical transformation using hemoproteins is one of the most representative and well-studied models of biocatalysis. As exemplified by pioneering studies on the engineering of cytochrome P450s for carbene[2-4] and nitrene[5-8] transfer reactions, hemoproteins have demonstrated versatile catalytic activities not only for naturally occurring reactions found in nature but also for a variety of abiotic chemical transformations required for modern synthetic chemistry[9-21]. In spite of these great advances, recombinant expression systems for hemoproteins still need to be improved in order to put these biocatalytic tools into more practical applications. Because the biosynthesis of heme cofactor is tightly regulated in host organisms[22], overexpression of recombinant hemoproteins often leads to the undesired accumulation of inactive apoenzymes. The exogenous addition of 5-aminolevulinic acid (5-ALA) into the culture media is known to partially increase the production of holoenzymes. However, the cost of 5-ALA accounts for approximately 60% of the total cost of *E. coli* cell culture[23], which would be a drawback for the practical application of hemoprotein-based biocatalysis. To overcome this problem, the author here carried out the metabolic engineering of heme biosynthetic pathway in *E. coli* to enable recombinant expression of active holohemoproteins.

Heme biosynthesis begins with the production of 5-ALA[24]. In most bacteria including *E. coli*, 5-ALA is synthesized via the C5 pathway, which involves two key enzymes, glutamyl-tRNA reductase (GluTR) and glutamate-1-semialdehyde aminomutase (GSAM) (Fig. 2-1a, pathway in green)[25]. GluTR promotes the reduction of glutamyl-tRNA to produce glutamate-1-semialdehyde, and GSAM converts glutamate-1-semialdehyde into 5-ALA via PLP-mediated transamination reaction. Because the activity of GluTR is strictly regulated by feedback inhibition of the end-product heme[22], the synthesis of 5-ALA generally serves as a bottleneck in the production of the heme cofactor. Previous studies have demonstrated that engineering the intrinsic C5 pathway can partially enhance holohemoprotein expression in *E. coli*. For example, overexpression of GluTR enhances 5-ALA supply, leading to increased heme biosynthesis; the resulting accumulation of heme renders GluTR intrinsically unstable and triggers its degradation[23]. In other work, excess free heme was shown to impose an additional layer of feedback control by repressing the transcription of GSAM, thereby slowing the conversion of glutamate-1-semialdehyde to 5-ALA and restricting pathway flux[26]. More recently, modular optimization of the C5 pathway has led to improved the heme production; however, this system remains highly sensitive to metabolic imbalance. Even modest overexpression of certain

downstream genes results in the accumulation of porphyrin intermediates, which are cytotoxic and severely impair cell growth and hemoprotein assembly[27]. Thus, despite pathway engineering, the C5 pathway remains under stringent feedback regulation, and also excessive GluTR overexpression ultimately causes growth inhibition, as discussed below. To address this issue, the author focused on a heterogeneous biosynthetic pathway of 5-ALA, so called C4 pathway, which is conserved in α-proteobacteria, fungi, and yeast (Fig. 2-1a, pathway in yellow). The C4 pathway involves only one enzyme, 5-aminolevulinic acid synthase (ALAS), which produces 5-ALA by condensation of succinyl-CoA with glycine[28-31]. Since the activity of heterogeneous ALAS is not likely to be affected by the intrinsic regulation system of *E. coli* cell, the co-expression of ALAS is expected to increase the intracellular concentration of 5-ALA via the heterogeneous C4 pathway, thereby improving the efficiency of the heme cofactor incorporation into the recombinant hemoproteins (Fig. 2-1b). Based on this concept, the author here constructed an ALAS-based synthetic C4 pathway for "self-supplementation" of 5-ALA in *E. coli* host cells and applied the engineered strain to whole-cell and lysate-based biocatalysis using various types of heme-dependent enzymes.

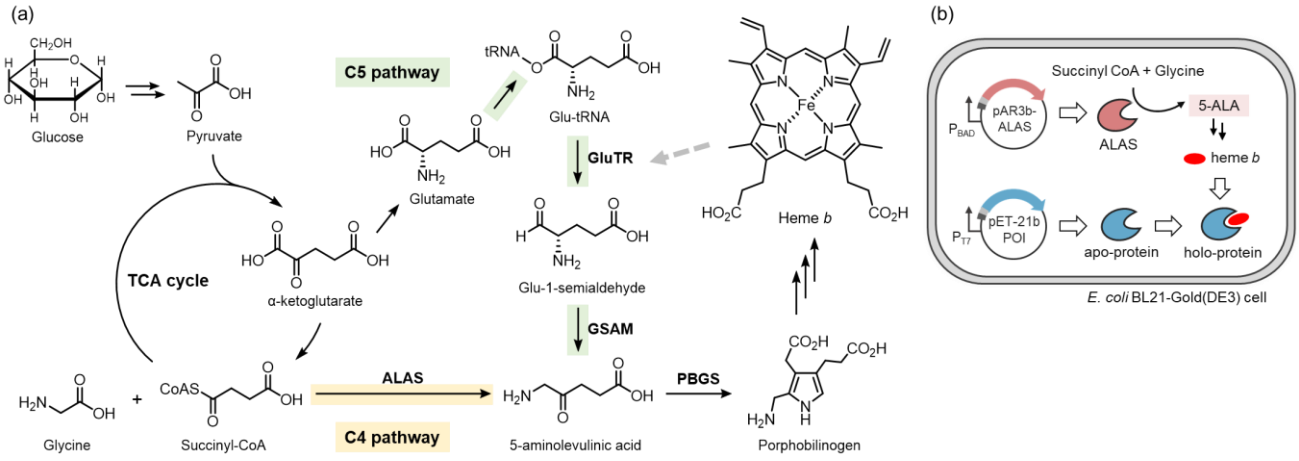


Figure 2-1. (a) C5 and C4 pathways for the biosynthesis of 5-ALA. (b) Self-supplementation strategy of 5-ALA via heterogeneous C4 pathway for the recombinant expression of holohemoproteins.

2-2. Results and discussion

Screening of ALAS and GluTR

The author first screened a panel of ALASs for the recombinant expression of holohemoproteins. The genes of ALASs from eight different microorganisms were selected from UniProt database (Table 2-1) and cloned into pAR3b vector[32] to construct a helper plasmid, pAR3b-ALAS, for self-supplementation of 5-ALA via the C4-pathway. In addition, helper plasmids, pAR3b-GluTR, which express 15 different types of GluTRs were also prepared to enhance the flux of the intrinsic C5 pathway as a comparison (Table 2-2)[23,26,27]. These two types of helper plasmids were then transformed into *E. coli* BL21-Gold(DE3) strain, and the resulting cells harboring pAR3b-ALAS or pAR3b-GluTR were used for recombinant expression of hemoproteins based on the pET system. In the initial screening, protoglobin from *Aeropyrum pernix* (ApPGb, UniProt ID: Q9YFF4) was selected as a model hemoprotein for the following three reasons: (i) ApPGb has been widely utilized as a biocatalyst for abiotic chemical transformations[33-38]. (ii) ApPGb is able to be expressed at high levels in *E. coli.* (iii) Recombinant expression of

ApPGb is known to require the addition of 5-ALA in the culture medium. Accordingly, the *E. coli* cells harboring pAR3b-ALAS/GluTR were transformed with the expression plasmid for ApPGb (pET21b-ApPGb) and cultivated in a normal LB medium using a 96-well microplate. During the log growth phase, the expression of ApPGb and ALAS/GluTR was induced by adding IPTG and arabinose, respectively, to investigate the effect of 5-ALA self-supplementation. The results showed that *E. coli* cell pellets expressing several ALASs and GluTRs exhibited characteristic orange color corresponding to holo-ApPGb compared to negative control cells without the helper pAR3b plasmids. In particular, ALAS from *Bradyrhizobium diazoefficiens* (BdALAS, UniProt ID: P08262), ALAS from *Paracoccus denitrificans* (PdALAS, UniProt ID: P43089), and ALAS from *Caulobacter segnis* (CsALAS, UniProt ID: D5VJ52), gave a relatively high concentration of holo-hemoproteins as estimated by UV-vis absorbance in the supernatant of *E. coli* cell lysates (Fig. 2-2). Co-expression of these three ALASs did not interfere with the final concentration of *E. coli* cells nor the expression of ApPGb (Fig. 2-3, 2-4), while co-expression of GluTRs mostly resulted in lower cell densities and decreased expression levels. The excessive consumption of glutamyl-tRNA by GluTR may have disturbed protein synthesis and *E. coli* cell growth. These initial screening results led us to select BdALAS, PdALAS, and CsALAS for further investigations.

Table 2-1. List of 5-aminolevulinate synthases (ALAS) and Glutamyl-tRNA reductase (GluTR)

Abbreviation	Organism	NBRC number	Taxonomy	UniProt ID	M.W. (kDa)
BdALAS	*Bradyrhizobium diazoefficiens*	14792	*Pseudomonadota (Alphaproteobacteria)*	P08262	45.7
PdALAS	*Paracoccus denitrificans*	13301	*Pseudomonadota (Alphaproteobacteria)*	P43089	45.7
MeALAS	*Methylorubrum extorquens*	15686	*Pseudomonadota (Alphaproteobacteria)*	A0A2N9AN23	63.6
CsALAS	*Caulobacter segnis*	15250	*Pseudomonadota (Alphaproteobacteria)*	D5VJ52	45.2
RbeALAS	*Rhizobium etli*	15573	*Pseudomonadota (Alphaproteobacteria)*	Q2K3J3	45.3
GtALAS	*Geobacillus thermoglucosidasius*	107763	*Bacillota*	A0A1Y3PCE6	46.3
KsALAS[a]	*Kitasatospora setae*	14216	*Actinomycetota*	E4NJF0	44.8
SrALAS[a]	*Streptosporangium roseum*	3776	*Actinomycetota*	D2BCN4	45.1

[a]annotated as 8-amino-7-oxononanoate synthase, a similar PLP-dependent enzymes

Table 2-2. List of 5-aminolevulinate synthases (ALAS) and Glutamyl-tRNA reductase (GluTR)

Abbreviation	Organism	NBRC number	Taxonomy	UniProt ID	M.W. (kDa)
EcGluTR	*Escherichia coli*	3301	*Pseudomonadota* (*Gammaproteobacteria*)	P0A6X1	47.5
PpGluTR	*Pseudomonas putida*	14164	*Pseudomonadota* (*Gammaproteobacteria*)	A5VYG4	47.5
CmGluTR	*Cupriavidus metallidurans*	102507	*Pseudomonadota* (*Betaproteobacteria*)	Q1LIF4	48.7
LmnGluTR	*Lebetimonas natsushimae*	112478	*Pseudomonadota* (*Epsilonproteobacteria*)	A0A292YF95	49.5
HtGluTR	*Hydrogenophilus thermoluteolus*	14978	*Pseudomonadota* (*Hydrogenophilia*)	A0A2Z6DWL2	46.9
GkGluTR	*Geobacillus kaustophilus*	102445	*Bacillota*	Q5KWK4	50.9
DrGluTR	*Deinococcus radiodurans*	15346	*Deinococcota*	Q9RRE5	38.7
FjGluTR	*Flavobacterium johnsoniae*	14942	*Bacteroidota*	A5FLE3	47.9
LlGluTR	*Luteolibacter luteus*	114341	*Verrucomicrobiota*	A0A858RN55	37.6
DdGluTR	*Deferribacter desulfuricans*	101012	*Deferribacterota*	D3PCG4	49.6
HgtGluTR	*Hydrogenobacter thermophilus*	102181	*Aquificota*	D3DG42	47.8
TsaGluTR	*Thermosipho africanus*	109656	*Thermotogota*	B7IHG8	44.7
TvGluTR	*Thermoplasma volcanium*	15438	*Euryarchaeota* (*Archaea*)	Q97B68	47.9
ApGluTR	*Aeropyrum pernix*	100138	*Crenarchaeota* (*Archaea*)	Q9Y9J2	46.4
SutGluTR	*Sulfurisphaera tokodaii*	100140	*Thermoproteota* (*Archaea*)	Q976H4	48.5

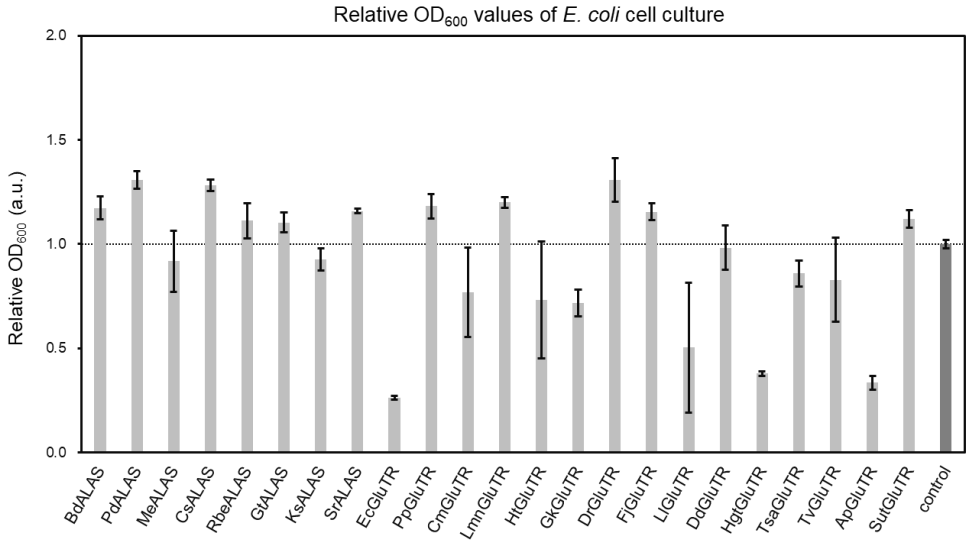


Figure 2-2. Relative OD_{600} values of the *E. coli* cell cultures harboring pET21b-ApPGb and pAR3b-ALAS/GluTR. Mean ± SD (n = 4, biological replicates). control: *E. coli* cells harboring only pET21b-ApPGb.

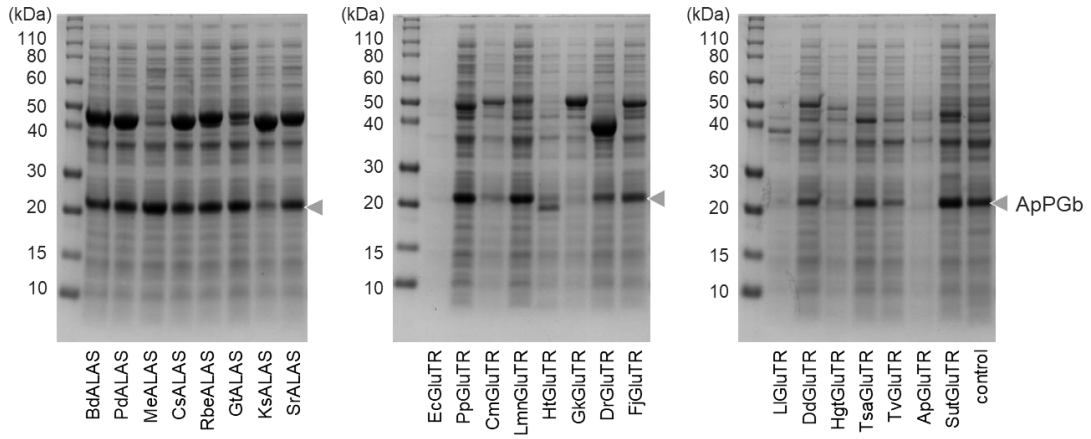


Figure 2-3. SDS-PAGE analysis for *E. coli* cells harboring pET21b-ApPGb and pAR3b-ALAS/GluTR. Molecular weights of each ALAS and GluTR were summarized in Table S1–S3. Molecular weight of ApPGb is calculated to be 24.5 kDa. control: *E. coli* cells harboring only pET21b-ApPGb.

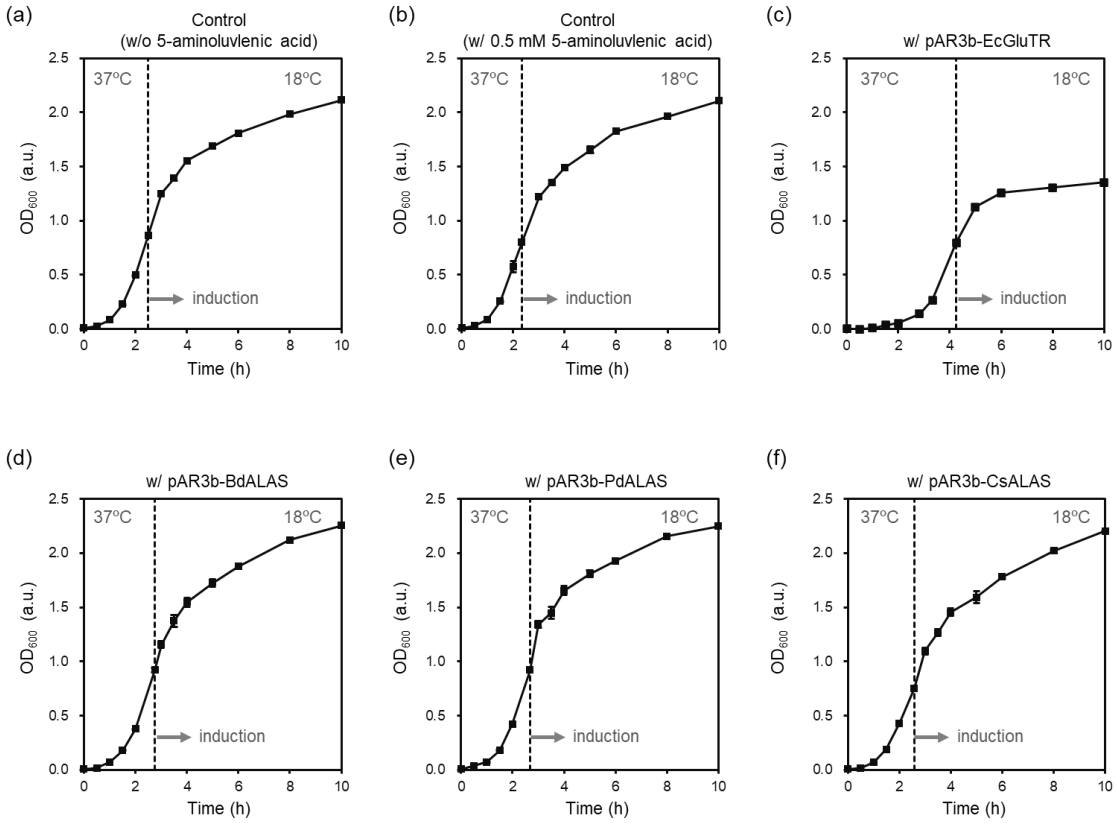


Figure 2-4. Growth curve of the *E. coli* cells harboring pET21b-ApPGb and pAR3b-ALAS/GluTR indicated by OD_{600} values. After the OD_{600} values reached approximately 0.7–0.9, IPTG (final conc. 0.20 mM) and arabinose (final conc. 2.0 mg/mL) were added to induce the expression of ApPGb and ALAS/GluTR, and the cultivation was continued at 18 ºC and 150 rpm. Mean ± SD (n = 2, biological replicates). (a) *E. coli* cells harboring only pET21b-ApPGb. (b) *E. coli* cells harboring only pET21b-ApPGb. The LB medium was supplemented with 0.50 mM 5-ALA. (c) *E. coli* cells harboring pET21b-ApPGb and pAR3b-EcGluTR. (d) *E. coli* cells harboring pET21b-ApPGb and pAR3b-BdALAS. (e) *E. coli* cells harboring pET21b-ApPGb and pAR3b-PdALAS. (f) *E. coli* cells harboring pET21b-ApPGb and pAR3b-CsALAS.

Construction of ALAS co-expression system

Next, the author investigated the influence of ALAS co-expression in details on a preparative scale using a 500 mL baffled flask. In addition to the pAR3b helper plasmid for BdALAS, PdALAS, and CsALAS, the helper plasmid for *E. coli* GluTR (EcGluTR) was also utilized as a negative control of the intrinsic C5 pathway similar to the previous studies[23,26,27]. The *E. coli* cells harboring pET21b-ApPGb and pAR3b-BdALAS/PdALAS/CsALAS/EcGluTR were cultivated in a normal LB medium in 100 mL scale, and the expression of ApPGb and ALASs or EcGluTR was induced by adding IPTG and arabinose after OD_{600} values reached approximately 0.7–0.9 (Fig. 2-5). As observed in the initial screening described above, the expression of EcGluTR largely inhibited the *E. coli* cell growth (Fig. 2-6). After 16 hours of cultivation time, the mass of the cell pellets expressing EcGluTR was less than half of the mass of the positive control cells with only pET21b-ApPGb (Fig. 2-7). On the other hand, the *E. coli* cells expressing ALASs exhibited a good growth curve comparable to that of the positive control cells (Fig. 2-6). The co-expression of these three ALASs did not affect the mass of obtained cell pellets (Fig. 2-7) nor the expression level of target hemoprotein (Fig. 2-8). Furthermore, pyridine hemochromagen assay[39] revealed that the content of heme in ApPGb has been significantly increased through the incorporation of the ALAS-based C4 pathway (Fig. 2-9). In particular, the co-expression of PdALAS provided the highest concentration of heme cofactor. Although the exogenous addition of 0.5 mM 5-ALA into the LB medium partially increased the production of holohemoproteins, PdALAS still gave better performance rather than such conventional expression methods. This is also true for the ApPGb solution after the protein purification (Fig. 2-10a). The production of 5-ALA in the cell was confirmed by LC-MS analysis (Fig. 2-10b, c). As the author expected, the incorporation of the PdALAS-based C4 pathway significantly increased the intracellular concentration of 5-ALA, whereas exogenous addition of 5-ALA into the medium did not largely contribute to the intracellular 5-ALA content. This might be due to the rapid consumption of 5-ALA during the cell cultivation and/or the poor activity of 5-ALA transport system in *E. coli*[40]. Continuous production of 5-ALA within the cell is considered to be crucial for increasing expression levels of holohemoproteins. LC-MS analysis also revealed increased levels of heme cofactor production within the cells, consistent with the results of the pyridine hemochromagen assay. On the other hand, the concentration of protoporphyrin IX, an intermediate in heme biosynthesis, was not affected by the co-expression of PdALAS. Since the biosynthetic intermediates of the heme cofactor exhibit cytotoxicity, this feature could provide benefits for cell growth.

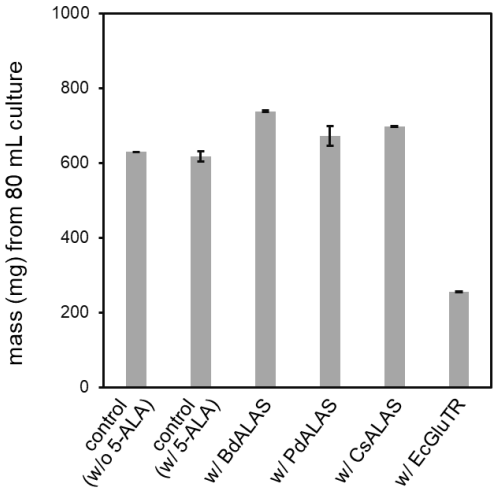


Figure 2-5. Mass of the *E. coli* cell pellets harboring pET21b-ApPGb and pAR3b-ALAS/GluTR obtained from 80 mL cultures. Mean ± SD (n = 2, biological replicates). Controls: *E. coli* cells harboring only pET21b-ApPGb. The cells were cultivated in the LB medium supplemented with (w/) and without (w/o) 0.50 mM 5-ALA.

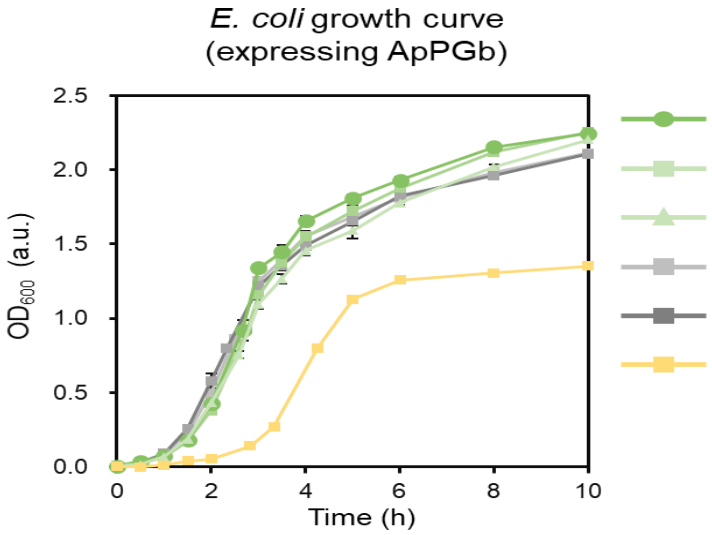


Figure 2-6. Growth curves of *E. coli* cells harboring pET21b-ApPGb and pAR3b-ALAS/GluTR indicated by OD_{600} values (w/o 5-ALA: *E. coli* cells harboring only pET21b-ApPGb were cultivated in the absence of 5-ALA. w/ 5-ALA: *E. coli* cells harboring only pET21b-ApPGb were cultivated in the presence of 0.50 mM 5-ALA.). After the OD_{600} values reached approximately 0.7–0.9, IPTG (final conc. 0.20 mM) and arabinose (final conc. 2.0 μg/mL) were added to induce the expression of ApPGb and ALAS/GluTR.

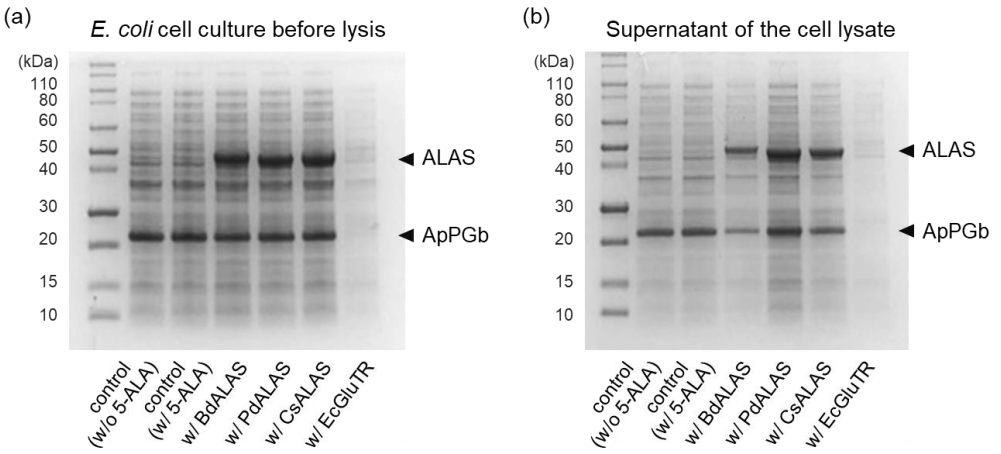


Figure 2-7. SDS-PAGE analysis on the *E. coli* cells harboring pET21b-ApPGb and pAR3b-ALAS/GluTR. (a) *E. coli* cell culture before lysis. (b) Supernatant of the *E. coli* cell lysate (ApPGb: 24.5 kDa, BdALAS: 45.7 kDa, PdALAS: 45.7 kDa, CsALAS: 45.2 kDa, and EcGluTR: 47.5 kDa). (controls: *E. coli* cells harboring only pET21b-ApPGb. The cells were cultivated in the LB medium supplemented with (w/) or without (w/o) 0.50 mM 5-ALA. BdALAS: *E. coli* cells harboring pET21b-ApPGb and pAR3b-BdALAS. PdALAS: *E. coli* cells harboring pET21b-ApPGb and pAR3b-PdALAS. CsALAS: *E. coli* cells harboring pET21b-ApPGb and pAR3b-CsALAS. EcGluTR: *E. coli* cells harboring pET21b-ApPGb and pAR3b-EcGluTR.)

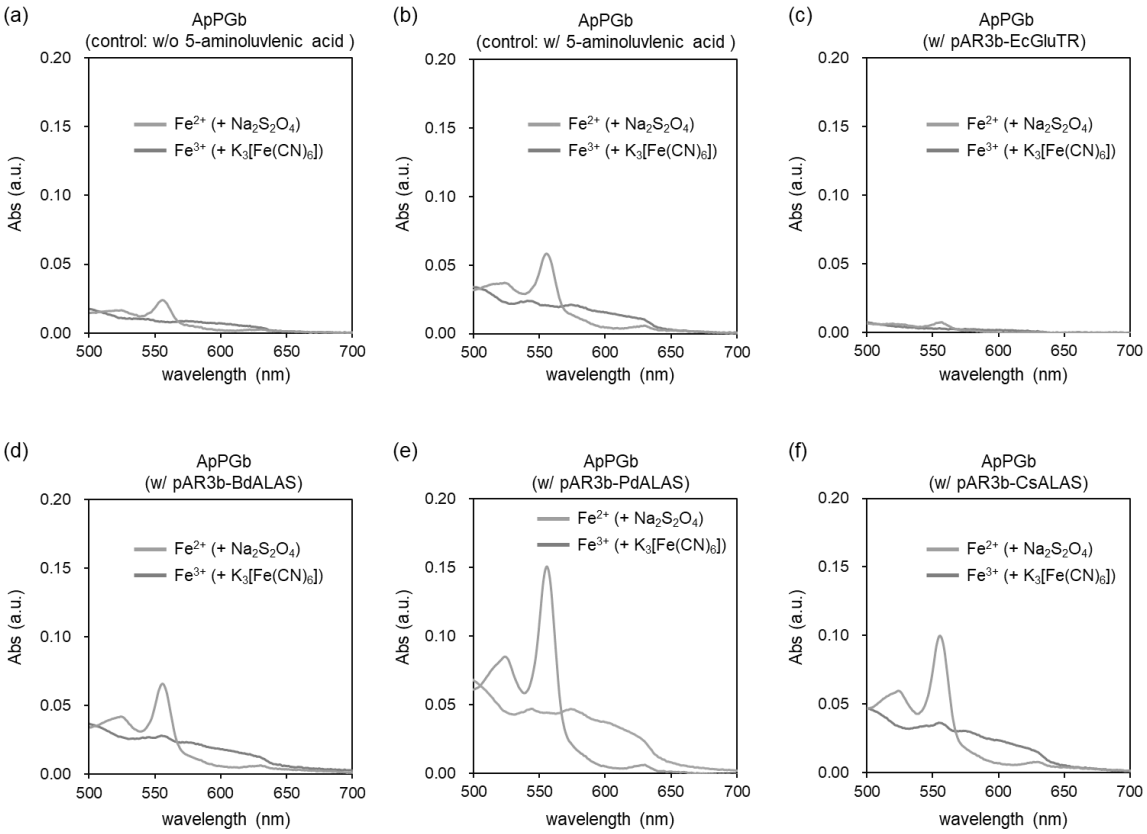


Figure 2-8. Pyridine hemochromagen assay for the *E. coli* cells harboring pET21b-ApPGb and pAR3b-ALAS/GluTR. UV-vis spectra of pyridine hemochromagen in the reduced samples and in the oxidized samples were shown in red and gray, respectively. (a) *E. coli* cells harboring only pET21b-ApPGb. (b) *E. coli* cells harboring only pET21b-ApPGb. The cells were cultivated in the presence of 0.50 mM 5-ALA. (c) *E. coli* cells harboring pET21b-ApPGb and pAR3b-EcGluTR. (d) *E. coli* cells harboring pET21b-ApPGb and pAR3b-BdALAS. (e) *E. coli* cells harboring pET21b-ApPGb and pAR3b-PdALAS. (f) *E. coli* cells harboring pET21b-ApPGb and pAR3b-CsALAS.

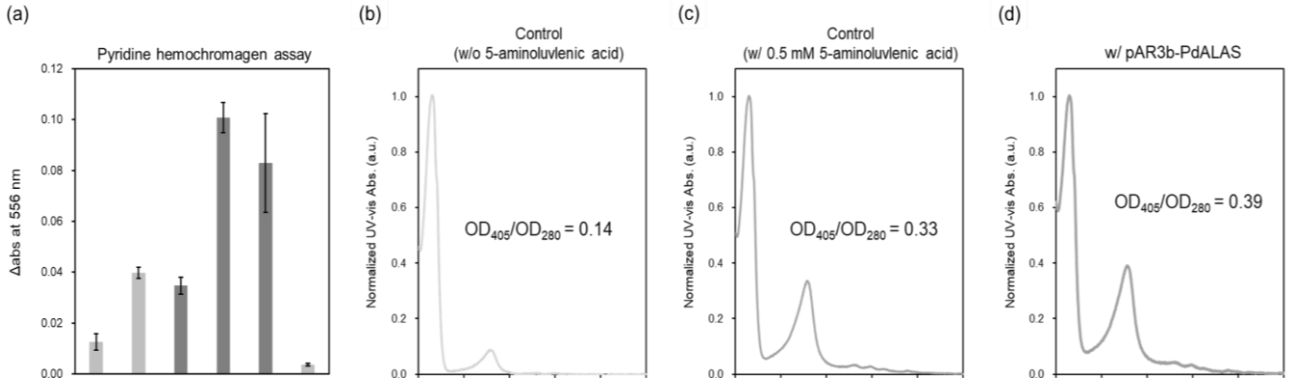


Figure 2-9. (a) Heme concentrations in the supernatant of *E. coli* cell lysates expressing ApPGb. The concentrations of heme were calculated based on the pyridine hemochromagen assay. (b) UV-vis spectra of the purified samples of ApPGb without (w/o) 5-ALA normalized at 280 nm. (c) UV-vis spectra of the purified samples of ApPGb with (w/) 0.50 mM 5-ALA normalized at 280 nm. (d) UV-vis spectra of the purified samples of ApPGb w/ pAR3b-PdALAS normalized at 280 nm.

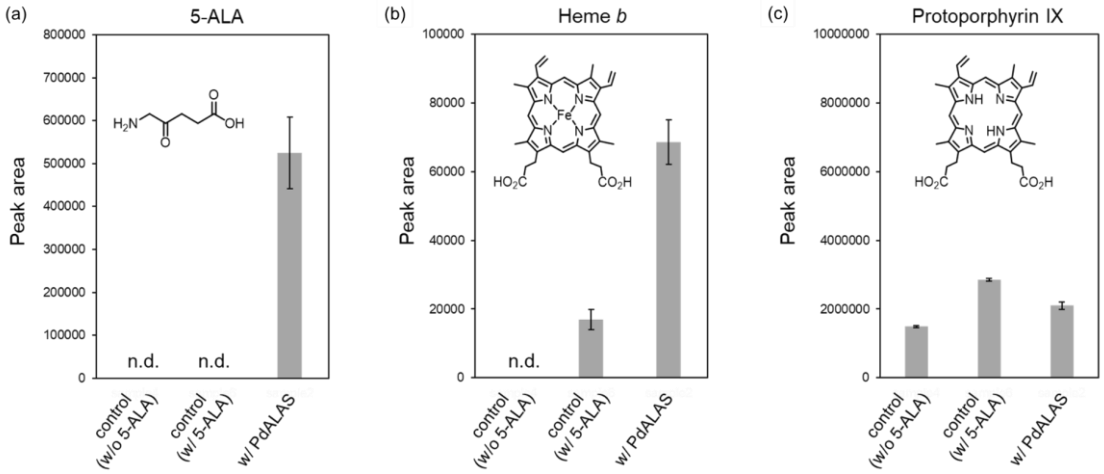


Figure 2-10. LC-MS analyses of 5-ALA (a), of heme *b* (b) and of protoporphyrin IX (c). The *E. coli* cells with or without pAR3b-PdALAS were used for the expression of ApPGb. After cultivation for 10 h, the cells were harvested by centrifugation, and the intracellular metabolites were extracted by bilayer extraction and analyzed by LC-MS. Peak areas of 5-ALA in LC-MS chromatograms are shown in bar graphs. Mean ± SD (n = 3, biological replicates).

Generality of PdALAS-enhanced *E. coli* for recombinant hemoprotein production

Motivated by these promising results of the PdALAS-based C4 pathway, the author next examined the generality of the engineered *E. coli* cell for recombinant expression of diverse hemoproteins. In addition to ApPGb, the *E. coli* cells incorporated with pAR3b-PdALAS were found to significantly increase the contents of the heme cofactor in various classes of hemoproteins (Fig. 2-11, Table 2-3). Particularly, the engineered cell was able to be widely applied to the expression of myoglobin (UniProt ID: P02185), bacterial hemoglobin (UniProt ID: A8IPS1), flavohemoglobin (UniProt ID: P49852), cytochrome b_{562} (UniProt ID: P0ABE7), peroxynitrite peroxidase (UniProt ID: O64527), dye-decolorizing peroxidase (UniProt ID: P76536), catalase (UniProt ID: P14412), catalase-related peroxidase (UniProt ID: B7X4G2), cytochrome P450BM3 (UniProt ID: P14779), NO synthase (UniProt ID: O34453), tryptophan 2,3-dioxygenase (UniProt ID: A0A1M6U789), aldoxime dehydratase (UniProt ID: UPI000400A70A),

latex clearing protein (UniProt ID: D1ADK3), and oxidative *N*-demethylase (UniProt ID: A4XXY9) as confirmed by the pyridine hemochromagen assay and SDS-PAGE. In all cases, the *E. coli* cells harboring pAR3b-PdALAS notably gave higher heme contents rather than that of the control cells cultivated by conventional methods.

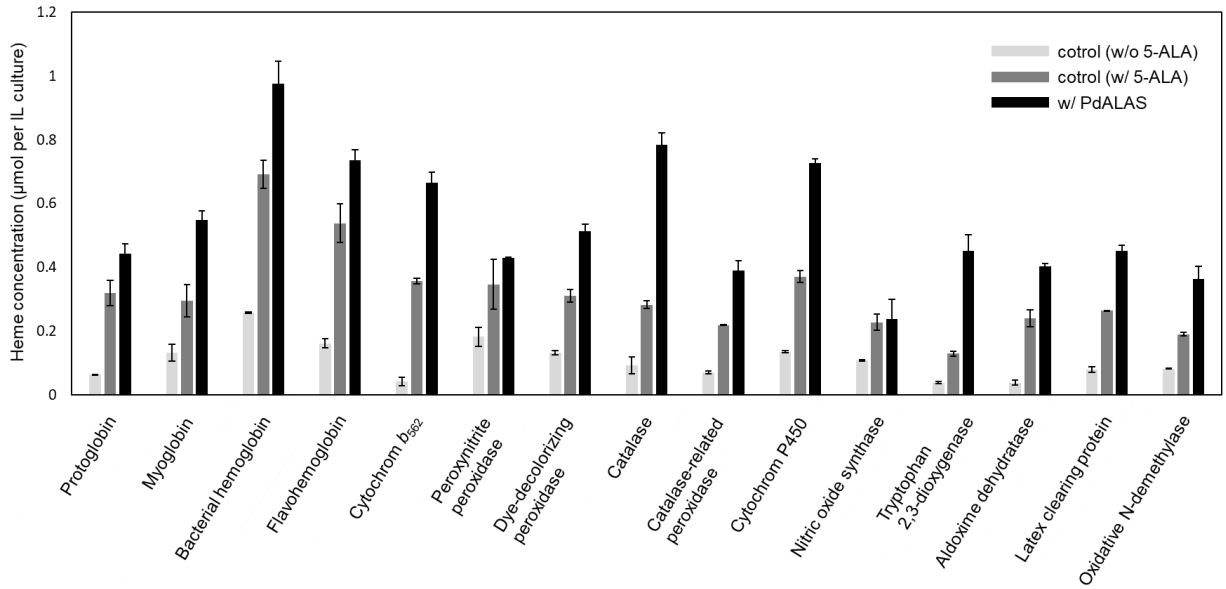


Figure 2-11. Heme concentrations in the supernatant of *E. coli* cell lysates expressing various hemoproteins.

Table 2-3. List of hemoprotein used in this study

Protein	Organism	UniProt ID	Expression vector	M.W. (kDa)
Protoglobin	*Aeropyrum pernix*	Q9YFF4	pET-21b	24.5
Myoglobin	*Physeter catodon*	P02185	pDEST	19.4
Bacterial hemoglobin	*Azorhizobium caulinodans*	A8IPS1	pET-21b	14.8
Flavohemoglobin	*Bacillus subtilis*	P49852	pET-21b	46.3
Cytochrome b_{562}	*Escherichia coli*	P0ABE7	pET-21b	13.9
Peroxynitrite peroxidase	*Arabidopsis thaliana*	O64527	pET-21b	20.5
Dye-decolorizing peroxidase	*Escherichia coli*	P76536	pET-21b	34.7
Catalase	*Geobacillus stearothermophilus*	P14412	pET-21b	84.5
Catalase-related peroxidase	*Comamonas testosteroni*	B7X4G2	pET-21b	35.6
Cytochrome P450	*Priestia megaterium*	P14779	pET-28a	117.8
Nitric oxide synthase	*Bacillus subtilis*	O34453	pET-21b	44.0
Tryptophan 2,3-dioxygenase	*Pseudonocardia thermophila*	A0A1M6U789	pET-21b	32.9
Aldoxime dehydratase	*Amycolatopsis thermoflava*	UPI000400A70A	pET-21b	42.2
Latex clearing protein	*Thermomonospora curvata*	D1ADK3	pET-21b	45.8
Oxidative *N*-demethylase	*Pseudomonas resinovorans*	A4XXY9	pET-21b	41.1

[a] for cytochrome P450 BM3 heme domain. [b] for full-length cytochrome P450 BM3.

Activity evaluation of hemoproteins expressed via the ALAS co-expression system

Finally, as a demonstration, biocatalysis using a series of heme-dependent enzymes was performed to take advantage of the engineered *E. coli* cells with the PdALAS-based C4 pathway (Fig. 2-12). The author first tested biocatalytic nitrene transfer reactions using an ApPGb variant, termed as HYA-5294, reported by F. H. Arnold and E. Alfonzo *et al*. (Fig. 2-12a)[37]. The *E. coli* cells supplemented with or without pAR3b-PdALAS were cultivated for the expression of ApPGb HYA-5294, and the lysates obtained from the same amount of cell culture were subjected to the heme-nitrene-mediated amination reaction of 4-fluorophenylboronic acid (**1**). Consequently, the cells with the C4 pathway were found to efficiently catalyze the target amination reaction and afforded 4-fluoroaniline (**2**) in 61% yield, while the cells without the C4 pathway show little activity (Fig. 2-12a). The introduction of the PdALAS-based C4 pathway significantly promoted the "holo" expression of ApPGb HYA-5294, thereby improving the performance of the lysate-based biocatalyst. The engineered cell was also able to be applied to abiotic carbene transfer reactions using bacterial hemoglobins from *Azorhizobium caulinodans* (Uniprot ID: A8IPS1) (Fig. 2-12b)[41]. The initial rate of cyclopropanation reaction of styrene (**3**) with ethyl diazoacetate (**4**) has significantly improved by the cell lysate

with the PdALAS-based C4 pathway (Fig. 2-12b). The desired product, ethyl 2-phenylcyclopropanecarboxylate (*S*,*S*)-**5,** was obtained in 66% yield with very high diastereo- and enantio-selectivities (>99% de, >99% ee). In contrast, the yield of (*S*,*S*)-**5** has decreased to less than half in the absence of the C4 pathway (Fig. 2-12b). Furthermore, the *E. coli* cells with pAR3b-PdALAS also accelerated a wide range of biocatalytic transformations, including hydroxylation reaction of benzene (**6**) using cytochrome P450BM3 with a decoy system[42-45] (Fig. 2-12c), dehydration reaction of octanal oxime (**8**) using aldoxime dehydratase[46,47] (Fig. 2-12d), degradation of natural rubber latex **10** using latex clearing protein[48] (Fig. 2-12e), peroxidation of ABTS using dye-decolorizing peroxidase[49] (Fig. 2-12f). In all cases, the incorporation of the C4 pathway significantly improved the catalytic performance of the whole-cell and lysate-based biocatalysts compared to the cells without the C4 pathway. These results clearly demonstrate the versatility of our PdALAS-based C4 pathway for the preparation of various types of hemoproteins and their biocatalysis.

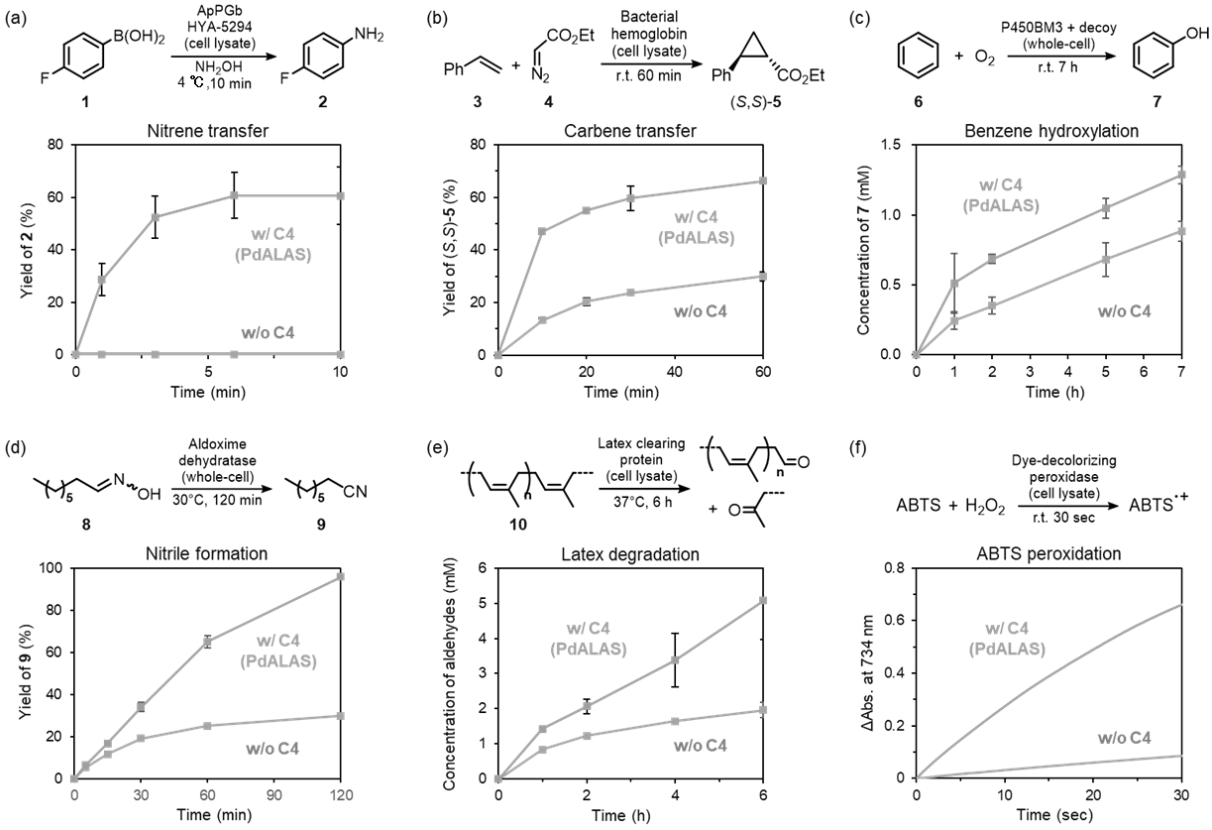


Figure 2-12. Heme concentrations in the supernatant of *E. coli* cell lysates expressing various hemoproteins.

2-3. Summary

In summary, the author here engineered the heme biosynthetic pathway in *E. coli* to develop an efficient cofactor supplementation system for the recombinant expression of hemoproteins. Through a series of enzyme screenings, ALAS from *Paracoccus denitrificans* (PdALAS), which efficiently increases the intracellular concentration of 5-ALA, was identified for the metabolic engineering. The incorporation of the PdALAS-based heterogeneous C4 pathway significantly increased the expression level of holohemoproteins. Notably, the heme contents in the engineered cells were even higher than that in conventional cultivation method in which 5-ALA is externally added into culture media. Thus, the engineered *E. coli* cells were shown to be versatile for the expression of various hemoproteins (including 15 examples). Furthermore, we applied the engineered *E. coli* cells for whole-cell and lysate-based biocatalysis using a series of heme-dependent enzymes, including protoglobin, cytochrome P450, aldoxime dehydratase, and so on. In all cases, the engineered *E. coli* cells with the heterogeneous C4 pathway exhibited improved catalytic activity rather than the normal *E. coli* cells without C4 pathway. Given the increasing demand for biocatalysis in recent years, the author is convinced that the system developed in this study will provide a powerful and practical platform for the implementation of the hemoprotein-based biocatalysis.

2-4. Experimental section

Instruments

Ultrapure water was demineralized using a Merck Millipore Milli-Q integral 3 system. PCR was performed using Bio-Rad T100™ Thermal Cycler. *E. coli* cells were cultivated using TAITEC BioShaker G·BR-300, BioShaker BR-23FP, BioShaker M·BR-024, and DWMax M·BR-034P, harvested using TOMY Suprema 21, Eppendorf centrifuge 5910R, 5430R, and HITACHI High speed Micro Centrifuge CF15RN, and disrupted using Qsonica Ultrasonic Homogenizer Q700. UV-vis spectra were measured with a Shimadzu UV-2700 spectrophotometer and Molecular Devices SpectraMax iD5 Multi-Mode Microplate Reader. Optical density was measured using a Shimadzu UV-2700 spectrophotometer and Molecular Devices SpectraMax iD5 Multi-Mode Microplate Reader. The GC experiments were performed on a Shimadzu GC-2010 Plus gas chromatograph equipped with a DB-1 column (Agilent Technologies, Inc.) or a SUPELCO Beta DEXTM 120 fused silica capillary column (Merck Ltd.). LC-MS experiments were performed on Bruker compact QTOF mass spectrometer connected with Shimadzu Nexera HPLC equipped with YMC-Triart C18 column or a liquid chromatography-quadrupole time-of-flight/mass spectrometer (LC-QTOF/MS, LCMS-9050, Shimadzu, Kyoto, Japan) equipped with a Discovery® HS F5 HPLC column (Merck, Darmstadt, Germany) or an Acquity UPLC peptide BEH C18 column (Waters, Milford, MA, USA).

Materials

All reagents of the highest guaranteed grade were purchased from TCI Co., Ltd., Merck Ltd., FUJIFILM Wako Pure Chemical Corporation and Nacalai Tesque, Inc., and used as received unless otherwise noted. Oligonucleotides were obtained from Merck Ltd. and Eurofins Scientific SE, Inc. The gene of ApPGb HYA-5294 was purchased from Twist Bioscience Corp. The genes of the other enzymes were obtained by PCR from genomic

DNA of the corresponding bacteria purchased from Biological Resource Center, National Institute of Technology and Evaluation (NBRC). The genes then cloned into pAR3b vector (for 5-aminolevulinic acid synthases and Glutamyl-tRNA reductases) or pET-21b vector (for hemoproteins) for protein expressions. Nucleotide sequences were determined by Eurofins Scientific SE, Inc.

Preparation of the expression plasmid pAR3b-ALAS and pAR3b-GluTR

The expression plasmids pAR3b-ALAS and pAR3b-GluTR were constructed according to the standard protocol of NEBuilder® HiFi DNA Assembly Cloning Kit (New England Biolabs Japan). Each insert genes for ALAS and GluTR were amplified by PCR from genomic DNA of corresponding bacteria using PrimeSTAR® GXL DNA Polymerase (Takara Bio Inc.) (Tables 2-1, 2-2, 2-4, 2-5, 2-6). The PCR products were then purified by agarose gel electrophoresis and assembled with a linearized pAR3b vector using the NEBuilder HiFi DNA Assembly Cloning Kit (New England Biolabs Japan). The assembled products were then transformed into the chemically competent *E. coli* DH5α cell, and transformants were directly transferred into 15 mL of LB medium containing chloramphenicol (20 μg/mL). After overnight cultivation at 37 ºC, the plasmids were purified using a NucleoSpin® Plasmid purification kit (Takara Bio Inc.) and subjected to the screening as follows to identify promising enzymes which can improve the production of holohemoproteins.

Table 2-4. Primers used for the cloning of ALAS into pAR3b vector

Primer name	DNA sequence
pAR3b vector (forward)	TAATAATTGCCCTGCACCTCGCAGAAATAAACAAAC
pAR3b vector (reverse)	TGTGGTCTCGTTATCTTTGATCTTCGTCATTG
BdALAS (forward)	AAAGATAACGAGACCACAATGGATTACAGCCAGTTCTTTAATTCCG
BdALAS (reverse)	GGTGCAGGGCAATTATTACTCCGCCGCCAGCGACTTTTGCTTGAG
PdALAS (forward)	AAAGATAACGAGACCACAATGGACTATTCAGCTGCCCTCGATCAG
PdALAS (reverse)	GGTGCAGGGCAATTATTAGGCAGCCGAAGTTGAACGGTTCAGTTTGC
MeALAS (forward)	AAAGATAACGAGACCACAATGCAAAGGACCACCGATCAATTGATGC
MeALAS (reverse)	GGTGCAGGGCAATTATTACGAGACCTCGCCCCAGCCCAGGCGTGAAC
CsALAS (forward)	AAAGATAACGAGACCACAGACTACAAAGCCGCGTTCCGCAGCGCCGTCGATC
CsALAS (reverse)	GGTGCAGGGCAATTATTAGGCCGCGTAGCCGCCCATCCGGGCGACGTTG
RbeALAS (forward)	AAAGATAACGAGACCACAATGGATTTCGAAGCATTTTTCAAAAACGAGCTG
RbeALAS (reverse)	GGTGCAGGGCAATTATTAGGCGACGTGCCTTGCCAGCGCGCAACG
GtALAS (forward)	AAAGATAACGAGACCACAATGTATGCCGAGATTCTCAGCGACAAG
GtALAS (reverse)	GGTGCAGGGCAATTATTATGCGTACACATCTGCTGCCGACTGC
KsALAS (forward)	AAAGATAACGAGACCACAATGAACCAATACCTGGAGATCTTCTCG
KsALAS (reverse)	GGTGCAGGGCAATTATTATTCCCGGGCCCGCGGCACGCCCAGCTC
SrALAS (forward)	AAAGATAACGAGACCACAACAAAAGTCTCCACCCGGCCCCACGTCTTC
SrALAS (reverse)	GGTGCAGGGCAATTATTACGCGCGAGCGAGGCACGATTCCAGGGCGTATGC

Table 2-5. Primers used for the cloning of GluTR into pAR3b vector

Primer name	DNA sequence
pAR3b vector (forward)	TAATAATTGCCCTGCACCTCGCAGAAATAAACAAAC
pAR3b vector (reverse)	TGTGGTCTCGTTATCTTTGATCTTCGTCATTG
EcGluTR (forward)	AAAGATAACGAGACCACAATGACCCTTTTAGCACTCGGTATCAACC
EcGluTR (reverse)	GGTGCAGGGCAATTATTACTCCAGCCCGAGGCTGTCGCGCAGAATATTCAG
PpGluTR (forward)	AAAGATAACGAGACCACAATGGCCTTTCTTGCACTTGGTATCAACC
PpGluTR (reverse)	GGTGCAGGGCAATTATTATTGCGGGGATTTGTCCGTGGAGCCCTCGTTG
CmGluTR (forward)	AAAGATAACGAGACCACAATGCAACTGCTCGCGATCGGTATCAATCAC
CmGluTR (reverse)	GGTGCAGGGCAATTATTAGCGCTCGGAGTGGCTGCTGTGGCGGAACAG
LmnGluTR (forward)	AAAGATAACGAGACCACAATGTATTTTATAATTAGTTTTAACTATAGAAATTCAG
LmnGluTR (reverse)	GGTGCAGGGCAATTATTATTTGAGTATTCCCTTATCCATATGATATTCAC
HtGluTR (forward)	AAAGATAACGAGACCACAATGCCCTTTTTCGCGATTGGCCTCAAC
HtGluTR (reverse)	GGTGCAGGGCAATTATTATCGTTGCGTCTTCTCCCAACCAAAGAG
GkGluTR (forward)	AAAGATAACGAGACCACAATGCAAATCGTAGTCGTTGGCGTCGAC
GkGluTR (reverse)	GGTGCAGGGCAATTATTAGCGGGCGGCACGGACCGCTTCCGCGTCTTG
DrGluTR (forward)	AAAGATAACGAGACCACAATGCCGCAGCCCGCACCGCTCGATTTTGTG
DrGluTR (reverse)	GGTGCAGGGCAATTATTAATCACACGCCAAGGCCAGCTCCGCTTG

Table 2-6. Primers used for the cloning of GluTR into pAR3b vector

Primer name	DNA sequence
pAR3b vector (forward)	TAATAATTGCCCTGCACCTCGCAGAAATAAACAAAC
pAR3b vector (reverse)	TGTGGTCTCGTTATCTTTGATCTTCGTCATTG
FjGluTR (forward)	AAAGATAACGAGACCACAATGGAAAACAATAACGTACCGAAACACC
FjGluTR (reverse)	GGTGCAGGGCAATTATTAAGATGCTTTTATTTTGAAGACTTTTTCGATCC
LlGluTR (forward)	AAAGATAACGAGACCACAATGGAACTCGTCTGCGTCGGTCTGAATC
LlGluTR (reverse)	GGTGCAGGGCAATTATTACGTACCGGGTAAATTCAGCTTGATCAG
DdGluTR (forward)	AAAGATAACGAGACCACAATGCAATTAGCTGTTGTAGGGATAAATCAC
DdGluTR (reverse)	GGTGCAGGGCAATTATTACTCCTTTAATTTAAATAATATTTCAGCCGCTTCAG
HgtGluTR (forward)	AAAGATAACGAGACCACAATGGATCGCATATTTGTATGGGGGATTAAC
HgtGluTR (reverse)	GGTGCAGGGCAATTATTAAGCTCCATCAGCTCTGTTATGGACATAGG
TsaGluTR (forward)	AAAGATAACGAGACCACAATGCTGAATAATCTAAAAATGATAGGCATAGG
TsaGluTR (reverse)	GGTGCAGGGCAATTATTATTCACCCTTTAAATATTGGATATGATAACTTGC
TvGluTR (forward)	AAAGATAACGAGACCACAATGTTAATGAATATAGTTACTTTGATTTCGTG
TvGluTR (reverse)	GGTGCAGGGCAATTATTAGGATTTTTGCAATAACTGACGAGTTCG
ApGluTR (forward)	AAAGATAACGAGACCACAATGATAGACAGGCTCGCCATGATAGGGGTAAACG
ApGluTR (reverse)	GGTGCAGGGCAATTATTACCCGGTGCTACCGTTTTTAAACCCGGAGTTC
SutGluTR (forward)	AAAGATAACGAGACCACAATGAGTGACGAATTTATAGATATAAACAATTATATAGC
SutGluTR (reverse)	GGTGCAGGGCAATTATTATTTTTCCTTAGCCTCCTCGGTCTTAGAG

Procedure for the screening of ALAS and GluTR

The expression plasmids pAR3b-ALAS and pAR3b-GluTR were transformed into chemically competent *E. coli* BL21-Gold(DE3) cell (Agilent Technologies, Inc.) which harbors pET21b-ApPGb for the expression of *Aeropyrum pernix* protoglobin. The resulting transformants were plated on LB agar medium containing ampicillin (100 μg/mL) and chloramphenicol (20 μg/mL) and incubated at 37 ºC overnight. Four single colonies obtained were then inoculated into a 96-well microplate filled with 100 μL of LB medium containing ampicillin (100 μg/mL) and chloramphenicol (20 μg/mL) and cultivated at 37 ºC and 1,200 rpm for 12 h. The culture (7.5 μL) was then transferred into another 96 deep-well plate filled with 750 μL of LB medium containing ampicillin (100 μg/mL) and chloramphenicol (20 μg/mL). After incubation at 37 ºC and 1,200 rpm for 2.5 h, IPTG (final conc. 0.20 mM) and arabinose (final conc. 2.0 mg/mL) were added to induce the expression of ApPGb and ALAS/GluTR, and cultivation was continued at 18 ºC and 1,200 rpm for 20 h. Cell concentrations in the culture were evaluated with OD_{600} values using Microplate Reader (Fig. 2-2), and the expression of ApPGb and ALAS/GluTR was examined by SDS-PAGE (Fig. 2-13). The *E. coli* cells were then harvested by centrifugation at 4,300 *g* for 10 min, resuspended in 100 μL of Tris-HCl buffer (100 mM Tris-HCl, 150 mM NaCl, 1.0 mM EDTA, pH = 8.0), and stored at −20 °C. The frozen cells were then thawed at 4 °C for 2 h and lysed by adding 50 μL of Tris-HCl buffer (100 mM Tris-HCl, 150 mM NaCl, 1.0 mM EDTA, pH = 8.0) containing 10 μg lysozyme, 12.5 U benzonase® nuclease, and 0.5 % Triton X-100. After incubation at 37 °C for 1 h, the lysed cells were centrifuged at 4,300 × g for 15 min. The contents of holohemoproteins in the supernatants were roughly measured by differential absorbance between 400 nm and 450 nm using the microplate reader.

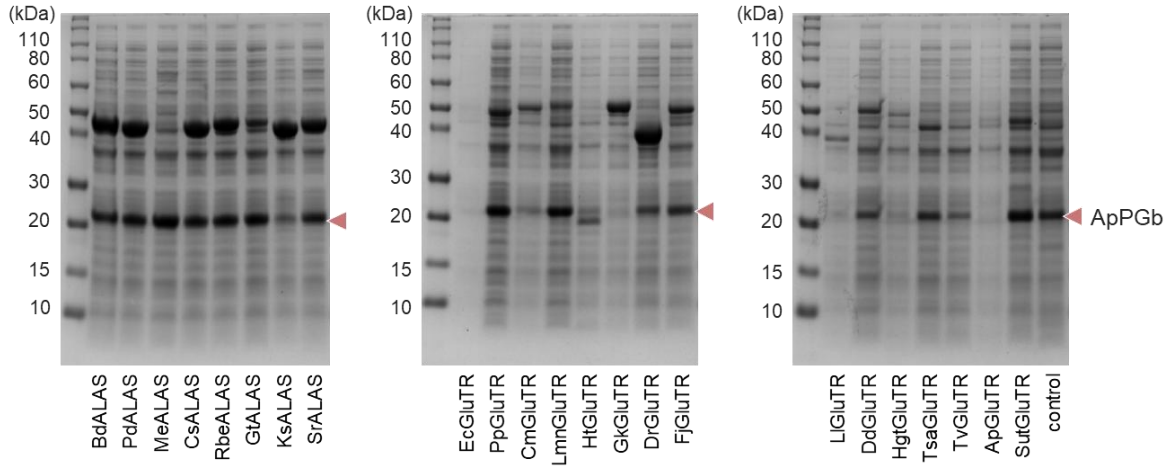


Figure 2-13. SDS-PAGE analysis for *E. coli* cells harboring pET21b-ApPGb and pAR3b-ALAS/GluTR. Molecular weights of each ALAS and GluTR were summarized in Tables 2-1 – 2-3. Molecular weight of ApPGb is calculated to be 24.5 kDa. control: *E. coli* cells harboring only pET21b-ApPGb.

Comparison of BdALAS, PdALAS, CsALAS and EcGluTR

The pAR3b plasmids encoding the gene for BdALAS, PdALAS, CsALAS and EcGluTR were transformed into chemically competent *E. coli* BL21-Gold(DE3) cell (Agilent Technologies, Inc.) which harbors pET21b-ApPGb for the expression of *Aeropyrum pernix* protoglobin. The resulting transformants were then plated on LB agar medium containing ampicillin (100 μg/mL) and chloramphenicol (20 μg/mL) and incubated at 37 ºC overnight. The

obtained single colonies were inoculated into 10 mL of LB medium containing ampicillin (100 μg/mL) and chloramphenicol (20 μg/mL) and cultivated at 37 ºC and 180 rpm for 12 h. The culture (1.0 mL) was then transferred into 100 mL of LB medium containing ampicillin (100 μg/mL) and chloramphenicol (20 μg/mL) and cultivated at 37 ºC and 150 rpm for 2.5 h. When OD_{600} values reached approximately 0.7–0.9, IPTG (final conc. 0.20 mM) and arabinose (final conc. 2.0 mg/mL) were added to induce the expression of ApPGb and ALAS/GluTR, and cultivation was continued at 18 ºC and 150 rpm for 20 h. As control experiments, the *E. coli* BL21-Gold(DE3) cells which did not possess the expression plasmids for ALAS/GluTR were also cultivated in LB medium supplemented with or without 5.0 mM of 5-aminolevlinic acid at the same time. During the cultivation, the cell growth was monitored by using OD_{600} values, and the expression of ApPGb and ALAS/GluTR was examined by SDS-PAGE. The *E. coli* cells were then harvested by centrifugation at 6,000 *g* for 10 min, and stored at −20 °C. The frozen *E. coli* cells were thawed on water bath at room temperature and resuspended in 3.0 mL of Tris-HCl buffer (100 mM Tris-HCl, 150 mM NaCl, 1.0 mM EDTA, pH = 8.0). The cells were then disrupted by using Qsonica Ultrasonic Homogenizer Q700 (amplitude: 40, process time: 30 sec × 6, pulse-ON time: 1 sec, pulse-OFF time: 1 sec) and the resulting lysate was centrifuged at 4,300 *g* and 4 ºC for 10 min. The supernatants (1.0 mL) were then transferred to another tube and further centrifuged at 20,000 *g* and 4 ºC for 3 min for pyridine hemochromagen assay. The supernatant (0.50 mL) was mixed with 0.5 mL of potassium ferricyanide solution (500 μM $K_3Fe(CN)_6$ in 0.2 M $NaOH_{aq}$ containing 40 v/v% pyridine), and UV-vis spectra of the oxidized samples were recorded from 400 nm to 800 nm. The oxidized samples were then treated with 10 μL of sodium dithionite solution (0.5 M $Na_2S_2O_4$ in 0.5 M $NaOH_{aq}$), and UV-vis spectra of the resulting reduced samples were recorded from 400 nm to 800 nm. The concentrations of pyridine hemochromagen in the samples were calculated from the difference between the absorbance at 557 nm of the reduced sample and the absorbance at 540 nm of the oxidized sample ($\Delta\varepsilon$ = 23.98 mM^{-1} cm^{-1}) according to the literature[39].

General procedure for the expression of hemoproteins with PdALAS

The pET-21b expression plasmids encoding the gene for the hemoproteins were transformed into chemically competent *E. coli* BL21-Gold(DE3) cell (Agilent Technologies, Inc.) harboring pAR3b-PdALAS helper plasmid. The resulting transformants were plated on LB agar medium containing ampicillin (100 μg/mL) and chloramphenicol (20 μg/mL) and incubated at 37 ºC overnight. The obtained single colony was then inoculated into 10 mL of LB medium containing ampicillin (100 μg/mL) and chloramphenicol (20 μg/mL) and cultivated at 37 ºC and 180 rpm for 6 h. The culture (1.3 mL) was then inoculated into 130 mL of LB medium containing ampicillin (100 μg/mL) and chloramphenicol (20 μg/mL). After incubation at 37 ºC and 150 rpm for 2.5 h, IPTG (final conc. 0.20 mM) and arabinose (final conc. 2.0 mg/mL) were added to induce the expression of hemoproteins and PdALAS, and the cultivation was continued at 18 ºC and 150 rpm for 16 h. For the expression of hemoproteins with high molecular weight (catalase and cytochrome P450BM3), pET expression system was first induced by IPTG (final conc. 0.20 mM) and after incubation at 18 ºC and 150 rpm for 3 h, the expression of PdALAS was induced by arabinose (final conc. 1.0 μg/mL). As control experiments, the *E. coli* BL21-Gold(DE3) cells which did not harbor pAR3b-PdALAS were also cultivated in LB medium supplemented with or without 5.0 mM of 5-aminolevlinic acid at the same time. Finally, the *E. coli* cells were harvested by centrifugation at 8,800 rpm for 10 min and stored at −80 °C until further use.

Procedure for pyridine hemochromagen assay

Pyridine hemochromagen assay was conducted according to the literature with slight modifications.[39] The frozen *E. coli* cells expressing hemoproteins (from a 130 mL culture) were thawed on a water bath at room temperature and resuspended in 3.0 mL of Tris-HCl buffer (100 mM Tris-HCl, 150 mM NaCl, 1.0 mM EDTA, pH = 8.0). The cells were then disrupted by using Qsonica Ultrasonic Homogenizer Q700 (amplitude: 40, process time: 30 sec × 6, pulse-ON time: 1 sec, pulse-OFF time: 1 sec) and the resulting lysate was centrifuged at 4,300 *g* and 4 ºC for 10 min. The supernatants (1.0 mL) were then transferred to another tube and further centrifuged at 20,000 *g* and 4 ºC for 3 min. Next, the supernatant (0.50 mL) were mixed with 0.5 mL of potassium ferricyanide solution (500 μM $K_3Fe(CN)_6$ in 0.2 M NaOH solition containing 40 v/v% pyridine), and UV-vis spectra of the oxidized samples were recorded from 400 nm to 800 nm. The oxidized samples were then treated with 10 μL of sodium dithionite solution (0.5 M $Na_2S_2O_4$ in 0.5 M NaOH solution), and UV-vis spectra of the resulting reduced samples were recorded from 400 nm to 800 nm. The concentrations of pyridine hemochromagen in the sample were calculated from the difference between the absorbance at 557 nm of the reduced sample and the absorbance at 540 nm of the oxidized sample ($\Delta\varepsilon$ = 23.98 mM^{-1} cm^{-1}) according to the literature.[39]

Procedure for LC-MS analysis on *E. coli* cells

The *E. coli* BL21-Gold(DE3) cells harboring pET21b-ApPGb and pAR3b-PdALAS were cultivated following the procedure described above. When OD_{600} values reached approximately 0.7–0.9, IPTG (final conc. 0.20 mM) and arabinose (final conc. 1.0 μg/mL) were added into the media, and the cultivation was continued at 18 ºC and 150 rpm. After 10 h of cultivation, the OD_{600} values were measured to estimate the cell density, and 4.5 mL of the cell culture was collected and centrifuged at 10,000 rpm and 4 ºC for 2 min. The supernatants were separated by decanting and pipetting, and the resulting cell pellets were resuspended in 10 mL of PBS buffer. The cell suspension was then centrifuged again at 10,000 rpm and 4 ºC for 2 min. The cell pellets were stored at −80 ºC until further analysis. Intracellular metabolites were extracted by adding 1.6 mL of methanol, 1.6 mL of chloroform and 640 μL of water. After vortexing and sonication for 1 min each, the tubes were centrifuged at 2900 *g* and 4 ºC for 20 min. The upper layer (500 μL) and lower layer (1500 μL) were collected and evaporated to dryness at room temperature using a centrifugal evaporator (CVE-2100, EYELA, Tokyo, Japan). The dried residue of the upper layer was dissolved in 100 μL of water and subjected to 5-ALA analysis using a liquid chromatography-quadrupole time-of-flight/mass spectrometer (LC-QTOF/MS, LCMS-9050, Shimadzu, Kyoto, Japan) equipped with a Discovery® HS F5 HPLC column (Merck, Darmstadt, Germany) as previously described.[51] The dried residue of the lower layer was dissolved in 100 μL of methanol and subjected to heme *b* and protoporphyrin IX analysis using LC-QTOF/MS equipped with an Acquity UPLC peptide BEH C18 column (Waters, Milford, MA, USA) as previously described.[52] The peak areas of the extract ion chromatograms of 5-ALA $[M + H]^+$ (*m*/*z* 132.066), heme *b* $[M]^+$ (*m*/*z* 616.177) and protoporphyrin IX $[M+H]^+$ (*m*/*z* 561.251) were used for relative quantitation.

Procedure for amination catalyzed by ApPGb HYA-5294

The amination reaction using ApPGb HYA-5294 was performed following the procedure of literature with slight modification.[37] *E. coli* BL21-Gold(DE3) cells with and without pAR3b-PdALAS were transformed with a

pET expression plasmid encoding the gene of ApPGb HYA-5294 (M39V/W59A/Y60G/S123P/K125R/P148L/I149N variant of ApPGb) and cultivated as described above. The resulting cell pellets from 130 mL culture were suspended in 3.0 mL KPi buffer (50 mM KPi, pH 8.0) and disrupted by using Qsonica Ultrasonic Homogenizer Q700 (amplitude: 40, process time: 30 sec × 6, pulse-ON time: 1 sec, pulse-OFF time: 1 sec). The cell lysates were then centrifuged at 6,000 *g* and 4 ºC for 10 min, and the supernatants were directly used for the catalysis. The supernatant (170 μL) was first diluted with 170 μL of KPi buffer (50 mM KPi, pH 8.0), and sodium dithionite in H_2O (20 μL, final conc. 2.5 mM), 4-fluorophenylboronic acid (**1**) in EtOH (20 μL, final conc. 2.5 mM), and hydroxylamine hydrochloride in H_2O (20 μL, final conc. 7.5 mM) were added into the solution in a glove box. The resulting solution was incubated at 4 °C for 10 min. After addition of 1,3,5-trimethoxybenzene (1.0 μmol) as an internal standard, the reaction mixture was extracted with 800 μL of ethyl acetate and analyzed by GC-FID equipped with a DB-1 column (Separation method: 1.0 μL injection, injector temperature: 200 °C, detector temperature: 270 °C, gradient: column temperature set at 40 °C, held at 40 °C for 7 min, then 30 °C/min to 100 °C, then 50 °C/min to 260 °C, and held at 260 °C for 10 min, with a total run time of 22.20 min).

Procedure for cyclopropanation catalyzed by bacterial hemoglobin

E. coli BL21-Gold(DE3) cells with and without pAR3b-PdALAS were transformed with a pET expression plasmid encoding the gene of *Azorhizobium caulinodans* bacterial hemoglobin (Uniprot ID: A8IPS1) and cultivated as described above. The resulting cell pellets from 130 mL culture were suspended in 3.0 mL of Tris-HCl buffer (100 mM Tris-HCl, 150 mM NaCl, 1.0 mM EDTA, pH = 8.0) and disrupted by using Qsonica Ultrasonic Homogenizer Q700 (amplitude: 40, process time: 30 sec × 6, pulse-ON time: 1 sec, pulse-OFF time: 1 sec). The cell lysates were then centrifuged at 6,000 *g* and 4 ºC for 10 min, and the supernatants were directly used for the catalysis. The supernatant (10 μL) was first diluted with 223 μL of Tris-HCl buffer (100 mM Tris-HCl, 150 mM NaCl, 1.0 mM EDTA, pH = 8.0), and sodium dithionite in H_2O (37 μL, final conc. 20 mM), styrene (**3**) in MeOH (15 μL, final conc. 10 mM), and ethyl diazoacetate (**4**) in MeOH (15 μL, final conc. 20 mM) were added into the solution in a glove box. The resulting solution was incubated at 25 °C for 1 h. After addition of benzyl alcohol (0.60 μmol) as an internal standard, the reaction mixture was extracted with 400 μL of ethyl acetate and analyzed by GC-FID equipped with a SUPELCO Beta DEXTM 120 fused silica capillary column (Separation method: 1.0 μL injection, injector temperature: 250 °C, detector temperature: 250 °C, gradient: column temperature set at 60 °C, then 3.0 °C/min to 150 °C, then 2.0 °C/min to 180 °C, and then 120 °C/min to 210 °C, and held at 210 °C for 5 min, with a total run time of 50.25 min).

Procedure for benzene hydroxylation catalyzed by cytochrome P450BM3

The hydroxylation reaction using cytochrome P450BM3 was performed following the procedure of literature with slight modification.[45] *E. coli* BL21-Gold(DE3) cells with and without pAR3b-PdALAS were transformed with a pET expression plasmid encoding the gene of *Priestia megaterium* cytochrome P450BM3 (Uniprot ID: P14779) and cultivated as described above. The resulting cell pellets from 130 mL culture were washed twice with reaction buffer (93 mM Na_2HPO_4, 16 mM KH_2PO_4, 85 mM NaCl, 7.0 mM $MgSO_4$, 0.1 mM $CaCl_2$, 20 μM H_3BO_3, 1.5 μM $CoCl_2$, 0.5 μM $CuSO_4$, 4.0 μM $MnCl_2$, 0.5 μM $ZnSO_4$, and 1.0 μM Na_2MoO_4, pH 7.4). The cell

pellets were then incubated with 995 μL of the reaction buffer (25 mg/mL) containing decoy molecule (*N*-Heptyl-l-prolyl)-l-phenylalanine (C7-Pro-Phe) (100 μM) and glucose (40 mM) at 25 °C and 1,200 rpm for 40 min. Benzene (**6**) in DMSO (5.0 μL, final conc. 10 mM) was then added into the cell suspension, and the reaction was performed at 25 °C with shaking at 1,200 rpm for 7.0 h. After addition of 1,3,5-trimethoxybenzene (2.0 μmol) as an internal standard, the reaction mixture was extracted with 600 μL of ethyl acetate and analyzed by GC-FID equipped with a DB-1 column (Separation method: 1.0 μL injection, injector temperature: 200 °C, detector temperature: 270 °C, gradient: column temperature set at 40 °C, held at 40 °C for 7 min, then 30 °C/min to 100 °C, then 50 °C/min to 260 °C, and held at 260 °C for 10 min, with a total run time of 22.20 min).

Procedure for nitrile synthesis catalyzed by aldoxime dehydratase

E. coli BL21-Gold(DE3) cells with and without pAR3b-PdALAS were transformed with a pET expression plasmid encoding the gene of *Amycolatopsis thermoflava* aldoxime dehydratase (Uniprot ID: UPI000400A70A) and cultivated as described above. The resulting cell pellets from 130 mL culture were suspended in 15 mL of KPi buffer (100 mM KPi, pH = 7.0) and directly used for whole-cell catalysis. Into the cell suspensions (250 μL), a solution of octanal oxime (**8**) in hexane (50 mM, 250 μL) was added. The resulting mixture was then shaken at 30 °C and 1,000 rpm for 1 h. After addition of cyclohexanol (11 μmol) as an internal standard, the reaction mixture was extracted with 500 μL of ethyl acetate and analyzed by GC-FID equipped with a DB-1 column (Separation method: 1.0 μL injection, injector temperature: 200 °C, detector temperature: 270 °C, gradient: column temperature set at 40 °C, held at 40 °C for 7 min, then 30 °C/min to 100 °C, then 50 °C/min to 260 °C, and held at 260 °C for 10 min, with a total run time of 22.20 min).

Procedure for the catalysis of latex clearing protein

E. coli BL21-Gold(DE3) cells with and without pAR3b-PdALAS were transformed with a pET expression plasmid encoding the gene of *Thermomonospora curvata* latex clearing protein (Uniprot ID: D1ADK3) and cultivated as described above. The resulting cell pellets from 130 mL culture were suspended in 3.0 mL of KPi buffer (50 mM KPi, pH = 7.0) and disrupted by Qsonica Ultrasonic Homogenizer Q700 (amplitude: 40, process time: 30 sec × 6, pulse-ON time: 1 sec, pulse-OFF time: 1 sec). The cell lysate was then centrifuged at 6,000 g and 4 ºC for 10 min, and the supernatant was directly used for the catalysis. Into a 0.5 w/v% solution of natural rubber latex **10** in 500 μL of KPi buffer (50 mM KPi, pH = 7.0), the supernatant (100 μL) of *E. coli* cell lysate was added. The resulting mixture was shaken at 37 °C and 1000 rpm. After the required time, the reaction was quenched by adding 600 μL of EtOH. To quantify the progress of latex degradation, Schiff's reagent (Merck Ltd.) was added into the mixture, and the solution was further incubated at 37 °C for 30 min. After centrifugation at 10,000 g and 4 °C for 5 min, the concentration of aldehydes was determined by measuring the absorbance at 547 nm with UV-vis spectrometer. Calibration curve for the aldehyde degradation products was prepared using propionaldehyde. For LC-MS analysis, degradation products were extracted with EtOAc. After removing organic solvent under reduced pressure, the residues were dissolved in CH_3CN and analyzed by LC-MS equipped with YMC-Triart C18 column (H_2O/CH_3CN).

Procedure for ABTS oxidation catalyzed by dye-decolorizing peroxidase

E. coli BL21-Gold(DE3) cells with and without pAR3b-PdALAS were transformed with a pET expression plasmid encoding the gene of *Escherichia coli* dye-decolorizing peroxidase YfeX (Uniprot ID: P76536) and cultivated as described above. The resulting cell pellets from 130 mL culture were suspended in 3.0 mL of HEPES buffer (50 mM HEPES, pH = 5.6) and disrupted by using Qsonica Ultrasonic Homogenizer Q700 (amplitude: 40, process time: 30 sec × 6, pulse-ON time: 1 sec, pulse-OFF time: 1 sec). The cell lysates were then centrifuged at 6,000 *g* and 4 ºC for 10 min, and the supernatants were directly used for the catalysis. The supernatant (100 µL) was first diluted with 500 µL of HEPES buffer (50 mM HEPES, pH = 5.6), and an ABTS solution in HEPES buffer (200 µL, final conc. 1.0 mM), and a H_2O_2 solution in HEPES buffer (200 µL, final conc. 2.0 mM) were added into the solution. The resulting mixture was incubated at 25 °C, and the reaction progress was monitored with UV-vis spectrometer by measuring absorbance at 730 nm derived from ABTS cation radical species.

Procedure for H_2O_2 degradation catalyzed by catalase

E. coli BL21-Gold(DE3) cells with and without pAR3b-PdALAS were transformed with a pET expression plasmid encoding the gene of *Geobacillus stearothermophilus* catalase (Uniprot ID: P14412) and cultivated as described above. The resulting cell pellets from 130 mL culture were suspended in 3.0 mL of KPi buffer (100 mM KPi, pH = 7.0) and disrupted by using Qsonica Ultrasonic Homogenizer Q700 (amplitude: 40, process time: 30 sec × 6, pulse-ON time: 1 sec, pulse-OFF time: 1 sec). The cell lysates were then centrifuged at 6,000 *g* and 4 ºC for 10 min, and the supernatants were directly used for the catalysis. The supernatant (20 µL) was first diluted with 756 µL of KPi buffer (100 mM KPi, pH = 7.0), and a H_2O_2 solution in KPi buffer (224 µL, final conc. 20 mM) were added into the solution. The resulting mixture was incubated at 25 °C, and the consumption of H_2O_2 was monitored with UV-vis spectrometer by measuring absorbance at 240 nm.

Preparative scale synthesis of nitrile 9 catalyzed by aldoxime dehydratase

E. coli BL21-Gold(DE3) cells harboring pAR3b-PdALAS were transformed with a pET expression plasmid encoding the gene of *Amycolatopsis thermoflava* aldoxime dehydratase (Uniprot ID: UPI000400A70A) and cultivated as described above. The resulting cell pellets (3.4 g) from 520 mL culture were suspended in 6.8 mL of KPi buffer (100 mM KPi, pH = 7.0) and directly used for whole-cell catalysis. In, a 200 mL round bottom flask, the cell suspensions (c.a. 8.0 mL) were diluted with 32 mL of KPi buffer (100 mM KPi, pH = 7.0), and a solution of octanal oxime (**8**) (573 mg, 4.0 mmol) in hexane (40 mL) was added into the suspension. The reaction mixture was then stirred at 30 °C for 1 h using a magnetic stirrer. The hexane layer was then corrected, and residual organic compounds in the aqueous layer was extracted with hexane and EtOAc. The combined organic phase was then dried over Na_2SO_4, and organic solvents were removed under reduced pressure to afford octanenitrile (**9**) as colorless oil (483 mg, 97% yield). The chemical structure and purity were confirmed by ^{1}H and ^{13}C NMR spectroscopy. ^{1}H NMR (400 MHz, $CDCl_3$): 2.33 (t, J = 7.2 Hz, 2H), 1.62–1.69 (m, 2H), 1.40–1.48 (m, 2H), 1.28–1.35 (m, 6H), 0.89 (t, J = 6.8 Hz, 3H). ^{13}C NMR (100 MHz, $CDCl_3$): 120.01, 31.61, 28.75, 28.55, 25.49, 22.64, 17.26, 14.14. The control experiment using *E. coli* BL21-Gold(DE3) cells without pAR3b-PdALAS was also performed following the same protocol as described above. In this control experiments, 246 mg of octanenitrile (**9**) was obtained as a mixture with

starting material (49% yield).

DNA Sequence

BdALAS:

ATG*ACGAAGATCAAAGATAACGAGACCACA*ATGGATTACAGCCAGTTCTTTAATTCCGCCCTCGATCGCCTCCACACTGAAC
GGCGTTACCGCGTGTTCGCCGATCTGGAACGCATGGCGGGCCGATTTCCGCATGCGATCTGGCACTCGCCCAAGGGCAAG
CGCGACGTCGTGATCTGGTGCTCCAACGACTATCTCGGCATGGGTCAGCATCCGAAGGTCGTCGGCGCCATGGTCGAGAC
CGCAACGCGCGTCGGCACCGGCGCGGGCGGCACCCGCAACATCGCCGGCACGCATCATCCGCTGGTGCAGCTCGAGGCC
GAGCTCGCCGATCTCCACGGCAAGGAAGCCGCGCTGCTGTTCACCTCGGGCTATGTCTCGAACCAGACCGGCATCGCGA
CCATCGCAAAGCTCATTCCGAACTGCCTGATCCTGTCGGACGAGCTCAACCACAATTCAATGATCGAGGGCATCCGCCAG
TCCGGCTGCGAGCGGCAAGTGTTCCGCCACAACGATCTCGCCGACCTCGAAGCGCTGTTGAAGGCGGCGGGTGCGAAC
CGGCCGAAGCTGATCGCCTGCGAGAGCCTCTATTCCATGGACGGCGACGTCGCTCCGCTCGCCAAGATCTGCGATCTCGC
CGAGAAATATAACGCGATGACCTATGTCGACGAAGTCCACGCGGTCGGCATGTACGGCCCGCGCGGCGGCGGCATCGCC
GAGCGTGACGGCGTCATGCATCGCATCGACATTCTCGAAGGCACGCTGGCCAAGGCGTTCGGCTGCCTCGGCGGCTACAT
CGCCGCCAACGGCCAGATCATCGACGCCGTGCGCTCCTATGCGCCGGGCTTCATCTTCACCACCGCGCTGCCGCCGGCGA
TCTGCTCGGCCGCGACCGCCGCGATCAAGCACCTGAAGACCTCGAGCTGGGAGCGCGAGCGCCACCAGGACCGCGCCG
CCCGCGTCAAGGCGATCCTCAACGCCGCCGGTCTCCCGGTGATGTCGAGCGACACCCACATCGTGCCGCTGTTCATCGGC
GATGCCGAGAAGTGCAAGCAGGCCTCCGACCTGCTGCTCGAAGAGCACGGCATCTACATCCAGCCGATCAACTATCCGA
CCGTCGCCAAGGGCTCCGAGCGCCTGCGCATCACGCCCTCGCCCTATCACGATGACGGCCTGATCGATCAGCTCGCCGAA
GCCCTGTTGCAAGTGTGGGACCGCCTCGGCCTGCCGCTCAAGCAAAAGTCGCTGGCGGCGGAG

(*italic*: translation enhancing element)

PdALAS:

ATG*ACGAAGATCAAAGATAACGAGACCACA*ATGGACTATTCAGCTGCCCTCGATCAGGCCATCGGCAAGCTGCACGAAGAG
GGGCGCTACCGGACCTTCATCGACATCGAGCGCCGCAAGGGGGCCTATCCGCAGGCGGTCTGGACGCGGCCGGACGGGA
CCGAAACCCGGATCACCGTGTGGTGCGGCAACGACTACCTGGGCATGGGCCAGCATCCCGTCGTGCTGGCGGCGATGCA
TGAGGCGCTGGACGCCACCGGCGCGGGTTCGGGCGGGACGCGCAACATCTCGGGCACCACGGTCTATCACAAGCGGCT
GGAAGCCGAGCTGTCCGACCTGCACGGGAAAGAGGCCGCGCTGGTCTTTTCCAGCGCCTATATCGCCAACGACGCGACG
CTCTCGACCCTGCGCAAGCTGTTTCCCGGCCTCATCATCTATTCGGACGAGTTGAACCACGCCTCGATGATCGAGGGGAT
CAAGCGGTTCGACGGCGCCAAGCGCATCTTCCGCCACAACGACGTGGCGCATCTGCGCGAGTTGCTGGCGGCCGACGAT
CCCGAGGCGCCGAAGCTGATCGCCTTTGAATCCATCTATTCGATGGACGGCGATTTCGGCCCGATCAAGGCGATCTGCGA
CCTTGCGGACGAATTCAACGCGCTGACCTATCTGGACGAGGTGCATGCCGTTGGCATGTATGGTCCGCGCGGCGGTGGCG
TGGCCGAGCGCGACGGGCTGAGCCATCGCATCGACATCTTCAACGGCACACTGGGCAAGGCGTTCGGCGTCTTCGGCGG
CTATATCGCCGCTTCGGCCAGGATGGTGGATGCGATCCGCTCCTATGCGCCCGGGTTCATCTTCACCACCTCGCTGCCCCC
GGCGGTGGCGGCGGGCGCGGCGGCCTCGATCGCCTTCCTCAAGACGGCCGAGGGGCAGTTGCTGCGCGACCAACAGCA
GCTGAACGCCCGCATCCTGAAGATGCGGCTGCGCGGCCTCGGCATGCCGATCATGGACCATGGCAGCCATATCGTGCCGG
TGCATGTCGGCAACCCGGTGCATTGCAAGGCGCTGTCGGACATGCTGCTGGCCGATTTCGGCATCTATGTGCAGCCGATC
AACTTCCCGACCGTGCCGCGCGGGACCGAACGTCTGCGTTTCACGCCCTCTCCGGTGCATGATCCCAAGCAGATCGACC
ATCTGGTGAAGGCCATGGACAGCCTGTGGTCGCAGTGCAAACTGAACCGTTCAACTTCGGCTGCC

(*italic*: translation enhancing element)

MeALAS:

ATG*ACGAAGATCAAAGATAACGAGACCACA*ATGCAAAGGACCACCGATCAATTGATGCTTTCCGTTGGGCTGCGCTGCCGCT
GCCCGCGCTGCGGCGAGGGGCGCCTGTTTAACGGCTTCATCACCTTGAAGCCACGCTGCGAGGCGTGCGGCCTTGATTAT
AGCTTCGCTGACCCAGCCGATGGACCCGCCTTCTTCATCATGATGACGATGGCCTTCCCGGTGACAGCCTTCGGCATTTGG
TTCGAGCTCGCATACGAACCGCCGGTCTGGGTTCATGCGGTCGTGACGCTCCCGCTTCTCTTGCTGGCCTGCGTGCCGGT
CATCCGGCCGCTGAAGGGGGCTCTTCATCGCCAGCCAGTACATCAACAAGGCGGGAGAAGGCCGCCTGGCGACTTCGGC
AGCACCCAACACGAGTCCTACGACCGGAGACTGACCCTGCCGCTCCACCGCGCGGTCCCGGGCAGACGCGCACCGGCG
GCATCGCCCGACGCTGGGCTTGCCATGACTTCATCCGACCTGACGAGGACCGGGACGATGCTCCCCTATTCCGACGTGTT
CGAGGCTTCCGTCCGGAAGCTTCGCGAGGACGGCTGTTACCGGACGTTCATCGAGCTTGAGCGTAATGTCGGCACATCCC
CGGCTGCCATCTGGAGGCATCCAGACGGCAGCCGCCGGCCGGTCACGGTCTGGTGCAGCAACGATTACCTTGGGATGGG
ACACAGCCCCCAGGTCATTAACGCCATGCATGCGGCCCTGGACCGCTACGGTGCCGGCGCGGGCGGCACACGCAACATC
TCCGGCACCGCCCACGAGCACGTGCTGCTGGATCACGACCTGGCCGACCTGCATGGGAAGGAGGCCGCGCTCCTGTTCA
CCTCGGGCTACGTCTCGAACCTCGCGGCTCTGAGCGTGCTCGGCCAAGTGCTGCCGGACAGCGTTATCCTCTCGGACGCC
GGCAACCACAACTCGATGATCGAGGGCATCCGCCGCTCGGGAGGCGCGAAGGCGATCTTCCCGCACAACGACGTCGCCG
CGCTCGACAGGCTGCTCGCGCAGTTCGATCCTGAACGGCCCAAGATCGTCGCGTTCGAGAGCGTCTACAGCATGGACGG
CGACGTGGCGCCCATCGCCGAGATCTGCGACGTCGCGGAGCGCCACGGGGCGCTCACCTACCTCGACGAGGTGCACGCG
GTCGGGATGTACGGCCCGCACGGCGCAGGCATTGCGGAGCGCGAGGGCGTCGCCCATCGCGTCACCCTGATCGAGGCGA
CGCTCGGCAAGGCCTTCGGCGTCATGGGCGGCTACGTCGCTGGGCCCTCCACGGTCGTCGACGTCATCCGCAGCCATGC
GGCGGGCTTCATCTTCACGACCTCGCTGTGCCCGCACCTGGCCGCTGGCGCACGGGCGGCGGTGCGGCACCTCAGGGAC
AGCCAAGCGGAACGGGCAACGCAGCAACGGGCTGCGGCGATCTTGATGGCCATGCTGCGCAAGGCAGGCCTGCCGGTC
CTGCCGAGTCAGAGCCACATCTTGCCGGTGATGGTCGGCGACGCCCACCTCTGCCGGAGGATCAGCGAGGAGTTGCTGG
AGCGCCACGGCATCTACGTCCAGCCGATCAACTATCCAACCGTGCCGCGCGGCGGCGAGCGGTTGAGGATCACCCCGAC

TCCGCTCCACACCGAGGAGCACATGCGGGCGCTCGTGGGGGCGCTCGTCGAGGTTCGTTCACGCCTGGGCTGGGGCGAG
GTCTCG

(*italic*: translation enhancing element)

CsALAS:

ATG*ACGAAGATCAAAGATAACGAGACCACA*GACTACAAAGCCGCGTTCCGCAGCGCCGTCGATCAGATCCGCGACGAAGGT
CGTTACCGCGTTTTCGCCGACCTGAAGCGTCAGCGCGGCGCTTTCCCTCGGGCCAGCTGGACCCGCCAGGACGGCTCGG
AACGCGAAGTCGTGGTCTGGTGCAGCAACGACTATCTCGGCCAGGGCCAGAACCCCGTCGTTCTGGACGCCATGAAGGC
GGCGGTCGACGCGCATGGCTCGGGCTCGGGCGGCACGCGCAACATCTCCGGCACGAACCACGACCATGTCCTGCTGGAG
CAGGAACTGGCCGATCTGCACGGCAAGGACGCCGCGCTGTTGTTCACCTCGGGCTATGTCTCGAACGAAGCGACTCTGT
CGGTCGTCCAGAAGATCCTGCCGGGCCTGATCATCTTCTCGGACGAGTTGAACCACGCCTCGATGATCGCCGGCATCCGC
AACGGCGGCGGCCCGCGCAAGATCTTCAAGCATAATGACTTGGCGCATCTCGAGGAGCTGCTGGCCGCGGCGCCGGCGG
ACGCGCCCAAGCTGATCGCCTTCGAAAGCGTCTATTCGATGGACGGCGACATCGCCGACATCGCCGGCACCATCGCGCTG
GCCAAGAAGTACGGCGCCATGACCTATCTGGACGAAGTCCACGCGGTCGGCATGTACGGTCCGCGCGGCGGCGGCGTCG
CCGAGCGCGAAGGCCTGATGGGCGACATCGACATCATCGAAGGCACGCTGGGCAAGGCGTTCGGCGTGATGGGCGGCTA
TATCACCGGCGACACCGAAGTGATCGACGCCATCCGCCTGATGGCGGCCGGCTTCATCTTCACCACCTCGCTGCCCCCAG
CCCTGGTGGCCGGCTCGTTGGCCAGCGTCCGTTGGCTGAAGGCCCACCCGGAAGTGCGCGAGATCCATCAGGAGCGCGC
GGCGACCCTGAAGGCCATGTTCAAGGCCGCCGGCCTGCCGGTGATGGAGAACGACAGCCACATCGTCCCGGTGCTGGTT
GGCGATCCCGTCCACTGCAAGATGATCAGCGACATGCTGCTGGCCGATCACGGCGTCTATGTGCAGCCGATCAACTATCC
GACCGTTCCGCGCGGCACCGAGCGCCTGCGCTTCACGCCCACGCCGTTCCACAGCGACGAGATGATGCGCAAGCTGGTC
TCCGCCATGGAAGCCCTGTGGGCCCACTGCAACGTCGCCCGGATGGGCGGCTACGCGGCC

(*italic*: translation enhancing element)

RbeALAS:

ATG*ACGAAGATCAAAGATAACGAGACCACA*ATGGATTTCGAAGCATTTTTCAAAAACGAGCTGGACGGGCTTCATGCCGAG
GGCCGCTACCGCGTTTTTGCCGATCTCGAACGTCAGCGCGGCCACTTTCCGCGCGCCACGCGCCATACGGCCGATGGTGA
AAAGGACGTCACGGTCTGGTGCTCCAACGACTATCTCGGCATGGGCCAGAACCCCAAGGTGATCGAGGCGATGAAGGCC
GCTATCGACCACTGTGGCGCGGGTGCGGGAGGCACCCGGAATATTTCTGGCACCAACCACTATCACGTCCTGCTCGAGCG
TGAGCTTGCCGATCTGCACGGCAAGGAAGCAGCCCTGATCTTCACGTCAGGCTATGTCTCCAACTGGGCCTCACTCGGCA
CGCTCGGCGGGAAAATTCCCGGCCTGATCATCTTCTCCGATGCGCTCAACCATGCCTCGATGATCGAGGGCATCCGTCATG
CCAAATGCGACAAAGTGATCTGGAAACATAATGACGTCGCCGATCTCGAAGCCAAGCTGAAAGCCGCCGATCCGAAGGC
GCCGAAGCTGATCGCCTTCGAGAGCGTCTATTCGATGGACGGCGACATCGCTCCGATCAAGGAGATCTGCGACCTCGCCG
ACCAATACGGCGCGATGACCTATCTCGACGAGGTGCATGCGGTCGGCATGTACGGCCCGCGCGGCGGCGGCATTGCCGA
GCGCGAGGGGCTGATGGATCGGCTGACGGTCATCGAAGGCACGCTCGGCAAGGCCTTCGGAGTGATGGGCGGCTATATC
GCCGCGTCGGCAGCGCTGTGCGACTTCATCCGCTCGTTTGCCTCCGGCTTCATCTTCACCACGGCGCTGCCGCCCGCATT
GGCAGCCGGCGCCGTCGCCTCGATCCAGCATCTGAAGGTCAGTCAGTTCGAGCGCGCCCGCCACCAGGACCGGGTGCGC
AAGCTCAGAGCCATGCTCGACCAGCGCGGCATTCCGCATATGCACAATCCCAGCCATATTGTGCCGGTGATGGTTGGCGAT
GCGGCCAAATGCAAGTGGATCTCCGATCTGCTGCTCGACAATTGCGGCGTCTACGTCCAGCCGATCAATTATCCCACCGTA
CCGAAGAAAACCGAACGGCTGCGCATCACCCCGACACCGCTGCATTCCGACGCCGATATCGCCCATCTCGTCGACGCCCT
GCATTCGCTCTGGTCGCGTTGCGCGCTGGCAAGGCACGTCGCC

(*italic*: translation enhancing element)

GtALAS:

ATG*ACGAAGATCAAAGATAACGAGACCACA*ATGTATGCCGAGATTCTCAGCGACAAGCTCAATTCTTTGAAAGAAAGTGGAC
AATACCGTGAATTCGTTACGATTAATCGGATATGTGGTCAGTATCCATTGGCAAAGTTGAATGGTAAGGAAGATGAGCAAT
CTGTTGTTGTGTGGTGTAGCAATGACTATTTAGGAATGTCTCAGCATCCTGTGGTTACTGCAGCGATGCACGATGCGATCA
GATTATATGGCGCCGGTTCAGGCGGATCACGGAACATAGGTGGCACACACTACCATTACACTTTGCTCGAATCATCACTAG
CAGACTGGCACGGTAAGGAGACTGCATTGGTTTTTCCGACTGGATACAGTTCAAATGATGCAACATTACAATGCTTGTTG
CGTCTGTTTCCTAATTGCATAGTGTTCTCCGACGAACTTAACCATGCTTCGATTATCAATGGAATACGAAGCGCTAAAGCTG
ACCGTGCTATATTTAGACATAATGATGTCGACCATCTGGAGGAATTACTTGCTTCTCAGCCACGTAATCGAGCAAAAATCAT
CGTATTCGAGTCGATATATTCGATGGACGGTGATATCGCGCCAATCGAAAAGATTACGAACCTTGCTAGTAAATATAACGCT
CTAACATTCCTCGATGAAGTGCATGCCATCGGTATGTACGGTCCACGTGGAGCAGGGATGGCTGCAGAACTCGGCGTTGC
AGATCGTATAGACATCATTCAGGGAACAATGGCGAAGGCGATAGGGGTGATAGGCGGATATATTGCTTCGTCAGCACTACT
GATTGACGCTGTTCGCTCTTTTGCATCTGGTTTCATTTTTACTACATCTCTGCCGCCAGCAGTTGTCGCTGCATGCTATGCC
AGCGTCGAGTACTTGAAATCCTCCGATAAGGAAAGAAAAGAACTGCATAGGAAGACTATTATGTTAAGGGAAACACTCA
CTCAGGCCGGTATTCCAGTGATGCAATCGAGTGAAACACACATTCTTCCCGTACTGATCGGGGATGCAAAAAAATGTAAA
GCTGCTGCTCAAAGACTACTTGAAAAACATAAGATCTATCTACAGCCTATTAACTCGCCGACCGTTCCTATCGGTACGGAA
CGTTTTCGAGTCAATGTTACACCTAACCACACCGAAGAACAGATATTACAGCTAACCGATGCATTGAAGGAAGTTTTTCA
CTACTTTGATATTCCTTTTGCGCAGTCGGCAGCAGATGTGTACGCA

(*italic*: translation enhancing element)

KsALAS:

ATG*ACGAAGATCAAAGATAACGAGACCACA*ATGAACCAATACCTGGAGATCTTCTCGCGGCGCATGCGTGAAGGGGGATCCC
CGAAGGCGGAGCGGGAGTTCCTGGAGATCAGCCGGATCGCCGGGAAATTCCCGGCGGCCCGCAGCCCGCTGGGCGGCG
CCGCCGCCGAGGTCAGCGTGTGGTGCAGCAACGACTACCTGGGGATGGGCCAGCACCCGCTGGTCCTGGCGGCCACCC
GGGAGGCCCTCGACGAGCACGGCGCGGGCTCAGGCGGCTCCCGGAACATCGGCGGCACCAACCACTACCACGTGCTGC
TGGAGCGCGAACTGGCGGACCTGCACGGCAAGGCGGACGCCCTCCTCTTCAGCTCCGGCTACACCGCCAACGACGGGG
CCCTCACCGTCCTGGCCGGCCGGCCGGGGGACTGCGTGGTCTTCTCCGACGAGATGAACCACGCCTCGATCATCGACGG

ACTCCGCCACAGCGGCGCCGAGAAGCGGATATTCCGGCACAACGACACGGCGCACCTGGAGGAATTGCTCTCCGCCGCC
GACCCCGACCGCCCGAAGATGATCGTCATGGAATCGGTCTACTCGATGGCGGGTGACGTCGCCCCGCTCGCCGAGATCGC
CCGGATCGCCCCGGAAGTACGGCGCGATGACCTTCCTGGACGAGGTCCACGCGGTCGGGATGTACGGGCCGGAAGGCGCC
GGAATCGCCGCCAGTCTGGGCATCGCCGACCAGTTCACCGTCATCATGGGAACGCTCGCCAAGGGATTCGGCACCACCG
GCGGATACATCGCGGGCCCCGCCGAGCTGGTCGACGCGGTGCGCGGCCTCTCCCGCTCCTTCATCTTCACCACCGCCCTG
CCCCCGGCGGTGGTGGCGGGCGCGCTCGCCGCCGTCCGGCACCTGCGCGGCTCGGAGGAGGAGCGCGACCGGCTGCAC
GCCAACGCGCGGCTGACCCACCGGCTGCTCACCGAGCGCGGCATCCCCTTCGTCTCCGACGGCTCCCACATCGTCTCGAT
CTTCGTCGGGGACGACGCGCTCGCCCAGCGGGTCTCCGCCCTGCTGCTGGAGCGCCACGGCATCTACGTGCAGGCGATC
AACGCGCCGAGCGTCCGCGCCGGGCAGGAGATCCTCCGCAGCGCGCCCGGCGCCGTCCACCAGCCCGCGCAGATCGAG
GGGTTCGTCGAGGCCCTGGACGGGATCTGGCGGGAGCTGGGCGTGCCGCGGGCCCGGGAA

(*italic*: translation enhancing element)

SrALAS:

ATG*ACGAAGATCAAAGATAACGAGACCACA*ACAAAAGTCTCCACCCGGCCCCACGTCTTCGAAACCATTGAGAACAAGCTC
CGGGAGCTGAAAAGCAACGGCCTGTACCGGCATTACCTCCCCACCGCGCACATGGCGGCCAGCCCGGGCCAGACACTGC
GTCTGGGGGAAGAGGTCCAGGTGTGGTGCAGCAACGATTATCTCGGCCTGAGCCAGCACCCGGATCTCATCAGGGCGCA
GATCGAGTCGACCGCGTTGCACGGCACCAGCATGGGCGGCTCGCGCAACATCGGCGGCACGAGCACCACGCACGTCGC
GCTGGAGTCGGAGCTGGCCGGCTGGCACGGGAAGGAGCGCGCGCTCATCTTCTCCAGCGGCTACGTGGCGAACTTCGAG
ACGCTCAGCGTGCTGCTGTCGGCGGTGCCGGACATGGTTGTCCTCTCGGACGAGAACAACCACCGCTCCCTGATCGAGG
GGATCCGCCGAGCGCGATGCGAAAAACGGATATTTCCACATAACGACCTGGTCGGGCTCGAACGCTGCCTGGCCGAGTA
CGACGAGTCGCGGCCCAAGATGATCGTGTTCGAGTCGGTGTACTCGATGGACGCCGACGCGTCCCCGATCAGCGCGATAT
GCGACCTGGCGCAGAAGTACAACGCCCTGACCTACCTGGACGAGACCCACGCCATCGGGGTCAAGGGCCCGACCGGCG
CGGGGATCTGCGAGGAGATCGGGGAGACCCGGCCGACCTTCGTCCAGGGCGTCTTCGGCAAGGCCATCGGGACGGTCG
GCGGATACGTCGCGGGCCCCGACGCGGCCCTGGACTACGTGCGCTCCTACGCGCCCGGCTTCATCTTCACGACCTCCCTT
CCGCAGGCGTGCATGGACGCCACGCTGAAGGGCCTCGAACTCGTACGGCACGGCACCGACCTGCGCCGGGCGCTGACC
GACAACTCACTCCGGATGAAAGCCGCTCTGCGGTCGGCGGACATCCCGTTCATCGACGGGGAGCACCACATCATCCCGG
TGATGGTGCCCGGCGGCGACCGGGTCAGGAAGGTGGCCGACCTCCTCCTGGAGGACCACCTCATCTACGTCCAGCCGAT
CAACTTCCCGTCCGTTCCCCTCGGGACGGAGCGGCTGCGCGTCACCGTCGCCCCGTATCGGACCGGCGACCAGATCGAG
TACTTCGCATACGCCCTGGAATCGTGCCTCGCTCGCGCG

(*italic*: translation enhancing element)

EcGluTR:

ATG*ACGAAGATCAAAGATAACGAGACCACA*ATGACCCTTTTAGCACTCGGTATCAACCATAAAACGGCACCTGTATCGCTGC
GAGAACGTGTATCGTTTTCGCCGGATAAGCTCGATCAGGCGCTTGACAGCCTGCTTGCGCAGCCGATGGTGCAGGGCGGC
GTGGTGCTGTCGACGTGCAACCGCACGGAACTTTATCTTAGCGTTGAAGAGCAGGACAACCTGCAAGAGGCGTTAATCC
GCTGGCTTTGCGATTATCACAATCTTAATGAAGAAGATCTGCGTAAAAGCCTCTACTGGCATCAGGATAACGACGCGGTTA
GCCATTTAATGCGTGTTGCCAGCGGCCTGGATTCACTGGTTCTGGGGGAGCCGCAGATCCTCGGTCAGGTTAAAAAAGCG
TTTGCCGATTCGCAAAAAGGTCATATGAAGGCCAGCGAACTGGAACGCATGTTCCAGAAATCTTTCTCTGTCGCGAAACG
CGTTCGCACTGAAACAGATATCGGTGCCAGCGCTGTGTCTGTCGCTTTTGCGGCTTGTACGCTGGCGCGGCAGATCTTTG
AATCGCTCTCTACGGTCACAGTGTTGCTGGTAGGCGCGGGCGAAACTATCGAGCTGGTGGCGCGTCATCTGCGCGAACAC
AAAGTACAGAAGATGATTATCGCCAACCGCACTCGCGAACGTGCCCAAATTCTGGCAGATGAAGTCGGCGCGGAAGTGA
TTGCCCTGAGTGATATCGACGAACGTCTGCGCGAAGCCGATATCATCATCAGTTCCACCGCCAGCCCGTTACCGATTATCG
GGAAAGGCATGGTGGAGCGCGCATTAAAAAGCCGTCGCAACCAACCAATGCTGTTGGTGGATATTGCCGTTCCGCGCGAT
GTTGAGCCGGAAGTTGGCAAACTGGCGAATGCTTATCTTTATAGCGTTGATGATCTGCAAAGCATCATTTCGCACAACCTG
GCGCAGCGTAAAGCCGCAGCGGTTGAGGCGGAAACTATTGTCGCTCAGGAAACCAGCGAATTTATGGCGTGGCTGCGAG
CACAAAGCGCCAGCGAAACCATTCGCGAGTATCGCAGCCAGGCAGAGCAAGTTCGCGATGAGTTAACCGCCAAAGCGTT
AGCGGCCCTTGAGCAGGGCGGCGACGCGCAAGCCATTATGCAGGATCTGGCATGGAAACTGACTAACCGCTTGATCCAT
GCGCCAACGAAATCACTTCAACAGGCCGCCCGTGACGGGGATAACGAACGCCTGAATATTCTGCGCGACAGCCTCGGGC
TGGAG

(*italic*: translation enhancing element)

PpGluTR:

ATG*ACGAAGATCAAAGATAACGAGACCACA*ATGGCCTTTCTTGCACTTGGTATCAACCATAAGACTGCCTCGGTAGACGTAC
GCGAGCGCGTGGCGTTTACCCCAGAGCAGCTGGTAGACGCCCTGCAGCAGCTCTGCCGACTGACTTCCAGCCGCGAGGC
GGCGATCCTGTCGACCTGCAACCGCAGCGAGCTCTATATAGAGCAGGACCACCTGTCCGCCGACGCCGTGCTGCAATGGC
TGGCCGATTATCACCGCCTCAGCCTGGACGAGCTGCGCGCCAGCGCCTACGTGCATGAAGAGCACGATGCGGTAAAGCA
CATGATGCGCGTGGCTTCCGGCCTGGACTCATTGGTGCTCGGCGAGCCGCAGATCCTCGGCCAGATGAAGTCCGCCTACG
CCGTGGCGCGCGAGGCCGGCACCGTCGGCCCGCTGCTCGGGCGCCTGTTCCAGGCCACCTTCAGCGCTGCCAAGCAGGT
GCGTACCGACACCGCCATCGGTGAAAACCCGGTATCGGTGGCGTTTGCCGCGGTCAGCCTGGCCAAGCAGATCTTCAGC
GACCTGGGCCGTAGCCAGGCCTTGTTGATCGGTGCCGGCGAAACCATCACCCTGGTCGCCCGCCACCTGCATGAGCAAG
GCGTGCGGCGTATCGTCGTGGCCAACCGCACCCTGGAGCGGGCCAGTATCCTGGCCGAGCAGTTCGGCGCGCACGCCGT
ATTGCTGGCCGACATCCCCCAGGAACTGGCCAACAGCGACATCGTCATCAGCTCCACCGCCAGCCAACTGCCAATCCTGG
GCAAGGGCGCGGTCGAGAGTGCGCTGAAACAGCGCCGGCACAAGCCGATCTTCATGGTCGACATTGCCGTACCGCGTGA
CATCGAACCTGAAGTCGGCGAGCTGGACGACGTCTACCTGTACACTGTCGATGACTTGCACGACGTGGTGGCGGAAAAC
CTCAAGAGCCGCCAGGGCGCCGCCCAGGCTGCCGAAGAGCTGGTGTCGGTGGGCGCCGAAGATTTCATGGTGCGCTTGC
GCGAACTGGCTGCGGTGGATGTGCTCAAGGCCTATCGCCAGCAAAGCGAGCGCCTGCGCGACGAAGAACTGCAAAAGG
CCCAGCGCCTGCTGGCCAACGGCGGCAACCCCGAGGACGTACTGGCCCAACTGGCCCGGGGGCTGACCAACAAACTTC

TGCATGCGCCCAGCGTGCAGTTGAAAAAGCTCTCGGCCGAGGGCCGCCTTGATGCGCTGGCCATGGCCCAGGAACTCTT
TGCCCTCAACGAGGGCTCCACGGACAAATCCCCGCAA

(*italic*: translation enhancing element)

CmGluTR:

ATG*ACGAAGATCAAAGATAACGAGACCACA*ATGCAACTGCTCGCGATCGGTATCAATCACACCACGGCACCCGTCTCGCTCC
GCGAACGTGTGGCGTTTCCGCTTGAGCAGATCAAACCCGCGCTTGGCGCACTGCGCACCCACCTCTCGGGTCGCAACGG
TACCGAAGCCGCCATTCTCTCCACCTGCAACCGCACCGAGATCTACTGCGCGACCGACGTGCTGAAGCCGGGCGAGGAA
GGTTTCGAGCACACGCTGCGCTGGCTGGCGCAGCATCACAACGTCCCCGCTTCTGAATTGGCGCCGCACCTGTACGCGCT
GCCCCAGTCGGAAGCCGTGCGCCATGCGTTTCGCGTGGCCAGCGGCCTGGACTCGATGGTGCTCGGCGAAACGCAGATC
CTGGGGCAGTTGAAGGATGCGGTGCGCACCGCCGGTGAGGCCGGCGCGCTGGGCACGTACCTGAACCAGCTTTTCCAGC
GCACGTTCGCGGTGGCCAAGGAAGTCCGCGGCCAGACCGAGATCGGCGCGCATTCAGTGTCGATGGCGGCCGCTGCGGT
TCGCCTGGCGCAGCGCATTTTCGAGAGCGTCTCCACGCAGCGCGTGCTGTTCATCGGCGCCGGCGAGATGATCGAACTGT
GCGCCACGCACTTCGCCGCGCAGACGCCGCGCCAGATCGTGGTGGCCAACCGTACCGTCGAACGCGGCGAAAAGCTGG
CCGAACAGTTGTCCGAGCAGGGGCTGACCACCCAGGCGATCCGCCTGCAGGACCTTGGCGACCGTCTGCATGAATTCGA
CATCGTCGTCTCCTGCACCGCGAGTTCGCTGCCGATCATCGGCCTGGGCGCGGTCGAACGCGCGGTCAAGCGCCGCAAG
CATCGCCCGATCATGATGGTCGATCTTGCCGTACCGCGTGACGTGGAGCCTGAAGTTGCACGCCTGGATGACGTGTTCCT
GTACACCGTCGACGACCTTGGCGCCGTCGTGCGCGAAGGCAACGCGCTGCGTCAGGCTGCCGTGGCGCAGGCCGAGGC
CATCATCGATTCCCGCGTGCTGAATTTCATGCACTGGCTGGAGACGCGCAGCGTCGTGCCCGTCATCCGCGAACTGCAAT
CGCAGGGCGAGGCGATCCGCCAGGCCGAAGTCGAACGCGCGCGCCGGATGCTGGCGCGCGGTGACGACCCCGCGGCCG
TGCTCGAGGCGCTCTCTGGCGCGCTGACCCGCAAGTTCCTGCACGGCCCGACCCACGCGCTGAACCACACCCAGGGCGA
GGACCGCGAGGCGCTGCTGCGCCTGGTGCCGGGCCTGTTCCGCCACAGCAGCCACTCCGAGCGC

(*italic*: translation enhancing element)

LmnGluTR:

ATG*ACGAAGATCAAAGATAACGAGACCACA*ATGTATTTTATAATTAGTTTTAACTATAGAAATTCAGATATAACTCTTAGGGGA
AAGTTAGCAAAACTTAAATTAGAAGATTTTAAAAATTATAAAGAGGTTATGGTTTTAAGTACATGTAACAGATTTGAAGTT
TATTTTGATAAAAAATATGATTTAAACGAACTGTATAAAAATATTTTTTCTAAAGTTATAGATGAAGAAGAATTTAAAAAAG
CAGAAATTTATGAAGGAAAAGATGCGATAAGGCATACTTTCAGGGTTGCTGCAAGTCTTGATTCAATGGTGGTGGGTGAG
GCTCAGATTACAGGGCAGCTAAAAGAGGCTTTTATGGAAAGTTATGAAAAACATTATATGGCTCAGGATTTGACAAGACT
TATTCATTTTTCTTTTAAATGTGCTAAGAAAGTAAGAAACCAAACACAGATTTCAAGCGAACCTGTCTCAGTAGCTTCCAT
CGCTGTAAAAAAAGCAAAAGAAAAATTGAATGATCTAAGCGGATATTCAGCGGTTGTTGTAGGTGTCGGTGATACGGCAA
AAATTGTTTGCAAAAATTTAATAAAAGAGGGTGTTAATATAATATTGGTAAACAGAACGGTTGAAAATGCATTTGCCCTGA
AAGAAGAATTAGGGGATGAAGTTAATATTGATGTTCATCCTTTGGAAAAGCTTCCAAAACTTATAAATAATTACAGACTTC
TTTTTTCAGCAACAGCTTCAAAAGAACCGATTATTAAAAATGAATTTATTAAAGACACCTCTTATAAAAGAATATGGTTTG
ATTTGGCAATCCCTTGTGATATAGAAAATGTCGAATGTACGAATGTAGAAATAATCAAAGTTGATGATTTAAAAAATATTTC
TGAGGAAAACCTCAGAAAAAGAAAAAAAGAGCTTGTTTTTGCTAATGATTTAATAGAAAAATGTGTTGTAGAATTTTACA
AATATCTTCAGTCTGTATCAATAGAGCCGGTAATAAAATTTTTGCAAGACAAAGCGAAAGAATGTGCTACTATGTCTTTAA
AAAATGCGGTGAAGAAAAAATATATTCCAGCTGAATATGAAGAAGATGTTGAAAAAATACTTCATAATGCATTTAAAAGAT
TTTTACACAATCCGAATTTGACTCTTAGAAAAATGGCCGATTCACCAGAAGTCGATATTTTAGTATCATCTTTAAAAAGACT
TTTTGGAATAAAAGGTGATATCTTAGATATTAATAAATGTGAATATCATATGGATAAGGGAATACTCAAA

(*italic*: translation enhancing element)

HtGluTR:

ATG*ACGAAGATCAAAGATAACGAGACCACA*ATGCCCTTTTTCGCGATTGGCCTCAACCACCACTCTGCGCCGGTGCCGGTGC
GTGAACAACTTGCGGTTGCTCCGTCCGAGCTACCCGAGCTTTTGCGCGCGCTCGTCGCTGCGGGGATCGGCGTTCACGA
AGCGGCGCTCTTGTCGACGTGCAACCGAACCGAATGTTACGTCGCGGCGAGCGACCCGCACGCGGTCTTCGCGTGGCTC
TGTGCCCACCGCCACGCCGATCTGGCGCAGGTCACACCCCACCTCTTCATTCATCGGGATAGCGAAGGGGTGCGACACCT
CTTTCGTGTCGCTTCGGGCCTCGATTCGATGGTCCTGGGCGAGACCCAGATCGTCGGGCAATTCAAAGAGGCGCTGCGTC
TTGCGAAAGCGGCGGGGACGCTCGGCAAGCACGTCCAGACCGTGATGCAGATGGCGCTTTCGGTCGCGAAAGAGGTGC
GCAGCCAAACCGCGATCGGTGCCAACGTCGTCTCGATGGCCGCCGCCGCTGTTCGCCTTTCCCAACGGGTTTTCGGGCCG
GTGGCGGAGCAGCGGGTGCTCTTCGTCGGTGCAGGGGAGATGATCGAAACGTGCGTCGCCCATTTCGCCGCAGGGCAGC
CGCAGCGGATCGCGATCGTGAACCGGACGGTGGCGCGGGCCGAGCAACTGGCTGCTCGTTTTGCCGCCGAGGCGCATCC
GCTCGATCGGTTGCCCGAACTGTTGCCGGAGTTCGATACGGTCGTCGCCAGTACCGCCAGCCCGTTGCCGTTGATCGGGT
TGGGGATGGTCGAGCGGGCGCTCAAGCAGCGGCGCCACCGTCCATTCGTGATGGTCGACCTTGCCGTGCCGCGCGACAT
CGAGCCGGAAGTGGGCGCGCTGCAGGACGTCTTCCTCTACGCGGTCGACGATCTGGCGCAAATCGTGCAGGAGGGACG
GGAAAGCCGCGCGCAGGCGGTTCGGGACGCCGAAGCGATCATCGACGCCCGCCTGGCCGAGTTTGCCCAGTGGGTGAG
CGCGCAAGAGATGGTGCCGCTCATTCGCCAGTTGCGCACCCACGCAGAGACGATCGCCACCGCAGAACGCGAGCGGGC
ATTGGCGAAATTGCGGGCGGGCGGGGATCCGGAAGCGGTGATCGCGGCGCTCACCCACGCGCTGACGAACAAATGGTTG
CATGCGCCAACCACCTTTTTTCGTCAAGCCCCGCCGGAAGCACGTCAGGCGTTGAGCCGCTGGGCGCCACAACTCTTTG
GTTGGGAGAAGACGCAACGA

(*italic*: translation enhancing element)

GkGluTR:

ATG*ACGAAGATCAAAGATAACGAGACCACA*ATGCAAATCGTAGTCGTTGGCGTCGACTATAAAACCGCCCCTGTAGAAATCC
GCGAAAAGCTCGCGTTTGCAGAAGCGGAACTCGGTGCGGCGATGAAACAGCTCGCCAAGCAAAAAAGCGTGCTCGAAA
ATGTGATCGTTTCGACGTGCAACCGGACGGAAGTTTATGCAGTGGTTGATCAACTGCATACCGGACGTTACTATATGAAAG
CATTTTTAGCCGAATGGTTTGGCGTCAAAGTGGAAGCGATTGCTCCGTATTTGCGTGTGCTTGAAGGAGAAGCGGCCATA

AAGCATTTGTTCCGCGTGGCGGCCGGCCTTGATTCGATGGTGCTTGGGGAAACGCAAATTTTAGGGCAAGTGAAAGACA
GCTATTTGCTCGCTCAAGAGGTCGGGACGAGCGGCACGATTTTCAATCATCTGTTCAAGCAGGCGGTGACCTTTGCGAAG
CGCGCCCACTCGGAAACGGGCATCGGCGCGCACGCTGTATCGGTCAGCTATGCGGCGGTTGAGCTGGCGAAGAAAATTT
TCGGCCGCCTTGCCGGCAAGCACGTCTTGATTATCGGGGCCGGCAAAATGGGGACGCTGGCGGCGCAAAACTTGTACGG
CAGCGGCGTCGGGAAGGTGACGGTTGTCAATCGGACGCTTGAAAAAGCGAAACAGCTTGCTAAGCAGTTTGCCGGCGA
AGCGAAGCCGCTCGGCGAATTGTCATGCGCTTTGCTGGAAGCGGATATCGTCATCAGCTCGACGGGAGCCAAAGGCTATA
TTTTGACGAAGGAAATGGTGGCGCCGCTTGAGAAAATGCGCAAAGGCCGCCCGCTCTTTATGGTTGACATCGCGGTGCC
GCGCGATTTGGATCCGGCGTTGGCTGATTTGGAAACGGTGTTTTTGTACGACATTGACGATTTGCAAGATGTGGTGGCGG
CCAACTTGGCGGAACGGCAAAAGGCAGCGGCTCGCATTGAAACGATGATCGAAGCGGAACTTATGGCGTTCAGCCAATG
GCTGCAGACGCTCGGCGTCGTGCCAGTCATTGCCGCATTGCGCGAAAAGGCGCTGGCCATTCAAGCAGAAACGATGAAA
AGTTTGGAGCGGAAACTGCCGCATTTGTCGGAGCGCGACTGGAAAGTGTTGAATAAGCATACGAAAAGCATTATTAACCA
GCTGCTCCGCGATCCGATTTTGCAGGCGAAGGAACTCGCCGCCGGCCCGAATGCCGAGGAGGCGCTTTTGCTGTTTATGA
AAATTTTCAATATCGAAGATGCGGTGAAAGCCGAGCGGCATATAGAGCAGGCGAAATCCGTGCAATGCGATGAACAAGA
CGCGGAAGCGGTCCGTGCCGCCCGC

(*italic*: translation enhancing element)

DrGluTR:

ATG*ACGAAGATCAAAGATAACGAGACCACA*ATGCCGCAGCCCGCACCGCTCGATTTTGTGGTGGTCGGCCTCAATCACCAGA
CCGCGCCAGTCGAGGTCCGCGAGCGCGTCGCCGTGCGGCCCGAGGAAGAAGGCGCGCTGCTCGGCCACCTCGCGCGCC
ACGCCGACGAGGTGCTGCTGCTCGCCACCTGCAACCGCACCGAGGTCTATCTCGCCGGGGTGCACGGCGACCCGCTCGC
CGCCTTCGAGGGCGCCTGGGGCCACGCGCTGCTCGATCACCTCTACGTGTACCGGGGCGAGGCCGCCGTGCGGCACCTC
TACCGCGTGACGGCGGGGCTCGACAGCCTCGTCATCGGCGAAACCCAGATTCAGGGACAGGTCAAACGTGCCTGGCAA
AGTGCCCGCGAGCGCGGTCTGAGCGGCACCCTGATGAACAAAGTGGTGCAGGGCGCACTGGCGGCGGGCAAGCGGGTG
CGCTCGCACACCGGCCTGAGCGACAAGGTGGTCAGCGTGTCGAGCGCCGCCGTGGAACTCGCGCAGGCCGCGCTCGGT
GAGCTCTCGCAGCGCCGCGCCCTGATTCTGGGGGCGGGCGAAACCGCCGAGCTGACTCTGACCCACCTGCGGGCGGCA
GGCGTGCAGGACGTGCTGGTGGTCAACCGCACCGCCGAGCGGGCCCGCGCCCTCGCCGAAAAACTGGGGGGCCGCGCC
TGCCCCGCCGAGGAACTGTCCGCCGCGCTCCCCGAAGTCGACGTGGTCATCGCATCGAGCGCCGCGCCGCACTACGTGG
TCACCGCCCAGAACGTGCGCGAGGCGCTCGCCGGGCGTCCGGGCCGCGCCATGTTCCTGATTGACATCAGCGTGCCGCG
CATCCTTGACCCCGAGATTGCCAGCGTGCCCGGCGCGCACCTCTACAACCTCGACGACCTGACCGCCGTCGTGCAGCGC
AATATGCAGAGCCGCCGCGCCGCGCTCCCGCAGGCCGAAGCGATCATCCGCGAACTCGGCTCGGACCTCAGCCGCTGGT
ATCTGACCCGTGAGACGCAGCTCGCCCGGCAAGCGGAGCTGGCCTTGGCGTGTGAT

(*italic*: translation enhancing element)

FjGluTR:

ATG*ACGAAGATCAAAGATAACGAGACCACA*ATGGAAAACAATAACGTACCGAAACACCTTTATTTTTACTCAGTTGGTCTGA
GTTATAAAAAAGCTGATGCTGAGGTTAGAGGTCAATTTAGTTTGGATGCCGTTGCCAAAACGCGATTGCTGGAACAAGCT
AAAAACGATGGAATAGAAAGTTTACTAGTTACTTCAACTTGCAACAGAACCGAAATCTACGGTTTTGCCGAACATCCATT
TCAATTAATAAAACTTATCTGCGATAATAGTAACGGATCTGTAGACGCTTTTCAAAAAGTTGGTTTCGTTTACAAAAATCAG
GAAGCGATTAATCATATGTTTCGCGTAGGAACTGGTTTAGACAGTCAGATCTTAGGCGATTTCGAAATTATATCTCAAATAA
AAACATCTTTTACGCATTCAAAATCAATGGGATTAGCCAATGCTTTTATGGAAAGATTGGTAAATGCGGTAATTCAGGCAA
GCAAAAGAATTAAAACGGAAACAGAAATCAGTTCTGGTGCTACTTCAGTTTCTTTTGCATCTGTACAATATATTTTGAAGA
ATGTTGAAGATATCAGTAACAAAAACATTTTACTTTTTGGAACTGGTAAAATCGGAAGAAATACGTGTGAGAATTTAGTAA
AACACACTAAAAACGAGCATATCACTTTAATCAACCGAACTAAAGATAAAGCAGAGAAATTAGCAGGAAAGTTAAATCTT
ATTGTTAAAGATTATTCTGAATTACACTTAGAACTTCAAAAAGCTGATGTTGTAGTTGTAGCAACCGGCGCGCAAAACCCA
ACGGTTGACAAAGCAATCTTAAATCTTAAAAAACCTTTGTTGATCCTGGATTTATCGATTCCGAAAAACGTAAATGAAAAC
GTTGAGGAATTAGAAGGTGTAACTTTAATTCACATGGATTATTTGTCTCAATTGACAGATGAAACTTTGGAAAACAGAAA
ATTACATATTCCCGCTGCTGAAGCAATCATCGAAGAAATCAAAGAAGAATTTGTTACTTGGATGAAAGGAAGAAAGTTCG
CTCCAACAATCAATGCTTTAAAAGAGAAATTAAACGCTATTAAAGCTTCGGAACTAGATTTTCAAAGCAAAAAAATCGCC
GATTTTAATGAAGAGCAAGCTGAAATTATCAGTAACAGAATCATTCAAAAAATCACTACACATTTTGCAAATCATTTAAAA
GACGACGATACTATGGTCGATGAAAGTATCGAATGGATCGAAAAAGTCTTCAAAATAAAAGCATCT

(*italic*: translation enhancing element)

LlGluTR:

ATG*ACGAAGATCAAAGATAACGAGACCACA*ATGGAACTCGTCTGCGTCGGTCTGAATCACCGCACCGCGCCCGTCGAGGTT
CGCGAGCGCTTCGCCGTGCCCCAAGGGAGGCTGGGCGCCTCCGCCAAGGAACTCCTCGGGATCGACGGGCTGGCGGAG
AGCGTGGTGCTTTCCACCTGCAACCGCACCGAATTCTACCTCGCGGGCGACCATGCCGAAATGGCTGCAGCCGAACTCC
GGCGCCGCCTCGCGCAGGCGCACGGCGCTGACTCGGATCCGCATTGGTATGAGCATCATCGGATCCAAGCGGCGAAGCA
TCTGTGCCGCGTGGTCAGCGGGCTGGACTCGATGGTGCTGGGAGAAACGGAAATCTTTGGCCAAACCAAGGATGCTTAC
CAGCAGGCACTCAGCGCGGGAGCGACATCCGGTGTCCTGAACCGTGTCTTCCAGCGCGCTTTCGGGATCGGGAAGAAAG
TCCGCACGGATACCCGGATCCAAGAAGGGGCAACTTCGGTAGCTGGAGCCGCCGTCGAGCTTGCGGAGAAAATTTTCGG
CAAGCTGGCCGGTTGCCGGGTGATCGTGATCGGGGCGGGTGAGATGAGCCGCCAGACCGCGCAGGCTCTCGTTTCACGT
GGAGCCTCCACGGTCTTCGTGACCAACCGCTCCTACGACAAGGCCGTGGGCTTGGCGGAGGAGATGGGCGGGCGCGCT
GTTCATTTCGACGAATGGCAGTCCGTGCTTGCGGGCGTGGACGTGGTGATTTCCTCGACCAGCGCGCCGCATCCGGTGGT
GCTGCCGCATCATATCGAATCCGTGCGCCGTATCCGGAAATTCCGGCCGCTGTTCCTGATCGACATCGCCGTGCCGCGCGA
CATTGATCCGGCCTGCGGCGAGATCGAAGAGGCCTACCTTTACGACATCGACACCCTCGAGCAGCTCGCTGGTGAAGCCC
GCGCGCGGCGGGAAAAGCAGATCGCCGAGTGCGACCGCATCATCGAGGAGGAACTGATCAAGCTGAATTTACCCGGTAC
G

(*italic*: translation enhancing element)

DdGluTR:
ATG*ACGAAGATCAAAGATAACGAGACCACA*ATGCAATTAGCTGTTGTAGGGATAAATCACAATACTGCTCCTGTAGAAATTAG
AGAAAAATTATCATTGGATGATTCTCAATTAAAAGATGAATATGAATTGATCCTTGGTAATGAGAGAATTTATGAAGCACTT
ATTATATCTACATGCAATAGGGTGGAGTACTATATTGTAACTGATGACTTTTTATGTAATGTAGAGAGTGTTATAAACCGCTT
TGCTGAACGGATTGGTGAAGATGTGTATGAGATTAAAAAATATATTTATATTTATTGTGGTAATGAAGCATTAAAACACTTAT
TTAAAGTAGCTTGCGGTCTTGATTCTTTAGTTTTAGGTGAGCCTCAAATATTGGGGCAGGTAAAAGATGCTTTTGATAAAG
CGAAAATGTATGGCAGATATGATACGTATTTAAAACAGTTAGAACAATATACTTTAAAAACAGCGAAAAAGGTGAGAACT
CACACCGGTATTTCAGAAAATCCAGTTTCTGTAAGTTATGCTGCAGTTGAATTAGCAAAGAAAATTTTTGGTGATTTAAAA
AATAATATAGCTTTGATTATTGGTGCAGGTGAAATGTGTGAATTGGCAGCTAAACACTTAGTGACTTCAAATATTAAAAAG
ATATATGTTACAAATAGGACATTTTCTCGAGCTGAGATATTAGCTGAAGAAATTAATGGGGAAGCTATTCCATTTGATAATTT
TTATAACAAATTGAACGAGGTGGATATAGTTATAAGTTCTACTGGAGCGCCAACTTATATTTTGACCTATGAGCAAGTTAAG
TCAGTTATGAAGCAGAGAAAATATTCACCAATGTTTTTTATAGATATAGCAGTTCCAAGAGATATTGACCCAGAAATAGAA
CGGCTTGATAATGTTTATGTTTATGATATTGACGATTTAAAAGAGGTTGTGGAAGCTAATAAAAGGGAAAGACAAAAAGA
AGCAGCGAAAGCGTTAAAATATATTGAGCAATCAGTAGAAGATTTTAATAGGTGGCTAAAATCTCTAAATATTGTTCCGGT
TATAAAGCTTATCAGATCAACATTTGAGGACTTAAAAGAGAGTGAACTTGAGAGATTTTTTAAGAAAAATAAGATAGAAG
ATGAGGCGCTTAAAAAGCAGATTTCTTACCTTTTGACTTCATATATGAATAAAGTTTTACACAATCCTCTTAATGTTTTGAA
GAGTAAAAGTGCAGATAATGCAAAATATACTATCGCTGAAGCGGCTGAAATATTATTTAAATTAAAGGAG
(*italic*: translation enhancing element)

HgtGluTR:
ATG*ACGAAGATCAAAGATAACGAGACCACA*ATGGATCGCATATTTGTATGGGGGATTAACTTTAAAACTGCCCCTGTTGAGTA
CAGAGAAGGGCTTGCCTGTAGCAGAGAGGAAACCGCTTATTTGCTTAGCATCTTAAAGACCATCAAAGGTGTTGAGGAG
CTAATCCTTCTCTCAACCTGTAATAGAGTTGAGCTTTACGCGGTAGCTCAAGAGTATGCCTGTATGGAAAACTTAGTGAAT
ACTTTGCTTGAGCTCAAAGGTGCAAGTTGGGATCTAAAGAGATACTCCTTCCTTTTGCAGGGCAAAGAAGCTATACATCA
CATATTCAAAGTAGCTTCAAGCCTTGACTCTATGGTAGTGGGTGAGACGCAGATAACCTCCCAATTTAAAGATGCCTTCAG
CATTGCTAGAAATGTAGGCACTGTTGGAAAGGTGTTGCACAGGCTATACGAAAAAGCTCTCAGGACTGCAAAGAGGGTC
AGAACCGAGACGGGTATAAGTAAGAATGCGGTATCTGTTAGTTATGTAGCTGTAGACCTTGCCAGGAAGATTTTTGGAAAT
CTCAAAAAGGCAAAGGTGCTTTTGGTGGGTGCGGGGGAAATGGGAGAGCTTGCTGCAAGATACTTAAAAAAGCTTCAG
GCGAGCCTGTCTATAACTAATAGAACTTACGAAAAGTCGGTAGATCTCGCCAGAGAACTGGAAGGGCATGCCTTGAGGTT
TGAAAGTTTGGAAGATTACCTTTACGAATTTGATATAGTGATACTTTCAACCGCTTCAAAAGAGCCTATCCTGAAAAAAGA
TATGGTTAAAAAAGCTATAAAGCTTAGAAATTACAAGCCCATGTTTATCATAGACATATCTGTACCAAGAAATGCAGACCCT
TCCATCAACGACCTTGACGAAGTTTTTTTATACAACATAGATGACCTGAGAAGCATTGCGGAAAAAAATCTCTCCGAGAG
GCTAAAGGAGAAAGAAAAAGGCGAGATCATAGTATGGGACGAGGTAGAGAAGTTAGTAAAGTGGCTTGAACTTCTAAAG
GTGGAAAGTTACATCATAAAAATAAAAAACAGATGGAAGGATGTAGAAGCCAGAGAGCCGGCAGTGAGAAAGCTCATCC
ACTCAGTTATAGAAGAGATAAGAAAACAACCATCTTCAGCGGAGAGATTGTTTAAAATATTCGTTCAGGAGGTAGATGAT
GGAGACACGTTCAGAGGGTTATCCTATGTCCATAACAGAGCTGATGGAGCT
(*italic*: translation enhancing element)

TsaGluTR:
ATG*ACGAAGATCAAAGATAACGAGACCACA*ATGCTGAATAATCTAAAAATGATAGGCATAGGGAGAAATGCTCCTCTTTATAT
TTTGGAAAAGTTTGATTTTGATGAAAAAGAAATTATTGAGCTTTTAAAAAGTAAAGTAGATGAAATCGCCGTGCTTAAAA
CGTGCCATAGAAGAGAAATATATTTTATTGGAGATTTAAAAAAACTACCTTTTGATTTAGATGAAAATGTAGAAGGATATTT
GATACAAAGAACAGGGCTTGATGTTGTAAGACATCTATTTAAAGTTTCATCAGGACTTGATTCCATGGTTCTTGGGGAGCA
TCAAATTCTTTCACAAGTAAAAAATACATACAAAAATTTTTGTGAAGGAAAATTGTTGAAGCGAATATTTAATGAAGCAAT
TTCAGTCGGAAAAGAGGTTAGGGAAAAAACTGGAGTTTCAAAATTTCCACTTTCAATAAGTTATATTGCTGTAAAGTTAAT
TGAGGAATTAAAAGGAAAAATTTCAGAAAAAGACATTTTTGTGATAGGTACAGGCCAAATGGGGCAAAAGGTGGTTAAG
TATCTTGTTGATAGAAATGCAAATGTATATATATCCAACAGAACAAAGTCCAAGGCTTTAGAAATTAAAAATAAATATCCGG
GAGTACATTTGGTTGATTTTTCAAAAAAGTATGAGTTTATTTCAAAGAGTGATGTTGTAATTAGTGCTACTAATGCCCCACA
CTATGTCGTTGAAAAGAAAAAAGTTAATACAAGAAAAAAAATATTGTTTATTGATCTTTCAATGCCAAGAAATATAGATCC
AAAGCTTTCAAAGTTACATGATCTATACACACTTGATGATCTACAAAAGATTTCTGAAAAGTATAGCTTATTAAGAAAAGA
AAAGATAGATATGATGCAAAAAATTTTGGAGCAAAGAATAGAAAAATTTTTGAATTGGTATTATTCACGAAATTTGAAAGA
AAAGATAGAAGATGTAATAAAGATGAGAGACATTGTTGTGGAAGAAGAATTTAAAAGGCTTGTTAATAAAGTTGAGGATA
ACAAAAATCTTGAAAAGATAAAGGAAAGTCTTAGAAGATGCGCAAATAGAATGGCAAGTTATCATATCCAATATTTAAAG
GGTGAA
(*italic*: translation enhancing element)

TvGluTR:
ATG*ACGAAGATCAAAGATAACGAGACCACA*ATGTTAATGAATATAGTTACTTTGATTTCGTGGGACTTTAAAAGAAATAATGA
ATCATTTCAAAGGGCAATTATTAATGGATATGATTATTGGTCACGTATATTGGACGATCATGGAGTAGAAAAATACGTTATAC
TCTTGACATGCAACAGAGTAGAGCTTTATTATAGGGGCGACCCGTTCGATGTTCAGGAAAAAGGTTATAACATAATTTCTG
ACGATATGGCAATAAATCACCTATTTCACGTTGCTGCAGGATTAGATTCAATGAGTATTGGTGAAAACGAAGTCTTGAAAC
AGGTAAAGCAAGCCTATGAAAAGTCTTCTTCTATGGGGAAGAGTGACAAGTTTCTATCCCTAATTTTTCAGCGTGCCATAA
GTGTTGGCAAGCTTGTAAGGTCAAAAACAGGCATAGGCAAGGGGAAAGTATCTATCCCATCGATTGTATATGATATTGTCC
GAAAGAATGGTGGCAATAAGATACTTCTCGTAGGAAACGGAATGCTAGCATCTGAAATTGCTCCCTATTTTTCATACCCGC
AGTACAAGGTCACAGTTGCCGGTAGGAATATAGATCACGTAAGAGCTTTTGCTGAAAAGTATGAATACGAGTACGTACTTA

TAAACGATATAGACTCTTTGATAAAGAATAATGACGTAATAATAACAGCAACTTCTTCGAAGACACCAATAGTGGAAGAAC
GATCATTGATGCCTGGAAAACTCTTCATAGATCTTGGGAATCCGCCTAACATTGAACGCGGAAATAATGTAATAACCTTGG
ACGAAATTTATGAGATTTCAAAAAAGAACGAGATGTTACGGGAGGAGAAGATAAACCAGGCTGAAATACTTATAGAGAA
CGAAATGAAAGCAACGATGAACAAGATAAAGGATCTAATGATAGACGACATATTCTCTCAATTCTATAGATTTGCCTCCGT
GGTTCAAACCATGGAGATACAGAAATTCAGGAAAATGCATCCAGAGGTAAACGAAAATGATCTTGAAGCTCTTGCACATT
CAATAATAAACAAAATACTTAACGTACCTGTAACGACACTCAAAGCGGTTTCCAGATCTCAGGGCAACTCAGATTTCAAC
AGATTATTTGAATCATTCTCAAGCAATTTCAACGATATCGTGTCTGCTGCCCTTCAGAGCTACGAAGGTCTTCGAGATACCC
AAAGTCTACGAGACCGAACTCGTCAGTTATTGCAAAAATCC

(*italic*: translation enhancing element)

ApGluTR:
ATG*ACGAAGATCAAAGATAACGAGACCACA*ATGATAGACAGGCTCGCCATGATAGGGGTAAACGTTAAAACCGCCTCCAGG
GAGCACGTGGCCAGGCTTGAGAAAGAGTGGGAGAAACACCTAGACACTATAGGTTATGCATCGAGAGGAACCGTCATAA
TAGCAACGTGCAACAGGTTCGAGGTCTATCTAGACAGCCCATCCAGGCTAGTGGAGGACCTCGCCTCCAGCATAGCCTCC
CCCGGTGGAGAAGGCCTAGTAAGGCTACAAGGTATCGATGCCGCCAGACACCTCTTCAGAGTGGCCTCGGGCCTCGAGT
CCCAGATAATAGGGGATCACGAGGTCCTCGGGCAGGTACGCAGAGCCTGGCTTAAGTCTAGGGAGAAGGGGTTCACCAC
GCCTCTGCTCGACGAGGTGTTCCACAGGGCCCTCAAGACTGGGGCCAGGGTTAGAAGCGAGTCGGCCATATCGTCGGGT
GGAGTGGGGTACTCCAGCGCGGCGGTGTCCCTAGCTGCCAGCCTCCTAGGAGGTGGGCTTGACGGGGCGAGAGTTGGC
ATAGTGGGGGCGGGCATGGCTGCCGTAGGCATAGCCAGAGCATTGTGCACCAGGTGGAGGCCGAGAGTTGTAGCGGTGT
TTAACAGGACCCCTGAGAGGGGTTGGGAGGTCGCTGGCAAGTGCAGGGGCGTGGAGTCCCTAGTATTACCGCTTGACGA
GCTGGCGAAGCTTATAAATGAATTAGACGCCCTCTTCGTCGCCATAGCAGGCTCTACCAATATTCTGGAGAGGGGGAGGG
TTGAGAGGGGCGTGAGCCCCAGGGTTATAGTAGACATCTCAAACCCGCCGGTTACCCCAAAGGTGGCGGGCAGGGTTTT
CCACATGCCCGAGGTTGAGGAGGAGGCTAAGAGGATGATGGAGGAGAGGCTGCGTTGGATACCTGCCGCCGAGGCGATA
ATAGAGGAGGAGCTGGAGGCCCTGCTGGATGCCCTCTCTAGGAGAAGGGCTAGAGAGTCTTCGAGATCCGTCATGAGGG
CCCTCTCCATACTCGCCGAGAGGGAGTATGAGAGAACGCTTGCCGGCCTTAGGAACGGCGTAGACCCCCGCGAGGCCGT
GGAGCTCGCGCTCAACTCCTACACAAAAAAGGTGGGGGGCGCGTTGAGAAGGCTTCTCGAGGAGGCTAGTGACAGGGG
TCAACTGTCCCTGGAGGACATAGAGGCTATACTAGTCAGCGAGTTCGCCAGGATAGCCGAGAACTCCGGGTTTAAAAACG
GTAGCACCGGG

(*italic*: translation enhancing element)

SutGluTR:
ATG*ACGAAGATCAAAGATAACGAGACCACA*ATGAGTGACGAATTTATAGATATAAACAATTATATAGCAATAGTATATACATAC
AAAACAGTTGGAATAAGTAAGTTATATGAACATTATGTTAAAGATCAAGAATTGTTATTGCTAAAGGGACTAATAAAGGGA
GAAATTAGTGTATTACAAACATGTAACAGAGCAGAGACATACTTATATACATATAACAAAGAAGAATTTAAAGATTTTTTAC
AGAAATTAGATGAAATTCATGGAAAACAGATTAGTAAAGATGCTATGATCTTAAAAGGGGAAGATGCAGTAAAGCATTTG
TTTGAGGTAGCATCTGGTTTAGACTCACTTGCTATAGGCGAATACGAAATACTTAGACAATTGAAAGAAAGCATTGAAAA
AAGTAAAAAACTTGGATTAAGCAGTGAAAAACTAGAATTTCTTTTTAAAAATGCTATAAAGGTAGGAAGAAAAATTAGAC
AACAAACGGAAATTTCAAAAGGAAAAACTGGTATATATGCATTAGCTGTTGAATATGCTAAACATGTATCAAATAATAACA
TAGGCAATGTAAAAATTGCTATAGTAGGAGCCGGAGAAATTGGAAATAAACTAGCTCTAATGTTGAAGAATGAAGGAGCT
CAAAATGTTACAATATTTAACAGAACATACGAAAAAGCGTTAGAAGTTGCCAATAAGTATGGTTTTAAAGCAGAACCATTA
GATTTTTATAAAATAAATAATTATGATATTGTATTTGTTGCAATATATTATGATAAAAAAATAAATCTACCAAATCCTAAACTA
GTAATTGATCTTTCTGTTCCCCAGATTGTTTTAGGTAACAATGTTATTACGTTAGAAAATTTGAGATCTATCTCAGATAAAAT
AATGGAAACAAAAATATTAAGTTTACAGAAAGCTGAGGAATTAATCCATATAGAGATAGAGAATTTTAAGAATGAAATTAT
TAAATATAATCAAAATAGACTTATTTCTAAATTTATGAAAAGAATAGAAGATATTAGGGAAGCTGAAATAAATAGAGCTTAT
GCAGAAATTTTAAAACATGCTAATGATAAAGAAGAGATAAAGAATATTATTGATAAAATGACTAATTCAATGCTTAAAAAA
ATCTTTTCACCGCTTTTTGAAACCGTTAGAAAAAATGAAGATATGGCAAATTACATTAACAACATTTTCGAAATATTAAGTA
ATGGTAACATTTCCAACTCTAAGACCGAGGAGGCTAAGGAAAAA

(*italic*: translation enhancing element)

ApPGb (Q9YFF4):
ATGACCCCAAGTGATATCCCTGGATACGACTACGGTAGAGTGGAGAAAAGCCCTATAACCGACCTGGAGTTCGATCTTCT
GAAGAAAACAGTTATGCTCGGTGAAAAAGATGTAATGTACCTAAAGAAGGCCTGCGATGTGCTAAAGGACCAGGTTGAC
GAGATACTGGATCTATGGTACGGCTGGGTCGCCTCGAACGAGCACCTAATCTACTACTTCTCAAATCCGGATACTGGTGAG
CCTATCAAAGAATATCTTGAGCGGGTTAGGGCCAGATTCGGGGCCTGGATCCTGGACACCACATGCCGAGACTATAACAG
GGAGTGGCTAGATTACCAGTATGAGGTAGGGCTGAGGCATCATAGGAGTAAGAAGGGAGTTACAGATGGAGTGAGGACA
GTGCCGCACATACCACTAAGGTATTTAATAGCATTCATTTATCCAATAACAGCTACAATAAAGCCATTCCTAGCAAAGAAA
GGTGGCAGCCCAGAGGATATCGAGGGAATGTATAACGCGTGGTTCAAATCAGTAGTCCTCCAAGTAGCCATTTGGAGCCA
TCCATACACAAAAGAAAACGACTGG**GGTGGTAGTGGCGGTTCTAGCGCT**TGGAGCCACCCGCAGTTCGAAAAA

(**bold**: GS linker, underline: *Strep*-tag II)

ApPGb_HYA-5294:
ATGACTCCCTCGGACATCCCGGGATATGATTATGGGCGTGTCGAGAAGTCGCCCATCACGGACCTTGAGTTTGACCTTCTG
AAGAAGACTGTCATGTTAGGCGAAAAGGACGTAGTGTACTTGAAAAAGGCGTGTGACGTTCTGAAAGATCAAGTTGATG
AGATCCTTGACTTGGCGGGTGGTTGGGTAGCATCAAATGAGCATTTGATTTATTACTTCTCCAATCCGGATACAGGAGAGC
CTATTAAGGAATACCTGGAACGTGTACGCGCTCGCTTTGGAGCCTGGATTCTGGACACTACCTGCCGCGACTATAACCGTG
AATGGTTAGACTACCAGTACGAAGTTGGGCTTCGTCATCACCGTCCAAAGAGAGGGGTCACAGACGGAGTACGCACCGT
GCCCCACATCCCACTTCGTTATCTTATCGCACTTATCTATCTTAATACCGCCACTATCAAGCCATTTTTGGCTAAGAAAGGTG

GCTCTCCGGAAGACATCGAAGGGATGTACAACGCTTGGTTCAAGTCCGTAGTTTTACAAGTTGCCATCTGGTCACACCCT
TATACTAAGGAGAATGACTGG**GGTGGTAGTGGCGGTTCTAGCGCT**TGGAGCCACCCGCAGTTCGAAAAA

(**bold**: GS linker, underline: *Strep*-tag II)

Myoglobin (P02185):

ATGTGGTCGCATCCGCAGTTTGAGAAAGAAA**ACCTGTACTTTCAGGGGAAA**GTGCTGTCTGAAGGCGAATGGCAACTG
GTCCTTCACGTTTGGGCTAAAGTCGAAGCCGATGTAGCGGGTCATGGTCAGGACATCCTGATTCGTCTGTTCAAAAGCCA
TCCGGAAACGTTGGAGAAGTTCGATCGCTTTAAACACCTGAAAACCGAAGCTGAGATGAAAGCCTCCGAGGACTTGAAG
AAACATGGCGTTACCGTGTTAACAGCACTTGGTGCAATCCTCAAGAAGAAAGGTCATCACGAAGCTGAACTCAAACCAC
TGGCACAGAGTCATGCGACTAAACACAAAATCCCGATCAAATATCTGGAGTTCATTAGCGAAGCCATTATTCACGTGTTAC
ACTCACGTCATCCTGGCAATTTTGGCGCGGATGCGCAAGGAGCAATGAACAAAGCGCTGGAATTATTTCGCAAGGATATT
GCGGCCAAATACAAAGAACTGGGCTATCAGGGG

(**bold**: GS linker, underline: *Strep*-tag II)

Bacterial hemoglobin (A8IPS1):

ATGTGGTCGCATCCGCAGTTTGAGAAA**GAAAACCTGTACTTTCAGGGGAAA**ATGACCCCGAGCCAAGTGGAACTGGTG
CAGTCCTCTTTCGCCAAGGTGGCGCCCATCGCCGAGACCGCAGCCGGCCTGTTCTATGGCCGGCTGTTCGAGATCGCGCC
GGAGGTGAAGCCCCTCTTCAAGGGCGATATTTCGGAGCAGGGGAAGAAGCTGATGGCCACCCTCTCCGTGGTGGTGAAC
GGCCTCACCAAGCTCGACGCCATCGTGCCGGCTGCGCAGGCGCTGGCCCGCCGCCACGTCGCCTATGGCGTGACGCGCG
AACACTATGCCCCGGTCGGCGCCGCCTTGCTCTGGACGCTGGAACAGGGCCTCGGCCCCGACTTCACGCCCGAGGTGAA
GGCCGCCTGGGCGGAGGCTTATGGGCTGCTCTCCGGCGTGATGATCGAGGCGGCCGAGGGCGCTGCCGTCCCGGCGGAA

(**bold**: TEV cleavage site, underline: *Strep*-tag II)

Flavohemoglobin (P49852):

ATGTTAGATAACAAAACAATCGAAATTATTAAAAGCACTGTACCCGTATTGCAACAGCATGGAGAAACAATCACTGGCCG
TTTTTACGATCGGATGTTTCAAGACCATCCAGAGCTTTTGAACATTTTTAATCAAACAAACCAAAAGAAAAAAACACAGC
GAACTGCACTGGCAAATGCCGTTATTGCAGCTGCGGCAAACATTGACCAATTAGGAAACATCATTCCGGTTGTCAAACAA
ATCGGCCACAAGCACCGCAGTATCGGAATTAAGCCTGAGCACTACCCAATCGTCGGTAAATATTTGCTGATTGCGATTAAA
GATGTATTGGGAGACGCTGCAACTCCTGACATTATGCAGGCATGGGAAAAAGCGTACGGAGTCATTGCTGACGCGTTCAT
CGGAATTGAAAAAGACATGTATGAACAGGCTGAAGAGCAAGCCGGCGGCTGGAAGGAGTATAAGCCATTCGTTATCGCA
AAAAAAGAGCGGGAAAGCAAAGAAATTACATCCTTCTATTTGAAACCGGAAGACAGCAAGCCGTTACCTGAATTCCAAG
CAGGGCAATATATCAGCATCAAAGTGCGGATTCCTGATTCTGAATATACGCATATCCGCCAGTACAGCCTGTCTGATATGCC
GGGAAAAGACTATTATCGAATTTCAGTGAAGAAAGATGGTGTCGTGTCTTCCTACTTACACGATGGGCTGCAGGAGGGAG
ATTCAATAGAGATCAGCGCACCGGCAGGGGACTTTGTTTTAGATCATGCATCACAAAAAGATCTCGTTTTGATCAGTGCCG
GAGTTGGCATTACACCAATGATCAGCATGCTGAAAACATCTGTTTCCAAACAGCCTGAACGGCAAATTCTGTTCATTCATG
CGGCGAAAAACAGTGAATATCATGCATTGCGCCATGAAGTAGAAGAAGCAGCAAAACATTCTGCTGTTAAAACAGCATTT
GTGTATCGCGAGCCGACAGAGGAAGACCGTGCAGGTGATCTGCATTTTCATGAAGGACAGATTGATCAGCAATTCCTCAA
AGAACTGATTGCCAACACAGATGCGGATTACTATATTTGCGGTTCACCGTCGTTTATTACGGCAATGCATAAGCTTGTATCA
GAGCTCGGATCAGCGCCGGAGTCTATCCATTACGAGCTATTCGGCCCGCAATTAAGTTTGGCGCAGTCCGTT**GGTGGTAG**
TGGCGGTTCTAGCGCTTGGAGCCACCCGCAGTTCGAAAAA

(**bold**: GS linker, underline: *Strep*-tag II)

Cytochrome b_{562} (P0ABE7):

ATGTGGTCGCATCCGCAGTTTGAGAAAGAAA**ACCTGTACTTTCAGGGGAAA**GCTGATCTTGAAGACAATATGGAAACC
CTCAACGACAATTTAAAAGTGATCGAAAAAGCGGATAACGCGGCGCAAGTCAAAGACGCGTTAACGAAGATGCGCGCC
GCAGCGCTGGATGCGCAAAAAGCAACGCCGCCGAAGCTCGAAGATAAATCACCGGACAGCCCGGAAATGAAAGATTTC
CGCCACGGTTTCGACATTCTGGTCGGTCAGATTGACGACGCGCTGAAGCTGGCAAATGAAGGTAAAGTAAAAGAAGCGC
AGGCTGCTGCAGAGCAACTGAAAACGACCCGCAACGCCTATCACCAGAAGTATCGT

(**bold**: TEV cleavage site, underline: *Strep*-tag II)

Peroxynitrite peroxidase (O64527):

ATGTGGTCGCATCCGCAGTTTGAGAAA**GAAAACCTGTACTTTCAGGGGAAA**AATCAACTGCAACAACTGCAAAATCCG
GGCGAGAGTCCGCCGGTTCATCCGTTCGTGGCACCGCTGTCCTATCTGCTGGGTACCTGGCGCGGCCAGGGTGAAGGCG
AGTATCCGACCATTCCGAGCTTTCGCTATGGCGAAGAGATCCGTTTCAGCCATTCGGGTAAACCGGTGATTGCCTATACCC
AAAAAACGTGGAAACTGGAATCGGGTGCACCGATGCACGCAGAGAGTGGTTATTTTCGCCCGCGTCCGGATGGTTCTATT
GAAGTGGTTATCGCACAGTCGACCGGTCTGGTGGAAGTTCAAAAAGGCACGTATAATGTGGATGAGCAGAGTATTAAACT
GAAATCTGACCTGGTGGGCAACGCGTCCAAAGTTAAAGAAATCAGCCGCGAATTCGAGCTGGTTGACGGTAAACTGAGT
TATGTGGTTCGTATGAGCACGACCACGAATCCGCTGCAACCGCACCTGAAAGCCATCCTGGACAAACTG

(**bold**: TEV cleavage site, underline: *Strep*-tag II)

Dye decolorizing peroxidase (P76536):

TCTCAGGTTCAGAGTGGCATTTTGCCAGAACATTGCCGCGCGGCGATTTGGATCGAAGCCAACGTGAAAGGGGAAGTTG
ACGCCCTGCGTGCGGCCAGTAAAACATTTGCCGACAAACTGGCAACTTTTGAAGCGAAATTCCCGGACGCGCATCTTGG
TGCGGTGGTTGCCTTTGGTAACAACACCTGGCGCGCTCTGAGCGGCGGCGTTGGGGCTGAAGAGCTGAAAGATTTTCCG
GGCTACGGTAAAGGCCTTGCGCCGACCACCCAGTTCGATGTGTTGATCCACATTCTTTCTCTGCGTCACGACGTAAACTTC
TCTGTCGCCCAGGCGGCGATGGAAGCCTTTGGTGACTGCATTGAAGTGAAAGAAGAGATCCACGGCTTCCGTTGGGTGG
AAGAGCGTGACCTGAGCGGCTTTGTTGACGGTACAGAAAACCCGGCGGGTGAAGAGACGCGTCGCGAAGTGGCGGTTA

TCAAAGACGGCGTGGATGCCGGCGGCAGCTATGTGTTTGTGCAGCGTTGGGAGCACAACCTGAAGCAGCTCAACCGGAT
GAGCGTTCACGATCAGGAGATGATGATCGGGCGCACCAAAGAGGCCAACGAAGAGATTGACGGCGACGAACGTCCGGA
AACCTCTCACCTCACCCGCGTTGATCTGAAAGAAGATGGCAAAGGGCTGAAGATTGTTCGCCAGAGCCTGCCGTACGGC
ACCGCCAGTGGCACTCACGGTCTGTACTTCTGCGCCTACTGCGCGCGTCTGCATAACATTGAGCAGCAACTGCTGAGCAT
GTTTGGCGATACCGATGGTAAGCGTGATGCGATGTTGCGTTTCACCAAACCGGTAACCGGCGGCTATTATTTCGCACCGTC
GCTGGACAAGTTGATGGCGCTG<u>GGTGGTAGTGGCGGTTCTAGCGCT</u>**TGGAGCCACCCGCAGTTCGAAAAA**

(**bold**: GS linker, <u>underline</u>: *Strep*-tag II)

Catalase (P14412):
ATGGGGAACCAACAAAATGCTTCCAAATGTCCGTATCACGGCAGCGTCACAAGCTACAACTCAAATCGAACAACCAATA
AAGACTGGTGGCCGAACCAGCTGAACTTAAACATTCTCCATCAACACGACCGAAAAACAAATCCTCATGATGAAGAGTT
CAATTATGCCGAGGAGTTTCAAAAACTCGACTATTGGGCGCTCAAAGAAGATTTGCGCAAACTGATGACCGAAAGCCAA
GATTGGTGGCCGGCCGATTATGGCCATTACGGTCCGCTGTTCATCCGCATGGCGTGGCATTCGGCAGGAACGTACCGCATC
GGCGACGGTCGCGGCGGCGGTTCGACCGGCACGCAGCGCTTTGCCCCGTTAAACAGCTGGCCGGATAACGCCAACTTGG
ATAAAGCGCGGCGGTTGCTGTGGCCGATCAAGAAAAAATACGGCAACAAAATTTCTTGGGCTGACTTGATGATTTTGGCC
GGCAATGTCGCCATTGAATCGATGGGCGGCAAAACGATCGGCTTTGGCGGCGGCCGGGAAGATGTCTGGCATCCGGAAG
AAGACATTTATTGGGGCGCGGAAAAAGAGTGGCTCGCTTCGGAACGCTACAGCGGGGATCGCGAACTGGAAAATCCGCT
TGCGGCTGTGCAGATGGGGCTGATCTATGTCAACCCGGAAGGCCCTGACGGCAAGCCGGATCCGAAAGCGGCAGCGCGC
GACATTCGCGAGACGTTCCGCCGCATGGGGATGAACGACGAAGAAACGGTCGCCTTGATCGCCGGCGGCCACACGTTCG
GCAAAGCGCATGGCGCAGGCCCTGCTTCCCACGTCGGCCCCGAGCCGGAAGCCGCTCCGATTGAAGCGCAAGGATTGGG
ATGGATCAGCTCATACGGAAAAGGAAAAGGCCGCGACACGATCACGAGCGGCATCGAAGGCGCGTGGACGCCGACACC
GACGAAGTGGGATATGTCGTATTTCGATATGCTGTTTGGCTATGACTGGTGGCTGACGAAAAGCCCATCTGGGGCATGGCA
ATGGATGGCAGTTGACCCGAAAGAAGAGCATCTCGCACCGGATGTCGAAGACCCATCGAAAAAAGTTCCGACGATGATG
ATGACAACCGACCTGGCGCTTCGCTTTGATCCGGAATTCGAAAAAATCGCCCGCCGCTTCCATGAAAATCCGGATGAGTT
CGCGGATGCGTTCGCCCGCGCTTGGTTCAAACTGACGCATCGCGATATGGGGCCAAAAACGAGATACTTAGGTCCGGAA
GTGCCGAAAGAAGACTTCATCTGGCAGGACCCGATTCCAACGGTCGACTATGAATTAACCGATGCCGAAATTGAAGAAAT
CAAAGCGAAGATTTTGAACTCGGGTCTGACGGTTAGTGAACTCGTCAAAACCGCTTGGGCCTCAGCCAGCACGTTCCGC
AACTCCGATAAACGAGGCGGAGCCAACGGCGCCCGCATACGCCTTGCGCCGCAAAAAGATTGGGAAGTGAACGAACCA
GAGCGGCTCGCCAAAGTGCTTTCGGTGTATGAAGACATCCAGCGCGAGCTGCCGAAGAAAGTCAGCATCGCCGATCTCA
TCGTTCTTGGCGGCAGCGCAGCGGTTGAAAAGGCGGCGCGCGACGCTGGCTTTGATGTCAAAGTGCCGTTTATTCCAGG
ACGGGGTGATGCGACGCAAGAACAAACTGACGTCCAGAGCTTTTCCGTACTGGAGCCGTTTGCCGACGGATTCCGCAAC
TATCAAAAGAAAGAGTACAGCGTCGGTCCGGAAGAATTGCTCATCGACAAAGCGCAGCTTCTAGGGTTGACCGCACCTG
AGATGACCGTGCTCATCGGCGGTCTGCGGGTATTGGGCGCGAACTATCGCGATCTCCCGCACGGGGTTTTCACTGATCGC
GTCGGGGTGCTGACGAATGACTTCTTTGTCAACTTAGTCGACATGAACTACGAATGGGTGCCGACTGAAGGCGGCATTTA
TGAAATCCGCGACCGGAAAACAGGCGAAGTGCGGTGGACGGCCACCCGGGTTGACCTTATTTTCGGAGCCAACTCAATC
CTTCGTTCGTACGCCGAATTTTACGCCCAAGACGACAACCGAGAAAAATTCGTCCGCGACTTTATCAACGCTTGGGTGAA
AGTGATGAACGCCGACCGCTTTGACATTCATTTGAAACAAACCAAAGAGTCGGTCACGGTT**GGTGGTAGTGGCGGTTC**
TAGCGCT<u>TGGAGCCACCCGCAGTTCGAAAAA</u>

(**bold**: GS linker, <u>underline</u>: *Strep*-tag II)

Catalase related peroxidase (B7X4G2):
ATG<u>TGGTCGCATCCGCAGTTTGAGAAA</u>**GAAAACCTGTACTTTCAGGGGAAA**GCCGAGCAGGAGGTGACGGCACCGCG
GGTGGTCCAGGCTCTGGAAGCGACCTTTGGCGTTCATCAGGGAGAGCGCCGCAATCACATCAAGGGGACCTGCGCGGTG
GGCGAATTCACCGCTACCGCCGAGGCCGCCAGATACTCGCGCTCTGCACTGTTTTCCGGCCAAGCCGTTCCGGTGATTGC
GCGCTTCTCGCTGGCAGGAGGAAACCCCAAGGTTCCAGATGTTACCCAAAGCGCGCGTGGAATGGCCCTGCAATTCAAG
CTCCCAAAGGGACAGTTGCACCAGATGTCCATGTTGAACACCCCCATGTTCGGCGCCGCCCACCCCGGAACGTTTCTGG
ACCTGACCGAGGCTCAGCGCCCCGATCCAGCCACCGGCAAACCGGATCCGGACAAGCTCAAAGCATTCAGGGCCTCCCA
TCCTGACAGCCTGGCTCAGGCGCAATACCTGGCCAGCCACAACCCTCCCGACAGCTACACCCGCAGCGCATTCTTTGGCA
TTCACACCTTCAAGTTCATCAATGCACAGGACAAGGTGACTCTGGTGCGCTGGCGCTTCGTACCGCAGGAAGGAGAGAA
GCCTCTAAGCAACGAGGCGCTGAAGACGGCTGGAACGGACTTTCTGGAAACCGCATTGATTAGCAGCACATCAAATAAA
CCGGCTCGCTGGGACATGCTGGTGACGGTCGGGCAGCCGGGTGACCCCCAGGACGACCCCACGCAATCATGGCCCGCAC
AGCGACCTGAGTTCAAGGCCGGCACCTTGACGATCACGAGCGCTTCGACTCAGAAAGGAGGCTTGTGCGAGCCGATCA
ACTTTGATCCGATGGTGATGGCCGACGGCATTGCGCCCACCAATGATCCGGTGCTCCGCTTTCGCTCCCAGGCCTATGCGG
TGTCATTTGGCAAGCGCTTGAGTGGTCAA

(**bold**: TEV cleavage site, <u>underline</u>: *Strep*-tag II)

Cytochrome P450 (P14779):
ATGACAATTAAAGAAATGCCTCAGCCAAAAACGTTTGGAGAGCTTAAAAATTTACCGTTATTAAACACAGATAAACCGGT
TCAAGCTTTGATGAAAATTGCGGATGAATTAGGAGAAATCTTTAAATTCGAGGCGCCTGGTCGTGTAACGCGCTACTTATC
AAGTCAGCGTCTAATTAAAGAAGCATGCGATGAATCACGCTTTGATAAAAACTTAAGTCAAGCGCTTAAATTTGTACGTG
ATTTTGCAGGAGACGGGTTATTTACAAGCTGGACGCATGAAAAAAATTGGAAAAAAGCGCATAATATCTTACTTCCAAGC
TTCAGTCAGCAGGCAATGAAAGGCTATCATGCGATGATGGTCGATATCGCCGTGCAGCTTGTTCAAAAGTGGGAGCGTCT
AAATGCAGATGAGCATATTGAAGTACCGGAAGACATGACACGTTTAACGCTTGATACAATTGGTCTTTGCGGCTTTAACTA
TCGCTTTAACAGCTTTTACCGAGATCAGCCTCATCCATTTATTACAAGTATGGTCCGTGCACTGGATGAAGCAATGAACAA
GCTGCAGCGAGCAAATCCAGACGACCCAGCTTATGATGAAAACAAGCGCCAGTTTCAAGAAGATATCAAGGTGATGAAC
GACCTAGTAGATAAAATTATTGCAGATCGCAAAGCAAGCGGTGAACAAAGCGATGATTTATTAACGCATATGCTAAACGGA
AAAGATCCAGAAACGGGTGAGCCGCTTGATGACGAGAACATTCGCTATCAAATTATTACATTCTTAATTGCGGGACACGA

AACAACAAGTGGTCTTTTATCATTTGCGCTGTATTTCTTAGTGAAAAATCCACATGTATTACAAAAAGCAGCAGAAGAAGC
AGCACGAGTTCTAGTAGATCCTGTTCCAAGCTACAAACAAGTCAAACAGCTTAAATATGTCGGCATGGTCTTAAACGAAG
CGCTGCGCTTATGGCCAACTGCTCCTGCGTTTTCCCTATATGCAAAAGAAGATACGGTGCTTGGAGGAGAATATCCTTTAG
AAAAAGGCGACGAACTAATGGTTCTGATTCCTCAGCTTCACCGTGATAAAACAATTTGGGGAGACGATGTGGAAGAGTT
CCGTCCAGAGCGTTTTGAAAATCCAAGTGCGATTCCGCAGCATGCGTTTAAACCGTTTGGAAACGGTCAGCGTGCGTGTA
TCGGTCAGCAGTTCGCTCTTCATGAAGCAACGCTGGTACTTGGTATGATGCTAAAACACTTTGACTTTGAAGATCATACAA
ACTACGAGCTGGATATTAAAGAAACTTTAACGTTAAAACCTGAAGGCTTTGTGGTAAAAGCAAAATCGAAAAAAATTCCG
CTTGGCGGTATTCCTTCACCTAGCACTGAACAGTCTGCTAAAAAAGTACGCAAAAAGGCAGAAAACGCTCATAATACGCC
GCTGCTTGTGCTATACGGTTCAAATATGGGAACAGCTGAAGGAACGGCGCGTGATTTAGCAGATATTGCAATGAGCAAAG
GATTTGCACCGCAGGTCGCAACGCTTGATTCACACGCCGGAAATCTTCCGCGCGAAGGAGCTGTATTAATTGTAACGGCG
TCTTATAACGGTCATCCGCCTGATAACGCAAAGCAATTTGTCGACTGGTTAGACCAAGCGTCTGCTGATGAAGTAAAAGG
CGTTCGCTACTCCGTATTTGGATGCGGCGATAAAAACTGGGCTACTACGTATCAAAAAGTGCCTGCTTTTATCGATGAAAC
GCTTGCCGCTAAAGGGGCAGAAAACATCGCTGACCGCGGTGAAGCAGATGCAAGCGACGACTTTGAAGGCACATATGAA
GAATGGCGTGAACATATGTGGAGTGACGTAGCAGCCTACTTTAACCTCGACATTGAAAACAGTGAAGATAATAAATCTAC
TCTTTCACTTCAATTTGTCGACAGCGCCGCGGATATGCCGCTTGCGAAAATGCACGGTGCGTTTTCAACGAACGTCGTAG
CAAGCAAAGAACTTCAACAGCCAGGCAGTGCACGAAGCACGCGACATCTTGAAATTGAACTTCCAAAAGAAGCTTCTTA
TCAAGAAGGAGATCATTTAGGTGTTATTCCTCGCAACTATGAAGGAATAGTAAACCGTGTAACAGCAAGGTTCGGCCTAG
ATGCATCACAGCAAATCCGTCTGGAAGCAGAAGAAGAAAAATTAGCTCATTTGCCACTCGCTAAAACAGTATCCGTAGAA
GAGCTTCTGCAATACGTGGAGCTTCAAGATCCTGTTACGCGCACGCAGCTTCGCGCAATGGCTGCTAAAACGGTCTGCCC
GCCGCATAAAGTAGAGCTTGAAGCCTTGCTTGAAAAGCAAGCCTACAAAGAACAAGTGCTGGCAAAACGTTTAACAATG
CTTGAACTGCTTGAAAAATACCCGGCGTGTGAAATGAAATTCAGCGAATTTATCGCCCTTCTGCCAAGCATACGCCCGCG
CTATTACTCGATTTCTTCATCACCTCGTGTCGATGAAAAACAAGCAAGCATCACGGTCAGCGTTGTCTCAGGAGAAGCGT
GGAGCGGATATGGAGAATATAAAGGAATTGCGTCGAACTATCTTGCCGAGCTGCAAGAAGGAGATACGATTACGTGCTTT
ATTTCCACACCGCAGTCAGAATTTACGCTGCCAAAAGACCCTGAAACGCCGCTTATCATGGTCGGACCGGGAACAGGCG
TCGCGCCGTTTAGAGGCTTTGTGCAGGCGCGCAAACAGCTAAAAGAACAAGGACAGTCACTTGGAGAAGCACATTTATA
CTTCGGCTGCCGTTCACCTCATGAAGACTATCTGTATCAAGAAGAGCTTGAAAACGCCCAAAGCGAAGGCATCATTACGC
TTCATACCGCTTTTTCTCGCATGCCAAATCAGCCGAAAACATACGTTCAGCACGTAATGGAACAAGACGGCAAGAAATTG
ATTGAACTTCTTGATCAAGGAGCGCACTTCTATATTTGCGGAGACGGAAGCCAAATGGCACCTGCCGTTGAAGCAACGCT
TATGAAAAGCTATGCTGACGTTCACCAAGTGAGTGAAGCAGACGCTCGCTTATGGCTGCAGCAGCTAGAAGAAAAAGGC
CGATACGCAAAAGACGTGTGGGCTGGGTAA

Nitric oxide synthase (O34453):
ATGTGGTCGCATCCGCAGTTTGAGAAA**GAAAACCTGTACTTTCAGGGGAAA**ATGGAAGAAAAAGAAATACTCTGGAAC
GAAGCGAAAGCGTTTATTGCCGCATGCTATCAGGAATTGGGAAAGGAGGAGGAAGTGAAAGACCGTCTCGCGGACATTA
AAAGTGAAATTGACCTGACCGGAAGCTATGTACATACGAAGGAAGAGCTGGAGCACGGAGCGAAAATGGCTTGGAGAA
ACAGCAACCGCTGCATCGGCAGATTGTTCTGGAATTCGCTGAATGTTATCGACAGACGAGACGTCCGGACGAAGGAGGA
AGTGCGTGATGCCCTCTTTCACCATATTGAAACCGCCACCAATAACGGGAAAATCAGACCGACCATTACGATTTTCCCTCC
GGAAGAGAAGGGTGAAAAGCAAGTCGAGATCTGGAATCATCAGCTGATCCGGTACGCTGGATATGAGTCAGACGGAGAA
AGAATCGGCGACCCGGCTTCCTGTTCCCTGACAGCAGCCTGCGAAGAGCTCGGCTGGCGCGGAGAGCGAACGGATTTTG
ACCTGCTGCCGCTCATTTTTCGCATGAAAGGGGACGAGCAGCCTGTCTGGTATGAGCTGCCGCGTTCACTTGTGATTGAG
GTTCCAATCACACATCCGGACATCGAGGCGTTTTCTGATTTGGAGCTGAAGTGGTACGGCGTGCCTATTATTTCTGATATG
AAGCTTGAGGTCGGGGGCATTCATTATAATGCCGCGCCATTTAACGGCTGGTATATGGGCACGGAGATCGGAGCGAGAAA
CCTCGCAGATGAAAAGCGGTACGACAAGCTCAAAAAAGTAGCGTCCGTGATCGGCATCGCCGCTGATTACAATACGGATT
TATGGAAGGATCAAGCGCTAGTTGAATTGAATAAAGCTGTGCTGCACTCGTATAAAAAGCAGGGTGTCAGCATCGTTGAC
CATCATACAGCGGCAAGCCAGTTTAAACGGTTTGAAGAACAGGAGGAAGAAGCGGGCAGAAAGCTGACGGGGGACTGG
ACGTGGCTGATTCCGCCAATTTCACCCGCTGCCACTCATATCTTCCACCGCTCCTATGATAACTCAATCGTTAAGCCGAACT
ATTTTTATCAAGATAAGCCTTATGAG

(**bold**: TEV cleavage site, underline: *Strep*-tag II)

Tryptophan 2,3-dioxygenase (A0A1M6U789):
ATGTGGTCGCATCCGCAGTTTGAGAAA**GAAAACCTGTACTTTCAGGGGAAA**ATGAGCGAACGCCTGACGTACGGCTCC
TACCTGCACCTGGACGAGCTGCTGTCCGCGCAGCACCCGCTGAGCTCGCCGCCGCAGCACGACGAGCTGCTGTTCATCG
TACAGCACCAGACCACCGAGCTGTGGATGAAGCTGGTGCTGCACGAGCTGCACGCGGTGCTCGACCGGATCGCGGCCG
ACGAGCTCCGACCGGCGCTGAAGGGGCTGGCGCGGGTCAAGCACATCCAGGACGTGCTCACCGACCAGTGGGCGGTGC
TGGCCACGCTCACCCCCACCGAGTACGCGCAGTTCCGCGGGTTCCTCGGGGCGTCGTCGGGGTTCCAGTCCGACCAGTA
CCGCGCGGTCGAGTTCCTGCTCGGGCACAAGGACGCAGCGATGCTGCGGGTGCTGGAGGGGGACGACCGGGCGACCGC
GCTGCTCACCGACGCGCTGCGGCGGCCGAGCCTGTACGACGAGTTCCTGCGCCACCTCGCCCGCGCCGGGCACCCGGTG
CCGCAGTCGGTGCTCGAGCGCGACGTCACCATCGCGCACGAGTTCACCGAGGAGTTGGTCCCGGTGTTCCGCACGATCT
ACGAGCACCCCGAGCAGCACTGGTCGGCGTACGAGACGTGTGAGGAGCTCGTCGACCTCGAGGACAACTTCCAGCTGT
GGCGGTTCCGGCACATGAAGACCGTCGAGCGGACCATCGGGTTCAAGCGGGGCACCGGTGGCACGGCGGGCGTGGCGT
TCCTGCGGCGAGCGCTGGAGCACTCGTTCTTCCCCGAGCTGTACGCGGTGCGGACGGAGATCGGCCGG

(**bold**: TEV cleavage site, underline: *Strep*-tag II)

Aldoxime dehydratase (UPI000400A70A):
ATGTGGTCGCATCCGCAGTTTGAGAAA**GAAAACCTGTACTTTCAGGGGAAA**ATGGAATCCGCAGTCGACAAGCACCTG
CAGTGCCCGCGCACCCGGTCGCGCCGGGTCGCCGACGACTACCGGCCCCCGTTCCCGATGTTCGTCGCTCGCGCCGCCG
AGGACCTCACCCACGTCGTCATGGGTTACTTCGGTGTCCAGTACCAGGGACCTGAACACCGCGCCGAGGCCCTCGCCGC

GCTGCGGGAGATCGTCGGGCACTTCGGACTCGATGACGGCCCCGGGGAGTACGACACGACGCACCACCAGGACCGTGA
AGGCGCCGACAATCTGATCGCGGTCGGCTACTGGCGCGACGCCGGCCGCTACCAGCGCTGGCTCTCCCGCCCGGAGGTG
GCAGGCTGGTGGAACTCCGCCGACCGCGAACGCGCCGGCGTCGGGTTCTTCCGCGAGATCGTTTCACCGCGAGCCGACC
AGTTCGAGACGCTCTACGCGTTCACCGACGGTTTCCCCGGCGTGGGCGCCATCATGGACGGCGTCAGCGGGGAGATCGA
AGAGCACGGCTACTGGGGCTCGATGCGGGACCGGTTGCCCATATCGCAGACCGACTGGCTCCCCGCGCGGGGCCAGACC
GTGGCCGTGACCGACGCCGCGACGCCTGGCCGGGTGATCGTGCGCGGCCACGACAACATCGCACTCATCCGGTCCGGCC
AGGACTGGGCCGACGCCGGCGACGACGAGCGTTCGCTCTACCTCGACGAGATCGAGCCCGTGCTGCGGGCCGGCATGG
ACTTCGTACGCGACCACGGCCAGGACGTCGGCTGCTACAGCAACCGGTACGTGCGCTACATCGATCTCGACGGCAACCC
GATTGACAAGTCGTACAACATCGGGCACTGGCGCTCACTCGACCTCCTGGAACGCTGGTCCGAGTCCCACCCGACGCAC
CTGCGGATCTTCACCACGTTCTTCCGCGTGGTCGAGCAACTGGACAAACTGCGCCTGTACCACGAGGTCTCCGTCTTCGA
CGCGAAAGACCAGTACTACGAATACATCAACTGTCACCCGGCGACCGGCATGCTGCGGGACGCGGCGGTGCCGTCGGTC
GCC

(**bold**: TEV cleavage site, underline: *Strep*-tag II)

Latex clearing protein (D1ADK3):
ATGTGGTCGCATCCGCAGTTTGAGAAA**GAAAACCTGTACTTTCAGGGGAAA**CGGCCCGTGTGGACGTGGTCTCCCGAA
GGCTCGGTCTTGGGCACCGGGACGGGTGCCGACCCGAGGGGAGTGTGGGACGAAGAGGCCGACCAGCTGGTGGCCGA
CATCATCCAGCGCGGCGATGTGCAGAAGGTCAACAAGGAGCTGCGCAAATGGCTCAAGAACGGCCAGCCGCTGCCCTCA
GGGCTGCCCAAGGACCTGAAGGACTTCATTGAGAAGGCCAAGCAGCTGCCGCCGTGGGCCGACAAGAACAAGCTGGCC
ACCGCCTTCCACTTCAACGAAAAGCGCGGGCTCTACCTCGGTGTCACCTACGGCTTCGTCAGCGGGATGATGAGCACCGT
CATCCCCCGGGAGGCGCGGGCGGTCTACTACTCCTGGGGCGGCGCGAACCTGCGGGACCGCATCACCAAGACCGCCAAG
CTGGGGTACGACATCGGCACCGCCAACGCCTACGAGCCGGACGGCGAGCTGATCGTGACCTGCATCAAGACCCGGCTGG
CCCACGCGGGCGTGCGGCACCTGCTGCCCAAGTCCCCCTACTGGAACAAGGTCGCCGAAGAAGAGATCCCGATCAGCCA
GGCCGACATGATGGTCACCTGGCACAGCCTGCCCACCAGCGTCATGCGGCAGCTGAAGACCTGGAAGGTGCCGATCCCG
GACAACGAGGCCGAGGCGTTCCTCCACTCCTGGCAGCTGTGCGCCTACATGCTCGGCATCAAGGAGGAGTACATCCCCA
ACTCCTGGGACCAGGCCGAGTCCCAGGCCCGGCAAGTGCTGGACCCGATCCTGGGCCCCACGCCCGAGGGCATCAAGCT
GGCCGACATGCTGCTCAACATCGGCACGCTGGTGCCGGGCGGGCCGCTGAAGTACGTCACCCGGCCCATCCTGGGCTCG
CTGACCCGCTACACGCTCGGCGACCAGATCGCCGACTGGCTGAAGATCCGGCGGGATCCGTTCTGGGACAACGTCTTCA
ACACCCTGTGGGAGCCCTTCATCGCCGTCCGCGAGGGCCTGCTGTCGTTGGAGAAGGCTCCGGGCGCCCTGTCGAAGTT
CTACTGGACCTTCGATGAGATCCTGCGCCTGGGCGTGCTGACCGTGCTGTCCGGCGCGCAGTTCCCGATCAGCATCGAGA
TCCCCTACTCCAACAACCCGAACTACCCCTCC

(**bold**: TEV cleavage site, underline: *Strep*-tag II)

Oxidative N-demethylase (A4XXY9):
ATGACCACCCTGACCTTCAAGCCGCTGGAGACCTACCGGGACGACTTCAGCTTCCGCAACAGCCCGGAGGCCATCGCTC
GCTTCCCCTTCCCCTTCCCGGAAGACCAGTACATGTACTCGGTGAACCTGGAACCGGCGGTGTCCCGCGACCCCGGCTCG
GTGTTCGAGCACCTGTTCGACGTGGACGAGCACTACGTGTCCGAGATGGCCGAGCGCGCCCGCGTGCTGGAGCGCGACC
CCGAGCGCTGCCTGGTGATGCCGCACATGGCCCCGGCCGCCTGGGACACCCTGGCGCTGCTGATGGAGAACCTGTCGCG
GGATTATCCACAGCACTTCCGCCTGGACCGCGAGGGCGACGCCTGGCACTGGCACAACCTCGCCCTGGGCATCGACCAG
CGCTTCACCTTCGGCGACCCGGCGACCCTGCCCTGCGAGCCGCTGGAGTACATCACCCGGCAGATGCAGGGCGACTTCG
CGGTGCTCGACCAGCGTGACGGCGACCTGTTCATGGACGCCGGCATGGTCACCTGCCCGGCCGACTGGTCCCTGCGCTT
CGACGCCGGCATGAGCTTCAAGCAGTGGCACTCTCCGGTGCCCATGGCCCACCAGATCGGGGTGTTCGACCGCGCCCTG
AAGTACCTGCTGAACATCCAGGTGGGCGCGCCGGTGCGTCGGCTGAACTGGACCCTGACCATCAACCCGCGCCTGGACA
CCTCCCCCGAGACCTACCACGAGTGGGGCAACGACCGCGGCAAGGTCACCCCGGACAACGTCGGCCGCCTGGTGCACC
TGCGCGTCGAGTTGCAGCTGATGGTCCGCCTGCCGCGCTCCAACGCCCTGCTGTTCGGCATCCGCACCTACCTGATCAGC
CTCGACGAGCTGGTCAGCAACCCGGCCTGGGCGCGGCGCATGCACCGCGTGATGCGCGACCTGCCCGCGCCCATCGCCG
ACTACAAGGGCATCACCCGCTACCGCCAGACGCTGGTCGACTGGCTGCGCCGCTTCGACCCCGAAGCC**GGTGGTAGTG
GCGGTTCTAGCGCT**TGGAGCCACCCGCAGTTCGAAAAA

(**bold**: GS linker, underline: *Strep*-tag II)

References

[1] E. O. Romero, A. T. Saucedo, J. R. Hernández-Meléndez, D. Yang, S. Chakrabarty, A. R. H. Narayan, "Enabling Broader Adoption of Biocatalysis in Organic Chemistry" *JACS Au* **2023**, *3*, 2073-2085.

[2] P. S. Coelho, E. M. Brustad, A. Kannan, F. H. Arnold, "Olefin cyclopropanation via carbene transfer catalyzed by engineered cytochrome P450 enzymes" *Science* **2013**, *339*, 307-310.

[3] P. S. Coelho, Z. J. Wang, M. E. Ener, S. A. Baril, A. Kannan, F. H. Arnold, E. M. Brustad, "A serine-substituted P450 catalyzes highly efficient carbene transfer to olefins *in vivo*" *Nat. Chem. Biol.* **2013**, *9*, 485-487.

[4] R. K. Zhang, K. Chen, X. Huang, L. Wohlschlager, H. Renata, F. H. Arnold, "Enzymatic assembly of carbon-carbon bonds via iron-catalysed sp^3 C-H functionalization" *Nature* **2019**, *565*, 67-72.

[5] E. W. Svastits, J. H. Dawson, R. Breslow, S. H. Gellman, "Functionalized Nitrogen Atom Transfer Catalyzed by Cytochrome-P-450" *J. Am. Chem. Soc.* **1985**, *107*, 6427-6428.

[6] J. A. McIntosh, P. S. Coelho, C. C. Farwell, Z. J. Wang, J. C. Lewis, T. R. Brown, F. H. Arnold, "Enantioselective Intramolecular C-H Amination Catalyzed by Engineered Cytochrome P450 Enzymes In Vitro and In Vivo" *Angew. Chem. Int. Ed.* **2013**, *52*, 9309-9312.

[7] T. K. Hyster, C. C. Farwell, A. R. Buller, J. A. McIntosh, F. H. Arnold, "Enzyme-Controlled Nitrogen-Atom Transfer Enables Regiodivergent C–H Amination" *J. Am. Chem. Soc.* **2014**, *136*, 15505-15508.

[8] C. K. Prier, R. K. Zhang, A. R. Buller, S. Brinkmann-Chen, F. H. Arnold, "Enantioselective, intermolecular benzylic C-H amination catalysed by an engineered iron-haem enzyme" *Nat. Chem.* **2017**, *9*, 629-634.

[9] A. Dennig, N. Lulsdorf, H. Liu, U. Schwaneberg, "Regioselective o-hydroxylation of monosubstituted benzenes by P450 BM3" *Angew. Chem. Int. Ed.* **2013**, *52*, 8459-8462.

[10] M. Bordeaux, V. Tyagi, R. Fasan, "Highly Diastereoselective and Enantioselective Olefin Cyclopropanation Using Engineered Myoglobin-Based Catalysts" *Angew. Chem. Int. Ed.* **2015**, *54*, 1744-1748.

[11] S. B. Kan, R. D. Lewis, K. Chen, F. H. Arnold, "Directed evolution of cytochrome *c* for carbon-silicon bond formation: Bringing silicon to life" *Science* **2016**, *354*, 1048-1051.

[12] S. B. J. Kan, X. Huang, Y. Gumulya, K. Chen, F. H. Arnold, "Genetically programmed chiral organoborane synthesis" *Nature* **2017**, *552*, 132-136.

[13] T. Betke, M. Maier, H. Gruber-Wölfler, H. Gröger, "Biocatalytic production of adiponitrile and related aliphatic linear α,ω-dinitriles" *Nat. Commun.* **2018**, *9*, 5112.

[14] Q. Zhou, M. Chin, Y. Fu, P. Liu, Y. Yang, "Stereodivergent atom-transfer radical cyclization by engineered cytochromes P450" *Science* **2021**, *374*, 1612-1616.

[15] M. Pott, M. Tinzl, T. Hayashi, Y. Ota, D. Dunkelmann, P. R. E. Mittl, D. Hilvert, "Noncanonical Heme Ligands Steer Carbene Transfer Reactivity in an Artificial Metalloenzyme" *Angew. Chem. Int. Ed.* **2021**, *60*, 15063-15068.

[16] L. E. Zetzsche, J. A. Yazarians, S. Chakrabarty, M. E. Hinze, L. A. M. Murray, A. L. Lukowski, L. A. Joyce, A. R. H. Narayan, "Biocatalytic oxidative cross-coupling reactions for biaryl bond formation" *Nature* **2022**, *603*, 79-85.

[17] I. Kalvet, M. Ortmayer, J. Zhao, R. Crawshaw, N. M. Ennist, C. Levy, A. Roy, A. P. Green, D. Baker, "Design of Heme Enzymes with a Tunable Substrate Binding Pocket Adjacent to an Open Metal Coordination Site" *J. Am. Chem. Soc.* **2023**, *145*, 14307-14315.

[18] S. Gergel, J. Soler, A. Klein, K. H. Schülke, B. Hauer, M. Garcia-Borràs, S. C. Hammer, "Engineered cytochrome P450 for direct arylalkene-to-ketone oxidation via highly reactive carbocation intermediates" *Nat. Catal.* **2023**, *6*, 606-617.

[19] K. Oohora, H. Meichin, L. Zhao, M. W. Wolf, A. Nakayama, J. Y. Hasegawa, N. Lehnert, T. Hayashi, "Catalytic Cyclopropanation by Myoglobin Reconstituted with Iron Porphycene: Acceleration of Catalysis due to Rapid Formation of the Carbene Species" *J. Am. Chem. Soc.* **2017**, *139*, 17265-17268.

[20] Y. Kagawa, K. Oohora, T. Himiyama, A. Suzuki, T. Hayashi, "Redox Engineering of Myoglobin by Cofactor Substitution to Enhance Cyclopropanation Reactivity" *Angew. Chem. Int. Ed.* **2024**, *63*, e202403485.

[21] S. Kato, M. Abe, H. Gröger, T. Hayashi, "Reconstitution of Myoglobin with Iron Porphycene Generates an Artificial Aldoxime Dehydratase with Expanded Catalytic Activities" *ACS Catal.* **2024**, *14*, 13081-13087.

[22] M. Schobert, D. Jahn, "Regulation of heme biosynthesis in non-phototrophic bacteria" *J Mol Microbiol Biotechnol* **2002**, *4*, 287-294.

[23] I. N. Harnastai, A. A. Gilep, S. A. Usanov, "The development of an efficient system for heterologous expression of cytochrome P450s in *Escherichia coli* using *hemA* gene co-expression" *Protein Expr. Purif.* **2006**, *46*, 47-55.

[24] G. Layer, "Heme biosynthesis in prokaryotes" *Biochim. Biophys. Acta, Mol. Cell Res.* **2021**, *1868*, 118861.

[25] M. Jiang, K. Hong, Y. Mao, H. Ma, T. Chen, Z. Wang, "Natural 5-Aminolevulinic Acid: Sources, Biosynthesis, Detection and Applications" *Front. Bioeng. Biotechnol.* **2022**, *10*, 841443.

[26] C. Feng, M. Pan, L. Tang, "5-Aminolevulinic acid level and dye-decolorizing peroxidase expression regulate heme synthesis in *Escherichia coli*" *Biotechnol. Lett.* **2022**, *44*, 271-277.

[27] J. Ge, X. Wang, Y. Bai, Y. Wang, Y. Wang, T. Tu, X. Qin, X. Su, H. Luo, B. Yao, H. Huang, J. Zhang, "Engineering *Escherichia coli* for efficient assembly of heme proteins" *Microb. Cell Fact.* **2023**, *22*, 59.

[28] W. Wang, Y. Xiang, G. Yin, S. Hu, J. Cheng, J. Chen, G. Du, Z. Kang, Y. Wang, "Construction of 5-Aminolevulinic Acid Microbial Cell Factories through Identification of Novel Synthases and Metabolic Pathway Screens and Transporters" *J. Agric. Food Chem.* **2024**, *72*, 8006-8017.

[29] T. Li, Y.-Y. Guo, G.-Q. Qiao, G.-Q. Chen, "Microbial Synthesis of 5-Aminolevulinic Acid and Its Coproduction with Polyhydroxybutyrate" *ACS Synth. Biol.* **2016**, *5*, 1264-1274.

[30] W. Pu, J. Chen, Y. Zhou, H. Qiu, T. Shi, W. Zhou, X. Guo, N. Cai, Z. Tan, J. Liu, J. Feng, Y. Wang, P. Zheng, J. Sun, "Systems metabolic engineering of *Escherichia coli* for hyper-production of 5-aminolevulinic acid" *Biotechnol. Biofuels Bioprod.* **2023**, *16*, 31.

[31] H. Zhou, C. Zhang, Z. Li, M. Xia, Z. Li, Z. Wang, G.-Y. Tan, Y. Luo, L. Zhang, W. Wang, "Systematic development of a highly efficient cell factory for 5-aminolevulinic acid production" *Trends Biotechnol.* **2024**, *42*, 1479-1502.

[32] J. Pérez-Pérez, J. Gutiérrez, "An arabinose-inducible expression vector, pAR3, compatible with ColE1-derived plasmids" *Gene* **1995**, *158*, 141-142.

[33] N. J. Porter, E. Danelius, T. Gonen, F. H. Arnold, "Biocatalytic Carbene Transfer Using Diazirines" *J. Am. Chem. Soc.* **2022**, *144*, 8892-8896.

[34] E. Danelius, N. J. Porter, J. Unge, F. H. Arnold, T. Gonen, "MicroED Structure of a Protoglobin Reactive Carbene Intermediate" *J. Am. Chem. Soc.* **2023**, *145*, 7159-7165.

[35] L. Schaus, A. Das, A. M. Knight, G. Jimenez-Osés, K. N. Houk, M. Garcia-Borràs, F. H. Arnold, X. Huang, "Protoglobin-Catalyzed Formation of cis-Trifluoromethyl-Substituted Cyclopropanes by Carbene Transfer" *Angew. Chem. Int. Ed.* **2023**, *62*, e202208936.

[36] E. Alfonzo, D. Hanley, Z.-Q. Li, K. M. Sicinski, S. Gao, F. H. Arnold, "Biocatalytic Synthesis of α-Amino Esters via Nitrene C–H Insertion" *J. Am. Chem. Soc.* **2024**, *146*, 27267-27273.

[37] D. Hanley, Z.-Q. Li, S. Gao, S. C. Virgil, F. H. Arnold, E. Alfonzo, "Stereospecific Enzymatic Conversion of Boronic Acids to Amines" *J. Am. Chem. Soc.* **2024**, *146*, 19160-19167.

[38] T. Rogge, Q. Zhou, N. J. Porter, F. H. Arnold, K. N. Houk, "Iron Heme Enzyme-Catalyzed Cyclopropanations with Diazirines as Carbene Precursors: Computational Explorations of Diazirine Activation and Cyclopropanation Mechanism" *J. Am. Chem. Soc.* **2024**, *146*, 2959-2966.

[39] I. Barr, F. Guo, "Pyridine Hemochromagen Assay for Determining the Concentration of Heme in Purified Protein Solutions" *Bio-protocol* **2015**, *5*, e1594.

[40] E. Verkamp, V. M. Backman, J. M. Björnsson, D. Söll, G. Eggertsson, "The periplasmic dipeptide permease system transports 5-aminolevulinic acid in Escherichia coli" *J. Bacteriol.* **1993**, *175*, 1452-1456.

[41] S. Kato, K. Takeuchi, M. Iwaki, K. Miyazaki, K. Honda, T. Hayashi, "Chitin- and Streptavidin-Mediated Affinity Purification Systems: A Screening Platform for Enzyme Discovery" *Angew. Chem. Int. Ed.* **2023**, *62*, e202303764.

[42] N. Kawakami, O. Shoji, Y. Watanabe, "Use of Perfluorocarboxylic Acids To Trick Cytochrome P450BM3 into Initiating the Hydroxylation of Gaseous Alkanes" *Angew. Chem. Int. Ed.* **2011**, *50*, 5315-5318.

[43] O. Shoji, T. Kunimatsu, N. Kawakami, Y. Watanabe, "Highly Selective Hydroxylation of Benzene to Phenol by Wild-type Cytochrome P450BM3 Assisted by Decoy Molecules" *Angew. Chem. Int. Ed.* **2013**, *52*, 6606-6610.

[44] O. Shoji, S. Yanagisawa, J. K. Stanfield, K. Suzuki, Z. Cong, H. Sugimoto, Y. Shiro, Y. Watanabe, "Direct Hydroxylation of Benzene to Phenol by Cytochrome P450BM3 Triggered by Amino Acid Derivatives" *Angew. Chem. Int. Ed.* **2017**, *56*, 10324-10329.

[45] M. Karasawa, J. K. Stanfield, S. Yanagisawa, O. Shoji, Y. Watanabe, "Whole-Cell Biotransformation of Benzene to Phenol Catalysed by Intracellular Cytochrome P450BM3 Activated by External Additives" *Angew. Chem. Int. Ed.* **2018**, *57*, 12264-12269.

[46] K. Chen, Z. Wang, K. Ding, Y. Chen, Y. Asano, "Recent progress on discovery and research of aldoxime dehydratases" *Green Synth. Catal.* **2021**, *2*, 179-186.

[47] A. Hinzmann, T. Betke, Y. Asano, H. Gröger, "Synthetic Processes toward Nitriles without the Use of Cyanide: A Biocatalytic Concept Based on Dehydration of Aldoximes in Water" *Chem. Eur. J.* **2021**, *27*, 5313-5321.

[48] L. Ilcu, W. Röther, J. Birke, A. Brausemann, O. Einsle, D. Jendrossek, "Structural and Functional Analysis of Latex Clearing Protein (Lcp) Provides Insight into the Enzymatic Cleavage of Rubber" *Sci. Rep.* **2017**, *7*, 6179.

[49] X. Liu, Z. Yuan, J. Wang, Y. Cui, S. Liu, Y. Ma, L. Gu, S. Xu, "Crystal structure and biochemical features of dye-decolorizing peroxidase YfeX from Escherichia coli O157 Asp143 and Arg232 play divergent roles toward different substrates" *Biochem. Biophys. Res. Commun.* **2017**, *484*, 40-44.

[50] R. Singh, B. Wiseman, T. Deemagarn, V. Jha, J. Switala, P. C. Loewen, "Comparative study of catalase-peroxidases (KatGs)" *Arch. Biochem. Biophys.* **2008**, *471*, 207-214.

[51] K. Nishimoto, N. Okahashi, M. Maruyama, Y. Izumi, K. Nakatani, Y. Ito, J. Iida, T. Bamba, F. Matsuda, "Lipidome and metabolome analyses reveal metabolic alterations associated with MCF-7 apoptosis upon 4-hydroxytamoxifen treatment" *Sci. Rep.* **2023**, *13*, 18549.

[52] S. Komori, N. Okahashi, J. Iida, F. Matsuda, "Lipidome variation of industrial Saccharomyces cerevisiae strains analyzed by LC-QTOF/MS-based untargeted lipidomics" *J. Biosci. Bioeng.* **2023**, *135*, 102-108

Chapter 3
Whole-Cell Aldoxime Dehydration in Organic Media Using Organic Solvent-Tolerant Bacterial Hosts

3-1. Introduction

Aldoxime dehydratase (Oxd) is a heme-dependent enzyme which catalyzes the dehydration of aldoximes to form the corresponding nitriles. This unique class of enzymes was first reported by Asano and co-workers, enabling a novel biocatalytic route for nitrile synthesis without the use of highly toxic cyanides or precious metal catalysts (Fig. 3-1a)[1,2]. Due to their ability to function under mild conditions and their chemoselectivity to suppress undesirable byproduct formation, Oxd has attracted considerable attention as green and sustainable catalyst for nitrile synthesis[3–5]. Despite these advantages, the practical application of Oxds still involves operational constraints. These enzymes are typically used in aqueous media, where substrate solubility, especially hydrophobic compounds, remains limited. Besides improved substrate solubility, conducting such biotransformations in pure organic medium would have the further advantage of a simplified downstream-processing, which consists of a separation of the product mixture from the biocatalyst by decantation instead of tedious extraction steps. Although several excellent strategies using specialized cell immobilization materials have been developed to enable the use of whole-cell catalysts in organic solvents[6–8], the low organic solvent tolerance of the conventional host strains such as *Escherichia coli* potentially restricts their use in non-aqueous environments.

To overcome this issue, the author focused on the use of organic solvent-tolerant bacteria as a host for the recombinant expression of Oxds. To date, several bacteria being tolerant towards organic solvents have been reported[9], beginning with the discovery and isolation of the toluene-tolerant strain Pseudomonas putida IH-2000 by Inoue and Horikoshi[10]. The earliest attempt to employ organic solvent-tolerant bacteria as a whole-cell catalyst in non-aqueous media was reported by Dias and co-workers, who utilized *Mycobacterium sp*. NRRL B-3805 as a whole-cell catalyst for the side-chain degradation of β-sitosterol[11]. Following these early studies, *Rhodococcus* species have emerged as particularly attractive hosts due to their exceptional tolerance to hydrophobic organic solvents enabled by their thick, hydrophobic cell walls and solvent-adaptive mechanisms[12,13]. This remarkable solvent tolerance is primarily attributed to the unique cell envelope architecture of *Rhodococcus* species, which is characterized by a mycolic-acid–rich outer layer covalently linked to arabinogalactan and peptidoglycan. That forms a highly hydrophobic permeability barrier, effectively restricting solvent penetration (Fig.3-1b)[14]. In particular, Ohtake and co-workers reported the use of *Rhodococcus opacus* B-4 as a whole-cell catalyst in anhydrous organic solvents or water-in-oil emulsion, demonstrating high catalytic activity and stability in the production of indigo from indole and *o*-cresol from toluene[15,16]. Therefore, the author speculated that this solvent-tolerant phenotype, combined with the protective effect of the cellular environment, may make *Rhodococcus* species attractive hosts for performing enzymatic aldoxime dehydration under anhydrous conditions in the presence of a whole-cell catalyst.

Based on this concept, the author developed a whole-cell catalytic system using the organic solvent-tolerant bacterium *Rhodococcus erythropolis* L88[17] as a host for Oxd expression (Fig. 3-1c). The system efficiently enabled preparative-scale synthesis of diverse nitriles under anhydrous conditions using hexane as an organic solvent. The developed process demonstrates the feasibility of a solvent-tolerant whole-cell system for aldoxime dehydration without laborious extraction steps or protective immobilization.

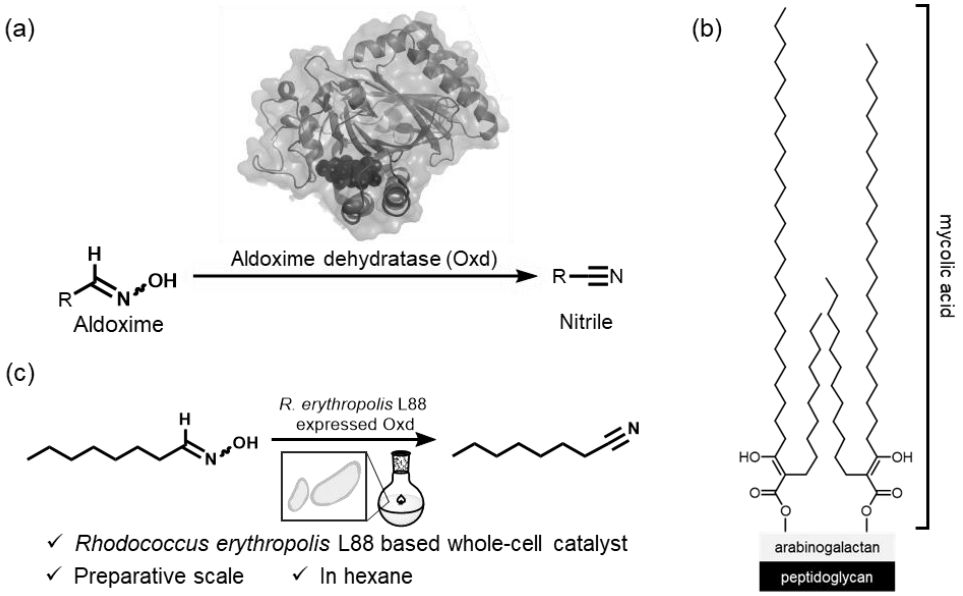


Figure 3-1. (a) Crystal structure of Oxd from *Rhodococcus erythropolis* PR4 (PDB : 3A15). (b) Representative structure of the cell membrane in *Rhodococcus erythropolis*. (c) Aldoxime dehydration using *Rhodococcus erythropolis* L88 as a whole-cell catalyst in this study.

3-2. Results and discussion

Verification of the whole-cell catalyst system based on *R. erythropolis* L88 bacteria in an organic solvent

In this study, *R. erythropolis* L88 was selected as the host strain for the whole-cell catalytic system, considering its high tolerance to organic solvents and the ease of genetic manipulation based on a recombinant expression system using the thiostrepton-inducible pTip-QT1 vector[17–19]. At first, the gene of *R. erythropolis* PR4 aldoxime dehydratase (ReOxd)[2,20] was cloned into the pTip-QT1 vector for the homogeneous overexpression in the host. The constructed plasmid was then transformed into *R. erythropolis* L88 cells, and the expression of ReOxd was induced by adding thiostrepton at exponential growth phase. After cultivation at 28 °C for 16 h, the cells were harvested by centrifugation, and the cell pellets stored at −80 °C were directly utilized for the whole-cell catalysis. To validate this concept, the author first tested the dehydration of octanal oxime (**1a**) as a model reaction for converting a hydrophobic substrate. The pellets of *R. erythropolis* L88 overexpressing ReOxd were suspended in hexane at the concentration of 15 mg/mL, and substrate **1a** was added at final a concentration of 100 mM to initiate the reaction. Notably, octanenitrile (**2a**) was found to be produced in 32% yield even under such non-aqueous conditions as determined by GC analysis, demonstrating the robustness of *R. erythropolis* L88 strain for the whole-cell catalyzed transformation in organic solvent (Fig. 3-2a). In contrast, when *R. erythropolis* L88 cells harboring an empty vector was used for the reaction, no detectable nitrile formation was observed, which underlines the

requirement of the ReOxd overexpression with pTip-QT1 vector for the desired biotransformation (Fig. 3-2b). Although *R. erythropolis* L88 also possesses the Oxd gene within its genome, the expression of the inherent Oxd may be strictly regulated under the cultivation conditions. Furthermore, the author also examined the influence of the reaction medium using ten different organic solvents (Table 3-1). The desired product **2a** was also generated in the presence of several other organic solvents, such as toluene and benzene, however, the activity was reduced or negligible, especially when utilizing organic solvents with lower logP_{ow} values. In general, organic solvents with logP_{ow} values below 2.4 are known to cause significant damage to cell membranes[10]. Although *R. erythropolis* is known to have excellent solvent tolerance[17,21], the use of organic solvents other than hexane was suggested to cause significant damage to cell membranes and decreased catalytic activity of ReOxd.

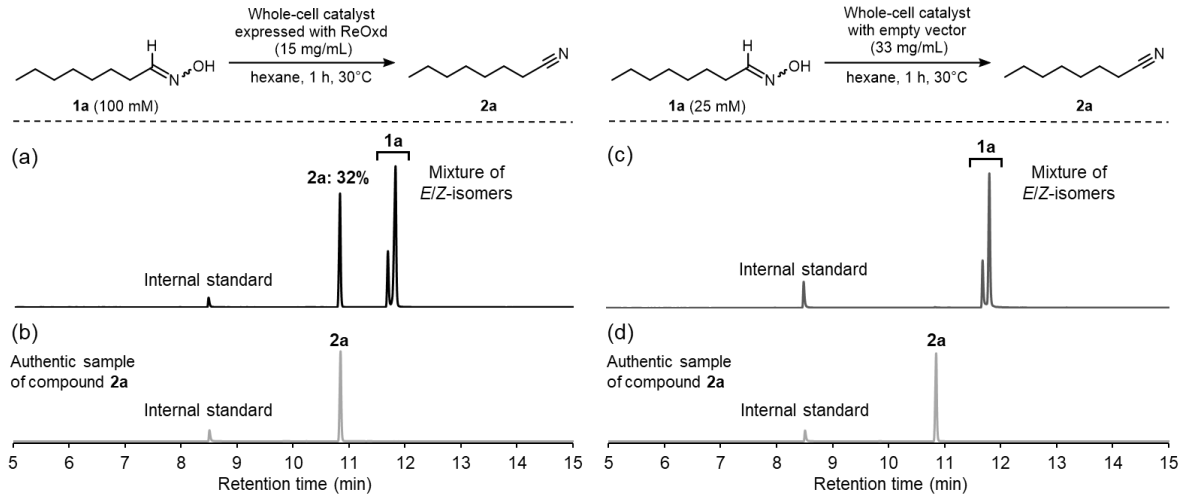


Figure 3-2. Aldoxime dehydration catalyzed by *R.erythropolis* L88 based whole-cell catalyst expressing ReOxd. (a) GC-FID chromatogram for the reaction mixture (**1a** → **2a**). (b) GC-FID chromatogram for authentic sample of **2a**. (c) GC-FID chromatogram for the reaction mixture (**1a** → **2a**). (d) GC-FID chromatogram for authentic sample of **2a**. Reaction conditions: **1a** (100 mM or 25 mM) in 250 μL of hexane and *R.erythropolis* L88 cells carrying ReOxd (7.5 mg) or empty vector (16.7 mg) in 250 μL of hexane at 30 °C for 1 h.

Table 3-1. Aldoxime dehydration in several organic solvents.

Organic solvent	log P_{ow}	Yield (%)
Hexane	4.0	32
Toluene	2.5	7
Benzene	2.1	6
Et_2O	0.89	3
Ethyl acetate	0.73	0.2
THF	0.46	n.d.
1,4-dioxane	-0.27	n.d.
Acetonitrile	-0.34	n.d.
DMF	-1.0	n.d.
DMSO	-1.4	n.d.

Screening of various biocatalysts

To improve the efficiency of the present whole-cell catalytic system, the author next performed an enzyme screening to identify an Oxd enzyme which shows higher catalytic activity under the chosen anhydrous conditions. Six Oxd candidates which had been examined in the previous studies[22,23] were selected for the screening based on the results of sequence similarity network (SSN) to ensure the diversity of the protein sequence space[24,25] (Fig. 3-3a). These six Oxds from different microorganisms were subsequently expressed in *R. erythropolis* L88 and evaluated for their catalytic activity under the low catalyst loading condition (15 mg/mL cell pellets, 100 mM substrate). Consequently, the Oxd from *Bacillus sp*. OxB-1 (BsOxd)[26] showed the highest performance among the tested Oxds, affording nitrile **2a** in 92% yield under the anhydrous condition (Fig. 3-3b). BsOxd is one of the most well-characterized aldoxime dehydratases, and it has been extensively investigated in the previous studies due to its broad substrate scope and robust activity[5,6,27–29]. In addition, BsOxd was found to be expressed at a higher level compared to ReOxd according to the SDS PAGE analysis (Fig. 3-4). The robust catalytic activity of BsOxd itself and its high expression level in the *R. erythropolis* L88 strain might have contributed to the superior catalytic performance of the BsOxd-based whole cell systems.

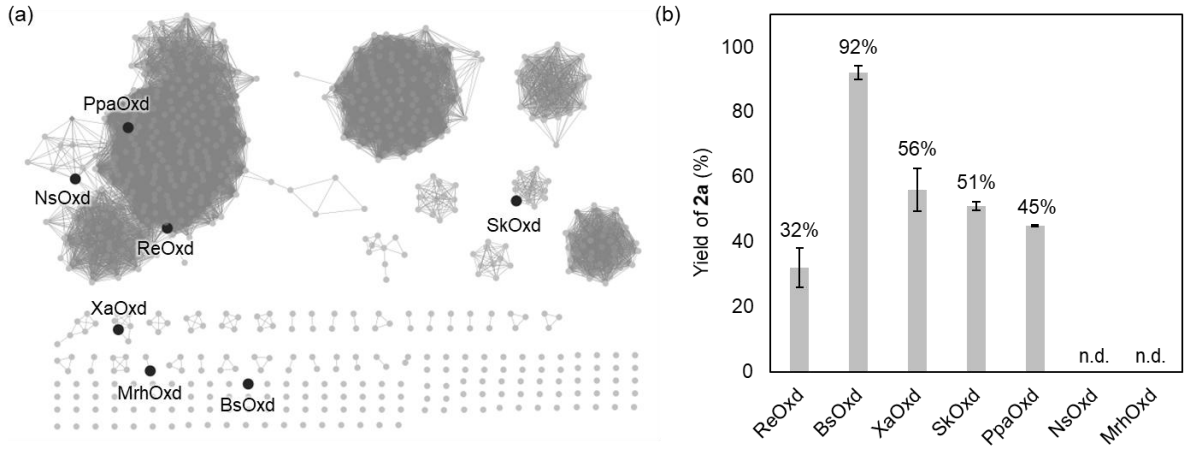


Figure 3-3. (a) SSN of aldoxime dehydratases generated by EFI-EST. Query sequence: ReOxd, database: UniProt, Node: 718, Edge: 18742 (>75%identity). A total of seven enzymes selected for screening are highlighted with black circles. (b) Concentration of **2a** catalyzed by various Oxds. Reaction conditions: [aldoxime **1a**] = 100 mM, [*R. erythropolis* L88 pellets] = 15 mg/mL in hexane (500 μL) at 30 °C for 1 h.

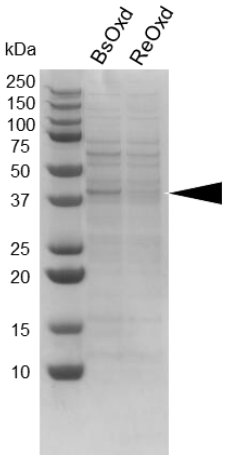


Figure 3-4. SDS-PAGE analysis of *R. erythropolis* L88 cells harboring pTip-QT1-BsOxd and pTiP-QT1-ReOxd. A 10 mg/mL cell suspension was disrupted using a ball mill, and 13 μL of the resulting supernatant was loaded.

Furthermore, *R. erythropolis* L88 cells expressing BsOxd exhibited retained catalytic activity under the lower catalyst loading conditions (Fig. 3-5). The desired nitrile **2a** was obtained in almost quantitative yield within 30 min even at a catalyst concentration as low as 5 mg/mL (Fig. 3-6a). In contrast, the *E. coli*-based whole-cell catalyst exhibited no catalytic activity under this non-aqueous condition using hexane as the organic solvent (Fig. 3-6a). Although *E. coli* exhibted a higher BsOxd expression level (Fig. 3-6b) than *R. erythropolis* (Fig. 3-4) as confirmed by the SDS–PAGE analysis, the present *R. erythropolis*-based catalytic system nevertheless demonstrated much higher catalytic activity. These findings highlight the intrinsic solvent tolerance and stress resistance of *R. erythropolis* L88, making strain a particularly promising biocatalyst for applications in organic solvents.

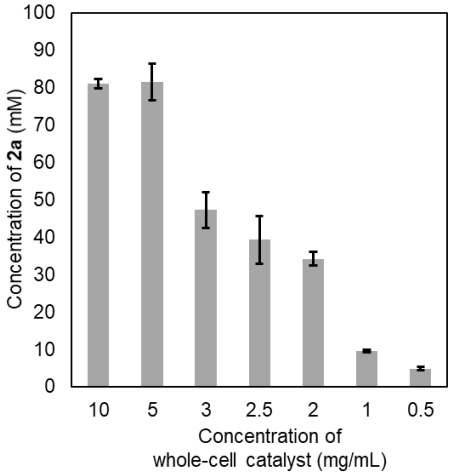


Figure 3-5. Aldoxime dehydration catalyzed by *R. erythropolis* L88 (BsOxd) based whole-cell catalysts. Reaction conditions: [aldoxime **1a**] = 100 mM in hexane (500 µL) at 30 °C for 30 min.

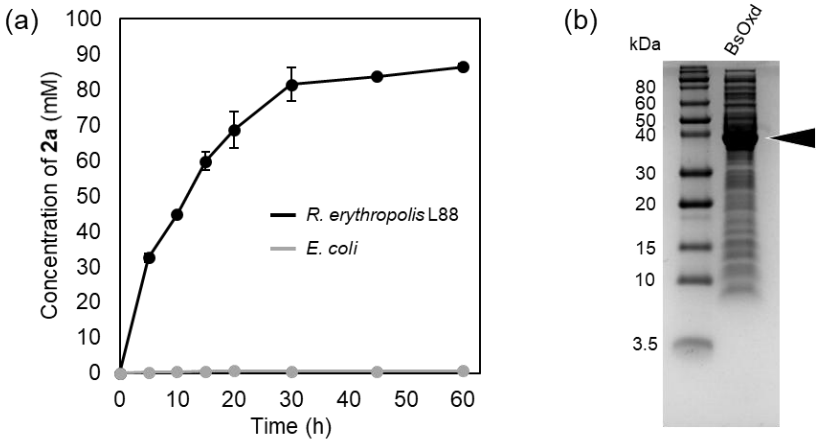


Figure 3-6. (a) Aldoxime dehydration catalyzed by whole-cell catalysts, *R. erythropolis* L88 (black) and *E. coli* (gray). Reaction conditions: [aldoxime **1a**] = 100 mM, [*R. erythropolis* L88 pellets and *E. coli pellets*] = 5 mg/mL in hexane (500 µL) at 30 °C for 1 h. (b) SDS-PAGE analysis of *E. coli* cells harboring pET21b-BsOxd. A 10 mg/mL cell suspension was disrupted by sonication, and 10 µL of the resulting supernatant was loaded.

Investigation of the substrate scope

Next, to evaluate the practicality of the catalytic system, the substrate scope of the whole-cell catalyst was examined under preparative-scale conditions (Fig. 3-7). The author performed the whole-cell catalysis at a 6.0 mmol scale using a conventional reaction apparatus in organic synthesis. Since the catalytic system does not require laborious extraction processes, which often cause cell lysis and result in viscous mixtures that resist phase separation, the generated nitriles were isolated through a simple workup involving only celite filtration, solvent evaporation, and flash chromatography to purify the products. For model substrate **1a**, octanenitrile (**2a**) was obtained in 86% isolated yield, demonstrating the applicability of the whole-cell catalytic system to preparative scale synthesis. Similarly, phenylacetylaldehyde oxime (**1b**), a known natural substrate of aldoxime dehydratase[1], was quantitatively converted into the desired nitrile **2b** in 95% isolated yield. Furthermore, structurally related aromatic aldoximes **1c**–**1g** were also found to be compatible with the developed catalytic system. The corresponding nitriles **2c**–**2g** were obtained in high or moderate isolated yields, highlighting the broad substrate versatility of BsOxd as well as the tolerance of the *R. erythropolis* host strain towards hexane as organic solvent. Particularly, furan-containing aldoxime **1c** was efficiently converted to the corresponding nitrile **2c** in 79% isolated yield. In contrast, nitriles **2e** and **2g** were produced in relatively low isolated yield, most likely due to the poor solubility of these aldoximes in hexane. Aliphatic aldoxime **1h** was also tolerated under these whole-cell conditions, although this aldoxime bearing a secondary carbon at the α-position exhibited reduced activity due to steric hindrance. Taken together, the processes using the developed BsOxd-based whole-cell catalyst represent a robust and versatile technology platform for the preparative-scale synthesis of structurally diverse nitriles.

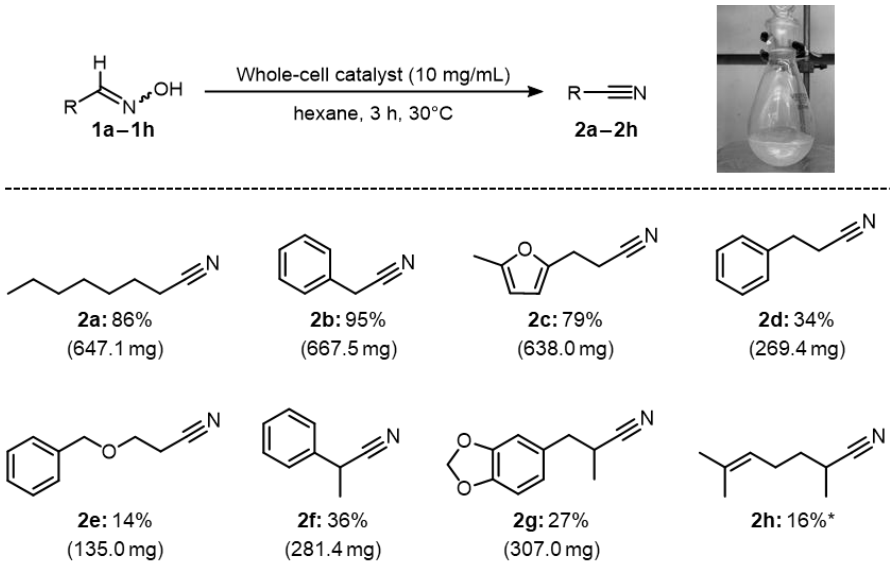


Figure 3-7. Substrate scope for aldoxime conversions catalyzed by whole-cell catalyst, *R. erythropolis* L88. Reaction conditions: [aldoximes **1a**–**1h**] = 100 mM, [R. *erythropolis* L88 pellets] = 10 mg/mL in hexane (60 mL) at 30 °C for 3 h. *The yield was determined by ^{1}H NMR.

3-3. Summary

In summary, the author developed a whole-cell catalytic system for nitrile synthesis using organic solvent-tolerant bacterium *R. erythropolis* L88 as a host strain. Particularly, *R. erythropolis* L88 cells expressing Oxd from *Bacillus sp*. OxB-1 (BsOxd) were found to exhibit high aldoxime dehydration activity under anhydrous conditions using hexane as an organic solvent. In contrast, conventional *E. coli*-based whole-cell system failed to maintain its catalytic activity after exposure to organic solvents. Furthermore, this system using *R. erythropolis* L88 was successfully applied to preparative-scale synthesis. Through a simple reaction work-up, a wide range of hydrophobic nitriles were efficiently obtained in moderate to good isolated yields. Considering its robustness, scalability and compatibility with hydrophobic substrates, this *R. erythropolis*-based whole-cell catalytic system is expected to provide a sustainable platform for nitrile production.

3-4. Experimental section

Instruments

^{1}H and ^{13}C NMR spectra were recorded on a Bruker NMR Advance III HD spectrometer (400 MHz) and Bruker NMR Advance 500 spectrometer (500 MHz). ^{1}H and ^{13}C NMR chemical shifts are reported relative to deuterated solvents or tetramethylsilane. ESI-TOF MS analyses were performed on a Bruker micrOTOF focus II mass spectrometer. The GC experiments were performed on a Shimadzu GC-2014 Gas Chromatograph equipped with DB-1 column (Agilent Technologies, Inc.). Ultrapure water was demineralized using a Merck Millipore Milli-Q integral 3 system. PCR was performed using a Bio-Rad T100TM Thermal Cycler. Electroporation was performed using a Bio-Rad Gene Pulser Xcell™ system. *E. coli* cells and *Rhodococcus erythropolis* L88 cells were cultivated using TAITEC BioShaker G·BR-300, G·BR-200, BR-23FP, BR-43FL, M·BR-024, and DWMax M·BR-034P and harvested using TOMY Suprema 21, Eppendorf centrifuge 5910R, 5430R, HITACHI High speed Micro Centrifuge CF15RN, and KUBOTA Tabletop Centrifuge, Model 4000. Flash chromatography of the synthesized compounds was performed using Biotage Isolera™ One and Biotage Selekt Enkel.

Materials

All reagents of the highest guaranteed grade were purchased from TCI Co., Ltd., Merck Ltd., FUJIFILM Wako Pure Chemical Corporation and Nacalai Tesque, Inc., and used as received unless otherwise noted. Aldoximes **1a**–**1h** were synthesized as described in the Supporting Information. Oligonucleotides were obtained from Merck Ltd. and Eurofins Scientific SE, Inc. The gene of BsOxd was purchased as a synthetic gene fragment from Twist Bioscience Corp. The genes of other aldoxime dehydratases were amplified by PCR from genomic DNA of the corresponding bacteria purchased from the Biological Resource Center, National Institute of Technology and Evaluation (NBRC). *R. erythropolis* L88 strain and pTip-QT1 vector were purchased from Hokkaido System Science Co., Ltd. pET-21b vector was purchased from Merck Ltd. and used for the protein expression in *E. coli*. Nucleotide sequences were determined by Eurofins Scientific SE, Inc.

Preparation of the expression plasmids for aldoxime dehydratases in *R. erythropolis* L88

The expression plasmids for Oxds were constructed using pTip-QT1 vector according to the standard protocol of NEBuilder HiFi DNA Assembly Cloning Kit (New England Biolabs Japan). The insert gene for BsOxd was purchased as a synthetic gene fragment from Twist Bioscience Corp, which contains 15–20 bp sequences overlapped with the pTip-QT1vector for the following cloning process. Insert genes for the other Oxds were amplified by PCR from the genomic DNA of corresponding bacteria using primers that contain the overlapped sequence with pTip-QT1 vector. The PCR products were then purified by agarose gel electrophoresis and assembled with a linearized pTip-QT1 vector using the NEBuilder HiFi DNA Assembly. The assembled products were then transformed into a chemically competent *E. coli* DH5α cell (Takara Bio Inc.), and the resulting plasmids were purified according to the standard protocol NucleoSpin Plasmid (Takara Bio Inc.).

General procedure for the expression of aldoxime dehydratase in *R. erythropolis* L88

The pTip-QT1 expression plasmids encoding the gene for the aldoxime dehydratases were transformed into chemically competent *R. erythropolis* L88 cells (Hokkaido System Science Co., Ltd.) by electroporation system (2 mm cuvette, 2.5 kV, 25 μF, 400 Ω). The resulting transformants were plated on LB agar medium containing tetracycline (5 μg/mL) and incubated at 28 ºC for 4 days. The obtained single colony was then inoculated into 10 mL of LB medium containing tetracycline (5 μg/mL) and cultivated at 28 ºC and 140 rpm for 2 days. The culture (500 μL) was then inoculated into 200 mL of LB medium containing tetracycline (5 μg/mL). After incubation at 28 ºC and 140 rpm for 24 h, thiostrepton (final conc. 0.2 μg/mL) were added to induce the expression of the aldoxime dehydratase, and the cultivation was continued at 28 ºC and 140 rpm for 24 h. Finally, the *R. erythropolis* L88 cells were harvested by centrifugation at 8,800 rpm for 10 min, and stored at −80 °C until further use.

Preparation of the expression plasmid for BsOxd in *E. coli*

The expression plasmid for BsOxd was constructed using the pET-21b vector according to the standard protocol of the NEBuilder HiFi DNA Assembly Cloning Kit (New England Biolabs Japan). The insert gene for BsOxd was purchased as a synthetic gene fragment from Twist Bioscience Corp. The linearized vector of pET-21b was prepared by PCR using KAPA HiFi HotStart DNA Polymerase (Nippon Genetics co. ltd). The PCR product was then purified by agarose gel electrophoresis and assembled with the BsOxd insert gene using NEBuilder HiFi DNA Assembly. The assembled product was then transformed into a chemically competent *E. coli* DH5α cell, and the resulting plasmid was purified using the NucleoSpin® Plasmid (Takara Bio Inc.).

Procedure for the expression of aldoxime dehydratase in *E. coli*

The pET-21b expression plasmids encoding the gene for aldoxime dehydratases were transformed into chemically competent *E. coli* BL21-Gold(DE3) cell (Agilent Technologies, Inc.). The resulting transformants were plated on LB agar medium containing ampicillin (100 μg/mL) and incubated overnight at 37 ºC. The obtained single colony was then inoculated into 10 mL of LB medium containing ampicillin (100 μg/mL) and cultivated at 37 ºC and 180 rpm for 6 h. The culture (1.3 mL) was then inoculated into 130 mL of LB medium containing ampicillin (100 μg/mL). After incubation at 37 ºC and 140 rpm for 3.5 h, IPTG (final conc. 0.20 mM) was added to induce the

expression of hemoproteins, and the cultivation was continued at 18 ºC and 140 rpm for 16 h. Finally, the *E. coli* cells were harvested by centrifugation at 8,800 rpm for 10 min, and stored at −80 °C until further use.

General procedure for aldoxime dehydration in a small scale

The frozen cell pellets of *R. erythropolis* L88 expressing Oxds (2.5 – 16.7mg) were resuspended in 250 μL of hexane. After shaking at 30 °C and 1000 rpm for 10 min, 200 mM aldoxime 1a in hexane (250 μL) was added (final concentration of 100 mM). The resulting mixture was then vigorously shaken at 30 °C and 1,200 rpm for 1 h using TAITEC BioShaker DWMax M·BR-034P. The reaction mixture was quenched by adding EtOAc (700 μL). For the product quantification, cyclohexanol (2.3 μmol) in acetonitrile (30 μL) was added to the reaction mixture as an internal standard. The reaction mixture was then centrifuged at 21,130 × g for 3 min, and the supernatants were analyzed by GC-FID equipped with a DB-1 column (Separation method: 1.0 μL injection, injector temperature: 200 °C, detector temperature: 270 °C, gradient: column temperature set at 40 °C, held at 40 °C for 7 min, then 30 °C/min to 100 °C, then 50 °C/min to 260 °C, and held at 260 °C for 10 min, with a total run time of 22.20 min).

Procedure for nitrile synthesis catalyzed by *E. coli*

The frozen cell pellets of *E. coli* expressing BsOxd (2.5 mg) were suspended in 250 μL of hexane. After stirring at 30 °C and 1000 rpm for 10 min, 200 mM aldoxime **1a** in hexane (250 μL) was added (final conc. 100 mM). The resulting mixture was then sheked at 30 °C and 1200 rpm for 1 h. The reaction mixture was quenched by EtOAc (700 μL). For the product quantification, cyclohexanol (2.3 μmol) in acetonitrile (30 μL) was added into the reaction mixture as an internal standard. The reaction mixture was centrifuged at 21,130 × g for 3 min, and the supernatants were analyzed by GC-FID equipped with a DB-1 column (Separation method: 1.0 μL injection, injector temperature: 200 °C, detector temperature: 270 °C, gradient: column temperature set at 40 °C, held at 40 °C for 7 min, then 30 °C/min to 100 °C, then 50 °C/min to 260 °C, and held at 260 °C for 10 min, with a total run time of 22.20 min).

General procedure for nitrile synthesis at a preparative scale

The frozen cell pellets of *R. erythropolis* L88 expressing BsOxd were added to a 200 mL round-bottom flask charged with a stirring bar and resuspended into 30 mL of hexane. After stirring at 30 °C for 10 min, aldoxime **1a**–**1h** (6.0 mmol) in hexane (30 mL) was added. The resulting mixture was then stirred at 30 °C for 3 h in the round-bottom flask being open to the atmosphere. After cooling at room temperature, the reaction mixture was filtered through celite, and the remaining celite cake was washed with EtOAc and $CHCl_3$. The obtained filtrate was concentrated by rotary evaporator. The residue was purified by silica flash column chromatography (hexane/EtOAc) to afford nitrile **2a**–**2h**. Chemical structures of the obtained products were confirmed by ^{1}H NMR, ^{13}C NMR, and ESI-TOS MS.

DNA Sequence

ReOxd :
ATGGAATCTGCAATCAGTGAACATCTTCAATGCCCGCGCACGCTGACCAGGCGCGTTCCGGATACCTATTCGCCACCATTT
CCCATGTGGGTCGGGCGTGCGGACGACACATTGCACCAGGTCGCGATGGGCTATCTCGGCGTGCAGTTCCGCGGCGAGG
ATCAGCGCTCGGCTGCACTGCAGTCCATGCGGGATATTGTCGCCGGCTTCGACTTGCCGGACGGACCGGCACATCACGAT
CTCACTCACCATGTCGACAACCAGGGCTACGAGAATCTGATCGTGGTCGGGTACTGGAAAGATGTTTCTTCCCAACATCG
TTGGAGCACATCAGCTCCGGTGGCCTCCTGGTGGGAGTCCGAGGACCGCTTGTCCGACGGATTGGGGTTCTTCCGGGAG
ATCGTGGCACCGAGAGCCGAACAATTCGAAACGCTCTACGCGTTCCAGGACGATCTCCCCGGAGTGGGAGCCGTCATGG
ACGGTGTCAGCGGCGAGATCAACGAGCACGGCTACTGGGGTTCGATGCGCGAGCGCTTTCCGATCTCCCAGACCGACTG
GATGCAGGCCTCGGGCGAACTACGGGTCGTCGCCGGTGACCCCGCCGCAGGTGGACGCGTAGTAGTGCGGGGGCACGA
CAACATCGCACTGATCAGATCCGGGCAGGACTGGGCCGACGCGGAAGCAGACGAGCGCAGCCTCTACCTCGACGAAATC
CTGCCGACTCTTCAATCGGGCATGGACTTCCTCCGCGACAACGGCCCGGCCGTCGGGTGCTACAGCAACCGTTTCGTACG
CAATATCGACATCGACGGAAACTTCCTCGACCTGAGCTACAACATCGGTCACTGGGCCTCACTCGACCAACTCGAGCGGT
GGTCGGAATCCCACCCGACCCATCTGCGGATCTTCACGACGTTCTTCCGGGTGGCCGAGGGCCTGTCGAAATTACGTCTC
TACCATGAGGTCTCGGTATTCGATGCCGCCGATCAGCTGTACGAGTACATCAACTGCCATCCCGGGACCGGGATGCTGCGC
GACGCGGTGACCACCGCCGCGCACTAA

BsOxd :
ATGAAGAACATGCCGGAAAATCATAATCCGCAGGCAAATGCATGGACCGCAGAATTTCCGCCTGAAATGAGCTATGTTGT
TTTTGCCCAGATTGGCATTCAGAGCAAAAGCCTGGATCATGCAGCAGAACATCTGGGTATGATGAAAAAATCATTTGATCT
GCGTACCGGTCCGAAACATGTTGATCGTGCACTGCATCAGGGTGCAGATGGTTATCAGGATAGCATTTTTCTGGCATATTG
GGATGAACCGGAAACCTTTAAAAGCTGGGTTGCAGATCCGGAAGTTCAGAAATGGTGGTCAGGCAAAAAAATCGATGAA
AATAGCCCGATTGGTTATTGGAGCGAAGTTACCACCATTCCGATTGATCATTTTGAAACCCTGCATAGCGGTGAGAATTAT
GATAATGGTGTTAGCCATTTCGTGCCGATCAAACATACCGAAGTTCATGAATATTGGGGTGCAATGCGTGATCGTATGCCG
GTTAGCGCAAGCAGCGATCTGGAAAGTCCGCTGGGTCTGCAGCTGCCTGAACCGATTGTTCGTGAAAGCTTTGGTAAAC
GTCTGAAAGTTACCGCACCGGATAACATTTGTCTGATTCGTACCGCACAGAATTGGAGCAAATGTGGTAGCGGTGAACGT
GAAACCTATATTGGTCTGGTTGAACCGACACTGATTAAAGCAAATACCTTTCTGCGTGAAAATGCAAGCGAAACCGGTTG
TATTAGCAGCAAACTGGTTTATGAACAGACCCATGATGGTGAGATTGTTGATAAAAGCTGCGTGATTGGCTATTATCTGAG
CATGGGTCATCTGGAACGTTGGACACATGATCATCCGACACATAAAGCAATTTATGGCACCTTTTACGAGATGCTGAAACG
CCATGATTTCAAAACCGAACTGGCACTGTGGCATGAAGTTAGCGTTCTGCAGAGCAAAGATATCGAACTGATTTATGTTAA
TTGCCATCCGAGCACCGGTTTTCTGCCGTTTTTTGAAGTTACCGAAATTCAAGAACCGCTGCTGAAAAGCCCGAGCGTTC
GTATTCAGTGA

XaOxd :
ATGGTCTTCCACGTCGAATATCCGCGCATCCTTCCCGAGCGCCGGCCGCCGGGCCATGAACCCGCCGCTCCGCGCTTCTC
CCTACGCTGGGAGCAGCCGGTGGGGCTCTTGGTCTGCGCCTATTTCGGCCTGCAGGGACAGAATCTGGCCTGGGACGAG
CAGAAGGCCTTCTTCGACCGCCTGGAAGCCTCCTTCGGCACGGACGGGCCGGTCGCCCACGAACTCATGCGCGCGAGCG
ACGAGACCGGCGCGGTGAACGCCATCCTCGTCGCCTACTGGCTCAATGCCACCACCCATGCTCGCTGGGAGCGCGCTGC
GCCCTTCATGGCGTGGTTTCGCGACCCCGCACGTCTCGAAGGCCCGCGCGGAGTATGGCGGGAGACCATGCACGTGCCC
TATGACCGGCACGAGACCATCTATTCCACGCCCAGCTACGCCATCGGCTTGGCCCGCACGCCCGGTGCGACGCGCGCATC
CATCACCACCAACGGCTATTTCGGTGCCATGCGCGACCGCATGCCCGTCTCCGCCATCGACACGCTGGAAAGCCCGCTCG
GCGCCATGCCGCCCCGGCGCACGCCTGTCTCCCTCGGCCGGCGGCTAAAGGCGACGTTTCCGCTCAACCTGATCTCGATC
CGGTCCGGCCAGTATTGGGAGGGGGCGGGTAACGAGCAGACCACCGACTATATCGACCATCTCCAGCCCAAACTCATGC
GCGGCATGGCTCACCTCGCCTCCCATCCGGAGGAGACTGGCACGCTGACACTGCGCATCATGACAAATCTGGATGCCGA
GGGCAGGCCCCGCGCCGAAACCTCAGTGCATGGCTATTTTCTCTCAATGGCGCATCTGGAAGAGTGGTCGCGCAGCCAC
GAGACCCATCTCGACATCTACCGGCACGCCATCGCCATGAACCGGCTCTACAAGGAGAAGCGCGAGGTGTTCACTTGGC
ACGAAGTGTTCGCGTTGCTGCCGGGCGCCCATGCTGAATATGCCAATTGCCACGGCGGCACCGGCCTGCTGCCGTATTTC
GCCGACGCCTGA

SkOxd :
ATGAGCTGGACCCCCGACTACCCGCGCACCGTCCCCGAGCGGCGGCCCCCCGGCCACCAGCCCCGGGCGCCCCGCTGGA
CCCTCGGCTTCGACGCGCCGGCCTCCCTGGTGACCAGCGACTACCTGGCGCTCCAGTGCGCCGGCCCCGACGACCCGGC
GGTCGGCCCGTTCCTGGAGCGGGTCCGCGCCTGCCACACCGGGCGGGACGGCGGAGACGCCCCCGAGGCGTGGGAACT
GCTCGCCTTCACCGACGAGGCGGGCCGCCACAACCTGGTCCACCTCGGCTACTGGCGGGACGCGACCTCCCACGCCCGC
TGGCTCGACACGGCCCCGCTCCCCCGCTGGTTCGCGGAACTCGACGCCGCCGCCGTGCCGTTCGGCGCCTGGCACGAAG
TGGTGCAGGTGCCGCTCGACCGGGTGGAGACGATCTACTCCGACCCGCGCCGCGCCTTCGGCCTCGCCGCCTGCCCGGG
GACCCGGCGCGAGTCGATGACGATGAACGGCTACTTCGGCGCCGCCCGCGACCGGCTCCCCGTCTCCGCGATCGACCCG
CTGGAGGCGGCGGCCCCGCACCGCCGCAGGGCGCGCCCGGCCGCCTCCGAGGGCCGCCGGCTGCGCGCCGAGTGCGGG
CACAACACCGCGGTGATCCGCTCGGGCCAGTACTGGCAGAACGCTCAGGGCGAGCAACTGGCCGACTACACCGAGGCG
CTGGAGCCCAAGCTGATGGCGGGCATGGCCCACCTGCGCGAGCAGGCCGACGCCGAGGGCACCCTGTCGCTGCGGGTG
ATGACCAGCCTGGACCGCGAGACCCTGCGCCCGCTGCGGGAGACCTCCGTCCTCGGCCACTTCCACACCCTCGCCGCGC
TGGAGGGATGGGCGGCCGGGCACGCCACGCACGCCGCGATCTACGAGCACGCCATCGCCAAGAACCGGCAGTACGGCG
AGGCCCGCACGGTCGTCACCTGGCACGAGGTCTTCGTCCTGCCCCGCACCGCCGCCTTCGCCTACGTCAACTGCCATCCG
GCGACGGGCATCCTGCCGTACGCCACCTCGGTGCTGGCGGTCGAGCCGGACGGCCCGGCGGAAAACTCCCCTGCCCCGT
ACGGAGGTTAA

PpaOxd :
ATGGAATCCGCGATCGACAAGCACCTCAAGTGCCCAAGAAGCCTGTCCCGCCGTGTGCCCGACGACTACCAACCGCCCT
TCCCCATGTGGGTGGCCCGCGCCGGCGAGCACATGCAGCAGGTGGTGATGGCTTACCTGGGCGTGCAGTACCAGGGCCA
GCAACACCAGCCCGCCGCGCTGCAGGCCATGGGCCAGATCGTGGCGAGCTTCAGCCTGGCCGATGGCCCGCTGAACCAT
GACCTGACCCACCACACCGACAACAGTGGCTACGACAACCTGATGGTGGTCGGCTACTGGAAAGACCCGGCCGCCTATG
GCCGCTGGCTGAACTCACCGGAAGTGGCCCAGTGGTGGGCAGCCGAAGCGCGGCTGCAGGATGGGCTCGGATATTTCCG
CGAGATCATCGCCCCACGGGCAGAACAGTTCGAAACGCTGTATGCCTTCCAGGACCGGCTGCCGGGTGTAGGCGCTGTA
ATGGACAGCACCAGCGGCGAGATCGAGGAACATGGCTACTGGGGCTCCATGCGCGACCGTTTCCCGGTGTCACAGACCG
ACTGGATGCTGCCCGACGGCGAATTGCGCATCGTCAGTGGTGACCCTGCCAAAGGCGGCCGGGTGGTGGTGCGCGGCCA
TGACAACATTGCGTTGATTCGTTCCGGGCAGGACTGGGTGGAGGCCGAGGCCGAGGAACGCTCGCTGTACCTTGACGAG
ATCCTTCCCACCCTGCAGGCAGGCATGGATTTCTTGCGTGACCAGGGGGCGCCACTGGGCTGCTACAGCAACCGCTTCGT
ACGCAATATCGACCTGCAGGGCAACCTGCTCGACTCAAGCTACAACATCGGCCACTGGCGGTCGGTTGAAAAGCTCGAG
CGCTGGGCCGAGTCGCACCCTACCCACCTGCGCATCTTCGTCACCTTCTTCCGCGTGGCAAGCGGCCTGGAAAAACTGC
GCTTGTACCATGAGGTGTCCGTGAGCGATGGCCGCCAGCAGCTGTTCGAGTACATCAACTGCCACCCCCATACCGGCATG
ATGCGCGATGCGCTACCCGCCGCTACCGGCTGCCCGCACCAGGCGCACGCATCATAA

NsOxd :
ATGGAATCAGCGATCGACACCCACCTGAAGTGCCCGCGCACCCTGTCGCGGCGGGTCGCCGACGACTACGCGCCGCCGT
TCCCGATGTTCGTCGGGCGCGGCCCGAAGGACCTGCAGCAGGTGGTCATGGCCTCGTTCGGCGTCCAGTACGCCGACGA
GGACCGCCGGCCGCAGGCCCTCGCCGCGCTGCGCCACATCGTCGGGACCTTCGAGCTCGCCGACGGCCCCGCGCACCAC
GACCTGACCCACCACGTCGACAACCAGGGGCACCACAACCTGATGGTGCTCGCCTACTGGGCCGACCCCGCGGCGTACT
GCCGGTGGCTGCGCTCCGACGAGGTCGCCGGCTGGTGGGCGTCGGACGAGCGGCTCACCGAGGGGCTGGGCTACTTCC
GCGAGATCGTCGCCCCGCGCGTCGAGCAGCTCGAGACCCTCTACGCGTTCACCGAGGACTTCCCCGGGGTCGGCACGCT
GATGCCGCAGGCCAGCGGGGAGATCGAGGAGCACGGCTACTGGGGCTCGGCCCGCGACCGGATGCCGATCTCCCAGAC
CGACTGGATGGAGGCCTCCGGCGAGCTGACCGTGGTCGAGGGCGATCCCGCGCAGGGTGGGCGGGTCGTCGTCCGGGG
GCACGACAACATCTGCCTGATCCGCTCCGGGCAGGACTGGCGCGCCGCCGGCCCCGACGAGCGCGACCTCTACGTCGAC
GAGATCCTGCCGACCCTCCAGGACGGCATGGACTTCCTCCGCGACAACGGCCAGGACCACGGCTGCTACAGCAACCGCT
TCGTCCGCAGCATCGACCTCGACGGCAACGAGCTCGACGAGAGCTACAACCTCGGGCACTGGCGCTCGCTCGACCTGCT
CGAGCGGTGGGCGGAGTCGCACCCCACCCACCTGCGGATCTTCGTGACCTTCTTCCGCGTGGTGACGGGGCTGGAGAAG
CTCCGGCTCTACCACGAGGTCTCGGTCTCCGACGGCCGCGACCAGACCTTCGAGTACATCAACTGCCACCCGGCCACGG
GGATGCTGCGCGACGCCCGCGTCCCGGTCGCCTAA

MrhOxd :
ATGGACGGGAGTGCCGTGGAGACTGGACGGCAGATCGGTGCGCGTGTGCTGGATACGGCGCCGCCAGAAGCTGTGGGC
GCTCCAGAGCGCCTCGCACCGCTGCGGAAGCCCCCTGGCTTCGTTCCCGCGGTTCAGCGCTGGTCGTTCCTGTTGCCGG
AGGGAGAGACCGCGATGCGCGTCGCCTTCTTCGGTGCACAGGCCGGATCGGCGGCCGCGCTCGACGCGCATCCGATGCG
GGACTGGATCCGCATCCATCTCACCGGTCACGCCAGCGGTCCGACCTGCTTCGACCATTCTCGAAACCGGCTCGCCGACG
GGCAGATGGAGCACGTCGTCTGTGCCTATTGGGTCTCGGAGGCCCGCTTCACGGCCTGGTCCGCCGACACCGCCGCCGA
GGGCTGGTGGCACCGGCCCGAGCGCCTCGTCGGGCCCTTCGGCGCGTGGCGTGAAGTCCTGCGGGTGCCGCGTGATCAT
CAGGAGAGCATCTACTGGAAGGATTACCCGGCCGGCTTGATGACGAGCCCGGATGTCGCGATCTTCCCGACCCCCTATTG
CGGCTATTACGGCGCCATGCGCGACCGGCTCCCGGCAGCCGCCATCGACGCCCTCGATGCGCCGGACAGCGCTGAACTC
GTGACCCGGCAGGAGCGGGTCGGTTACGGCGAACACTGGTCGGTCCGTCCGCCGCACAACCTCGCGCTGATCCGCTCCG
CCAGCACCTGGGGGCGAATGGATGCCGAACAACGCGCCGATTTCGATCTTAAGCTGCGCGTCCCTCTCAAGACCGGCAT
GGACTACCTTGCCGAGAACCCGCTTCCCTCCGGCTGTGCCTCCCTGCGTTGGCAGGAGACCACGGATCCCGAAGGTGCT
CCGAGGCCGGAAGCGCACGCGCACGCGTACTTCCTGTCTTTGCGCCACATGGAGCGTTGGGCGGAGGACCACGCCACCC
ATGCGGCCATCTTCAGGGCAGCGATCCAGCGCTACCGCCACTACGGACCGGCCAATCAACTCCGAACTTGGCATGAGGTC
TACATTCTTCCGGGGGACGGTCAGCGTTTCGAGTATCTCAACTGCGACCCGCAAACTGGCCTCCTGCGCTGGTTCGAGGC
GAAGCGCCTTGCCTGA

References

[1] Y. Asano, Y. Kato, "Z-phenylacetaldoxime degradation by a novel aldoxime dehydratase from *Bacillus sp.* strain OxB-1" *FEMS Microbiol. Lett.* **1998**, *158*, 185–190.

[2] H. Sawai, H. Sugimoto, Y. Kato, Y. Asano, Y. Shiro, S. Aono, "X-ray Crystal Structure of Michaelis Complex of Aldoxime Dehydratase" *J. Biol. Chem.* **2009**, *284*, 32089–32096.

[3] T. Betke, M. Maier, H. Gruber-Wölfler, H. Gröger, "Biocatalytic production of adiponitrile and related aliphatic linear α,ω-dinitriles" *Nat. Commun.* **2018**, *9*, 5112.

[4] A. Hinzmann, S. Glinski, M. Worm, H. Gröger, "Enzymatic Synthesis of Aliphatic Nitriles at a Substrate Loading of up to 1.4 kg/L: A Biocatalytic Record Achieved with a Heme Protein" *J. Org. Chem.* **2019**, *84*, 4867–4872.

[5] A. Hinzmann, M. Stricker, H. Gröger, "Chemoenzymatic Cascades toward Aliphatic Nitriles Starting from Biorenewable Feedstocks" *ACS Sustainable Chem. Eng.* **2020**, *8*, 17088–17096.

[6] A. Hinzmann, N. Adebar, T. Betke, M. Leppin, H. Gröger, "Biotransformations in Pure Organic Medium: Organic Solvent-Labile Enzymes in the Batch and Flow Synthesis of Nitriles" *Eur. J. Org. Chem.* **2019**, *2019*, 6911–6916.

[7] H. Mallin, J. Muschiol, E. Byström, U. T. Bornscheuer, "Efficient Biocatalysis with Immobilized Enzymes or Encapsulated Whole Cell Microorganism by Using the SpinChem Reactor System" *ChemCatChem* **2013**, *5*, 3529–3532.

[8] J. Wachtmeister, P. Mennicken, A. Hunold, D. Rother, "Modularized Biocatalysis: Immobilization of Whole Cells for Preparative Applications in Microaqueous Organic Solvents" *ChemCatChem* **2016**, *8*, 607–614.

[9] Y. Sardessai, S. Bhosle, "Tolerance of bacteria to organic solvents" *Res. Microbiol.* **2002**, *153*, 263–268.

[10] A. Inoue, K. Horikoshi, "A Pseudomonas thrives in high concentrations of toluene" *Nature* **1989**, *338*, 264–266.

[11] A. C. P. Dias, J. M. S. Cabral, H. M. Pinheiro, "Sterol side-chain cleavage with immobilized *Mycobacterium* cells in water-immiscible organic solvents" *Enzyme Microb. Technol.* **1994**, *16*, 708–714.

[12] C. C. De Carvalho, S. S. Costa, P. Fernandes, I. Couto, M. Viveiros, "Membrane transport systems and the biodegradation potential and pathogenicity of genus *Rhodococcus*" *Front. Physiol.* **2014**, *5*, 133.

[13] M. Pátek, M. Grulich, J. Nešvera, "Stress response in *Rhodococcus* strains" *Biotechnol. Adv.* **2021**, *53*, 107698.

[14] I. Kolouchová, O. Schreiberová, J. Masák, K. Sigler, T. Řezanka, "Structural analysis of mycolic acids from phenol-degrading strain of *Rhodococcus erythropolis* by liquid chromatography–tandem mass spectrometry" *Folia Microbiol* **2012**, *57*, 473–483.

[15] S. Yamashita, M. Satoi, Y. Iwasa, K. Honda, Y. Sameshima, T. Omasa, J. Kato, H. Ohtake, "Utilization of hydrophobic bacterium *Rhodococcus opacus* B-4 as whole-cell catalyst in anhydrous organic solvents" *Appl. Microbiol. Biotechnol.* **2007**, *74*, 761–767.

[16] K. Honda, S. Yamashita, H. Nakagawa, Y. Sameshima, T. Omasa, J. Kato, H. Ohtake, "Stabilization of water-in-oil emulsion by *Rhodococcus opacus* B-4 and its application to biotransformation" *Appl. Microbiol. Biotechnol.* **2008**, *78*, 767–773.

[17] Y. Mitani, X. Meng, Y. Kamagata, T. Tamura, "Characterization of LtsA from *Rhodococcus erythropolis*, an Enzyme with Glutamine Amidotransferase Activity" *J. Bacteriol.* **2005**, *187*, 2582–2591.

[18] N. Nakashima, T. Tamura, “A novel system for expressing recombinant proteins over a wide temperature range from 4 to 35°C” *Biotechnol. Bioeng.* **2004**, *86*, 136–148.

[19] N. Nakashima, T. Tamura, “Isolation and Characterization of a Rolling-Circle-Type Plasmid from *Rhodococcus erythropolis* and Application of the Plasmid to Multiple-Recombinant-Protein Expression” *Appl. Environ. Microbiol.* **2004**, *70*, 5557–5568.

[20] Y. Kato, S. Yoshida, S.-X. Xie, Y. Asano, “Aldoxime dehydratase co-existing with nitrile hydratase and amidase in the iron-type nitrile hydratase-producer *Rhodococcus* sp. N-771” *J. Biosci. Bioeng.* **2004**, *97*, 250–259.

[21] C. C. C. R. de Carvalho in *Biology of Rhodococcus* (Ed.: H.M. Alvarez), Springer International Publishing, Cham, **2019**, pp. 103–135.

[22] S. Kato, H. Nishiwaki, K. Endo, T. Hayashi, “Radical Ring-Opening Reaction of Non-Activated Oximes Catalyzed by Aldoxime Dehydratases” *Angew. Chem. Int. Ed.* **2025**, *64*, e202511590.

[23] T. Betke, J. Higuchi, P. Rommelmann, K. Oike, T. Nomura, Y. Kato, Y. Asano, H. Gröger, “Biocatalytic Synthesis of Nitriles through Dehydration of Aldoximes: The Substrate Scope of Aldoxime Dehydratases” *ChemBioChem* **2018**, *19*, 768–779.

[24] R. Zallot, N. Oberg, J. A. Gerlt, “The EFI Web Resource for Genomic Enzymology Tools: Leveraging Protein, Genome, and Metagenome Databases to Discover Novel Enzymes and Metabolic Pathways” *Biochemistry* **2019**, *58*, 4169–4182.

[25] N. Oberg, R. Zallot, J. A. Gerlt, “EFI-EST, EFI-GNT, and EFI-CGFP: Enzyme Function Initiative (EFI) Web Resource for Genomic Enzymology Tools” *J. Mol. Biol.* **2023**, *435*, 168018.

[26] D. Matsui, N. Muraki, K. Chen, T. Mori, A. A. Ingram, K. Oike, H. Gröger, S. Aono, Y. Asano, “Crystal structural analysis of aldoxime dehydratase from *Bacillus* sp. OxB-1: Importance of surface residues in optimization for crystallization” *J. Inorg. Biochem.* **2022**, *230*, 111770.

[27] S. Xie, Y. Kato, Y. Asano, “High Yield Synthesis of Nitriles by a New Enzyme, Phenylacetaldoxime Dehydratase, from Bacillus sp. Strain OxB-1” *Biosci. Biotechnol. Biochem.* **2001**, *65*, 2666–2672.

[28] D. Zheng, Y. Asano, “Biocatalytic asymmetric ring-opening of dihydroisoxazoles: a cyanide-free route to complementary enantiomers of β-hydroxy nitriles from olefins” *Green Chem.* **2020**, *22*, 4930–4936.

[29] A. Hinzmann, M. Stricker, H. Gröger, A. Hinzmann, M. Stricker, H. Gröger, “Immobilization of Aldoxime Dehydratases and Their Use as Biocatalysts in Aqueous Reaction Media” *Catalysts* **2020**, *10*, 1073.

Conclusion

This work advanced the practical application of hemoproteins as biocatalysts by utilizing chemical and biotechnological approaches. The author aimed to improve the catalytic activity and expand applicability of aldoxime dehydration reactions based on hemoproteins by deploying artificial metalloenzyme engineering, metabolic engineering, and reaction system engineering.

In Chapter 1, to overcome the substrate scope limitations of aldoxime dehydratase, the author reconstituted myoglobin with iron porphycene as a cofactor and demonstrated its function as an artificial aldoxime dehydratase. This artificial metalloenzyme catalyzed a broad range of aldoxime derivatives, achieving a maximum TON of 9300 and exhibited catalytic activity toward less reactive *O*-alkyl aldoximes, which are substrates not converted by natural aldoxime dehydratases. Furthermore, focusing on the reaction mechanism of aldoxime dehydratases, the author performed site directed mutagenesis within the heme pocket, substituting residues with serine, threonine, and tyrosine, to dramatically improve TOF. This design enabled the construction of artificial metalloenzymes with high catalytic diversity that can convert substrates inaccessible to natural enzymes.

In Chapter 2, to improve the production of heme *b* in overexpression *E. coli*, the author introduced the C4 heme biosynthetic pathway into *E. coli.* Specifically, the supply efficiency of heme was enhanced by co-expressing 5-aminolevulinic acid synthase from *Paracoccus denitrificans* together with heme proteins in *E. coli*. This approach achieved high yields of holoproteins without the need for costly external supplementation with 5-aminolevulinic acid. Notably, the heme content of the engineered method was even higher than that obtained by the conventional cultivation method. It also demonstrated enhanced activity in diverse heme protein catalysts, thereby establishing a versatile platform for heme production.

In Chapter 3, to address the limitation of enzyme reactions to aqueous conditions, the author employed the organic solvent-tolerant bacterium *Rhodococcus erythropolis* L88 as a whole-cell catalyst. The aldoxime dehydratase reactivity was compared with that of the conventional *E. coli*-based whole-cell catalyst, which lost its activity in hexane, whereas the *Rhodococcus*-based catalyst retained activity in hexane even at the low catalyst concentration of 5 mg/mL. Substrate scope evaluation further confirmed that this system is capable of converting a variety of aldoximes to nitriles on a preparative scale.

In conclusion, this study demonstrates that the utility of hemoprotein-based biocatalysts can be enhanced by systematically integrating (i) incorporation of artificial cofactors to improve catalytic function, (ii) metabolic engineering to alleviate intracellular heme limitations, and (iii) reaction system engineering to enable operation under non-aqueous conditions. The achieved improvements in catalytic efficiency, substrate scope (including activity toward non-natural substrates), reduction of cultivation costs for hemoproteins, and robustness under preparative conditions suggest the feasibility of applying hemoprotein catalysis in broader chemical contexts. This strategy provides a promising basis for the continued development of sustainable biocatalytic systems derived from hemoproteins.

List of Publication

1. Reconstitution of Myoglobin with Iron Porphycene Generates an Artificial Aldoxime Dehydratase with Expanded Catalytic Activities
   Shunsuke Kato,* Miteki Abe, Harald Gröger, Takashi Hayashi*
   ACS Catal., **2024**, *14*, 13081–13087.
   DOI: 10.1021/acscatal.4c03220

2. Metabolic Engineering of the 5-Aminolevulinate Biosynthetic Pathway in *E. coli* Improves Efficiency of Hemoprotein-Based Biocatalysis
   Shunsuke Kato,* Miteki Abe, Nobuyuki Okahashi, Shinya Ariyasu, Fumio Matsuda, Osami Shoji, Takashi Hayashi
   Angew. Chem. Int. Ed., **2025**, *64,* e202512156.
   DOI: 10.1002/ange.202512156

3. Organic Solvent Tolerant Bacteria as a Host for Whole-cell Biocatalysis: Enzymatic Dehydration of Aldoximes in Organic Medium
   Miteki Abe, Moeko Takeuchi, Shunsuke Kato*, Tomohisa Hasunuma, Harald Gröger, Takashi Hayashi*
   J. Porphyrins Phthalocyanines, accepted

Acknowledgements

The study presented in this thesis has been carried out at Department of Applied Chemistry, Graduate School of Engineering, The University of Osaka from April 2020 to March 2026. The author would like to express her immense gratitude to her supervisor, Professor Takashi Hayashi, for his dedicated guidance, constant discussions, and generous support of time throughout this research. The author also extends her profound thanks to Associate Professor Koji Oohora for his insightful advices and helpful suggestions. Additionally, the author acknowledges with profound appreciation Associate Professor Shunsuke Kato at Engineering Biology Research Center, Kobe University, for his penetrating comments, invaluable insights, and passionate commitment to research. Special thanks are extended to Professors Seiji Minakata and Masaya Nogi for reviewing this thesis and providing valuable suggestions.

Acknowledgements are also made to Professor Osami Shoji at Department of Chemistry, Graduate School of Science, Nagoya University and Associate Professor Shinya Ariyasu at Graduate School of Science and Engineering, Kindai University, for preparation of decoy molecule and cytochrome P450BM3 gene in Chapters 2. The author expresses her gratitude to Professor Fumio Matsuda and Associate Professor Nobuyuki Okahashi at Department of Biotechnology, The University of Osaka and Shimadzu Analytical Innovation Laboratories, Graduate School of Engineering, The University of Osaka, for LCMS analysis in Chapter 2. The author would like to thank Professor Tomohisa Hasunuma and Ms. Moeko Takeuchi at Department of Chemical Science and Engineering, Faculty of Engineering, Kobe University, for SDS-PAGE analysis and substrate scope investigation in Chapter 3. The author is very grateful to Prof. Harald Gröger at Industrial Organic Chemistry and Biotechnology, Faculty of Chemistry, Universität Bielefeld, for his kind guidance and the warm welcome during her stay in Bielefeld , and for granting her the valuable opportunity to pursue her studies abroad.

The author would like to express the gratitude to Mr. Shinya Kanbe, Mr. Hiroyuki Shibata and all staffs at Nagoya Criatio R&D Center, Toagosei Co., Ltd. for accepting the author under an internship program. Thanks to their kind guidance, the author learned a lot in the field of polymer engineering and its industrial use.

Acknowledgement is also made to Ms. Kiyomi Lee for her kind help in laboratory life. The author wishes to express sincere gratitude to Dr. Yoshiyuki Kagawa for his patient guidance and for imparting fundamental insights, which have been invaluable throughout this work. The author gratefully acknowledges Ms. Chihiro Sonoda, a fellow colleague, whose enthusiastic engagement in research has been deeply motivating throughout the course of this work. Furthermore, the author is grateful to all members of Prof. Takashi Hayashi's group and Prof. Harald Gröger's group for their discussions, encouragements and friendship.

The author expresses great gratitude to her family, Takanobu, Naoko, Shoma and Koma for their heartfelt assistance and encouragement.

Finally, the author is grateful for financial support from Interactive Materials Science Cadet Program.

Miteki Abe

January 2026